Understanding, inducing and exploiting actionable vulnerabilities in experimental glioma

Dissertation

zur Erlangung des Grades eines
Doktors der Naturwissenschaften

der Mathematisch-Naturwissenschaftlichen Fakultät
und
der Medizinischen Fakultät
der Eberhard-Karls-Universität Tübingen

vorgelegt
von

Bianca Armbruster (geborene Walter)
aus Herrenberg, Deutschland

2024

Tag der mündlichen Prüfung: 16.04.2024

Dekan der Math.-Nat. Fakultät: Prof. Dr. Thilo Stehle

Dekan der Medizinischen Fakultät: Prof. Dr. Bernd Pichler

1. Berichterstatter: Prof. Dr. Dr. Ghazaleh Tabatabai

2. Berichterstatter: Prof. Dr. Julia Skokowa, PhD

Prüfungskommission: Prof. Dr. Dr. Ghazaleh Tabatabai

                              Prof. Dr. Julia Skokowa, PhD

                              Prof. Dr. Jonas Neher

                              Prof. Dr. Katja Schenke-Layland

Erklärung / Declaration:

Ich erkläre, dass ich die zur Promotion eingereichte Arbeit mit dem Titel:

„Understanding, inducing and exploiting actionable vulnerabilities in experimental glioma"

selbständig verfasst, nur die angegebenen Quellen und Hilfsmittel benutzt und wörtlich oder inhaltlich übernommene Stellen als solche gekennzeichnet habe. Ich versichere an Eides statt, dass diese Angaben wahr sind und dass ich nichts verschwiegen habe. Mir ist bekannt, dass die falsche Abgabe einer Versicherung an Eides statt mit Freiheitsstrafe bis zu drei Jahren oder mit Geldstrafe bestraft wird.

I hereby declare that I have produced the work entitled „Understanding, inducing and exploiting actionable vulnerabilities in experimental glioma"*, submitted for the award of a doctorate, on my own (without external help), have used only the sources and aids indicated and have marked passages included from other works, whether verbatim or in content, as such. I swear upon oath that these statements are true and that I have not concealed anything. I am aware that making a false declaration under oath is punishable by a term of imprisonment of up to three years or by a fine.*

Tübingen, den ....
                          Datum / Date   Unterschrift /Signature

Contents

List of tables

List of figures

List of abbreviations

°C	Centigrade
AKT	serine/threonine kinase 1
ATM	ataxia telangiectasia mutated
ATP	Adenosine triphosphate
ATR	ataxia telangiectasia mutated and Rad3 related
ATRi	ATR inhibition
BBB	blood brain barrier
BCA	bicinchoninic acid
BER	base excision repair
bFGF	basic fibroblast growth factor
bHLH	basic Helix loop Helix
BSA	bovine serum albumin
CD	cluster of differentiation
CDK	cyclin dependent kinase
CDKN2A	cyclin dependent kinase inhibitor 2A
Chk1/2	checkpoint-kinase 1/2
CNS	central nervous system
CRISPR/Cas9	clustered regularly interspaced short palindromic repeats/Cas9
CTLA-4	cytotoxic T lymphocyte associated protein 4
DEG	differentially expressed gene
DDR	DNA damage response
DMEM	Dulbecco's modified eagle medium
DR	direct repair
DSB	double strand break
EGFR	epithelial growth factor receptor
ERCC3	ERCC excision repair 3, TFIIH core complex helicase subunit
EURACAN	European Reference Network on Rare Adult Cancers
f	forward
FA	Fanconi Anemia
FANC	Fanconi anemia complementation group

fc	fold change
FDA	Food and Drug Administration
GB	glioblastoma
GFAP	glial fibrillary acidic protein
Gt	goat
h	hour
hESC SFM	human embryonic stem cell culture serum- and feeder-free medium
HLA	human leukocyte antigen
HPRT	hypoxanthine phosphoribosyltransferase 1
HSCT	hematopoietic stem cell transfer
HR	homologous repair
i.p.	intra peritoneal
IDH	isocitrate-dehydrogenase
IL	interleukin
kb	kilobase
KEGG	Kyoto encyclopedia of Genes and Genomes
L	liter
LRT	likelihood ratio test
m	meter
MAP kinase	mitogen-activated protein kinase
MEM	minimal essential medium
MGMT	O6-Methylguanin-DNA-Methyltransferase
MHC	major histocompatibility complex
MHC	major histocompatibility complex
min	minute
MMR	mismatch repair
NCI	National Cancer Institute
NER	nucleotide excision repair
NFκB	nuclear factor kappa-light-chain-enhancer of activated B-cells
NF1	neurofibromin 1
NFDM	non-fat dry milk

NHEJ	non-homologous end joining
padj	adjusted p-value
PAGE	polyacrylamide gel electrophoresis
PARP	poly(ADP ribose) polymerase
PBS	phosphate-bufered saline
PCA	principal component analysis
PD-1	programmed death 1
PDGFRA	platelet derived growth factor receptor alpha
PD-L1	programmed death ligand 1
PDM	patient derived microtumor
PDX	patient derived explant
PFA	paraformaldehyde
PI	propidium iodide
PTEN	phosphatase and tensin homolog
PVDF	polyvinylidendifluorid
q-rtPCR	quantitative real-time polymerase chain reaction
r	reverse
RB	retinoblastoma
RCAS	replication competent avian leucosis and sarcoma virus
RIPA	radio-immunoprecipitation assay
RPA	replication protein A
rpm	revolutions per minute
RPMI	Roswell Park Memorial Institute
RT	room temperature
SBDS	SBDS ribosome maturation factor
SDS	sodium-dodecyl sulfate
sec	second
SSB	single strand break
ssDNA	single stranded DNA
TBS	tris-buffered saline
TCGA	The Cancer Genome Atlas

TERT	telomerase-reverse-transcriptase
TF	transcription factor
TIL	tumor infiltrated lymphocyte
TLS	translesion synthesis
TMZ	temozolomide
TNF	tumor necrosis factor
TP53	tumor protein p53
TSA	tumor specific antigen
tv-a	tumor virus a
V	volt
WHO	world health organization

Abstract

Glioblastoma (GB) are aggressive, primary brain tumors, for which standard therapy comprises surgical resection followed by radio-chemotherapy [1-3]. Despite this multimodal and aggressive treatment approach, overall survival of patients remains in the range of 1.5 years and almost all patients will suffer from progressive disease [1, 2, 4]. Hence, novel treatment options are urgently needed, however, identifying novel exploitable tumor vulnerabilities in GB remains challenging. Consequently, this thesis focuses on understanding, inducing and exploiting actionable vulnerabilities in experimental glioma.

This thesis includes the following three projects: First, Argyrin F a cyclic peptide that inhibits the proteasome from downregulating p27^{Kip1} [5], is evaluated for its anti-glioma efficacy. Second, the ATR inhibitor AZD6738 is molecularly analyzed to identify potential combination partners opening new therapeutic strategies. Lastly, this thesis discusses the accumulation of Fanconi Anemia (FA) germline mutations in the molecular tumor board (MTB) neuro-oncology cohort Tübingen.

Argyrin F showed promising anti-glioma efficacy in acute cytotoxicity and clonogenic survival assays *in vitro* (**Figure 12**). This anti-glioma efficacy was also detected in the *ex vivo* model of patient derived microtumors (PDMs) (**Figure 14**). Treating VM/Dk mice harboring SMA560 tumors with Argyrin F led to a significant prolongation of time until onset of neurological symptoms *in vivo* (**Figure 12Figure 13Figure 14**). Interestingly, brains harboring SMA560 tumors that were treated with Argyrin F displayed an increased influx of T cells into the tumor tissue (**Figure 13**), highly suggestive for an immunogenic activation upon Argyrin F treatment. This hypothesis was further validated using HLA ligandome analyses that showed treatment induced changes upon Argyrin F treatment (**Figure 15**). Also, PDMs co-cultured with autologous TILs that were treated with Argyrin F displayed a significant induction of cytotoxicity read-out, combination therapy using Argyrin F together with the PD-1 checkpoint inhibitor Nivolumab could significantly increase the cytotoxicity read-out compared to either monotherapy (**Figure 16**). In an animal experiment that also tested the combination of Argyrin F together with PD-1 checkpoint inhibition, symptom onset was delayed by ten days in the combination therapy compared to the mono-therapeutic setting (**Figure 17**).

ATR inhibition by AZD6738 and Berzosertib, respectively, lead to anti-glioma activity *in vitro* and displayed a modest phenotype *in vivo* (**Figure 18**, **Figure 19**, **Figure 20**). Further characterization of cells treated with ATR inhibition, showed differences in cell cycle regulation upon treatment (**Figure 21**). To elucidate these differences in more detail, transcriptomic analyses using bulk RNASeq were done and revealed shared, as well as distinctly regulated pathways (**Figure 22**). These findings could be validated using DigiWest protein profiling (**Figure 23**). Based on this, ATR inhibition was combined with standard therapy Temozolomide, the PARP inhibitor Olaparib and PI3K/mTOR inhibitors Paxalisib

and Everolimus (**Figure 24**, **Figure 25**, **Figure 26**, **Figure 27**, **Figure 28**, **Figure 29**). The analyses lead to different synergism read-outs depending on the cell line used, which can be explained with the distinct transcriptomic and proteomic signatures identified.

Lastly, genetic analyses of 216 glioblastoma patients revealed 23 germline mutations of which 9 were part of the FA pathway (**Table 4**). Somatically also an accumulation of FA mutations in GB patients could be detected (**Figure 31**). To elucidate the influence of FA mutations on GB development and/or propagation, five FA genes were used to model glioma development in the RCAS/tv-a mouse model *in vivo*. In one of the five genes a reduction of time until onset of neurological symptoms was seen (**Figure 33**). This was accompanied by a significantly higher level of Ki67 positive cell nuclei in the tumor tissue as well as histological features of high-grade glioma (**Figure 34**). An analysis of proliferation capacity of stable glioma cell lines did not lead to any significant changes upon FA knockdown (**Figure 36**), however, in clonogenic survival assays a significantly higher treatment sensitivity could be detected (**Figure 38**, **Figure 39**, **Figure 40**).

Taken together, this thesis presents novel insights into vulnerabilities in experimental glioma and might inform future clinical trials.

1. Introduction

1.1 Glioblastoma

1.1.1 Epidemiology, therapy and diagnosis

World-wide brain and nervous system tumors comprise 1.6% of all newly diagnosed cancers [6]. Glioblastoma (GB) are aggressive primary brain tumors with an incidence of 3.23 per 100 000 in the United States (US). It is the most common primary malignant tumor of the central nervous system (CNS), encompassing 14.3% of all CNS tumors and 49.1% of the group of malignant CNS tumors. According to retrospective analysis in the US, the incidence for glioblastoma in men is higher than in women [7]. Outside of clinical trials, standard therapy entails maximum safe resection of tumor mass, followed by radio-chemotherapy using Temozolomide (TMZ) as first-line treatment. This therapy regimen is widely known as "Stupp protocol" [1, 3, 4]. Despite this intensive treatment schedule median overall survival remains in the range of only 1.5 years [1, 2, 4, 8]. The majority of patients reveal first progression within seven to nine months after initial diagnosis [7, 9].

Until 2016, GB diagnosis relied mostly on histopathological features for diagnosis [10]. Histological features of GB include marked hypercellularity, nuclear atypia, microvascular proliferation and necrosis leading to pseudopalisading [11, 12]. However, due to inter-observer heterogeneity these diagnostic tools led to limited comparability and risk of misdiagnosis [13]. 2016 the purely histological diagnosis paradigm was broken and molecular features were incorporated into the diagnostic routine [14]. 2021 the fifth edition of the WHO Classification of Tumors of the CNS was published [15]. In this, the role of molecular diagnostics advances even more. Key diagnostic marker genes for GB diagnosis are, among others, mutations in the isocitrate-dehydrogenase (IDH), telomerase-reverse-transcriptase (TERT) promoter mutations, epithelial growth factor receptor (EGFR) amplification and copy number changes of chromosome 7 and 10 (**Figure 1**). Novel approaches using methylation analysis for CNS tumor diagnostics have been proposed and might even surpass classical diagnosis in the future [16], however, as of now, these approaches are acknowledged and recognized as grading option in the WHO classification, but are not a necessary tool, yet [17].

1.1.2 Molecular features

Glioblastoma are very heterogeneous and treatment refractory tumors [18, 19], hence, substantial research has been focused on defining markers to identify subclasses of GB patients and in turn improve therapeutic strategies based on those. One of the first prognostic markers described in the glioma background was the methylation of the O^6-methylguanine-DNA-methyltransferase (MGMT)
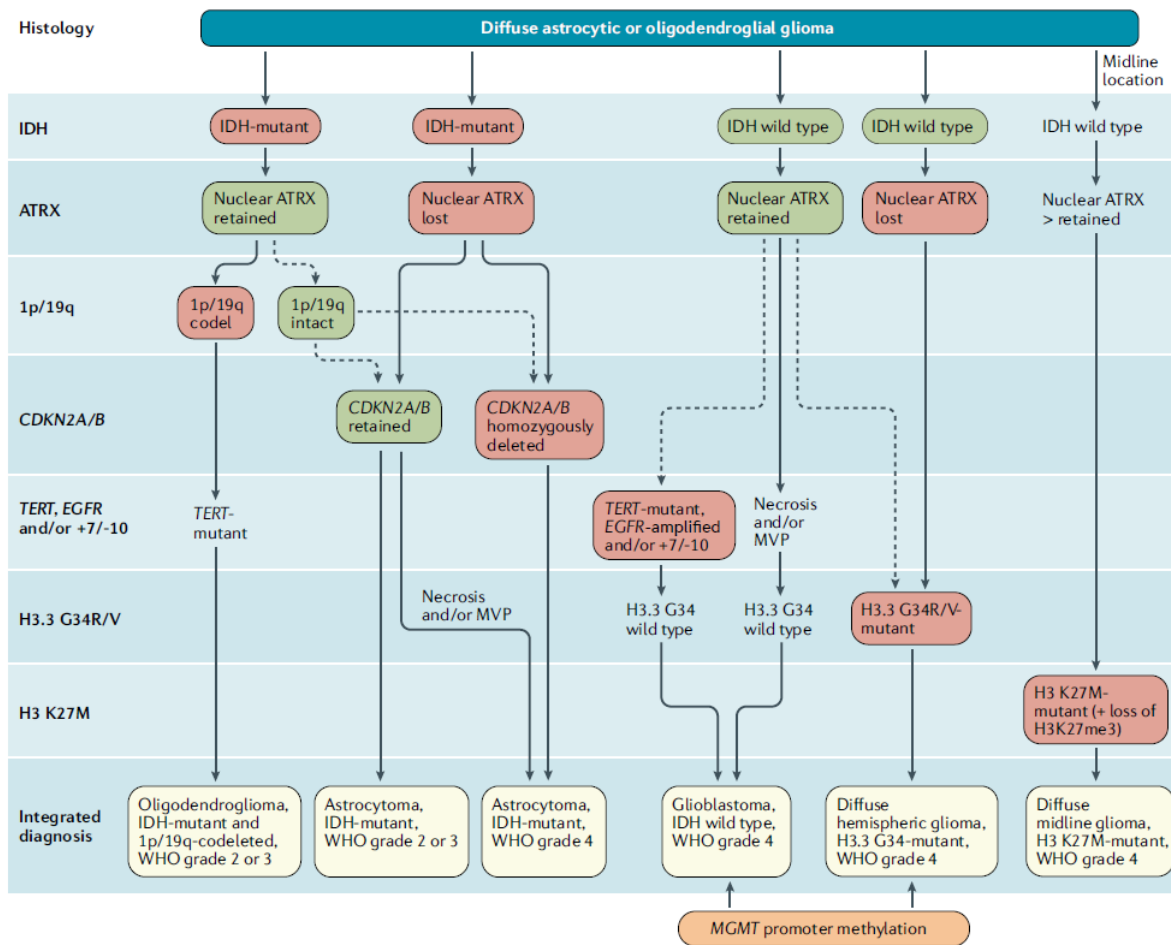
Figure 1: *Decision tree for diagnosis of diffuse astrocytic or oligodendroglial glioma*
Decision tree for diffuse glioma diagnosis according to the European Association of Neuro-Oncology (EANO), adapted from Weller et al. [3]

promoter. Methylation inactivates this DNA repair gene and in turn sensitizes brain tumors towards alkylating agents [20, 21]. In clinical trials, patients displaying methylated MGMT promoter show increased median overall survival when treated by radiotherapy with concomitant and maintenance Temozolomide compared to non-methylated patients regardless of age [22, 23]. IDH1 mutations are another example of prognostic and also diagnostic markers. They were described to occur more often in younger patients, show increased overall survival and are correlated with p53 mutations [24]. This mutation holds diagnostic power as grading of CNS tumors according to the WHO classification of CNS tumors is heavily influenced by IDH mutation status, i.e., adult-type glioma determined to be IDH wildtype are classified as GB [15, 17].
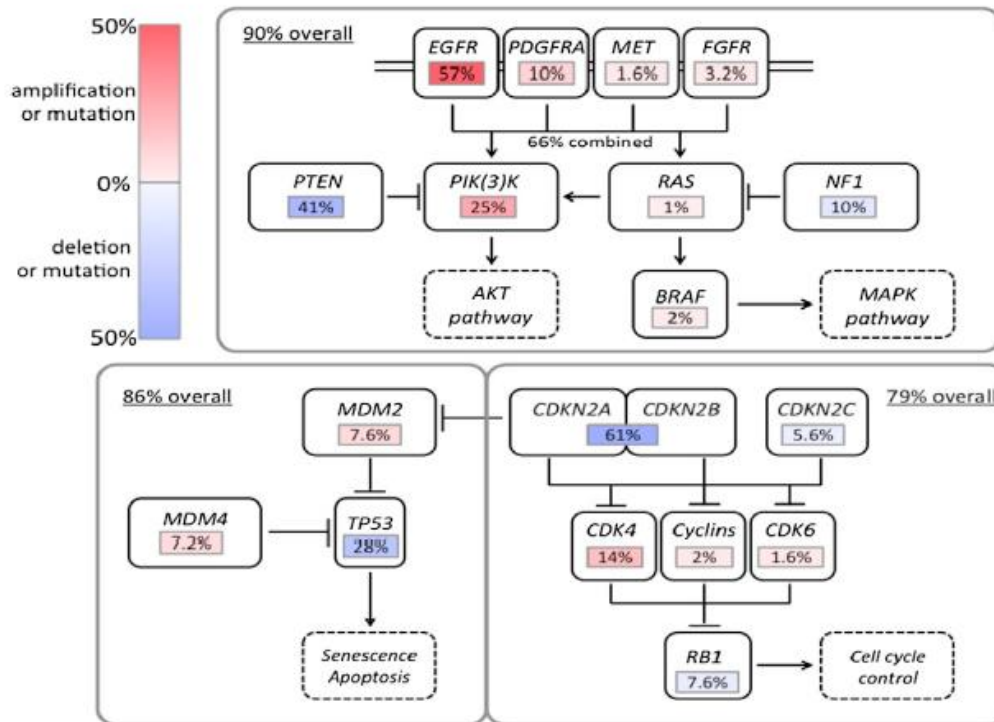
Figure 2 *Analysis of frequently mutated genes based on the TCGA data base.*
Figure adopted from Brennan et al. [25]

On a broader range, The Cancer Genome Atlas (TCGA) program by the national cancer institute (NCI) [26] collects and provides patient data for different cancer entities. Especially for more rare tumors this database provides an opportunity to conduct large scale analyses. Based on this data repository, GBs have been analyzed and divided into three molecular subtypes, namely, classical, mesenchymal and proneural. Proneural GBs tend to have alterations in the platelet derived growth factor receptor alpha (PDGFRA), IDH1 and p53. They are associated with younger patients, favorable outcome and with the oligodendrocytic lineage, hence, comprising a group of rather atypical GB. The classical subtype was described to carry chromosome 7 amplifications paired with chromosome 10 loss. Almost all are EGFR amplified while co-occurring dysregulation of the retinoblastoma (RB) pathway was linked to cyclin dependent kinase inhibitor 2A (CDKN2A) mutations. The mesenchymal subtype was linked to neurofibromin 1 (NF1) loss and phosphatase and tensin homolog (PTEN) mutations, both associated with the AKT serine/threonine kinase 1 (AKT1) pathway. Mesenchymal and classical subtypes show poorer outcome but higher benefit from therapy regimen compared to the proneural subtype [27, 28]. This might be due to the fact that IDH mutations, which have been shown to indirectly support resistance towards TMZ therapy through upregulation of homologous recombination (HR) [29], are mostly detected in the proneural subtype [27, 28].

In line with the determinant genetic alterations described by Verhaak et al. [27], TCGA analyses of most frequently somatically mutated genes reveal that 79% of GB harbor mutations in the CDKN2A/CDKN2B/RB1 pathway, 90% harbor mutations in the mitogen-activated protein kinase (MAP Kinase) and AKT pathway and 86% harbor mutations in the p53 pathway (**Figure 2**) [25]. Recent studies on the single cell level have revealed strong intra-tumoral heterogeneity, leading to detection of several subtypes in one tumor [30, 31]. This might also explain the frequent progression and evasion events preventing improvement of therapy success.

1.1.3   Implementation of Molecular Tumor Boards (MTB) at the University Hospital Tübingen

Despite intensive research efforts, novel treatment options remain elusive and although there are more than 1700 trials listed in the ClinicalTrials.gov repository, with more than 300 actively recruiting (search term "glioblastoma" at ClinicalTrials.gov July 2022 [32]), no major changes to standard therapy of GB have been made since the implementation of the "Stupp protocol" [2-4]. So far, the "one treatment for all" approach did not lead to long-term tumor control.
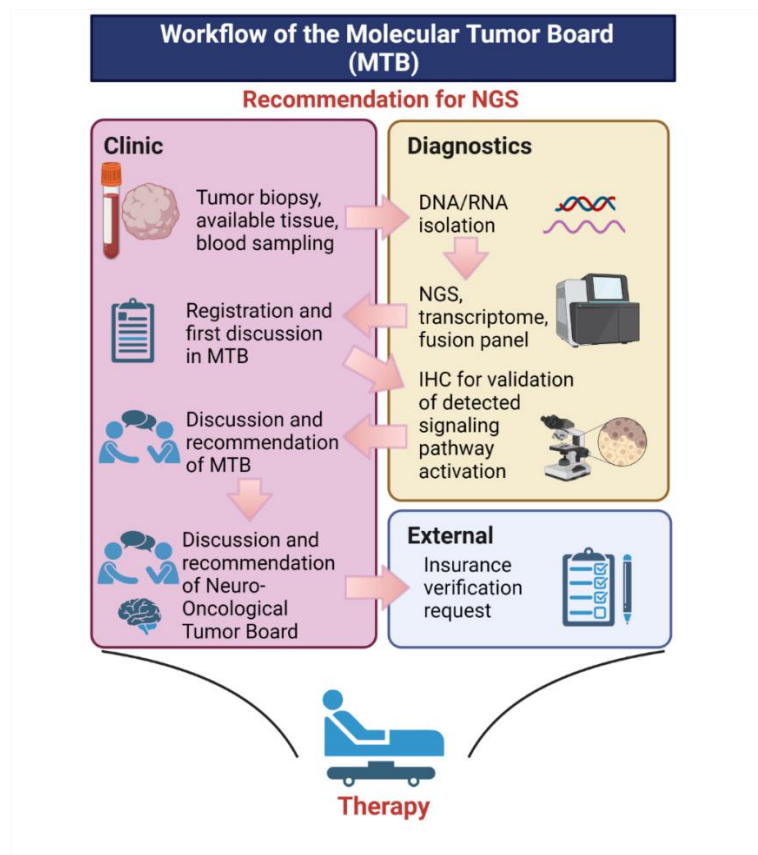
Figure 3 *Workflow of the Molecular Tumor Board (MTB) Tübingen.*
Created with BioRender.com

Rapid advances in next-generation sequencing (NGS) enable clinical trials to include molecular profiles into their study and treatment design moving towards personalized therapy approaches [33, 34]. Even in routine clinical care high-throughput molecular diagnostics have become available at lower costs, thus, leading to easily available genetic data of patients [35]. In recent years, targeted therapies for certain genetic changes like KIT mutations in gastrointestinal stromal tumors, have been successfully implemented into the clinical work-flows [36]. However, these treatment options are only available for a select small patient cohort of specific tumor entities. Especially in neuro-oncology, many patients cannot participate in clinical trials due to a lack of clinical trials for their specific tumor entity or because they do not meet the study inclusion criteria. Nevertheless, a substantial proportion of molecular diagnostics are currently performed outside of clinical trials, however, this data needs to be connected to relevant individual clinical data from which a personalized treatment can be deduced [37]. Consequently, the Center for Personalized Medicine Tübingen was founded and introduced a standardized, quality-controlled and transparent workflow. In a crosstalk between oncologists, geneticists, pathologists, pharmacologists, bioinformaticians, radiologists and molecular biologists, personalized treatment options based on molecular markers are discussed in and recommended by the molecular tumor board (MTB) (**Figure 3**). To evaluate the impact of this workflow on the clinical course and outcome of patients, the prospective observational study MTB@ZPM (NCT03503149) was implemented. Furthermore, the genetic data can also be used to identify novel molecular markers or genetic changes that might be of relevance to tumor biology or therapy which have not been recognized, yet.

1.2 Novel treatment options investigated in Glioblastoma research

As has been described above, GB treatment did not change much in the last almost two decades despite intensive research efforts [38]. Nevertheless, brain tumor patients still have a poor prognosis [2, 7] which emphasizes the need for novel treatment options. This thesis focuses on elucidating treatment options in cancer relevant research areas proteasome inhibitors, immune checkpoint inhibitors and DNA damage response pathways.

1.2.1 Proteasome inhibitors

The proteasome is a complex structure responsible for the protein turn-over in cells. It is made up of a core unit, called the 20S proteasome which is typically found in a complex with two 19S regulatory subunits, together building the 26S proteasome. In an adenosine triphosphate (ATP) and ubiquitin dependent manner the proteasome degrades proteins [39, 40]. However, the proteasome has been

found to not only degrade proteins but also prepare peptides for binding to major histocompatibility complexes (MHC) which will in turn migrate to the cell surface and function as an important control function for the immune system [41, 42].

In recent years, proteasome inhibitors have become quite an interesting novel drug class due to their successful implementation into the clinical use in multiple myeloma treatment [43]. Proteasome inhibitors affect the protein turnover in cells which ultimately leads to cell death. Bortezomib, a reversible inhibitor of the proteasome, showed cytotoxicity towards different human cancer cells [44, 45]. Following this finding, Bortezomib became the first-in-class Food and Drug Administration (FDA) approved proteasome inhibitor as a third-line therapy in myeloma. Following further treatment refinements and clinical trials, Bortezomib is now approved for first-line treatment in myeloma and other cancer entities [43]. Based on this success, Bortezomib as well as other second-generation proteasome inhibitors, e.g. Marizomib, an irreversible inhibitor of the proteasome with a broader inhibition of the 20S subunit [46], are now investigated in several other cancer entities, among them GB. Several pre-clinical studies have been conducted looking into Bortezomib and Marizomib in the GB context. They could detect good anti-glioma efficacy *in vitro* and *in vivo*. In general, Marizomib seems to have the more favorable chemical profile due to its good blood brain barrier (BBB) penetrance [47, 48]. Nevertheless, although clinical trials have shown inhibitory effects of Marizomib towards the proteasome [49], no improvement of overall survival or progression free survival was detected. Unfortunately, at the same time an increased amount of treatment related adverse events were reported [50].

Taken together, proteasome inhibitors remain an interesting drug class, however, at least for GB therapy, novel drugs with better profiles are needed. Here, the anti-glioma efficacy of the cyclic peptide and 20S proteasome inhibitor Argyrin F (**Figure 4**) is investigated [51]. Cyclic peptides are chemically highly interesting drug candidates as they have better biological activity than their linear counterparts conferred by their conformational rigidity. The cyclic build-up also makes them rather resistant towards hydrolysis by exopeptidases due to the lack of amino and carboxyl termini [52, 53].

Argyrin F, which is a more soluble analogue of Argyrin A [54], has been developed in an academic drug discovery program. It has been shown to specifically inhibit the proteasomal degradation of $p27^{Kip1}$, a cyclin dependent kinase (CDK) inhibitor that is involved in cell cycle control. The cell cycle is controlled via several CDK-cyclin complexes that lead to RB1 phosphorylation and in turn to cell cycle progression and proliferation [55]. $p27^{Kip1}$ together with $p21^{Cip1}$ inhibit the activity of the CDK2-cyclin E and CDK4-cyclin D complexes at G1-S-phase transition inhibiting cell cycle progression (**Figure 5**). Hence, low levels of either $p21^{Cip1}$ or $p27^{Kip1}$ lead to cell cycle progression [56-58]. In GB, among other cancer entities, low levels of $p27^{Kip1}$ have been described and associated with highly aggressive tumors [59].

Figure 4: Chemical formula of Argyrin F

Adopted from Bülow et al., 2010 [60]

Argyrin F has been reported to show anti-cancer efficacy in other pre-clinical cancer models, e.g., pancreatic cancer, reducing proliferation, migration, invasion while inducing apoptosis *in vitro* and blockage of tumor growth, neo-vascularization and metastasis formation *in vivo* [5]. Due to its involvement with cell cycle control, it is very interesting in the GB context. As has been mentioned before, approx. 79% of all GB patients display mutations in the CDKN2A/CDKN2B/RB1 signaling pathway (**Figure 2**), consequently leading to dysfunctional cell cycle control [25]. Additionally, it has been shown that loss of any of these genes as well as CDK4 amplification which disrupts the RB1 pathway, is associated with shorter survival [61]. Taking all of this into account, Argyrin F seems to hold great potential for GB treatment.

Figure 5: p27 and p21 in cell cycle regulation adopted from Abde M. Abukhdeir and Ben Ho Park, 2008 [55]

1.2.2 Immune checkpoint inhibition

The immune system is usually quite effective at preventing tumor onset, however, it has been shown that the immune system can also function in a tumor protecting manner [62]. Different mechanisms termed "cancer immunoediting" lead to the dual role of the immune system of host-protection and tumor-promotion [63]. Consequently, research has focused on those immune evasion mechanisms and potential treatment options to reinstall the anti-tumor function of the immune system in cancer [64, 65].

The starting point of immune therapies was the detection of tumor specific antigens (TSA) that were hypothesized to be treatable [66]. Consequently, therapeutic antibodies targeting TSAs were developed. One example for this is the targeting of human epithelial growth factor receptor 2 (HER2) which has no known natural ligand to bind but is frequently upregulated in certain cancers and plays a crucial role in cellular transformation and tumor propagation. Hence, it is an ideal candidate for antitumor treatment which was achieved using Trastuzumab a recombinant monoclonal antibody against HER2 [67, 68]. Unfortunately, this approach needs the expression of this specific TSA making these treatments only available for a selected subset of patients and resistance mechanisms are quite frequent [68].

Further research then proved that tumor cells display different mechanisms of immune escape, ranging from loss of antigen presentation, upregulation of anti-apoptotic effector molecules to establishment of an immunosuppressive state within the tumor microenvironment. The latter can be achieved by expression of immunosuppressive cytokines or recruiting and modulating of regulatory immune cells [63]. Naturally, the immune system is equipped with a very well-balanced control system that also entails negative regulators to prevent auto-immune reactions [69]. Examples for two of these negative regulators are the cytotoxic T lymphocyte associated protein 4 (CTLA-4) or programmed death 1 (PD-1). Upon interaction with their respective ligands, i.e., CD80 and CD86 for CTLA-4 [70] and programmed death ligand 1 (PD-L1) and PD-L2 for PD-1 [71], they lead to a reduced immune response of immune effector cells. Tumors often leverage this system in order to evade the immune surveillance of the host organism by up-regulation of, e.g., CTLA-4 [63].

Immune checkpoint blockade is supposed to disrupt these non-physiological immunosuppressive signals by the tumor. In 2011 the FDA approved Ipilimumab, a therapeutic antibody targeting CTLA-4, to treat late-stage melanoma. Studies had shown that median overall survival of patients treated with Ipilimumab was 10 months as compared to 6.4 months in the control group [72]. Together with the second-generation checkpoint inhibitors targeting the PD-1/PD-L1 axis, combination of Ipilimumab with Nivolumab in late-stage melanoma, leads to a 5-year survival rate of 52% [73]. Before immune checkpoint inhibition metastatic melanoma revealed, similarly to GB, devastating prognosis in

combination with high treatment refractory [72]. With the implementation of immune checkpoint inhibition now approximately 50% of patients show long-term treatment responses and improved overall survival [73]. Based on this success, immune checkpoint inhibition has been shown to be highly effective in a variety of tumor entities [74]. Consequently, also in brain tumors checkpoint inhibition has been tested.

In glioma high PD-L1 expression has been shown and correlated with glioma grade, i.e., high PD-L1 expression correlated with higher glioma grade [75-77]. Additionally, PD-1 expression has been detected on peripheral T cells and also correlated with disease progression and glioma grade [78]. Pre-clinical studies in glioma mouse models also showed promising results upon PD-1 blockade [79]. However, clinical studies failed to improve survival of glioma patients compared to standard therapy [80, 81]. This might be due to the fact that GB are immunologically rather quiet tumors as evidenced by low mutational burden, few tumor infiltrated lymphocytes (TILs) and low PD-1/PD-L1 expression compared to other immune checkpoint inhibition sensitive tumors [65, 82]. Still, although the CheckMate-143 study did not meet its primary endpoint, overall survival was comparable between Nivolumab and Bevacizumab groups, proving some level of efficacy nonetheless [80]. Major research efforts are ongoing to improve immune checkpoint inhibition in glioma patients. Some are investigating combination approaches enhancing immunogenicity which has been shown to be successful in different cancers [83]. Other approaches entail targeting of additional immune checkpoint molecules which might be more efficacious than targeting CTLA-4 or the PD-1/PD-L1 in glioma patients [84].

1.2.3 The DNA damage response

Every day thousands of DNA damaging events occur [85] which need to be repaired in order to maintain genomic integrity [86]. To do so, the cell has a plethora of proteins and pathways to repair DNA damage. There are eight "core pathways" of DNA damage response (DDR) (**Figure 6**) which are responsible for certain DNA damages but have been shown to interact and crosstalk in a vast network [87]. Three of those can be attributed to DNA double strand break (DSB) repair: the Fanconi Anemia (FA) pathway is activated in the presence of inter-strand crosslinks [88]; homologous recombination (HR) is activated to repair a double strand break in case an undamaged sister chromatid, which can serve as a template, is present (late S-phase or G2-phase) [89]; and thirdly, non-homologous end joining (NHEJ) repairs a double strand break without a sister chromatid and therefore is rather error prone [90]. Four other mechanisms are responsible for DNA single strand breaks (SSB): base excision repair (BER) corrects modified bases, abasic sites and DNA single strand breaks [91]; nucleotide excision repair (NER) corrects nucleotides that distort the structure of the DNA, mostly

induced by UV light [92]; and mismatch repair (MMR) which corrects replication errors of mismatched base-pairing, nucleotide insertions or deletions [93]. There are also some proteins which directly repair (DR) certain DNA damages, e.g., MGMT directly repairs O^6-methylguanine removing the nucleotide adduct and thus preventing the MMR to wrongly correct the DNA sequence from G:C to A:T [94]. Lastly, the translesion synthesis (TLS) mechanism prevents genetic instability at damaged DNA bases or base adducts that were not repaired before replication start. It enables the replication to proceed without stalling replication forks until they collapse which could in turn induce DNA single or double strand breaks.
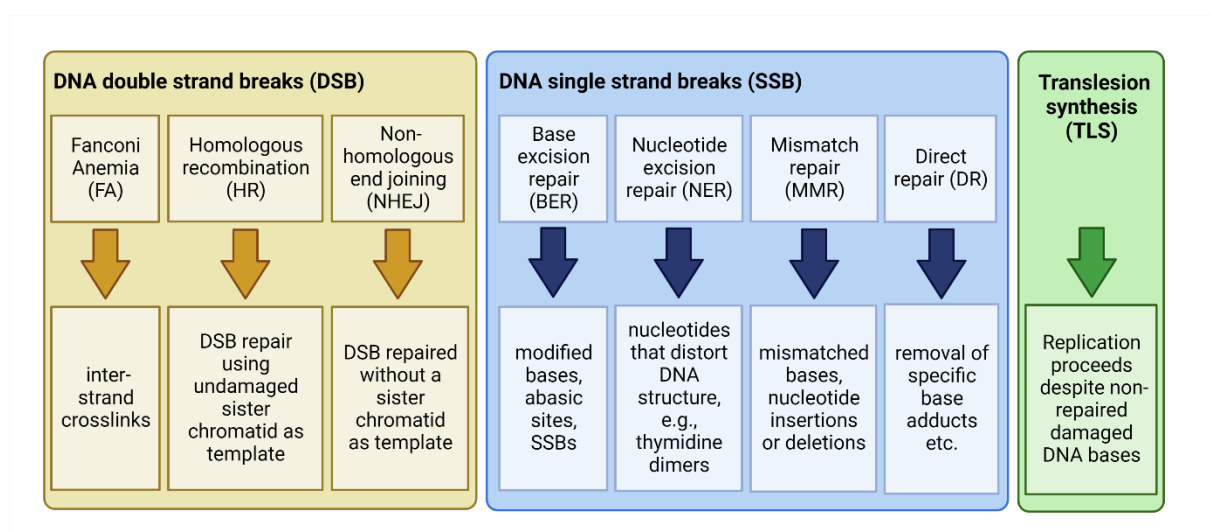
Figure 6: *DNA damage pathways divided by DNA double strand breaks (DSB) and single strand breaks (SSB). Created with BioRender.com*

In general, DDR is one of the main functions to ensure genomic stability. Moreover, in case the damage is too severe these pathways can also lead to cell death or senescence, a mechanism which prevents neoplasia. Their anti-cancer capabilities lie within their function to stop the cell-cycle and allow cells to repair any DNA damage [95].

Interestingly, targeting the DDR pathways is one central focus point in cancer therapy research. This is due to the fact that some key aspects of DDR are altered in cancer cells which render DDR proteins attractive drug targets for cancer therapy. Three main aspects for this include i) the loss of one or more DDR pathways leading to genomic instability, a hallmark of cancer [96], rendering the cells more dependent on the remaining pathways [97]; ii) an increased level of replication stress; and iii) an increased level of endogenous DNA damage due to the elevated proliferation rate in neoplasia [86, 96].

The idea of synthetic lethality, basically designing a therapy based on a dependency specific for tumor cells, e.g., acquired by mutation or gene silencing necessary for tumor development or propagation,

but well tolerable for healthy cells, has been discussed and studied for a long time [98]. In the DDR context this means that tumors which lost one or more DDR pathways can be pharmacologically targeted for a remaining DDR pathway [97]. The best known and studied example for this are poly(ADP-ribose) polymerase (PARP) inhibitors in BRCA1 or BRCA2 mutated cancers, e.g. ovarian cancers [99-101]. Olaparib, the most studied compound in this class, together with Rucaparib and Niraparib are approved in several therapeutic settings for ovarian cancer [102]. PARP inhibitors are in testing in several more cancer entities, many with a focus on BRCA1 or BRCA2 mutations [103]. Interestingly, non BRCA1 or BRCA2 mutated tumors have shown responses to PARP inhibitors as well [101]. Olaparib and Pamiparib, both shown to penetrate the BBB pre-clinically, are currently under clinical investigation in glioma [104, 105].

In glioma DDR also plays a very prominent role. Approximately 40% of GB patients have methylated MGMT promoters, a protein associated with DDR conferring resistance to alkylating chemotherapy [106]. Methylation inactivates MGMT and in turn sensitizes the tumors to Temozolomide (TMZ) treatment [21]. Furthermore, it has also been shown that progressive GB frequently show reduced expression for MMR pathway genes [107], e.g., MSH6, which in turn is associated with resistance to alkylating therapy in glioma cell lines [108]. One important mechanism described leading to radio resistance in progressive GB is the upregulation of the DNA damage checkpoint response [109]. Taken together, the DDR pathways seem to play an important role and might entail actionable novel targets for GB treatment. To elucidate novel treatment options in this context, treatment of the DDR targeting ataxia telangiectasia and Rad3 related (ATR) and the influence of the FA pathway on tumor onset, propagation and/or treatment efficacy will be analyzed in this thesis.

1.1.1.1 Ataxia telangiectasia and Rad3 related (ATR) DDR pathway

Very important sensors for DNA DSB, SSB and replicative stress are ataxia telangiectasia mutated (ATM) and ataxia telangiecatasia mutated and Rad3 related (ATR), respectively. Upon activation of either, several downstream targets involved in a variety of processes to maintain genomic integrity are activated (**Figure 7**).

Upon a DNA DSB induced by, e.g., ionizing radiation, ATM is recruited to the DSB by the MRE11/Rad50/NBS1 (MRN) complex. In turn, ATM then activates Chk2 and p53 which leads to cell-cycle arrest (**Figure 7**, left). As illustrated in **Figure 7**, ATM activation typically leads to G1 arrest. Some evidence suggests a role of ATM also in S-phase and G2-checkpoints [110].

ATR on the other hand, gets activated by single stranded DNA (ssDNA), sensed by replication protein A (RPA). ssDNA can occur in cells upon lesions in the DNA or nucleotide depletion leading to

dissociation of the DNA polymerase from the replication fork [111]. Subsequently, ATR signals through Chk1 again leading to cell-cycle arrest (**Figure 7**, right panel). ATR activation usually leads to intra S-arrest and plays a role in the G2-checkpoint [110].

In general, ATM and ATR are pro-survival pathways, giving the cells time to repair the DNA damage and subsequently proceed proliferation [95]. However, if the damage afflicted to the cells is too severe ATM and ATR signaling can also induce apoptosis [95, 112].
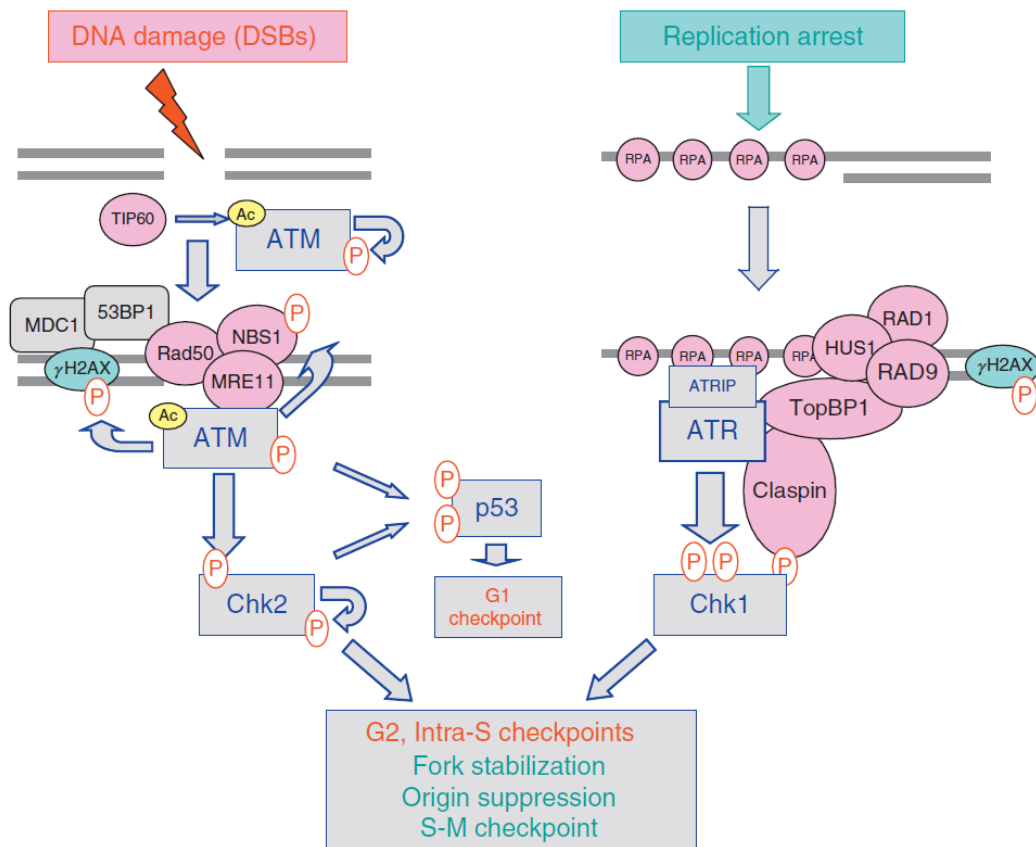
Figure 7: *Activation of ATM-Chk2 and ATR-Chk1 pathways upon DNA damage and downstream signaling. Adopted from Smith et al., 2010 [113]*

Due to their central regulatory function in sensing and reacting to DNA DSB and SSB, both, ATM and ATR, are targets for potential novel treatment options in cancers [102]. Furthermore, pre-clinical [114, 115] and clinical [116] data suggest that DDR inhibition does sensitize tumors to therapy. For ATM two inhibitors are in clinical testing. One is M3541 for which a clinical trial has been completed, but clinical development aborted due to absence of dose-response relationship and non-optimal pharmacokinetics profile [117]. The other ATM inhibitor, AZD0156, is currently undergoing a Phase I clinical trial (NCT02588105). Several ATR inhibitors are undergoing clinical trials as well, e.g., Berzosertib [118] and AZD6738 [119]. Interestingly, a previous preclinical study in the laboratory looking into the basic helix-loop-helix (bHLH) family which is frequently upregulated in glioma,

associated up-regulation of this network with ATR inhibitor sensitivity [120]. Based on this, here, ATR inhibition in different glioma models was evaluated and analyzed for functionally guided combination approaches.

1.1.1.2 The Fanconi Anemia pathway

The Fanconi Anemia (FA) pathway might be the least known pathway of all DDR pathways. The name is derived from the clinical manifestation of FA first described by Guido Fanconi 1927 [121]. FA is a rare disease presenting with panmyelopathy, early onset of aging, multiorgan congenital defects, bone marrow failure and a predisposition to malignancies [122, 123]. So far, there are 22 known members to this family, assigned based on biallelic germline mutations that cause the FA phenotype [123, 124]. Consequently, the FA family is a very diverse family made up of helicases, ligases, nucleases, polymerases etc. [123]. BRCA1 and BRCA2, both members of the FA family, are very well-known and play an important role in cancer onset of familial ovarian and breast cancer cases. Furthermore, BRCA1 (also known as Fanconi anemia complementation group S (FANCS)) and BRCA2 (also known as FANCD1) hold predictive value concerning treatment options using the synthetic lethality approach of PARP inhibitors in BRCA1/2 mutated cancers [100]. Defects in the FA protein family have also been associated with other cancers, e.g., the incidence of AML is 700 times higher in the FA deficient population [124].

The "canonical" FA pathway (**Figure 8**) starts with the recruitment of FANCM to stalled replication forks due to inter strand crosslinks [125]. Subsequently, the FA core complex is assembled which activates the FA core complex made up of FANCI and FANCD2, known as ID complex [126]. This FA ID complex will then activate the functional downstream units, among them BRCA1 and BRCA2, leading to DNA repair (**Figure 8**). Interestingly, further research has demonstrated additional functions of the FA pathway apart from DDR, like involvement in proliferation [127] and telomer regulation [128]. In the glioma context the FA pathway has not been studied in depth, nevertheless, Chen et al. [129] and Patil et al. [130] report an increased chemosensitivity of glioma cell lines upon FA inhibition. During data acquisition in the context of the MTB in Tübingen, an accumulation of FA mutations has been detected and will be further analyzed in this thesis.
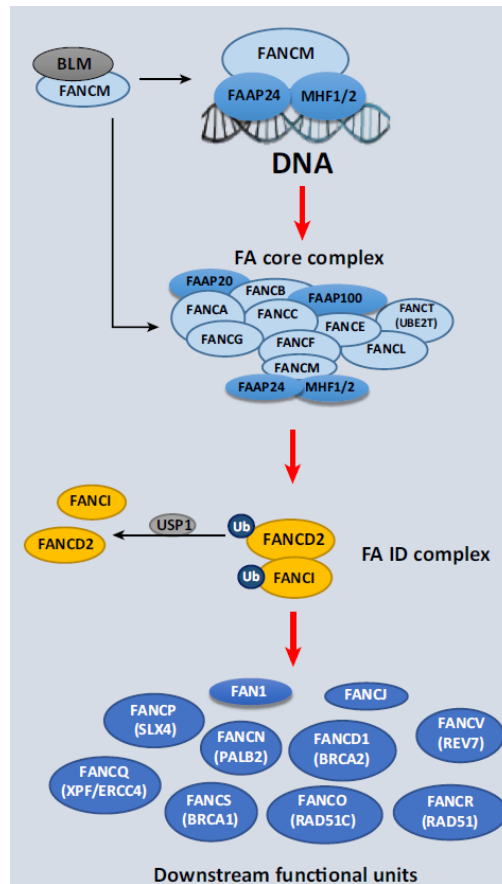
Figure 8*: Canonical Fanconi Anemia pathway.*

Adopted from Che et al., 2018 [123]

1.3 Animal models in glioma

To test novel treatment options and evaluate their clinical potential, it is of utmost importance to have good pre-clinical models. In cancer research, different *in vivo* models are used, each with specific advantages and disadvantages. In general, they can be divided in immunocompetent and non-immunocompetent. The latter provides the opportunity to use either patient derived explants (PDX) or human long-term cell lines, i.e., xenograft models, which are implanted orthotopically or into the flanks of mice [131]. Especially the PDX models are valued for the close representation of human tumors [132], however, the lack of immunocompetence also limits their usability for certain research questions.

Immunocompetent models can be syngeneic, derived from a tumor that occurred in a specific mouse strain either naturally, e.g., the glioma SMA560/VM/Dk model [133, 134], or was induced, e.g., the glioma GL261/C57/BL6 model [135]. Another option are models based on gene transfer, e.g., the RCAS/tv-a model [136, 137], which are also usually immunocompetent. With these models immunotherapies can be tested, however, they are not as closely related to human tumors as their

non-immunocompetent counterparts [131]. In this thesis, we used the SMA560/VM/Dk mouse model and the RCAS tv-a model.

SMA560/VM/Dk mouse model. This model is a syngeneic, immunocompetent mouse model. The SMA560 cell line is derived from a spontaneously occurring astrocytoma in the VM/Dk mouse line. This tumor was explanted by Serano et al. 1980 who then successfully established the SMA560 cell line [134]. The SMA560 cells can now be used for *in vitro* experiments, for example, testing novel treatment options. The same cells can then be re-implanted into VM/Dk mice and will grow up to form a tumor *in vivo* [134] which in turn can be treated with experimental novel treatment options [51, 138, 139]. The tumors mirror glioma phenotypically and morphologically regarding the ability to secrete immunosuppressive cytokines that are also secreted by human glioma. Transcriptomic analyses of SMA560 tumors grown in VM/Dk mice display upregulation of major histocompatibility complex (MHC) Class I and Class II [140]. Taken together, this model shows good representation of human glioma and allows to study immunotherapies [141].

RCAS tv-a model. This model is based on the replication-competent avian sarcoma-leukosis virus (RCAS) and its respective receptor tumor virus a (tv-a). The RCAS vector can be genetically engineered to carry inserts of up to 2.8 kilobases (kb), commonly used are oncogenes or shRNAs [142]. The RCAS vector is used to transfect DF-1 cells, which are used to produce the virus. The resulting virus is an avian virus that can only infect cells that express the tv-a receptor which mammalian cells usually do not (**Figure 9** A). Holland and Varmus established 1998 mouse lines carrying tv-a receptors under the control of glial fibrillary acidic protein (GFAP) promoter (Gtv-a) and nestin (Ntv-a) [136, 137]. The latter is a promoter that is mostly active in neuronal progenitor cells [143]. To incorporate the viral cDNA into the host genome, cell division of the target cells is required. Hence, infection rates are rapidly reduced after the neonatal stage [144]. Nevertheless, highly efficient tumor induction has been shown in p16/Ink4a (encoded by the Cdkn2a gene) deleted adult mice carrying the tv-a receptor controlled by the nestin promoter implanted with RCAS virus transferring platelet derived growth factor b (PDGFB) [145, 146]. Not only can tumors be induced in adult mice, the Cdkn2a deleted background is also highly relevant as 61% of human glioma also display CDKN2A/CDKN2B mutations (**Figure 2**) [25]. Both, the ability to insert a cDNA of choice and engineer mice that carry tv-a receptors controlled by lineage specific promoters make this model very versatile and attractive for the study of tumor biology [145] (**Figure 9** B).

In the laboratory this model was established using the 129S.Tg(NES-TVA)-Cdkn2a$^{-/-}$ mouse line which carries the tv-a receptor under the control of the nestin promoter [136, 145-148]. Due to the immunocompetence of the mice and the fact that genetic changes that lead to tumor development are induced in their own cells, this set-up very well mimics tumor onset in patients [149].
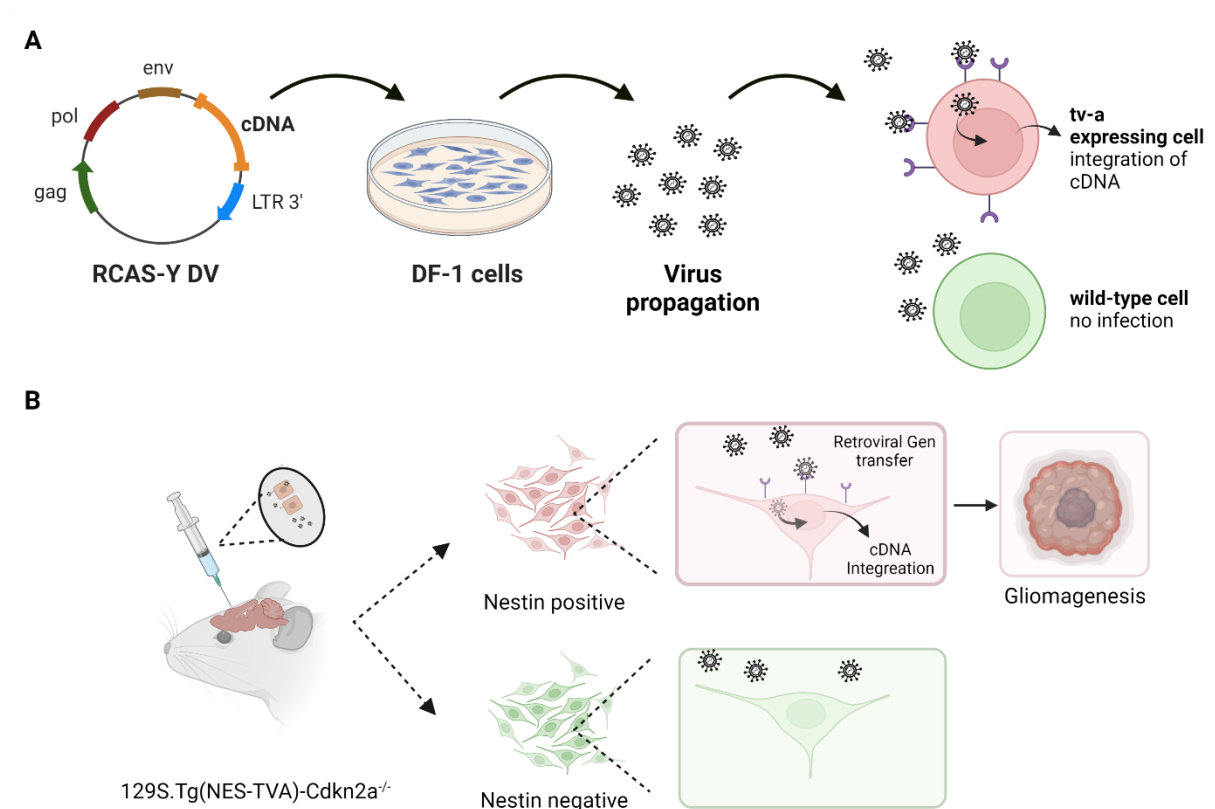
Figure 9*: RCAS/tv-a model principles adopted from Ahronian and Lewis, 2014 [142] and Becker et al., 2022 [148]*

A, *Graphical depiction of the RCAS vector that codes for the complete RCAS virus and can also carry a cDNA of choice to overexpress oncogenes or produce shRNAs to study knock-downs. Only cells that express the tv-a receptor will be infected (upper, red cell; no infection is possible in wild-type mammalian cells, lower, green cell) by the RCAS virus that in turn will integrate into the host genome.* ***B****, Schematic overview of an animal experiment using a nestin tv-a mouse line (129S.Tg(NES-TVA)-Cdkn2a$^{-/-}$) which is intracranially injected with DF-1 cells expressing RCAS virus carrying a cDNA of choice. The virus can only integrate into nestin positive cells (red, upper panel; nestin negative cells are not infected, green, lower-panel) in the mouse brain leading to cDNA expression exclusively in those which in turn can induce gliomagenesis.*

1.4 Scientific objectives

Despite multimodal treatment approaches, survival of GB patients remains in the range of 1.5 years [1, 2, 4]. Consequently, novel treatment options are pursued and urgently needed [150]. This thesis focuses on three distinct projects to improve the understanding of glioma biology and potential actionable vulnerabilities.

1. The 20S proteasome inhibitor Argyrin F was hypothesized to be a valuable novel treatment option in glioma due to its involvement in cell cycle control [5]. The scientific objectives were:

a. To analyze the molecular effects and anti-glioma efficacy of Argyrin F treatment in glioma long-term cell lines.

b. To evaluate Argyrin F treatment *ex vivo* using patient derived microtumors (PDMs).

c. To validate anti-glioma effects of Argyrin F *in vivo* using the SMA560/VM/Dk model.

d. To test potential novel combination therapies.

2. Based on the findings of Koch et al. [120] and the mounting evidence of a central role of the DDR in glioma [151], ATR inhibition (ATRi) was hypothesized to be a promising candidate for glioma treatment. The scientific objectives were:

a. To determine anti-glioma efficacy of ATRi using the SMA560/VM/Dk mouse model treated with AZD6738.

b. To analyze the anti-glioma efficacy of AZD6738 and Berzosertib in glioma long-term cell lines.

c. To evaluate transcriptomic and proteomic changes to glioma long-term cell lines by AZD6738 treatment in order to identify molecular mechanisms of ATRi.

d. To test evidence-based combination therapies and determine synergism signatures.

3. Upon detection of a substantial amount of germline mutations in the MTB neuro-oncology cohort Tübingen a functional impact of those mutations on GB development, propagation and/or treatment response was hypothesized. The scientific objectives were:

a. To characterize germline mutations of patients part of the MTB with a focus on GB patients.

b. To investigate the functional impact of gene silencing of selected FA pathway members in the RCAS tv-a model on tumor formation *in vivo*.

c. To assess the effect of gene silencing of FA genes on proliferation and treatment efficacy in glioma long-term cell lines *in vitro*.

Taken together, in this thesis, novel actionable tumor vulnerabilities are studied and characterized in depth. Additionally, potentially treatment relevant vulnerabilities are exploited.

Of note, parts of this thesis have already been published. The Argyrin F data was published in the Journal Advanced Therapeutics in June 2021 [51].

2. Material and Methods

2.1 Material

2.1.1 Consumables and instruments

Description	Manufacturer
Plastic ware	
0.2 mL skirted 96-well PCR plate	Thermo Fisher Scientific, Waltham, US
15 mL Falcons	Corning, Glendale, AZ, US
24 well culture plate	Greiner Bio-One GmbH, Kremsmünster, AUT
50 mL Falcons	Corning, Glendale, AZ, US
6-well culture plate	Greiner Bio-One GmbH, Kremsmünster, AUT
96-well culture plate	Sarstedt, Nürnbrecht, DE
96-well fast PCR plate white	Sarstedt, Nürnbrecht, DE
Bolt™ casettes	Thermo Fisher Scientific, Waltham, US
Cell culture flasks T25, T75, T175	Greiner Bio-One GmbH, Kremsmünster, AUT
CellSTACK® Culture Chamber 1 chamber/2 chamber	Corning, Glendale, AZ, US
Cryomolds	Sakura Finetek, Staufen im Breisgau, DE
Cryos.s™	Greiner Bio-One GmbH, Kremsmünster, AUT
Dual-chamber cell counting slides	Bio-Rad Laboratories GmbH, Munich, DE
Falcon® 5mL, 10 mL, 25 mL, 50 mL serological pipet	Corning, Glendale, AZ, US
Filter tips, 2.5 µL, 10 µL, 100 µL, 200 µL, 1 000 µL	JoJo life science, Giengen, DE
Millex®-HV PVDF 0.45µm filter unit	Sigma, Merck KGaA, Darmstadt, DE
Nitrile gloves, powder free	Abena, Zörbig, DE
Non-filter tips, 2.5 µL, 10 µL, 100 µL, 200 µL, 1 000 µL	Nerbe plus, Winsen/Luhe, DE
Parafilm PM996	Cole-Parmer, Wertheim, DE
Petri dishes	Corning, Glendale, AZ, US
Reagent reservoirs	vwr™, Radnor, PA, US
Tissue culture plate 6-wells	TPP®, Trasadingen, CH
Tubes 0.5 mL, 1 mL, 2 mL, 5 mL	Sarstedt, Nürnbrecht, DE

Glass ware

Beaker	Schott AG, Mainz, DE
Bottles 100-600 mL	Schott AG, Mainz, DE
Cover slips	R. Langenbrinck, Emmendingen, DE
Erlenmeyer flasks	Schott AG, Mainz, DE
Glass vials for drug storage	Fisher Scientific, Hampton, NH, US
Neubaur improved chamber for cell counting	Hecht-Assistant, Sondheim v.d. Rhön, DE
Pasteur capillary pipettes	WU, Mainz, DE
SuperFrost® Plus Slide, matt, edge white	R. Langenbrinck, Emmendingen, DE
ToPAS TopFrost extra white adhesive slides	Laboron, Hofheim, DE

Other consumables

0.05% Trypsin-EDTA	Gibco, Thermo Fisher Scientific, Waltham, US
Accutase	Sigma-Aldrich, Munich, DE
Ammonium persulfate (APS)	Sigma-Aldrich, Munich, DE
BLOXALL® Endogenous Blocking Solution, Peroxidase and Alkalin Phosphatase	Vector Laboratories, Burlingame, CA, US
Bovine serum albumin	Sigma-Aldrich, Munich, DE
Color-coded beads	Luminex, Austin, TX, US
Crystal Violet	Carl Roth, Karlsruhe, DE
Descosept	Dr. Schumacher GmbH, Malsfeld, DE
Difco™ Skim milk powder	BD Biosciences, Franklin Lakes, US
Dulbecco's Phosphate Buffered Saline	Gibco, Thermo Fisher Scientific, Waltham, US
Dynabeads Human T-Activator CD3/CD28	Thermo Fisher Scientific, Waltham, MA, US
Eosin G solution 0.5% aqueous	Carl Roth, Karlsruhe, DE
Ethanol absolute	AppliChem GmbH, Darmstadt, DE
Formaldehyde solution 4%	Sigma-Aldrich, Munich, DE
Incuwater-Clean™	AppliChem GmbH, Darmstadt, DE
LB Agar, Vegitone	Sigma-Aldrich, Munich, DE
LB Broth, Vegitone	Sigma-Aldrich, Munich, DE
LDS Lysis Buffer	Life Technologies, Carlsbad, CA, US
LE Agarose	Biozym Scientific, Hessisch Oldendorf, DE
Mayer's Haematoxylin Solution	Sigma-Aldrich, Munich, DE
Methanol	AppliChem GmbH, Darmstadt, DE
Nuclease-free water	Thermo Fisher Scientific, Waltham, US

NuPAGE 10% Bis-Tris precast gel	Thermo Fisher Scientific, Waltham, MA, US
NuPAGE 4-12% Bis-Tris precast gel	Thermo Fisher Scientific, Waltham, MA, US
Phycoerythrin (PE) labelled secondary antibodies	Dianova, Hamburg, DE
Propidium Iodide	Thermo Fisher Scientific, Waltham, US
Protease- and Phosphatase inhibitors	Roche Diagnostics GmbH, Mannheim, DE
QiaShredder Eppendorf tubes	Eppendorf, Hamburg, DE
Reducing agent	Thermo Fisher Scientific, Waltham, MA, US
Richard-Allan Scientific HistoGel	Thermo Fisher Scientific, Waltham, US
Roti Histo Kit Mounting Medium	Carl Roth, Karlsruhe, DE
S.O.C. medium	Invitrogen, Thermo Fisher Scientific, Waltham, US
Sample Buffer Laemmli 2x concentrat	Sigma-Aldrich, Munich, DE
SDS for molecular biology	AppliChem GmbH, Damrstadt, DE
Standard Earloop Face Mask	3M Germany, Neuss, DE
Tinfoil	Carl Roth, Karlsruhe, DE
Tissue-Tek® O.C.T™ Compount	Sakura Finetek Germany GmbH, Umkirch, DE
Triton X-100	Carl Roth, Karlsruhe, DE
Trypan Blue Stain (0.4%)	Gibco, Thermo Fisher Scientific, Waltham, US
Tween® 20	Merck, Milipore, Burlington, US
UltraCompeBeads	Thermo Fisher Scientific, Waltham, US
Xylene	AppliChem GmbH, Darmstadt, DE

Instruments

Autoclave DX-65	Systec GmbH, Linden, DE
Autoclave V-150	Systec GmbH, Linden, DE
Automated cutting plotter	Silhouette America, West Orem, UT, US
Axio Scan. Z1 Slide Scanner	Carl Zeiss, Oberkochen, DE
Axiofluor Zeiss microscope	Carl Zeiss Microscopy, Oberkochen, DE
Axiovert 200M	Carl Zeiss Microscopy, Oberkochen, DE
Bacterial incubator INFORS HT	INFORS HT, Bottmingen/Basel, CH
Bio-Rad ChemiDoc MP Imaging system	Bio-Rad Laboratories GmbH, Munich, DE
Centrifuge 5417R	Eppendorf, Mississauga, US
Centrifuge 5920R	Eppendorf, Mississauga, US
eCount™ Colony Counter, EA	Heathrow Scientific, Vernon Hills, IL, US

Epson Perfection V8000 Photo	Epson, Nagano, JPN
Gammacell® 40 Exactor	MDS Nordion, Ottawa, CA
GloMax Explorer	Promega, Madison, US
Hand piece counter "H 20"	Esska GmbH, Hamburg, DE
Heraeus HeraSafe clean bench	Thermo Fisher Scientific, Waltham, US
Kern ABJ	Sartorius, Göttingen, DE
LI-COR	LI-COR, Bad Homburg, DE
LSR Fortessa cytometer	Beckton, Dickinson & Company, Franklin Lakes, NJ, US
Luminex FlexMAP 3D	Luminex Corporation, DiaSorin, Saluggia, IT
MACSQuant flow cytometer	Miltenyi Biotech GmbH, Bergisch Gladbach
Magnetic mixer IKA® RH basic 2	IKA, Staufen im Breisgau, DE
Magnetic stir bar standard set	Neolab, Heidelberg, DE
Multifuge 1 S-R	Heraeus, Hanau, DE
Nanodrop-2000 Spectrophotometer	Thermo Fisher Scientific, Waltham, US
OK. ® Microwave	Imtron GmbH, Ingolstadt, DE
Olympus BXC1	Olympus, Tokyo, JPN
Pipetboy acu 2	INTEGRA Biosciences GmbH, Biebertal, DE
Pipette Eppendorf research 0.1-2.5μl,0.5-10μl, 10-100μl, 20-200μl, 100-1000μl, 1-5ml	Eppendorf, Mississauga, US
PowerEase 300W	Life technologies, Thermo Fisher Scientific, Waltham, US
PowerEase 500	Life technologies, Thermo Fisher Scientific, Waltham, US
Roche LightCycler 96	Roche Diagnostics International GmbH, Rotkreuz, CH
Sanyo MCO-18AIC(UV) CO2 Incubator	Marshall Scientific, Hampton, NH, US
TC20™ automated cell counter	Bio-Rad Laboratories GmbH, Munich, DE
Tecan 96-well plate reader	Tecan, Männedorf, CH
Thermomixer comfort heating block	Eppendorf, Mississauga, US
Transferpette S-8	Brand GmbH & Co. KG, Wertheim, DE
Vacuum pump VacuSafe	INTEGRA Biosciences GmbH, Biebertal, DE
Vortexer	Phoenix instrument, Garbsen, DE
Water bath 1083	GFL, Burgwedel, DE

2.1.2 Cell lines used in this thesis

Description	Characteristics	Source
Human		
LN229 [152]	Glioma long-term cell line, adherent, p53mut, PTENwt	ATCC, Wesel, DE
LNZ308 [152, 153]	Glioma long-term cell line, adherent, p53null, PTENmut	Kindly provided by Prof. Dr. Hegi, Centre Hospitalier Universitaire Vaudois, Lausanne, CH
HEK-293FT	Human embryonic kidney cells, adherent	Thermo Fisher Scientific, #R70007
Murine		
SMA560 [134]	Spontaneous murine mouse astrocytoma cell line, adherent	Kindly provided by Prof. Dr. Wick, Universitätsklinikum, Heidelberg, DE
GL-261 [135]	Chemically induced, mouse-derived glioma cell line, adherent	DSMZ, Wesel, DE
NIH3T3 t-va	Adherent cells, immortalized mouse fibroblasts	Kindly provided by Eric C. Holland, Fred Hutch, Seattle, US
Avian		
DF-1 [154]	Support avian retrovirus replication, adherent cells, cultured at 39°C	ATCC, Manassas, VA, US

2.1.3 Cell culture media and supplements

Description	Manufacturer
Media	
Advanced RPMI	Sigma Aldrich, St. Louis, MO, US

Dulbecco's Modified Eagle Medium (DMEM) 1X	Gibco, Thermo Fisher Scientific, Waltham, US
Opti-MEM, reduced serum media	Gibco, Thermo Fisher Scientific, Waltham, US
StemPro hESC SFM medium	Thermo Fisher, Waltham, US

Supplements

1xMEM Vitamins	Thermo Fisher Scientific, Waltham, US
B-27® Supplement (50x)	Gibco, Thermo Fisher Scientific, Waltham, US
bFGF (10 µg/mL)	Peprotech, Rocky Hill, NJ, US
Gentamycin 50 mg/mL	Gibco, Thermo Fisher Scientific, Waltham, US
Glutamine (200 mM)	Thermo Fisher Scientific, Waltham, US
Heat inactivated calf serum (CS)	Sigma, Merck KGaA, Darmstadt, DE
Heat inactivated fetal calf serum (FCS)	Gibco, Thermo Fisher Scientific, Waltham, US
Human AB serum 5%	Sigma Aldrich, St. Louis, MO, US
IL-15 (23.8 U/mL)	Peprotech, Rocky Hill, NJ, US
IL-2 (100 U/mL)	Peprotech, Rocky Hill, NJ, US
IL-7 (10 U/mL)	Peprotech, Rocky Hill, NJ, US
Primocin®	Invivogen, San Diego, CA, US

2.1.4 Treatment compounds *in vitro*

Compound	Diluent	Stock concentration	Manufacturer
Argyrin F	DMSO	5 mg/mL	Prof. M. Kalesse, Leibniz University Hannover, Prof. N. Malek University Hospital Tübingen [5]
AZD6738	DMSO	50 mM	Selleck Chemicals, Houston, TX, US
Berzosertib	DMSO	50 mM	Selleck Chemicals, Houston, TX, US
Everolimus	DMSO	10 mM	Selleck Chemicals, Houston, TX, US
Lomustine	DMSO/Ethanol	100 mM	Haupt Pharma Amareg, Regensburg, DE

Olaparib	DMSO	10 mM	Selleck Chemicals, Houston, TX, US
Paxalisib	DMSO	10 mM	Selleck Chemicals, Houston, TX, US
Temozolomid	DMSO	100 mM	Excella Pharmasource, Feucht, DE

2.1.5 Antibiotics

Description	Manufacturer
Ampicillin 100 mg/mL	AppliChem GmbH, Darmstadt, DE
Blasticidin 10 µg/µL	Gibco, Thermo Fisher Scientific, Waltham, US
Kanamycin 25 mg/mL	Thermo Fisher Scientific, Waltham, US
Puromycin 1 µg/µL	Sigma-Aldrich, Munich, DE

2.1.6 Antibodies

Description	Number	Dilution	Manufacturer
Primary antibodies			
Western Immunoblot			
GAPDH	2118	1:1000	Cell Signaling Technology, Danvers, MA, US
p21 [EPR3993]	Ab109199	1:1000	Abcam, Cambridge, UK
p27^{Kip1} (SX53G8.5)	3698	1:1000	Cell Signaling Technology, Danvers, MA, US
p53	Sc-263	1:1000	Santa Cruz, Dallas, TX, US
pRb1	8516	1:1000	Cell Signaling Technology, Danvers, MA, US
Rb1	9309	1:2000	Cell Signaling Technology, Danvers, MA, US

Immunohistochemistry

Anti-CD3-FITC		1:20	BioLegend, San Diego, CA, US
Anti-CD4-BV510		1:20	BioLegend, San Diego, CA, US
Anti-CD8-PerCP/Cy5.5		1:20	BioLegend, San Diego, CA, US
Anti-TNFa-BV711		1:20	BioLegend, San Diego, CA, US
CD11b	Ab133357	1:4000	Abcam, Cambridge, UK
CD3	Ab16669	1:100	Abcam, Cambridge, UK
CD31	553370	1:50	BD Biosciences
CD4	Ab183658	1:200	Abcam Abcam, Cambridge, UK
CD8	Ab22378	1:80	Abcam, Cambridge, UK

Flow cytometry

GFAP-GA5-L-U		1:400	Leica Biosystems
Ki67	Ab16667	1:100	Abcam, Cambridge, UK
p27	Ab137736	1:300	Abcam, Cambridge, UK
RFP	Ab62341	1:300	Abcam, Cambridge, UK

Secondary antibodies

Goat anti-rat IgG Antibody, mouse adsorbed (H*L), biotinylated	BA-9401	IHC 1:400	Vector Laboratories, Burlingame, CA, US
Goat pAb to mouse IgG (HRP)	Ab97023	WB 1:5000	Abcam, Cambridge, UK
Gota pAb to rabbit IgG (HRP)	Ab97051	WB 1:5000	Abcam, Cambridge, UK
Horse anti-rabbit IgG Antibody (H+L) biotinylated	BA-1100	IHC 1:400	Vector Laboratories, Burlingame, CA, US

The full antibody list for DigiWest protein profiling can be found in the Appendix in **Appendix Table 5**.

Plasmid		Supplier
Lenti dCas9-VP64_Blast	Addgene plasmid #61425	Generous gift from Feng Zhang (Addgene plasmid # 61425 ; http://n2t.net/addgene:61425 ; RRID:Addgene_61425) [155]
lentiCas9-Blast	Addgene plasmid #52962	Generous gift from Feng Zhang (Addgene plasmid # 52962; http://n2t.net/addgene:52962 ; RRID:Addgene_52962) [156]
pENTR-mRFP-H1		Generous gift by Eric C. Holland, Fred Hutch, Seattle, US
pLKO.1 puro	Addgene plasmid #8453	pLKO.1 puro was a gift from Bob Weinberg (Addgene plasmid # 8453 ; http://n2t.net/addgene:8453 ; RRID:Addgene_8453) [157]
pMD2.G	Addgene plasmid #12259	pMD2.G was a gift from Didier Trono (Addgene plasmid # 12259 ; http://n2t.net/addgene:12259 ; RRID:Addgene_12259)
psPAX2	Addgene plasmid #12260	psPAX2 was a gift from Didier Trono (Addgene plasmid # 12260 ; http://n2t.net/addgene:12260 ; RRID:Addgene_12260)
RCAS-Y DV		Generous gift by Eric C. Holland, Fred Hutch, Seattle, US

2.1.8 Competent E. coli

Description	Manufacturer
DH5α	Invitrogen, Thermo Fisher Scientific, Waltham, US
One Shot™ Stbl3™ chemically competent E. coli	Thermo Fisher Scientific, Waltham, US
Stellar™ Competent Cells	Takara Bio, Kusatsu, Shiga, JP

2.1.9 Restriction enzymes

Description	Manufacturer
Age1	NEB, Ipswich, US
Bgl2	NEB, Ipswich, US
EcoR1	NEB, Ipswich, US
XhO1	NEB, Ipswich, US
CutSmart Buffer	NEB, Ipswich, US

2.1.10 Commercially available Kits

Description	Manufacturer
Blocking Reagent for ELISA	Roche, Basel, CH
BlueBandit™	VWR, Darmstadt, DE
Calcein-AM	Thermo Fisher Scientific, Waltham, US
CellTiterBlue	Promega, Madison, WI, US
CellTiterGlo 3D	Promega, Madison, WI, US
CellTox Green Dye reagent	Promega, Madison, WI, US
FITC Annexin V Apoptosis Detection Kit I	BD Biosciences, Franklin Lakes, US
FIX&PERM Cell permeabilization kit	Thermo Fisher Scientific, Waltham, US
Gateway™ LR Clonase™ II Enzyme Mix	Invitrogen, Thermo Fisher Scientific, Waltham, US
High Capacity RNA-to-cDNA Kit	Thermo Fisher Scientific, Waltham, US
Liberase DH	Sigma Aldrich, St. Louis, MO, US

Lipofectamine 3000™	Invitrogen, Waltham, US
Pierce BCA Protein Assay Kit	Thermo Fisher Scientific, Waltham, US
Pierce ECL Western Blotting Substrate	Thermo Fisher Scientific, Waltham, US
PureYield™ Plasmid Maxiprep System	Promega, Madison, US
QIAamp DNA Blood Maxi Kit	Qiagen, Venlo, NL
QIAamp DNA Blood Midi Kit	Qiagen, Venlo, NL
QIAprep Spin Miniprep Kit	Qiagen, Venlo, NL
QIAquick® Gel Extraction Kit	Qiagen, Venlo, NL
qPCR Mastermix Plus for SYBR Green I	Roche Diagnostics International GmbH, Rotkreuz, CH
RNase-Free DNase Kit	Qiagen, Venlo, NL
RNeasy Mini Kit	Qiagen, Venlo, NL
SuperFect® Transfection Reagent	Qiagen, Venlo, NL
SyTox-Orange	Thermo Fisher Scientific, Waltham, US
T4 DNA Ligase	NEB, Ipswich, US
VECTASTAIN® Elite ABC-HRP Kit, Peroxidase (Standard)	Vector Laboratories, Burlingame, CA, US
Vector® NovaRED® Substrate Kit, Peroxidase (HRP)	Vector Laboratories, Burlingame, CA, US

2.1.11 Animal work

Description		Source
Mouse strains		
VM/Dk	Serano, Pegram, and Bigner 1980	Originally bought by Prof. Dr. Naumann, Hertie-Institute for clinical brain research, Tübingen, DE
129S.Tg(NES-TVA)-Cdkn2a$^{-/-}$	Serrano et al. 1996; Holland et al. 1998; Dai et al. 2001; Hambardzumyan et al. 2009	kindly provided by Prof. Gronych, DKFZ Heidelberg, DE

Instruments

Coldlight source KL 1500 LD	Leica Biosystems, Nussloch, DE
Cordless Micro drill, 220V	Stoelting, Wood Dale, US
Forceps	Fine Science Tools, Heidelberg, DE
Hamilton syringe	Hamilton Bonaduz AG, Bonaduz, CH
Hamilton syringe needles	Hamilton Bonaduz AG, Bonaduz, CH
Hippocampel Spatula Tool	Fine Science Tools, Heidelberg, DE
Hot bead sterilizer	Fine Science Tools, Heidelberg, DE
Ismatec perfusion pump	Cole-Parmer, Wertheim, DE
Malleus Bone Nippers	Fine Science Tools, Heidelberg, DE
Narrow Pattern Forceps	Fine Science Tools, Heidelberg, DE
Quintessential stereotactic injector	Stoelting, Wood Dale, US
Scissors	Fine Science Tools, Heidelberg, DE
Shaver Exacta	Aesculap Schermaschinen, Buchbach, DE
Side-ankled scissors	Fine Science Tools, Heidelberg, DE
Stereotactic Apparatus	Stoelting, Wood Dale, US
Warming mat	Eickenmeyer, Tuttlingen, DE

Consumables

BD Micro-Fine+ 30G	BD Biosciences, Franklin Lakes, US
Bepanthen®	Bayer Vital, Leverkusen, DE
Bone vax	Ethicon Inc., Raritan, NJ, US
Cotton swaps	Boettger, Bodenmais, DE
Disposable scalpel No. 11	FEATHER Safety Razor Co. , Osaka, JPN
Ethilon™	Ethicon Inc., Raritan, NJ, US
Hand warmers	Thermopad, Freudenstadt, DE
MoliNea®plus, Underpads	Hartmann, Heidenheim an der Brenz, DE
Safety-Multifly ®-Needle	Sarstedt, Nürnbrecht, DE
Secureline™ bone marker	Aspen surgical, Caledonia, MI, US

Narcotics, antidote, pain killer

Compound	Treatment concentration	Supplier
Atipamezole Nosedorm® 5 mg/mL	2.5 mg/kg	Alfavet, Neumünster, DE

Compound	Concentration	Supplier
Fentandon® 50 µg/mL for animal use	0.05 mg/kg	WDT, Garbsen, DE
Flumazenil Kabi 0.1 mg/mL	0.5 mg/kg	Fresenius Kabi AG, Bad Homburg, DE
Ketamin 100 mg/mL for animal use	120 mg/kg	WDT, Garbsen, DE
Medetomidin Dormilan 1 mg/mL	0.5 mg/kg	Alfavet, Neumünster, DE
Midazolam-hameln 5 mg/mL	5 mg/kg	Hameln, Hamelin, DE
Naloxon-hameln 0.4 mg/mL	1.2 mg/kg	Hameln, Hamelin, DE
Rimadyl® Carprofen 50 mg/mL injection solution for cattle	5 mg/kg	CP Pharma, Burgdorf, DE
Sedaxylan® 20 mg/mL for animal use	10 mg/kg	WDT, Garbsen, DE

Treatment compounds

Compound	*Concentration*	*Supplier*
Argyrin F	1 mg/kg	Prof. M. Kalesse, Leibniz University Hannover, Prof. N. Malek University Hospital Tübingen [5]
AZD6738	50 mg/kg	Selleck Chemicals, Houston, TX, US
IgG2a isotype control (C1.18.4)	10 mg/kg	In vivo Plus+ BXCell Lebanon, NH, US
Anti PD-1 (RPM1.14)	10 mg/kg	kindly provided by Roche Diagnostics, Penzberg, CH

2.1.12 PCR Primers

Target	**Sequence (5'-3')**	**Manufacturer**
Human		
HPRT_forward (f)	TGACACTGGCAAAACAATGCA	Sigma-Aldrich, Munich, DE

	Aithal, Rajeswari [158]	
HPRT_reverse (r)	GGTCCTTTTCACCAGCAAGCT	Sigma-Aldrich, Munich, DE
	Aithal, Rajeswari [158]	
FA-GENE1_f1	AGTCCAGTCTACCACACCAC	Sigma-Aldrich, Munich, DE
FA-GENE1_rev1	GAATCCTCCAAAGCACTACCATC	Sigma-Aldrich, Munich, DE
FA-GENE4_f1	GACTCTGCCGCTGTACCAAT	Sigma-Aldrich, Munich, DE
FA-GENE4_rev1	GGACAGGAAACATCATCTGCTTG	Sigma-Aldrich, Munich, DE

Murine

Hprt_f	TTGCTGACCTGCTGGATTACA	Sigma-Aldrich, Munich, DE
	Silginer et al. [159]	
Hprt_r	TTTATGTCCCCCGTTGACTG	Sigma-Aldrich, Munich, DE
	Silginer et al. [159]	
FA-Gene1_f3	CGTAAAGTGTCTTGTGGTGGATG	Sigma-Aldrich, Munich, DE
FA-Gene1_rev3	ACGAAAGTGAGTGGTGTATTTGAC	Sigma-Aldrich, Munich, DE
FA-Gene2_f4	GCTGCTCTTCAGGTTTTCACATC	Sigma-Aldrich, Munich, DE
FA-Gene2_rev4	GGATTGCTTCAGGGTGCTGG	Sigma-Aldrich, Munich, DE
FA-Gene3_f3	CAGAACAGAGGCGTGGTTATTC	Sigma-Aldrich, Munich, DE
FA-Gene3_rev3	AGTTTTTCCGAGCAGGACTTCA	Sigma-Aldrich, Munich, DE
FA-Gene4_f4	TACAGACACACAGACAGTTAGAGC	Sigma-Aldrich, Munich, DE
FA-Gene4_rev4	CAGGATCATTCGGTAAACAGCG	Sigma-Aldrich, Munich, DE
FA-Gene5_f3	TTACAGACCGCCCCTCAAGAA	Sigma-Aldrich, Munich, DE
FA-Gene5_rev3	GCCCTCAGAAAACTCACAAGCA	Sigma-Aldrich, Munich, DE

Sequencing Primers

pENTR	GTAACATCAGAGATTTTGAGACAC	Sigma-Aldrich, Munich, DE
pLKO1	GACTATCATATGCTTACCGT	Eurofins Scientific, Luxembourg
RCAS	CCCGTACATCGCATCGAT	Sigma-Aldrich, Munich, DE

2.1.13 shRNA Sequences

Name	Sequence (5'-3')	Source	Manufacturer

human

shLuciferase	CGTGATCTTCACCGACAAGAT	Generously provided by Daniel Merk, Tübingen, DE	Sigma-Aldrich, Munich, DE
shFA-GENE1_1	AGGACGAGAGGAACGTATTTA	MISSION® shRNA library by Sigma-Aldrich/Broad Institute	Sigma-Aldrich, Munich, DE
shFA-GENE1_2	GACTTCATGAAACTCTATAAT	MISSION® shRNA library by Sigma-Aldrich/Broad Institute	Sigma-Aldrich, Munich, DE
shFA-GENE4_1	GAAGAATGCAGGTTTAATA	Han et al. [160]	Sigma-Aldrich, Munich, DE
shFA-GENE4_2	GGGAAACACTCAGATTAAA	Han et al. [160]	Sigma-Aldrich, Munich, DE
Mouse			
shscramble	GCTCTACAACCGCTCATCATA	Generously provided by Frank Szulzewsky, Seattle, US	Sigma-Aldrich, Munich, DE
shFA-Gene1_1	GCTTACTGCCAGGTGGTAAGA	MISSION® shRNA library by Sigma-Aldrich/Broad Institute	Sigma-Aldrich, Munich, DE
shFA-Gene1_2	GTGATCACTAACCTACTAATT	MISSION® shRNA library by Sigma-Aldrich/Broad Institute	Sigma-Aldrich, Munich, DE
shFA-Gene2_1	AGTCTTGGATATGAGTCTATTC	BLOCK-iT™ RNAi Designer	Sigma-Aldrich, Munich, DE
shFA-Gene2_2	GGTGGAGCTGAAGGTATTAATC	MISSION® shRNA library by Sigma-	Sigma-Aldrich, Munich, DE

		Aldrich/Broad Institute	
shFA-Gene3_1	CAGTAAACTCAGTAGTATATAC	MISSION® shRNA library by Sigma-Aldrich/Broad Institute	Sigma-Aldrich, Munich, DE
shFA-Gene3_2	GTGATTACTTGAATGTATTTCC	MISSION® shRNA library by Sigma-Aldrich/Broad Institute	Sigma-Aldrich, Munich, DE
shFA-Gene4_1	GGACCAGACATTCAGGCAAAT	BLOCK-iT™ RNAi Designer	Sigma-Aldrich, Munich, DE
shFA-Gene4_2	GAGTATCAGGAAGTCTATATT	MISSION® shRNA library by Sigma-Aldrich/Broad Institute	Sigma-Aldrich, Munich, DE
shFA-Gene5_1	GCAGATGGGCTGCAAGTAAAG	BLOCK-iT™ RNAi Designer	Sigma-Aldrich, Munich, DE
shFA-Gene5_2	GCGGGCGACCATGAAGTATAA	BLOCK-iT™ RNAi Designer	Sigma-Aldrich, Munich, DE

Of note, the shRNA sequences were all used to produce a corresponding virus in the pLKO1 or RCAS-Y DV backbone, but these plasmids are not separately listed.

2.1.14 Software

Description	Manufacturer
ImageJ 1.53k	Wayne Rasband, National Institute of Health, Bethesda, US
GraphPad Prism 9	GraphPad, La Jolla, US
R/R Studio	
Zeiss Zen lite	Carl Zeiss Microscopy, Oberkochen, DE
AxioFluor 4.9.1.0	Carl Zeiss Microscopy, Oberkochen, DE

FloJo® v10.0.7	FloJo LLC, Ashland, US
LightCycler® 96 SW 1.1	Roche Diagnostics International AG, Rotkreuz, CH
Image Lab	Bio-Rad Laboratories GmbH, Munich, DE
BioRender	BioRender, Toronto, Ontario, CA
gProfiler web server	Raudvere et al. [161]
Image Studio	LI-COR, Bad Homburg, DE

2.2 Methods

2.2.1 In vitro methods

2.2.1.1 Cell culture

Culture conditions. Human and mouse cell lines were cultured at 37°C and 5% CO_2 atmosphere, the avian DF-1 cell line needed 39°C to grow. Standard culture medium for adherent cells is Dulbecco's modified eagle's medium (DMEM) supplemented with 10% fetal calf serum (FCS) and 0.1% Gentamycin (DMEM complete). NIH3T3 t-va cells needed calf serum (CS) instead of FCS (NIH3T3 medium). In serum-free treatment conditions media without FCS but including Gentamycin, was used.

Cell passaging. Cells were split at 70-90% confluence. Adherent cells were washed once with phosphate buffered saline (PBS), treated with Accutase or Trypsin and incubated for 3-5 min in the incubator. The cell suspension was topped up with DMEM complete, transferred to a centrifugation tube and centrifuged for 5 min at 1200 revolutions per minute (rpm). The resulting cell pellet was resuspended in DMEM complete, an aliquot was put back into the flask (1:2 - 1:20).

Cell freezing. For freezing cells, the cell pellet was resuspended in DMEM supplemented with 20% FCS, 0.1% Gentamycin and 10% dimethyl sulfoxide (DMSO). This was then distributed into cryogenic vials (1mL/aliquot), placed in a cryofreezing container filled with isopropanol and placed at -80°C. For long-term storage those cryogenic vials were transferred to a -150°C freezer.

Cell thawing. To thaw cells, vials were taken out of the storage freezer and put at 37°C in the water bath. Once vials were completely liquefied, the complete aliquot was then transferred to 10 mL of DMEM complete in a centrifugation tube. Cells were centrifuged for 5 min at 1200 rpm. Then, cells were resuspended in DMEM complete and seeded in an appropriate cell culture flask. The next day, medium was changed to remove cell debris from the culture.

2.2.1.2 Acute cytotoxicity

To determine acute cytotoxic activity of compounds used in this thesis, cells were seeded at 5 000 cells per well in 100 μL in a 96-well plate in DMEM complete. The next day, the medium was taken off and 100 μL of serum-free medium containing no treatment, vehicle or compound was added to the cells. For synergy analyses, mixtures of two compounds in a 4 by 4 matrix were generated based on IC_{25}- and IC_{50}-concentrations and evaluated for their efficacy compared to monotherapy treatment. The treatment was allowed to stay on the cells for up to 72 h.

After the treatment incubation time, 20 μL of CellTiterBlue reagent was added to each well and incubated for 3-4 h. Measurement was done using the pre-programmed "CellTiterBlue" program on a GloMax® instrument. The resulting values are first subtracted by the blank condition and second normalized to untreated cells. Statistical significance was determined using multiple T tests with the GraphPad 9 software, p-values<0.05 were considered significant.

2.2.1.3 Clonogenic survival assays

To evaluate clonogenic survival after different treatment conditions, cells were seeded at 250 - 1000 cells per well in a 6-well plate. The day after, cells were treated in serum free medium for 24 h either in monotherapy or combination therapy settings. On the third day, the medium was changed back to DMEM complete. Cells were allowed to grow up and form colonies for 7 days (SMA560), 10 days (GL261), 14 days (LN229) and 21 days (LNZ308). Afterwards, the medium was taken off and formed colonies were fixed and stained with Crystal Violet solution (0.5% w/v) containing 1% formaldehyde and 10% methanol for 5 min at room temperature. Then, the plates were rinsed with demineralized water and afterwards air dried.

Combination treatments using clonogenic survival assays were done referring to IC_{25}- and IC_{50}-concentrations of each compound, measuring area coverage after monotherapy or combination.

For evaluation of area coverage, plates were scanned using an Epson Scanner and evaluated by the ImageJ PlugIn ColonyArea as described in the publication by Guzman et al. [162]. Values were normalized to vehicle treated wells.

To calculate plating efficiencies and surviving fractions [163], a ColonyCounter Pen was used and total number of colonies determined. According to Franken et al., plating efficiency (PE) was calculated using:

$$PE = \frac{number\ of\ colonies\ formed}{number\ of\ cells\ seeded} * 100\%$$

The surviving fraction (SF) after treatment:

$$SF = \frac{number\ of\ colonies\ formed\ after\ treatment}{number\ of\ cells\ seeded * PE}$$

Statistical significance of monotherapy was determined using multiple T tests. To compare treatment sensitivities of different cell lines one-way ANOVA and two-way ANOVA analyses, respectively, were conducted. For both we used the GraphPad Prism 9 software, p-values<0.05 were considered significant.

2.2.1.4 Flow cytometry: Cell cycle and apoptosis analysis

Cell cycle analysis. To analyze the cell cycle status of cells, 200 000 cells were seeded in a T25 flask and treated the next day in serum-free medium. After treatment incubation, cells were detached and centrifuged. The pellet was washed twice in sample buffer (PBS + 1g/L glucose) and centrifuged at 700 g for 5 min. Next, cells were resuspended in 1 mL sample buffer and slowly 4 mL of ice cold (-20°C) ethanol (absolute) was added. This cell suspension was incubated for 15 min at -20°C. Cells were centrifuged at 500g for 5 min and cells were resuspended in sample buffer and left to rehydrate for 15 min. Afterwards, the staining solution (50 µg/mL propidium iodide (PI), 0.2% Triton X-100, 100 µg RNAse in sample buffer) was added to the cells and incubated for 15 min at room temperature (RT). Then, cell cycle status was analyzed using a MACSQuant Analyzer 10. The gating strategy can be found in the **Appendix Figure 3**.

Apoptosis analysis. To determine the apoptosis inducing properties of compounds, the FITC Annexin V Apoptosis Detection Kit I was used according to manufacturer's protocol. In brief, cells were seeded at 200 000 cells per 6-well plate and treated in serum-free medium the next day. After treatment incubation time, cells were carefully detached using Accutase and washed twice with ice cold PBS. Afterwards, cells were resuspended in staining solution (1x binding buffer, Annexin V, PI) and incubated for 15 min at room temperature in the dark. Samples were measured on the MACSQuant Analyzer 10 within 1 h.

Flow cytometry data analysis was done using the FloJo 10 software. The gating strategy can be found in **Appendix Figure 9**.

2.2.1.5 Synergy calculation: Bliss model and R package "synergyfinder"

Bliss model. To assess synergism of treatments in clonogenic survival assays the original Bliss Independence Criterion was utilized. For this, the actual effect (E) of two drugs together (E_{a+b}) was compared to the product of each individual drug concentration (E_a*E_b). If the effect of the two drugs together was equal to the product of each individual effect ($E_{a+b}=E_a*E_b$), additivity was assumed (**Figure**

10, option 1). In case $E_{a+b}>E_a*E_b$, synergism is assumed (**Figure 10**, option 2), in case $E_{a+b}<E_a*E_b$, antagonism is assumed [164] (**Figure 10**, option 3).
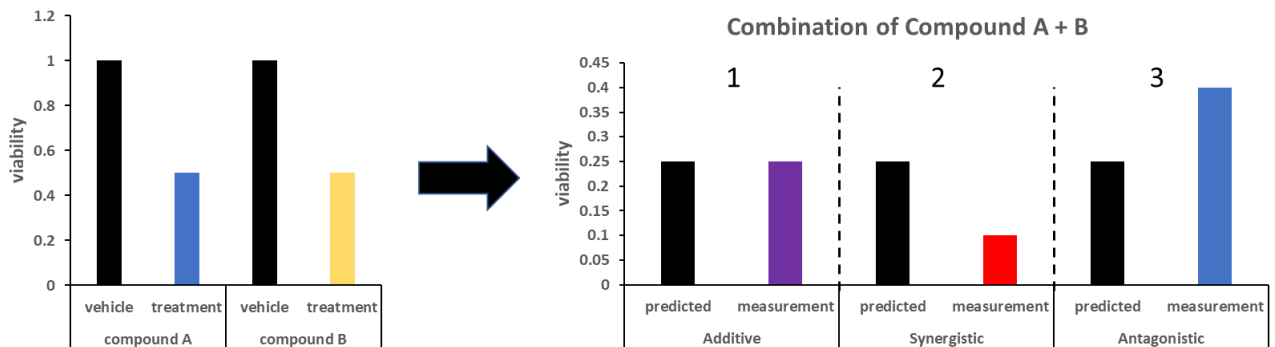
***Figure 10**: Evaluation of combinatorial effects based on the Bliss multiplication model*
Compound A and compound B lead to a reduction of viability of 50% alone (left). When combining A and B to assess the combinatorial effect the product of each monotherapy is calculated to achieve the "predicted" value. The predicted value is compared with the measurement derived from the actual combination treatment in a clonogenic survival assay. Option 1 shows additive results, option 2 is a synergistic read-out and option 3 depicts an antagonistic outcome (right).

Synergyfinder Package. To assess the synergism of treatments in acute cytotoxicity assays the R synergyfinder package was utilized [165]. In this package different synergy models are available, namely, HSA (highest single agent), Bliss, Loewe and ZIP (zero interaction potency). For this thesis, the ZIP model analysis was conducted according to the vignette provided by He et al. [165]. The ZIP model assumes minimal changes of the dose-response curves of two individual drugs compared to their combination. Synergy is assumed if the null-hypothesis of only minimal interaction is dismissed. Hence, it takes advantage of both the Loewe additivity and the Bliss independence model [166]. We assumed synergism of a given drug combination if at least in 2 combinatorial settings a ZIP synergy score of >10 was achieved.

2.2.1.6 pLKO1-shRNA constructs

Cloning strategy. Essentially this cloning strategy followed the Addgene cloning protocol provided for the pLKO.1-TRC cloning vector [167]. Small changes included the annealing strategy, we heated the Oligos to 95°C for 5 min and afterwards cooled them down from 90°C decreasing the temperature by 5°C every minute until reaching 25°C. The pLKO.1 puro vector was digested with AgeI and EcoRI in one step.

pLKO1-shRNA virus production. HEK293FT cells were seeded at a high density and left to attach overnight. The next afternoon, the medium was sucked off and replaced with OptiMEM. For

transfection of the cells the Lipofectamine 3000™ kit was used. For this, 700 µL OptiMEM was mixed with 10 µg pLKO1-shRNA plasmid, equimolar concentrations of packaging plasmids psPAX2 and pMD2.G and 50 µL P3000 in one reaction tube. A second reaction tube containing 700 µL OptiMEM plus 29 µL Lipofectamine 3000 was prepared. The mixture containing the pLKO1-shRNA plasmid was mixed into the reaction tube containing Lipofectamine 3000 and left undisturbed for 5 min at RT. Afterwards, the mix was added to the cell culture medium and cells were put back into the incubator. The next day, the medium was changed to DMEM complete. HEK293FT cells were allowed to produce virus for 48 h after which the medium was taken off, centrifuged 5 min at 1200 rpm and filtered through a 0.45 µm filter. The virus medium was then aliquoted and stored at -80°C.

Production of knock-down cell lines using Lentiviruses carrying pLKO1-shRNA constructs. At day one, cells were seeded at 200 000 cells per well in a 6-well plate. The next day, the medium was changed to DMEM complete including polybrene at 7.5 µg/mL for LN229 and 8 µg/mL for LNZ308 cells. pLKO1-shRNA virus was added in a range between 0 and 1000 µL to each well, shRNA sequences can be found in table "2.1.13 shRNA Sequences". Cells were put back into the incubator overnight. Then, cells were detached, counted and again seeded at 200 000 cells per well in a 6-well plate and left to attach overnight. The following day, Puromycin was added to the medium, at 1µg/mL for LN229 cells and at 2 µg/mL for LNZ308 cells. The selection was left undisturbed for at least 72 h when the non-infected control wells were checked for left-over surviving cells. Successfully transduced cells were expanded and validated for knock-down efficiency using quantitative real-time PCR (q-rtPCR). An shRNA targeting Luciferase served as control and was produced alongside the knockdown cells.

2.2.1.7 Proliferation assay

To assess proliferative capacity of different cell lines, 200 000 cells were seeded in four T25 flasks per cell line. After 24, 48, 72 and 96 h total cell number was determined and documented. Statistical significance was tested using one-way ANOVA with the GraphPad 9 software, p-values<0.05 were considered significant.

2.2.1.8 RCAS-shRNA constructs

Cloning strategy. Oligo annealing was done as is described under 2.2.1.6. For the RCAS cloning a two-step protocol was followed. First, annealed Oligos were ligated into the pENTR-H1-RFP vector that was cut open using Bgl2 and XhO1 (**Figure 11** A). shRNA, pENTR vector, 10x T4 DNA ligase buffer and T4 DNA ligase were incubated at 4°C overnight. The next day, DH5α competent E. coli were transformed by incubating a bacteria-ligation mix for 30 min on ice, followed by 45 sec heat shock in a water bath

at 42°C, followed by another 5 min incubation on ice. Then, SOC medium was added and the bacteria incubated for 1 h at 37°C in a bacterial shaker. Lastly, bacteria were plated on a plate containing kanamycin. The next day, clones were picked and minipreps using the QIAprep Spin Miniprep Kit performed according to manufacturer's protocol. Resulting DNA samples were sequenced at Eurofins Genomics and checked for successful integration of the shRNA sequence. Next, the Gateway Clonase II system was used according to manufacturer's protocol to transfer the shRNA-RFP sequence into the RCAS-Y DV vector leveraging the attL/attR cloning sites included in the vectors (**Figure 11**). Bacteria were transformed as has been described above, selection was done using ampicillin plates. Again, after QIAprep Spin Miniprep Kit DNA extraction, DNA was sequenced and successful shRNA-RFP sequence integration controlled.
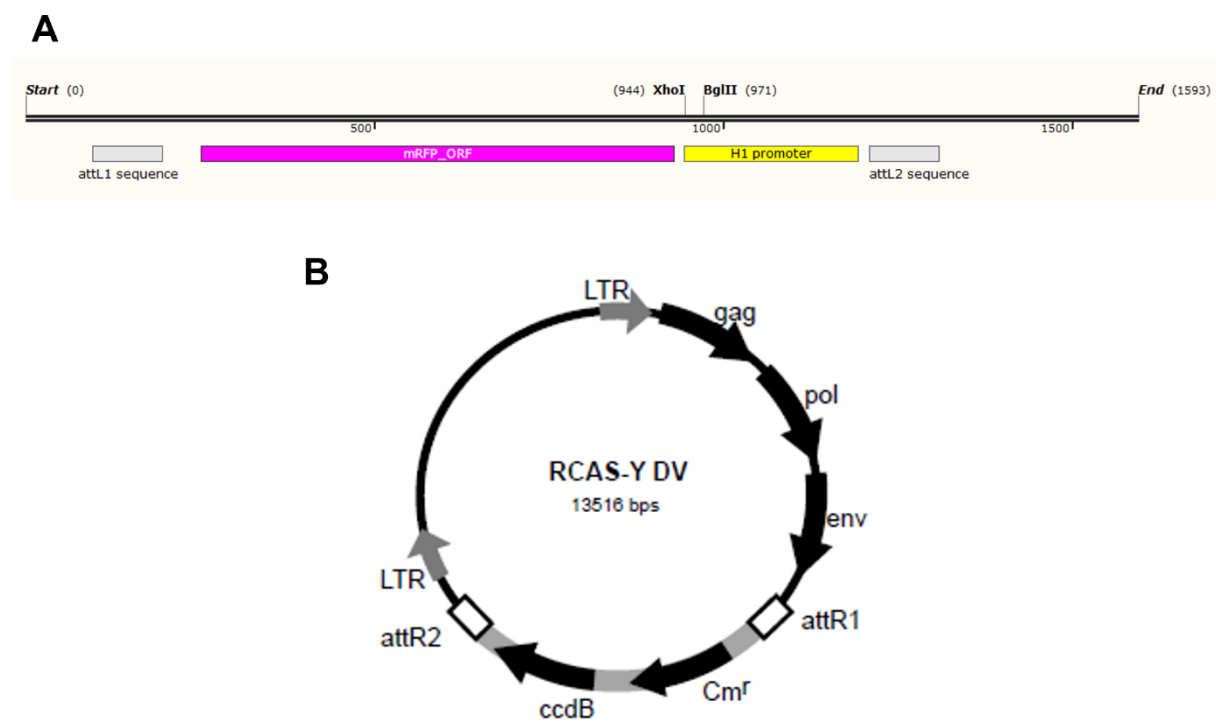
Figure 11: *Vector maps of pENTR-RFP (A, created with SnapGene viewer) and RCAS-Y DV (B, adopted from Loftus et al., 2001 [168]) indicating important cloning sites for the cloning strategy*

DF-1 virus production. DF-1 virus production was achieved according to the protocol proposed by von Werder et al. [169]. In summary, DF-1 cells were seeded at 250 000 cells and left to attach overnight. The next day, cells were washed once with PBS and fresh DMEM complete was added. For transfection the Qiagen Superfect kit was used. For this, 2.5 µg RCAS-shRNA plasmid plus DMEM without any supplement was mixed with 25 µL Superfect reagent. This mixture was incubated for 7 min at RT.

During the incubation time medium on the DF-1 cells was changed to 1 mL DMEM complete into which the transfection mix was added. Cells were incubated 3 h in the incubator, washed twice with DMEM complete and filled up with 5 mL DMEM complete again. The mixture was then incubated for at least two days after which fluorescence could be checked using an Axiovert 200M fluorescent microscope and successful transfection could be validated.

Determining RCAS-shRNA knock-down efficiency. As a model system *in vitro*, NIH3T3 tv-a cells could be transduced with RCAS-shRNA viruses. For this, DF-1 cells producing the RCAS virus of interest were seeded at 550 000 cells per T25 flask. The next day, the media of the DF-1 cells was changed to 50% DMEM complete, 50% DMEM supplemented with 10% CS and 0.01% Gentamycin (NIH3T3 medium). NIH3T3 tv-a cells were seeded at 75 000 cells per well in a 6-well plate. Virus was harvested from DF-1 cells, centrifuged and filtered using a 0.45 µm filter. The resulting virus medium was mixed with NIH3T3 medium 1:2 and 8 µg/mL polybrene was added. Medium from the NIH3T3 tv-a cells seeded in 6-well plates for transfection was taken off and 2 mL of virus medium was added. After approximately 8 and 16 h respectively additional 2 mL of virus medium were added to the cells. We incubated the cells for 2 days and afterwards the virus medium was aspirated and cells expanded. After another 2 days red fluorescence protein (RFP) presence was checked with the Axiovert 200M fluorescent microscope. Upon successful transduction, RNA was extracted and, using q-rtPCR, knock-down efficiency determined.

2.2.2 In vivo methods

2.2.2.1 Mouse models and procedures

Animal maintenance. Animals were kept and bred in the animal facility of the institute and regularly analyzed for infectious diseases. All animal experiments were approved by the regional council Tübingen and conducted in accordance with animal law under the license numbers N7/17, N1/20, N19/20 and N5/19.

Stereotactic injection into the right striatum. Mice were anesthetized using a 3 component (3K) anesthesia. Breathing and reflexes were constantly checked. After approximately 10 min the heads of the animals were shaved to clean out the surgical field. Pain killers were administered and once the inter-toe reflex vanished the head was prepared with iodine solution and a 1 cm central cut was administered using a disposable scalpel. Afterwards the Bregma was identified and approximately 1.5 mm to the right and 1 mm to the front a whole was drilled into the skull. Next, the mouse was fixed into a stereotactic device and corrected until a horizontal injection side is achieved. A Hamilton syringe

containing the cells to be injected into the right striatum was placed directly above the whole drilled into the skull. The needle was inserted 3 mm into the brain. After 1 min the cells were injected with a rate of 0.5 µL/min. For SMA560/VM/Dk 5 000 cells per mouse were injected into the right striatum, for RCAS tv-a 50 000 cells per mouse were injected. The needle was left in the tissue another 2 min, and then removed from the brain. Subsequently the animals were taken out of the stereotactic device. The whole in the skull was closed with bone wax and the central cut stitched closed with single stitches. Afterwards, the antidote was administered and animals were watched until full recovery from anesthesia and circulatory stable. During the whole procedure the bodies of the animals were kept warm using warming mats and their eyes are protected by Bepanthen® ointment.

Animal monitoring and treatment. During the course of the experiments animals were closely monitored [170], according to the licenses and animal law. Respective score sheets can be found in the Appendix (**Appendix Tables 1, 2**). Between N7/17 and the other licenses, regulatory changes lead to a change in scoring sheets, however, this did not impact the comparability of study outcomes. Blinding happened at the data analysis stage. Any treatments administered during the experiments are indicated in the respective figure and in the treatment schedules.

Perfusion and brain preservation. To collect brain tissue for subsequent analyses, animals were heavily sedated using the perfusion narcosis. Once the inter-toe reflex is gone, the abdominal cavity was opened and the heart freed. A butterfly needle which has been connected to the perfusion tube, was inserted into the left ventricle and perfusion with ice cold PBS started, shortly after the aorta abdominals was cut to flush out all the blood of the mouse. Perfusion status was controlled through color of the liver, once this was completely white, perfusion was deemed complete. Then, the needle was taken out of the heart. The animal's neck was broken using a Malleus Bone Nipper and the animal beheaded. The scalp was opened with a scalpel and folded to the side, exposing the skull. To extract the brain, the skull was cut open along the sutura sagittalis using a side angled bone cutting scissor starting at the medulla oblongata. Then the skull bones were detached from the brain tissue and the brain lifted out of the skull using a hippocampal spatula.

The extracted brains were either instantly frozen in 2-methyl-butan cooled down with dry ice or directly on a metal block cooled down with liquid nitrogen. Brains were then stored at -80°C. Alternatively, brains were placed into a 4% paraformaldehyde (PFA) solution and put on a roll mixer at 4°C for up to 72 h. Afterwards, brains were dehydrated in 15% and 30% sucrose. Before cutting on a cryotome, brains were embedded in cryomolds using TissueTek™.

The tissue was cut into 8 µm thin sections using a cryotome, slides were stored at -80°C until stained.

Survival analyses. Statistical analyses of symptom free survival were conducted using the Log-rank test (**Figure 13**, **Figure 18**), two-way ANOVA (**Figure 17**) and Gehan-Breslow-Wilcoxon (**Figure 18**), respectively. P-values <0.05 were considered significant.

2.2.2.2 Hematoxylin and Eosin stain

Hematoxylin and Eosin (H&E) staining procedure. For H&E stains, sections were selected and air dried for approximately 10 min at RT. Next, slides were fixed 10 min in acetone at -20°C and methanol at 4°C. Then, slides were washed twice for 5 min in PBS and put into filtered, 0.1% hematoxylin solution for 10 min. Afterwards, slides were put under running tab water. This was followed by 2 min in a 1% eosin solution. Then, slides were dipped in tab water until the streaking stopped. Lastly, the stains were dehydrated in an alcohol dilution series, two times 5 min in 70% and each 1 min at 95% and 100% ethanol. Slides were covered using Roti Histokit mounting medium and air dried overnight and evaluated under an Axiofluor Zeiss Microscope.

Tumor volume approximation by H&E stains. Overview pictures of H&E stained brains were produced using the MosaiX function on the Axio Vision 4.0 software of the Axiofluor Zeiss Microscope. Upper and lower limit of tumors were determined and respective surfaces measured in regular intervals using ImageJ. The surface areas multiplied with the thickness of the slides (calculated from slide one until the next slide with a determined tumor area) gave partial volumes. The sum of these volumes approximates the overall volume.

2.2.2.3 Immunohistochemistry

Staining procedure. Stains were air dried for 10 min at RT. Depending on the primary antibody, slides were fixated either in 4% PFA solution for 15 min or 10 min acetone at -20°C followed by 10 min 80% methanol at 4°C. Afterwards, slides were washed twice with PBS. The brain tissue was circled using a lipophilic marker and blocked for 10 min with BLOXALL™ solution to inactivate endogenous peroxidase activity. Then, slides were washed again with PBS, blocked for 1 h in 10% bovine serum albumin (BSA) in PBS-Tween 0.3%. The primary antibody was diluted in 2% BSA in PBS-T 0.06% for up to two nights at 4°C. Next, slides were washed three times with PBS and secondary antibody was incubated for 1 h at RT in 2% BSA PBS-T 0.06%. Slides were washed four times with PBS and incubated for 30 min in ELITE ABC reagent. Again, slides were washed in PBS, then, the peroxidase substrate NovaRED was added to the slides and incubated for 5 min at RT. Slides were washed for 2 min with distilled water. Next, slides were counterstained using hematoxylin for 45 sec and put under running tap water for 2 min. Lastly,

slides were taken through a series of alcohol dilutions, 2 min 70% ethanol, 2 min 90%, two times 2 min 100% and three times Xylene 5 min each. Slides were covered using Roti Histokit mounting medium.

Analysis and Quantification. Digitalization of slides was performed using the Axiofluor Zeiss and Olympus BXC1 microscope. Pictures were saved as TIFF and further analysis done using ImageJ. Counting was done using an ImageJ script. For this, pictures were background corrected and colors separated according to the RGB (red-green-blue-violet) system. Positive stained cells were filtered using a stable threshold limit which led to the generation of a binary data picture. Positive stained cells were automatically counted depending on their size. Statistical analysis was performed using unpaired t-tests in GraphPad Prism 9, p-values<0.05 were considered significant.

2.2.3 Molecular Tumor Board (MTB) Tübingen

The data analyzed here is part of the prospective, observational study "Molecular Tumor Board at the Center for Personalized Medicine Tübingen (MTB@ZPM)", ClinicalTrials.gov Identifier: NCT03503149. The two main inclusion criteria were (i) advanced tumor disease without further registered and guideline-based treatment options and (ii) rare disease as defined by European Reference Network on Rare Adult Cancers (EURACAN). The study focused on adult patients with tumors in the nervous system diagnosed in the time from February 2016 to May 2020. The ethical board of the University Hospital Tübingen approved the collection of data in a pilot phase of 132 patients (700/2020BO) and in the ongoing prospective observational study MTB@ZPM (883/2017BO1). After patient consent genome sequencing results were evaluated for actionable clinical targets in weekly interdisciplinary MTB conferences. For the present thesis diagnosis, germline mutation status, IDH status and Fanconi Anemia (FA) somatic mutations were evaluated and are presented here.

The NGS-panel sequencing dataset generated during this study are not uploaded in a public repository as these are patient samples with potentially identifiable germline information. Data access for researchers beyond the Center for Personalized Medicine Tübingen is possible upon request. This requires granting by the Data Use and Access Committee (DUAC) of the University Hospital Tübingen (https://www.medizin.uni-tuebingen.de/de/das-klinikum/einrichtungen/institute/informationstechnologie-und-medizininformatik/medic/duac). Following the granting of access, accounts are given to researchers and data can be accessed.

2.2.4 Miscellaneous

2.2.4.1 Agarose gel electrophoresis and DNA gel extraction

After enzymatic digest, vectors need to be cleaned up which was done by agarose gel electrophoresis. For this, a 1.5% agarose gel was prepared. The vector solution was mixed with 6x loading dye and the gel run at 100 V for 2 h. To extract DNA from agarose gels, the QIAquick® Gel Extraction Kit was used according to manufacturer's instruction.

2.2.4.2 RNA extraction

To perform RNA extraction from cells the RNeasy Mini Kit was used according to manufacturer's instruction including a DNase digest using the RNase-Free DNase Kit.

2.2.4.3 Quantitative real-time PCR

To determine knockdown efficacy and expression levels, quantitative real-time polymerase chain reaction (q-rtPCR) was performed. For this, RNA was translated into cDNA using the High Capacity RNA-to-cDNA Kit. The cDNA was then diluted 1:4 before usage in q-rtPCR. The qPCR Mastermix Plus for SYBR Green I was used to set-up master mixes containing respective primers. Hypoxanthine phosphoribosyltransferase 1 (HPRT) served as the reference housekeeping gene. Samples were run on a Roche LightCycler 96 with the following protocol:

1. 2 min 50°C
2. 10 min 95°C
3. 15 sec 95°C
4. 1 min 60°C
5. Repeat from (3) 40x
6. Melting curve: 15 sec 95°C, 1 min 60°C ramp to 15 sec 95°C

Raw data was annotated using the LightCycler® 96 SW 1.1 software. Relative quantification was done using the $2^{-\Delta\Delta Ct}$ method [171] referring to HPRT expression.

2.2.4.4 Immunoblot analyses

Cells were detached and washed twice with ice cold PBS. Using radio-immunoprecipitation assay (RIPA) buffer supplemented with protease and phosphatase inhibitors, cells were lysed for 30 min on ice, vortexing every 10 min. After 15 min spinning at 13 000 rpm at 4°C, cell lysate was transferred to a fresh 1.5 mL reaction tube. Protein concentration was measured using the Pierce bicinchoninic acid

(BCA) protein assay kit according to manufacturer's protocol. Lysates were diluted to desired protein concentrations, mixed with 2x Laemmli and denatured for 5 min at 95°C. Next, a standard ladder and the lysates were loaded onto sodium-dodecyl sulfate (SDS) gels, 10% or gradient 4-12% NuPAGE (polyacrylamide gel electrophoresis). Electrophoresis ran for approx. 30 min at 200 V. Afterwards, the proteins were transferred onto a methanol activated polyvinylidendifluorid (PVDF) membrane using a wet transfer. The transfer ran for 2-3.5 h at 25 V. Membrane was then blocked in non-fat dry milk (NFDM) or bovine serum albumin (BSA) for 1 h at RT. Primary antibodies were added to the membrane and incubated over night at 4°C. The next day, the membrane was washed three times 10 min with tris-buffered saline (TBS) supplemented with 0.1% Tween-100 (TBS-T). Then, the secondary antibody was added and incubated for 1 h at RT. Again, the membrane was washed three times with TBS-T. Development of protein signal was done using the Pierce ECL Western Blotting Substrate kit according to manufacturer's instructions and detected on a Bio-Rad ChemiDoc MP Imaging system.

2.2.5 Collaborations

2.2.5.1 Human leukocyte antigen (HLA) Ligandome Analysis

LNZ308 and LN229 cells were treated with the indicated concentrations of Argyrin F for 24 h in serum free media. Then, they were harvested, washed twice in ice cold PBS and stored at -80 °C until human leukocyte antigen (HLA) class I and II molecules were isolated using standard immune affinity purification methods, as described previously [172, 173]. The mass spectrometry proteomics data have been deposited to the ProteomeXchange Consortium via the PRIDE partner repository with the dataset identifier PXD021526.

2.2.5.2 Patient derived microtumors (PDMs)

The generation of patient derived microtumors (PDMs) from remaining tissue of freshly resected glioblastoma was approved by the Ethical Committee of the University Hospital Tübingen (ethical approval number 610/2020BO). The applied procedure for PDM and tumor infiltrated lymphocytes (TIL) isolation is adapted from the publication of Kondo et al. [174] and has been published in Walter et al. [51] and Anderle et al. [175]. In brief, fresh patient tissue was minced into small pieces and digested. After a series of filtering steps, PDMs were cultured in 60 mm dishes containing StemPro human embryonic stem cell culture serum- and feeder-free medium (hESC SFM) with addition of basic fibroblast growth factor (bFGF) and 1% Primocin at 5% CO_2 and 37°C in a humidified incubator. The flow-through containing single cells were collected and resuspended in T cell medium (Advanced Roswell Park Memorial Institute (RPMI), 200 mM Glutamine, 1x minimal essential medium (MEM)

Vitamins, human AB serum, Primocin) containing interleukin (IL)-15 (23.8 U/mL), IL-2 (100 U/mL), IL-7 (10 U/mL) and cluster of differentiation (CD) 3-/CD28-coated magnetic beads. TILs were expanded for approximately 10 days at 5% CO_2 and 37°C with expansion medium being exchanged every 2 days.

Characterization of PDM-derived TILs population by flow cytometry. The isolated TILs were fixed and permeabilized using a FIX&PERM Cell Permeabilization Kit according to manufacturer's instructions. For immune phenotyping, TILs were stained using Anti-CD3-FITC, Anti-CD4-BV510, Anti-CD8-PerCP/Cy5.5 and Anti-TNFa-BV711 and analyzed on a LSR Fortessa cytometer. Prior to analyses, color compensation was performed for each dye using compensation beads. Recorded events first passed through a routine light-scatter and doublet discrimination gate. Data analysis was performed using FlowJo v10.6.2 software, plotted are absolute or fold change values (normalization indicated in respective graphs). The gating strategy is displayed in **Appendix Figure 5**.

Luminescent PDM dose-finding assay. For assessment of treatment effects on PDM viability a CellTiterGlo 3D luminescent cell viability assay was performed according to manufacturer's instructions. Measurements were done on a 96-well plate reader after 48 h. Relative luminescence units were background corrected and plotted as absolute or fold change values (normalization indicated in respective graphs). Statistical significance of treatment-induced effects on PDM viability was analyzed using GraphPad Prism 8.

Co-culture experiments of PDM and TILs. PDMs were cultured in T cell medium without cytokines in 96-well clear-bottom microtiter plates together with autologous TILs at an effector:target cell ratio of 4:1 [176] in the presence of CellTox Green Dye reagent. CellTox Green dye fluorescence was measured at 48 h after treatment start using a multimode microplate reader (Excitation filter: 485 (20) nm, Emission filter: 535 (20) nm). Relative fluorescence units were background corrected and plotted as fold change values (normalization indicated in respective graphs). Statistical significance of treatment-induced increase in TILs cytotoxicity was analyzed using GraphPad Prism 8.

Immunohistochemistry and Live-Cell Imaging of PDMs: PDMs were fixed in 4% PFA solution at pH7 for 1 h at RT. Then, PDMs were stained with hematoxylin for 5 min, washed briefly in H_2O and incubated twice in 50% ethanol and 70% ethanol for 15 min each. PDMs were embedded into a gel matrix (Richard-Allan Scientific HistoGel) in a cryomold according to manufacturer's instructions. For immunohistochemistry analyses, gel-embedded PDMs were embedded into paraffin blocks. 5 µm sections were subjected to H&E staining as well as IHC staining using a DAB (3,3'-Diaminobenzidine) staining solution (Leica Biosystems). For IHC staining of Glial Fibrillary Acidic Protein (GFAP) in PDM sections, the GFAP-GA5-L-U was used at 1:400 dilution according to manufacturer's instructions. Stained sections were imaged on an Axio Scan.Z1 Slide Scanner. For live-dead cell staining, PDMs were

labelled with Calcein-AM to visualize viable cells and SyTox-Orange for visualization of non-viable cells, according to manufacturer´s instructions. Confocal z-stacks were generated from images taken at 25 µm intervals on a spinning disc confocal microscope (Axio Observer.Z1).

2.2.5.3 Transcriptomic analysis

RNA was prepared using the Qiagen RNeasy Mini kit. For each sample quality control was done using a nanodrop and at least 1 µg RNA was sent for sequencing. Sequencing was conducted by the center for next generation sequence at the University of Tübingen.

Resulting data was processed by the R package "DESeq2" [177]. First, reads were mapped to the reference genome and annotated. Next, differentially expressed genes (DEGs) were identified comparing treatment conditions with the respective control condition per cell line. Significant DEGs were defined as fold-change (fc) above or below |1| with a p-adjusted (padj) value<0.01. Results were then analyzed for Kyoto Encyclopedia of Genes and Genomes (KEGG) pathway association using gProfiler [161]. Additionally, the significantly differentially regulated genes between treated cell lines were analyzed using the likelihood ratio test (LRT). Significant LRT genes were re-aligned with DEG expression results and the ones with a significant fc and padj were again analyzed by gProfiler [161].

2.2.5.4 DigiWest Protein Profiling

Lysis and protein quantification for DigiWest. 20-30 µL of LDS lysis buffer, supplemented with reducing agent and protease- and phosphatase-inhibitor were added to cell pellets on ice. Proteins were denatured by heating to 95°C for 10 min before the lysates were transferred to QiaShredder Eppendorf tubes. After centrifugation (16000 g, 5 min, RT), eluates were stored at -80°C until further use.

Protein quantification was performed using in-gel staining. 1 µL of each original lysate was diluted 1:10 (v/v) in lysis buffer. The respective aliquots were denatured for 10 min at 70°C and 10 µL were run in a NuPAGE 4-12% Bis-Tris precast gel according to the manufacturer´s instructions. The gel was washed with water and proteins were stained with BlueBandit for 1 h. The gel was de-stained over night with ddH$_2$O before detection on a LI-COR instrument. Analysis and protein quantification was performed using ImageStudio.

DigiWest multiplex protein Analysis. DigiWest was performed as published previously [178]. In brief, 10 µg of cellular protein was loaded on an SDS-polyacrylamide gel and size-separated using the commercial NuPAGE system. Size-separated proteins were blotted onto a PVDF membrane and biotinylated on the membrane using NHS-PEG12-Biotin (50 µM) in PBST for 1 h. After drying of the membrane, the sample lanes were cut into 96 strips of 0.5 mm width using an automated cutting

plotter each corresponding to a defined molecular weight fraction. Each of the strips was placed in one well of a 96-well plate and 10 µL elution buffer (8 M urea, 1% Triton-X100 in 100 mM Tris-HCl pH 9.5) was added. The eluted proteins were diluted with 90 µL of dilution buffer (5% BSA in PBS, 0.02% sodium azide, 0.05% Tween-20) and each of the protein fractions was incubated with one distinct magnetic color-coded bead population coated with neutravidin. The biotinylated proteins bind to the neutravidin beads such that each bead color represents proteins of one specific molecular weight fraction. All 96 protein loaded bead populations were mixed resulting in reconstitution of the original lane. Such a bead-mix was sufficient for about 150 individual antibody incubations (**Appendix Table 5**). Aliquots of the DigiWest bead-mixes (about 1/200th per well) were added to 96 well plates containing 50 µL assay buffer (Blocking Reagent for ELISA supplemented with 0.2% milk powder, 0.05% Tween-20 and 0.02% sodium azide) and different diluted antibodies were added to the wells. After overnight incubation at 15°C in a shaker, the bead-mixes were washed twice with PBST and species-specific phyoerythrin (PE)-labelled secondary antibodies were added and incubated for 1 h at 23°C. Beads were washed twice prior to readout on a Luminex FlexMAP 3D.

For quantification of the antibody specific signals, the DigiWest Analyzer software was used; it automatically identifies peaks of appropriate molecular weight and calculates the peak area. Signal intensity was normalized to the total amount of protein loaded onto one lane. The software package MEV 4.9.0 was used for statistical analysis [179] along with GraphPad Prism 9. For all statistical tests, a p-value<0.05 was considered significant.

3. Results

3.1 Argyrin F Treatment-Induced Vulnerabilites Lead to a Novel Combination Therapy in Experimental Glioma

The data of this project have been published in the Journal Advanced Therapeutics in June 2021 [51].

3.1.1 Argyrin F shows anti-glioma activity *in vitro*
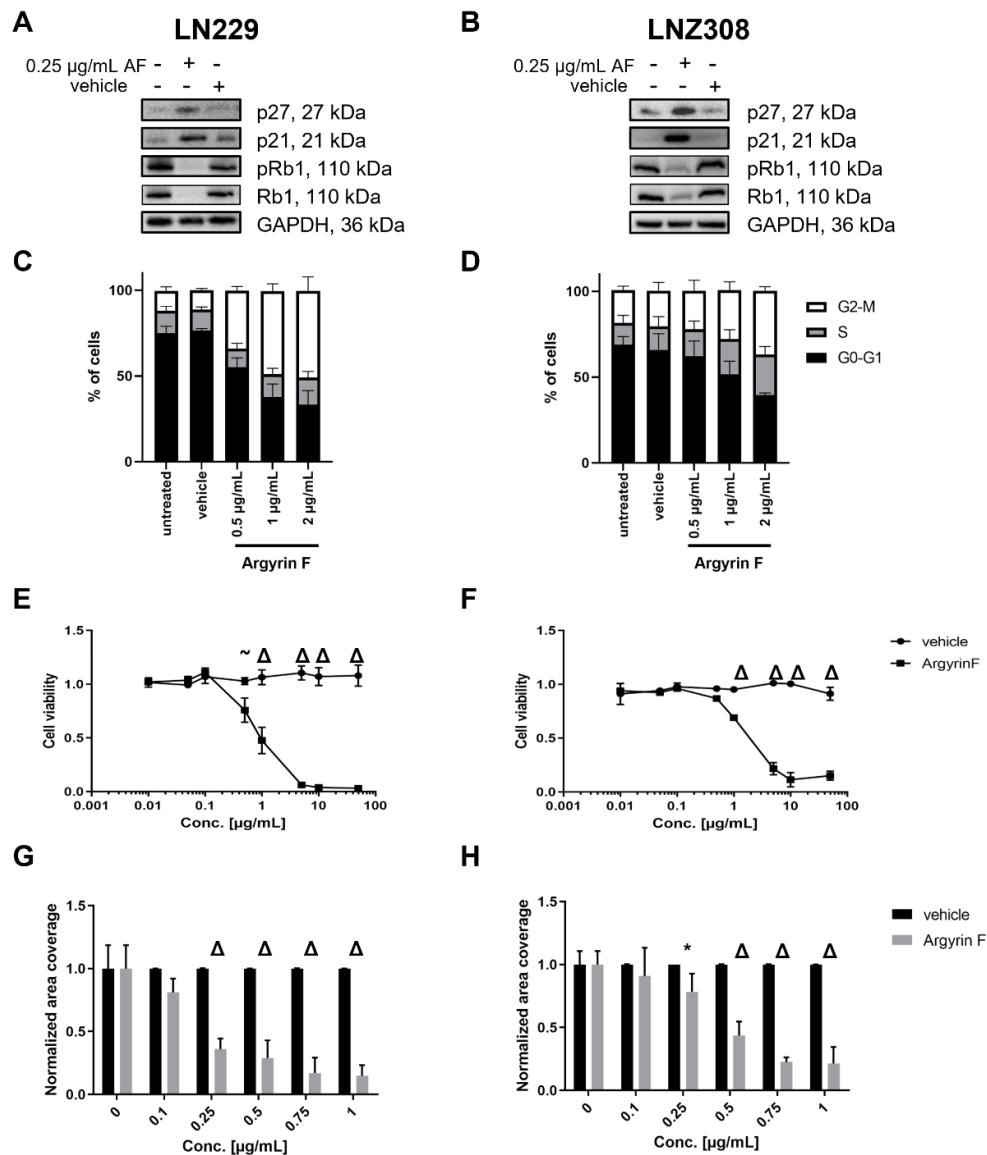
Figure 12*: Characterization of Argyrin F treatment in vitro*

*Immunoblot analyses of p27, p21, pRb1 and Rb1 levels in LN229 (A) and LNZ308 (B) cells after Argyrin F treatment. Cell cycle analyses of LN229 (**C**) and LNZ308 (**D**) cells treated with Argyrin F. Acute cytotoxicity and clonogenic survival assays comparing vehicle and Argyrin F treated LN229 (**E, G**) and LNZ308 (**F, H**) cells. (n=3) Statistical analysis was done using multiple t-tests with the Holm-Sidak method. * p < 0.05, ~ p < 0.005, Δ p < 0.0000001*

Argyrin F has been described to lead to an accumulation of p27 in cells [5], therefore, target engagement was looked at by immunoblots of p27 and p21 levels in glioma cells treated with Argyrin F for 48 h. We were able to detect an accumulation of both in LN229 and LNZ308 cells (**Figure 12** A, B). Next, we assessed the cell cycle stabilizing capabilities of Argyrin F. Hence, immunoblot analyses for retinoblastoma 1(Rb) and phospho-Rb1 (pRb1) were conducted (full pictures of all blots can be found in **Appendix Figure 1**). In both cell lines Rb1 was strongly downregulated (**Figure 12** A, B) and flow cytometry analyses of cell cycle status revealed an accumulation of cells in G2-M phase (**Figure 12** C, D) (the gating strategy for cell cycle analysis is illustrated in **Appendix Figure 3**). In acute cytotoxicity and clonogenic survival assays a dose-dependent reduction of cell viability and clonogenic survival could be detected (**Figure 12** E-H), comparable data was acquired using the glioma mouse cell lines GL261 and SMA560 (**Appendix Figure 2**).

3.1.2 Argyrin F treatment of SMA560 tumor bearing VM/Dk mice *in vivo*

As a next step, we wanted to determine the efficacy of Argyrin F therapy *in vivo*. For this, 5 000 SMA560 cells were intracranially injected into the right striatum of VM/Dk mice. Treatment started 7 days post-surgery using Argyrin F and a vehicle control, respectively, (**Figure 13** A, animal scoring sheet can be found in **Appendix Table 1**). Comparing the time until onset of neurological symptoms of both groups, Argyrin F treatment led to a modest but significant prolongation compared to vehicle treated animals (**Figure 13** B). From brain tissue collected of the mice in the project, target engagement of Argyrin F *in vivo* was determined and could show a clear increase of p27 signal in Argyrin F treated SMA560 tumors compared to vehicle treated tumors (**Figure 13** C). Histological approximation of tumor volume was also performed which showed a slight trend towards smaller tumors in Argyrin F treated animals, however statistical significance was not reached (**Figure 13** D). Further immune histological analyses revealed a significant influx of CD3$^+$, CD4$^+$ and CD8$^+$ T cells into Argyrin F treated SMA560 tumors (**Figure 13** E).
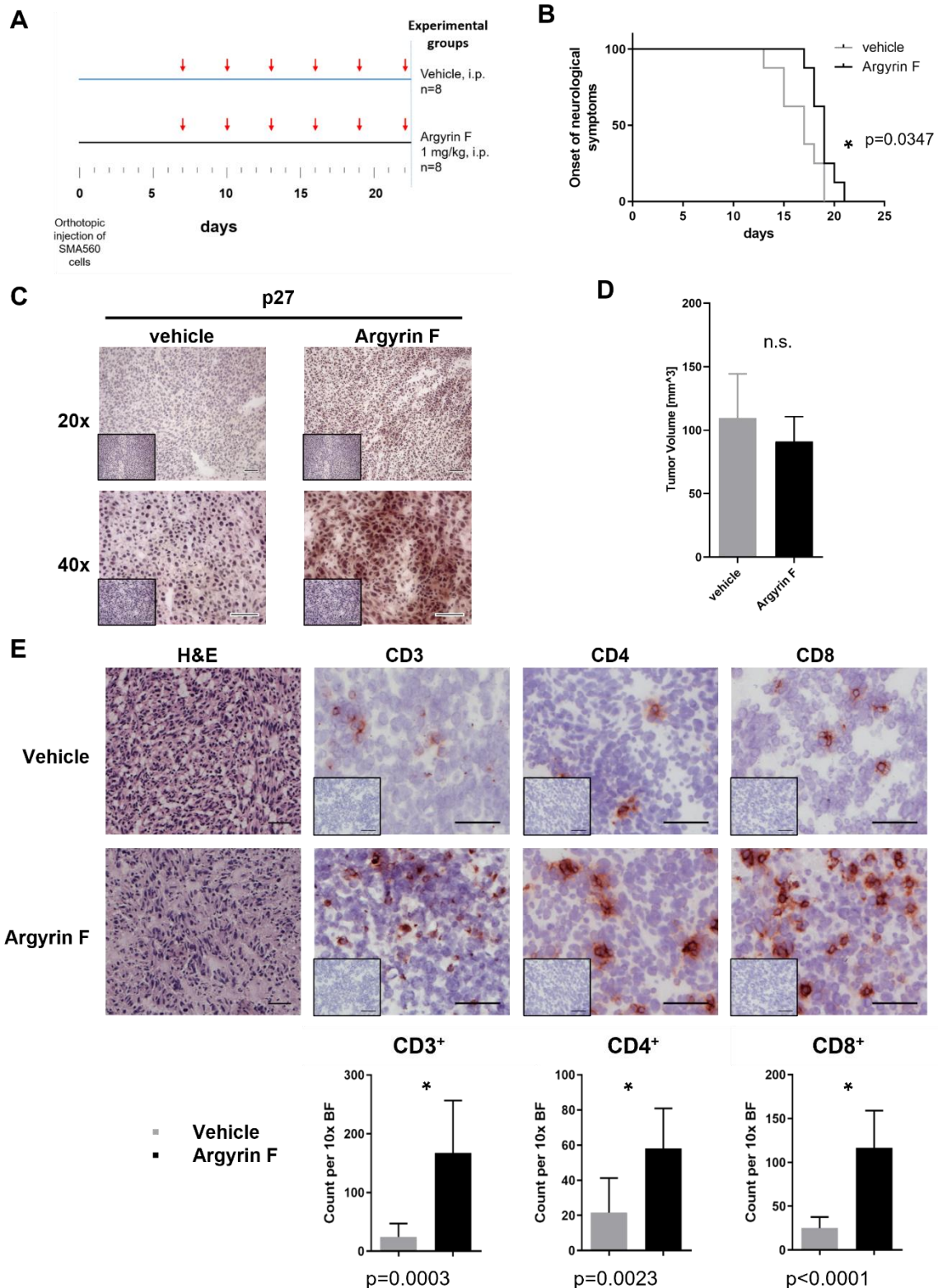
Figure 13: *SMA560 tumor bearing VM/Dk mice treated with Argyrin F show increased T cell infiltration in vivo*

*A, Treatment schedule, Argyrin F is administered every three days intraperitoneally (i.p.). **B**, Kaplan Meier curve depicting time until onset of neurological symptoms of Argyrin F and vehicle treated VM/Dk mice (n=8). **C**, Representative IHC stain for p27 levels. **D**, Histologically approximated tumor volume of Argyrin F and vehicle treated tumors (n=3). **E**, Histological panel including H&E, CD3, CD4 and CD8 staining of vehicle and Argyrin F*

3.1.3 Patient derived microtumors (PDMs), an *ex vivo* glioma model, treated with Argyrin F

As a next step, the anti-glioma activity of Argyrin F treatment on a novel *ex vivo* model was tested. For this, residual freshly resected primary glioma tissue from patients was used to extract patient derived microtumors (PDMs). Alongside the microtumors also autologous tumor infiltrating lymphocytes (TILs) were extracted, expanded and retained for co-culture experiments [51, 139, 175]. The resulting PDMs are viable and express the glioma marker glial fibrillary acidic protein (GFAP) (**Figure 14** A, B).

Argyrin F treatment of PDMs alone, i.e., the absence of autologous TILs, was able to reduce cell viability in a dose-dependent manner in PDM models leading to the identification of IC_{50} values (**Figure 14** C). At the same time, using concentrations up to 100 ng/mL Argyrin F treatment of TILs alone did not induce a cytotoxic read-out (**Figure 14** D). However, when co-culturing the PDMs with their autologous TILs a strong, significant induction of cytotoxic read-out can be detected already at doses of 10 ng/mL Argyrin F treatment (**Figure 14** E).

Together with the detection of an increased T cell influx into SMA560 tumors *in vivo* (**Figure 13**), an increased treatment-induced immunogenicity upon Argyrin F treatment was hypothesized.

3.1.4 The immunopeptidome of Argyrin F treated LN229 and LNZ308 cells show treatment-induced changes

After Argyrin F treatment, LN229 and LNZ308 cells were collected and their immunopeptidome was analyzed using mass spectroscopy. Graphs of LN229 data can be found in the **Appendix Figure 4** analogously to **Figure 15** for LNZ308 cells in the main text.

First, quality control was done analyzing the number of presented peptides (**Figure 15** A) which was not affected by Argyrin F treatment. Looking at the overlap of presented peptides it was highest between the two treatment conditions, suggestive for treatment-induced changes (**Figure 15** B). In the subsequent analysis significantly up- (red) and down- (blue) modulated peptides could be identified comparing the treatment conditions with the blank condition (**Figure 15** C). In **Figure 15** D five exemplary up-modulated peptides for the LNZ308 cells treated with 3 µg/mL Argyrin F are listed with their respective corrected p-value, the log2 fold change (cond1/cond2), the corresponding protein and gene. In LNZ308 cells the peptide SSVPGVRLL corresponding to vimentin (VIM) was detected, which
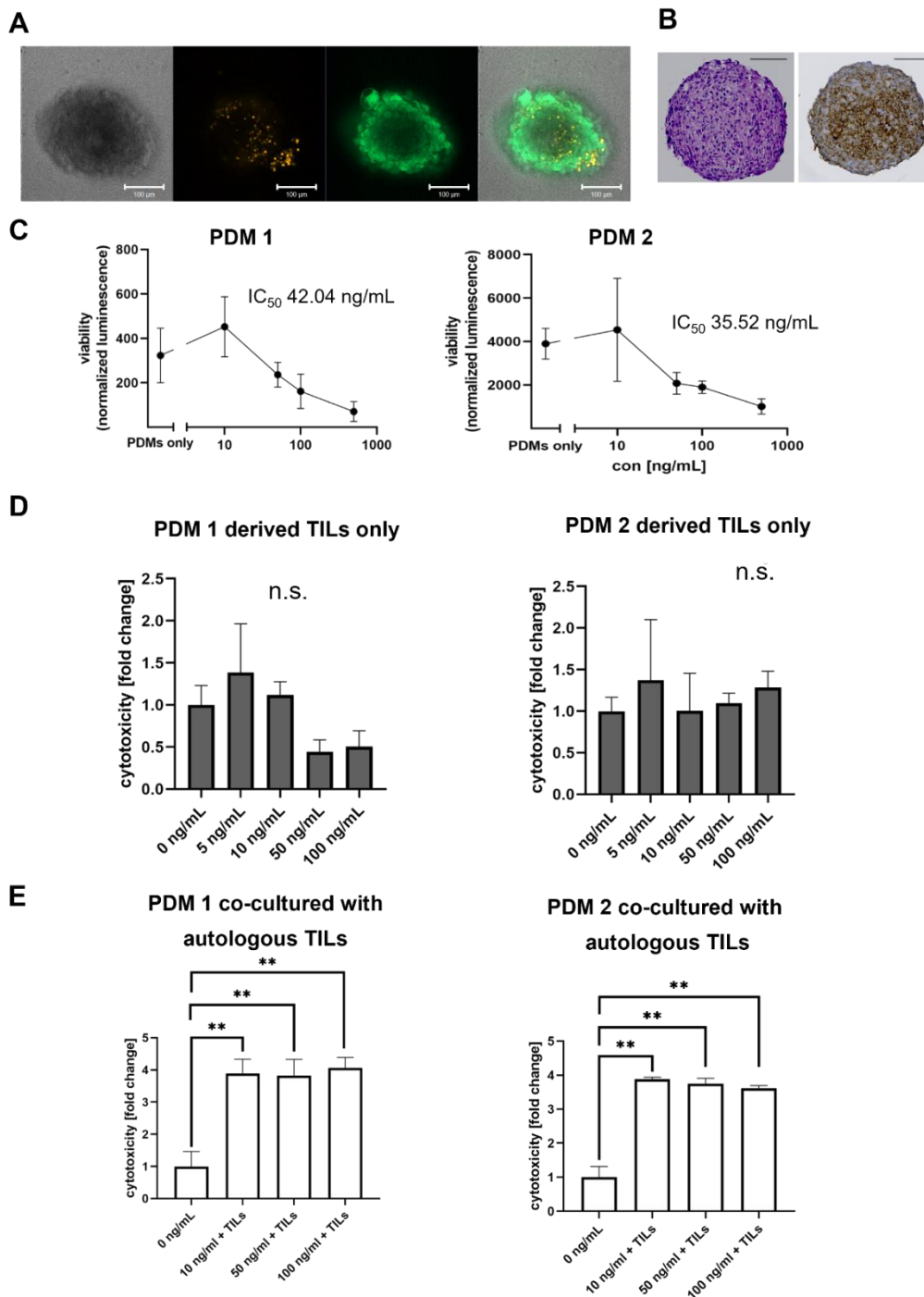
Figure 14: *Patient derived microtumors (PDMs) display sensitivity towards Argyrin F treatment and co-cultures with autologous tumor infiltrating lymphocytes (TILs) prove cytotoxic effects*

*A, Live- (green) and dead- (orange) stain of representative PDM. Scale bars 100 μm. B, Histological analysis of a PDM depicting H&E and glial fibrillary acidic protein (GFAP). Scale bars 100 μm. C, Dose-response curve of two PDM models treated with Argyrin F. IC_{50} values derived from dose-response curve are depicted. D, Cytotoxicity read-out of TILs treated with Argyrin F. E, Cytotoxicity read-out of co-culture of PDM with autologous TILs treated with Argyrin F. Statistical analysis using Two-way ANOVA with multiple testing using Dunnetts method. ** p < 0.001*

has been described to have immunogenic activity as it lead to an interferon gamma (IFNγ) response of T cells upon presentation in the immunopeptidome by Jarmalavicius et al. [180]. Further peptides included FYVDTVRAF (POLE), TYTYEKLLW (CTNNB1) which have been described in melanoma [181] and IYFEYSHAF (MSH3) described in breast cancer [182]. Novel treatment-induced peptides like TYmEASAKI (RRAS2), AWLSDSPLF (RB1), SQSTKPKKVRPSAS (PALLD), LDGTCSLH (PALLD), RLLGICLTSTVQLITQLmPFGC (EGFR), RMRSVLISLK (CLTA), LEPPQHGALQKEDGPQART (MCSP) and DCASGLCCARHFWSKICKP (DKK1) were also detected. A comprehensive list of cancer associated peptides can be found in **Table 1**.
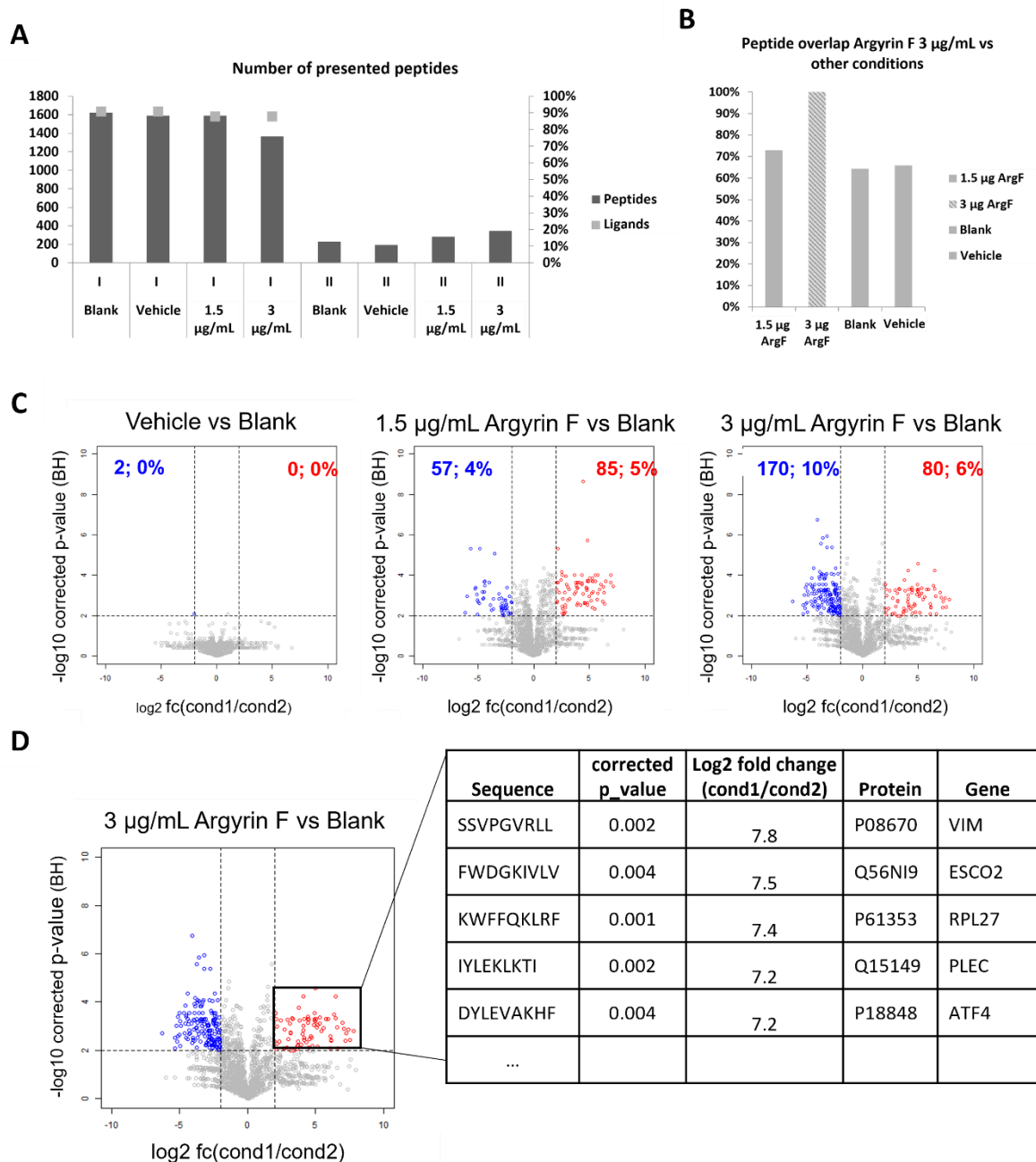
Figure 15: *HLA ligandome displays up- and downmodulated peptides upon Argyrin F treatment in LNZ308 cells*

*A, Number of presented peptides divided in class I and II peptides of LNZ308 cells treated with Argyrin F. **B**, Overlap of peptides comparing 3 µg/mL Argyrin F with all other treatment conditions. **C**, Volcano blots depicting detected peptides in vehicle, 1.5 µg/mL Argyrin F and 3 µg/mL Argyrin F compared to blank condition. Treatment conditions show up- (red) and down- (blue) modulated peptides upon Argyrin F treatment. **D**, Exemplary list of 5 upmodulated peptides in the 3 µg/mL Argyrin F treated LNZ308 cells. Sequences, corrected p-value, log2 fold change(cond1/cond2) protein, and gene names are depicted. SSVPGVRLL is a known immunogenic peptide [180]. ATF4, activating transcription factor 4; ESCO2, establishment of sister chromatid cohesion N-acetaltransferase 2; PLEC, plectin; RPL27, ribosomal protein L27; VIM, vimentin.*

Table 1: Treatment-induced peptides in the immunopeptidome of LN229 and LNZ308 cells after Argyrin F treatment

LN229		
Class I peptides		
Argyrin F 0.2 µg/mL		
Sequence	**Tumor association/known immunogenicity**	**Gene**
LEPPQHGALQKEDGPQART	Cancer immunity	MCSP
Argyrin F 0.4 µg/mL		
Sequence	**Tumor association/known immunogenicity**	**Gene**
DCASGLCCARHFWSKICKP	Cancer immunity	DKK1
LNZ308		
Class I peptides		
Argyrin F 3 µg/mL and 1.5 µg/mL		
Sequence	**Tumor association/known immunogenicity**	**Gene**
FYVDTVRAF	Uniprot	POLE
IYFEYSHAF	Uniprot	MSH3
TYTYEKLLW	Uniprot	CTNNB1

3 µg Argyrin F		
Sequence	**Tumor association/known immunogenicity**	**Gene**
SSVPGVRLL	Known IFNγ reaction	VIM
LYLLNTTKL	Uniprot	MLH1
SFDLAIKGV	Uniprot	MINPP1
TYmEASAKI	Uniprot	RRAS2
Argyrin F 1.5 µg/mL		
Sequence	**Tumor association/known immunogenicity**	**Gene**
AWLSDSPLF	Uniprot	RB1
Class II peptides		
Argyrin F 3 µg/mL and 1.5 µg/mL		
Sequence	**Tumor association/known immunogenicity**	**Gene**
FYDIDLDPETEQVNGLF	Uniprot	MTHFD1
SQSTKPKKVRPSAS	Uniprot	PALLD
YDIDLDPETEQVNGLF	Uniprot	MTHFD1
Argyrin F 3 µg/mL		
Sequence	**Tumor association/known immunogenicity**	**Gene**
DIDLDPETEQVNGLF	Uniprot	MTHFD1
LDGTCSLH	Uniprot	PALLD
NYLDRFLSL	Cancer immunity	CCND1
RLLGICLTSTVQLITQLmPFGC	Uniprot	EGFR

Abbreviations (alphabetical order): CCND1, cyclin D1; CTNNB1: catenin beta 1; DKK1, Dickkopf-related porotein; EGFR, epithelial growth factor receptor; MCSP, melanoma-associated chondroitin sulfate proteoglycan; MINPP1, multiple inositol-polyphosphate phosphatase 1; MLH1, human mutL homolog 1; MSH3, mutS homolog 3; MTHFD1, methylenetetrahydrofolate dehydrogenase 1; PALLD, palladin; POLE, DNA polymerase epsilon, catalytic subunit; RB1, retinoblastoma 1; RRAS2, RAS related 2; VIM, vimentin

3.1.5 Combination of Argyrin F with anti PD-1 treatment in PDM/TIL co-culture models

Taken together, the *in vivo* (**Figure 13**), *ex vivo* (**Figure 14**) and immunopeptidome data (**Figure 15**) suggest an immunogenic potential of Argyrin F therapy. To exploit this treatment-induced vulnerability, a combination of Argyrin F treatment together with immune checkpoint inhibition, i.e., anti PD-1 therapy, was used. For this, functional cytotoxic read-out generated by Argyrin F treatment combined with Nivolumab (anti PD-1) on PDM/TIL co-cultures was analyzed. PDM 3 with a high CD3$^+$ TIL population, i.e., more than 80%, and PDM 4 with a low CD3$^+$ TIL population of less than 10% (**Figure 16** A, the gating strategy for this can be found in **Appendix Figure 5**), were selected. The combination of 75 ng/mL Argyrin F with 50 µg/mL Nivolumab was able to significantly increase the cytotoxic read-out detected compared to either monotherapy in PDM 3, but not in PDM 4 co-cultured with their autologous TILs (**Figure 16** B, C). This observation might suggest that a treatment benefit is achieved via T cell-mediated cytotoxicity. Furthermore, in PDM 3 an increase of CD8$^+$TNFa$^+$ cells was seen (**Figure 16** B), with the highest levels being detected in the combination therapy (gating strategy depicted in **Appendix Figure 5**). Next, the novel combination was tested in the SMA560/VM/Dk mouse model *in vivo*.

3.1.6 Argyrin F in combination with anti PD-1 therapy in the SMA560/VM/Dk mouse model

VM/Dk mice injected with SMA560 cells were treated with vehicle, Argyrin F monotherapy, anti PD-1 monotherapy and the combination of both, five days after the surgery according to the treatment plan (**Figure 17** A, animal scoring sheet can be found in **Appendix Table 2**). In line with the first *in vivo* experiment, Argyrin F prolonged survival moderately (median survival control: 16 days, Argyrin F alone: 19 days), a similar effect was detected for PD-1 therapy alone (median survival: 22 days). The median time until onset of neurological symptoms was significantly prolonged by ten days in combination of Argyrin F and PD-1 blockade compared to the Argyrin F monotherapy (p=0.0019, two-way ANOVA) and by seven days compared with anti PD-1 treatment (p=0.0215, two-way ANOVA) (**Figure 17** B, C). Consequently, the histological work-up showed the previously detected increase in CD3$^+$, CD4$^+$ and CD8$^+$ T cells in the Argyrin F monotherapy group, which was even more pronounced in the combination therapy setting (**Figure 17** D).
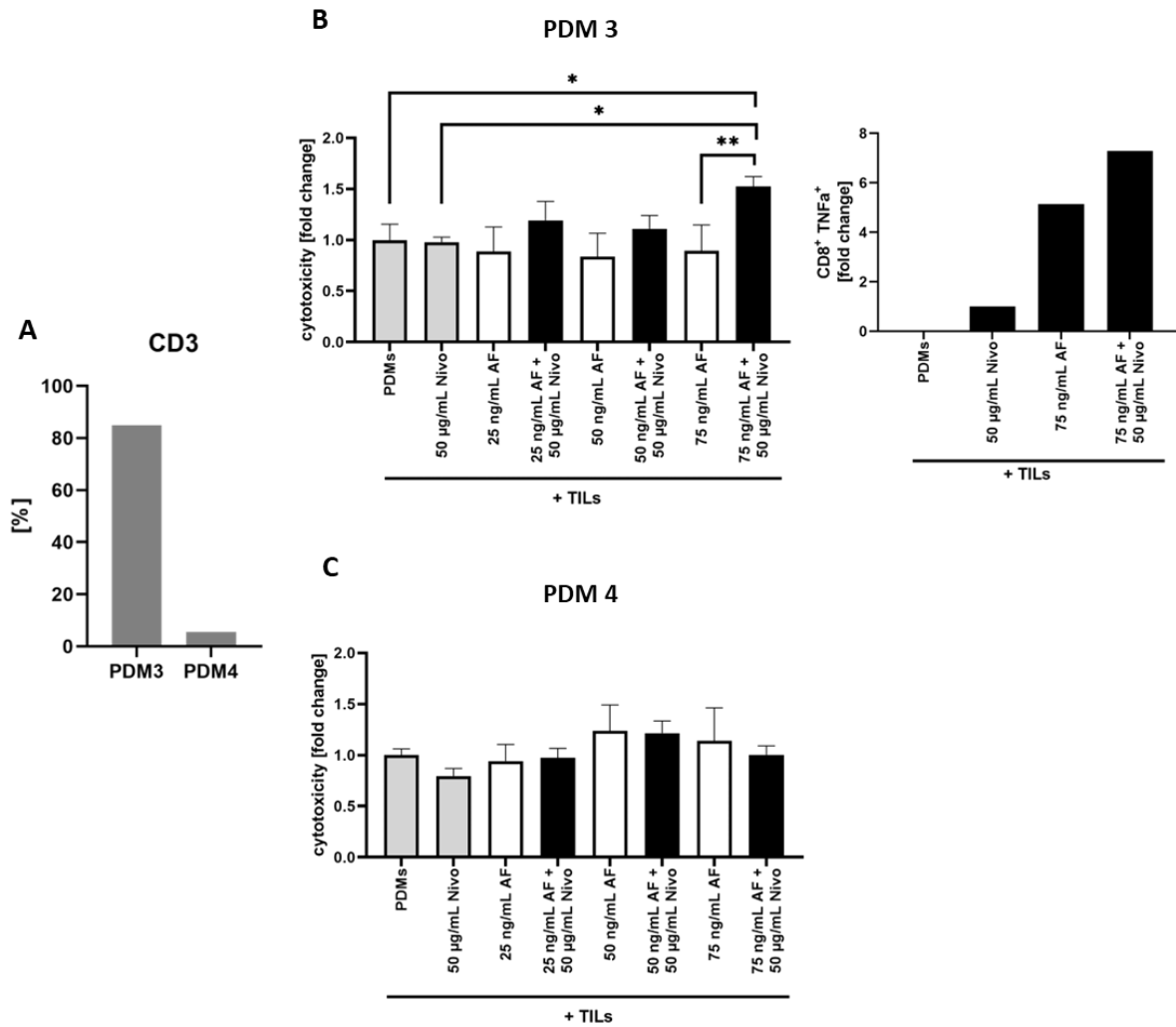
Figure 16: *Combination of Argyrin F with PD-1 blockade in PDMs co-cultured with their autologous TILs*

*A, Flow cytometry analysis of TILs derived from PDM3 showing a high abundance of CD3+ cells and PDM4 showing a low abundance for CD3+ cells. **B**, Cytotoxicity read-out of PDM3 co-cultured with autologous TILs treated with Nivolumab (Nivo), Argyrin F (AF) and a combination of both. Bar graph on the right side depicts levels of tumor necrosis factor alpha (TNFa) positive CD8 T cells in indicated treatment conditions. **C**, Cytotoxicity read-out of PDM4 co-cultured with autologous TILs. Values were normalized to PDMs plus TILs signal. Statistical analysis using Two-way ANOVA with multiple testing using Dunnett´s method. * p < 0.01, ** p < 0.01*
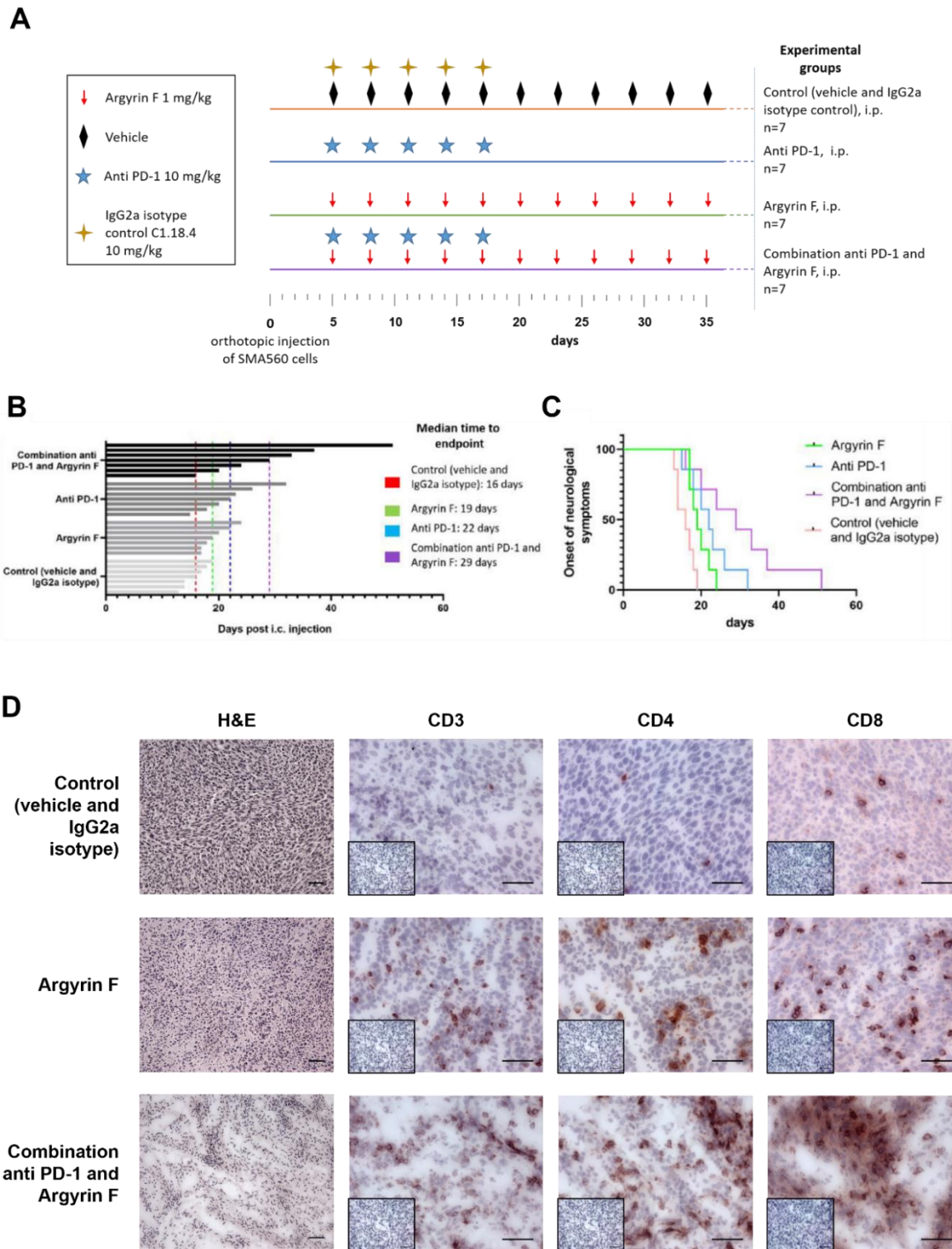
Figure 17: Combination of Argyrin F and PD-1 blockade in the SMA560/VM/Dk model is superior compared to each monotherapy

A, Treatment plan for all groups, start of treatment 5 days post-surgery. **B**, Waterfall plot depicting the time until onset of neurological symptoms in days after surgery per group. Median survival times for each group are indicated in the plot (n=7). **C**, Kaplan-Meier curve depicting time until onset of neurological symptoms. **D**, Representative pictures of histological panel depicting H&E, CD3, CD4 and CD8 staining for vehicle, Argyrin F and combination anti PD-1 and Argyrin F treated tumors. Scale bars 50 μm.

3.2 ATR inhibition in experimental glioma

Parts of this project have been published in the Journal of Experimental & Clinical Cancer Research [183].

3.2.1 ATR inhibition in the SMA560/VM/Dk mouse model

In glioma the basic Helix loop helix (bHLH) transcription factor (TF) family is frequently upregulated. Previous work in the laboratory linked this upregulation with a higher sensitivity towards ATR inhibition (ATRi) [120].

The present project aims to delve further into the novel treatment option of ATRi in glioma. For this, the anti-glioma efficacy of ATRi in different glioma models was further elucidated. First, an *in vivo* experiment using the SMA560/VM/Dk glioma mouse model was conducted. As illustrated in **Figure 18** A, the ATR inhibitor AZD6738 and the respective vehicle control DMSO were administered per oral gavage five days per week at 50 mg/kg followed by two days of drugs holidays, reflecting the therapy schedule of patients in the clinics. The resulting survival comparison shows a significant survival benefit (p=0.0345) for AZD6738 treated animals compared to vehicle treated ones (**Figure 18** B).
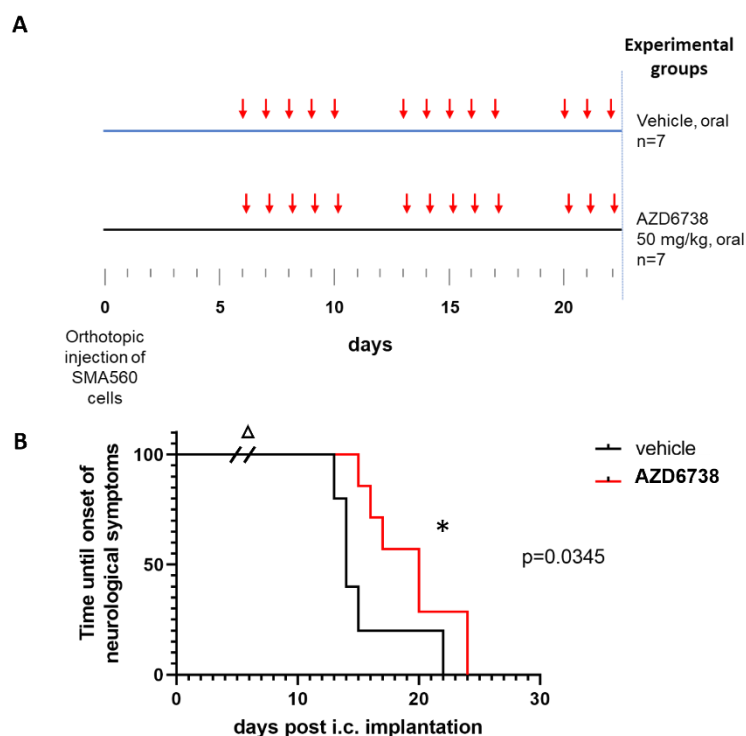
Figure 18: *Anti-glioma efficacy of AZD6738 in the SMA560/VM/Dk model*

A, Treatment schedule, treatment starts 6 days post-surgery. (n=7) B, Kaplan-Meier curve depicting the time until onset of neurological symptoms. Statistical analysis using Gehan-Breslow-Wilcoxon test, p-values < 0.05 considered significant. Δ Of note, two animals in the control group were taken out due to reasons unrelated to tumor development (post-surgery complication, eye infection).

3.2.2 Molecular characterization of ATR inhibition effects *in vitro*

Next, the anti-glioma efficacy of ATRi was assessed in human LN229 and LNZ308 and murine SMA560 and GL261 long-term glioma cell lines. AZD6738 served as the main ATR inhibitor used in this project. Berzosertib, a second ATR inhibitor, was used as a control and proof of principle compound for several of the experiments.

3.2.2.1 Acute cytotoxicity and clonogenic survival effects of ATR inhibition in vitro

As a first step, the influence of ATRi on cell viability and clonogenic survival treating LN229, LNZ308, SMA560 and GL261 cells with AZD6738 (**Figure 19**, **Appendix Figure 6**) and analogously Berzosertib (**Figure 20**, **Appendix Figure 7**) was analyzed. All experiments revealed a dose dependent reduction in cell viability and clonogenic survival. From those results, IC_{25}- and IC_{50}-values for both ATR inhibitors in both experimental set-ups were extracted (**Table 2**, **Table 3**).
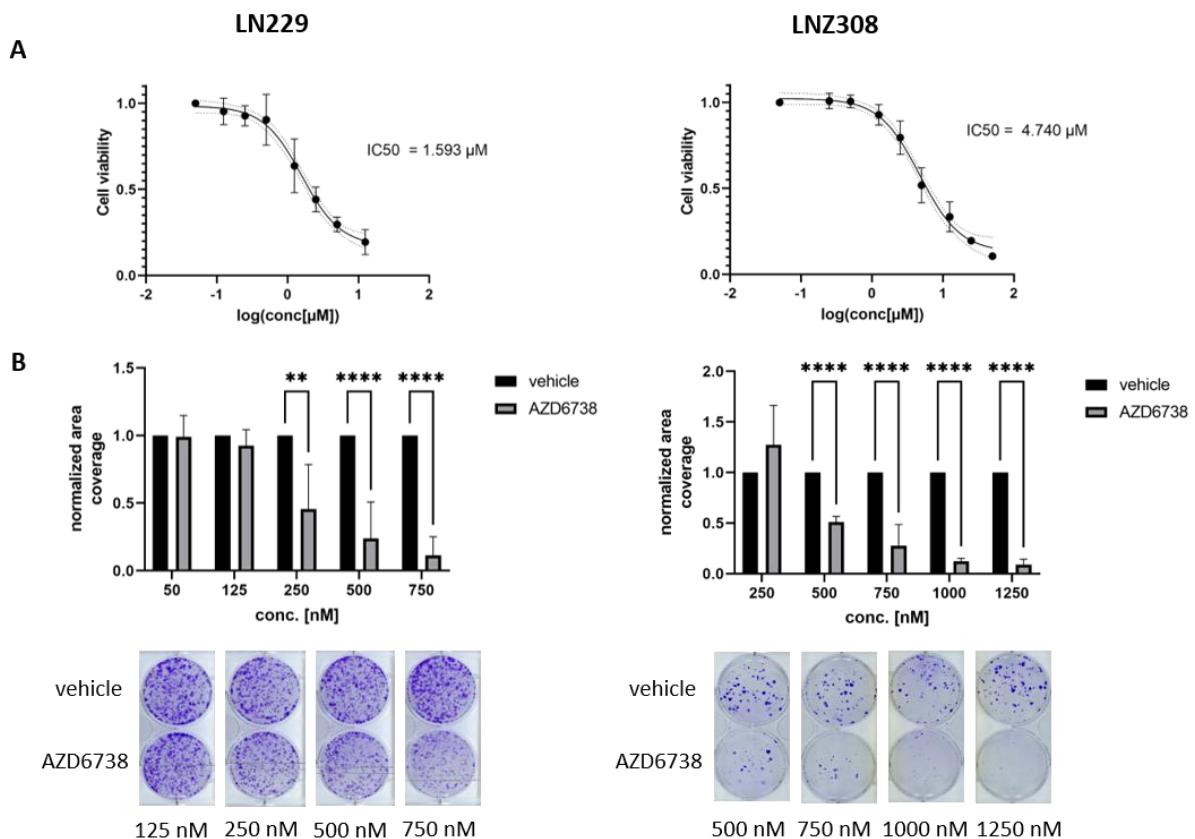
Figure 19: *Acute cytotoxicity and clonogenic survival assays in LN229 and LNZ308 cells treated with AZD6738*
A, *Dose dependent reduction of cell viability in LN229 and LNZ308 cell upon AZD6738 treatment. IC_{50}-values for each cell line are also indicated in the graph.* ***B,*** *Bar graphs depicting dose dependent reduction of clonogenic survival in LN229 and LNZ308 cells treated with AZD6738. Lower panel shows exemplary pictures of cells treated*
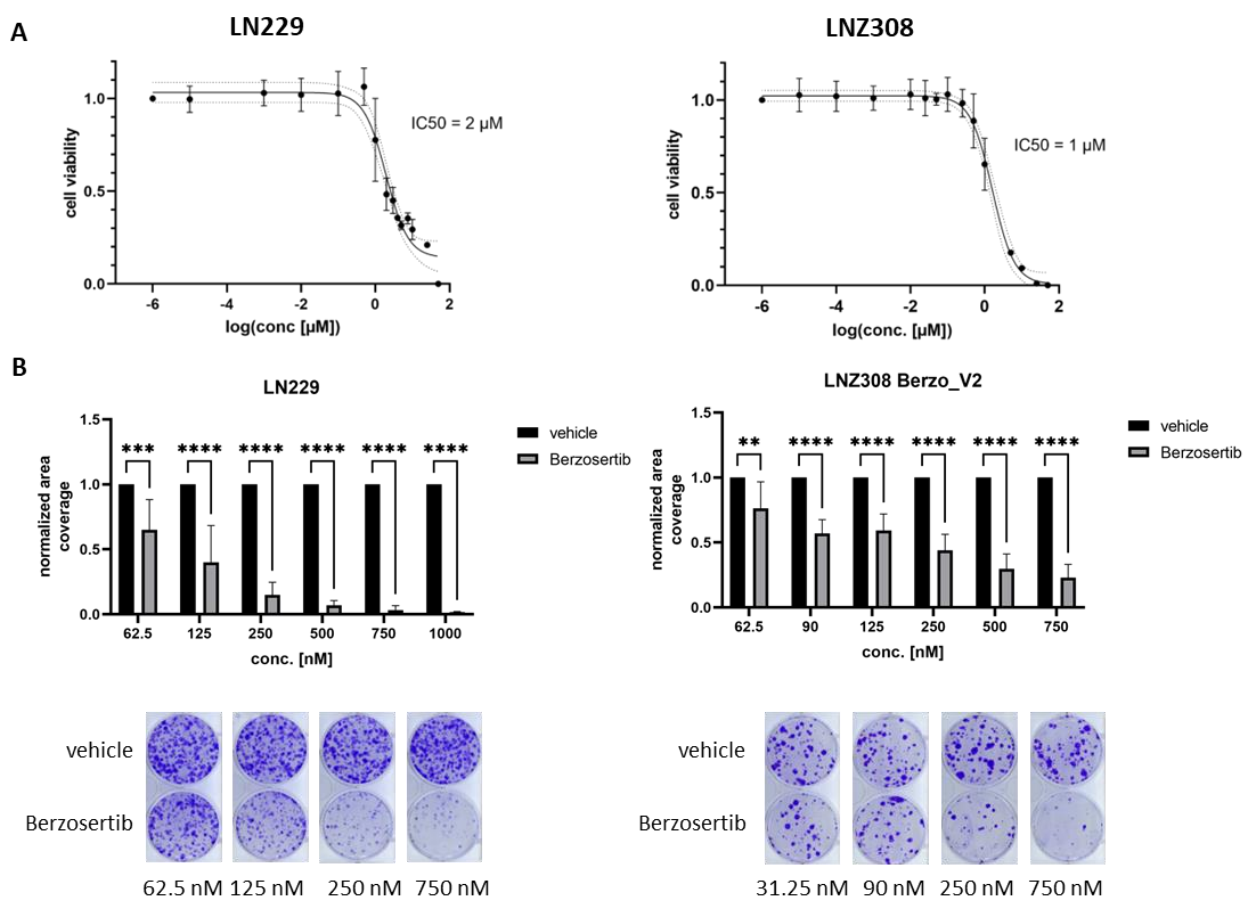
Figure 20: *Acute cytotoxicity and clonogenic survival assays in LN229 and LNZ308 cells treated with Berzosertib **A**, Dose dependent reduction of cell viability in LN229 and LNZ308 cell upon Berzosertib treatment. IC_{50}-values for each cell line are also indicated in the graph. **B**, Bar graphs depicting dose dependent reduction of clonogenic survival in LN229 and LNZ308 cells treated with Berzosertib. Lower panel shows exemplary pictures of cells treated in indicated concentrations and stained with Crystal Violet. Statistical analysis was done using multiple t-tests with the Holm-Sidak method. * p < 0.05, ** p < 0.01, *** p < 0.001, **** p < 0.0001.*

Comparing the IC_{25}- and IC_{50}-values for AZD6738 and Berzosertib treatment in each cell line, Berzosertib concentrations necessary to achieve an inhibition of 25% and 50%, respectively, are generally lower than AZD6738 concentrations also across experimental set-ups. Furthermore, fast proliferating cells, i.e., SMA560 and GL261, display lower IC_{25}- and IC_{50}-values than mediocre fast proliferating cells, i.e., LN229, or slow proliferating cells, i.e., LNZ308 (**Table 2**, **Table 3**). Nevertheless, AZD6738 remained the main focus compound due to its good BBB penetrance [184]. Studies on Berzosertib, on the other hand, have shown active efflux of Berzosertib at the BBB and strong binding to brain tissue [185].

Table 2: IC_{25}- and IC_{50}-values for acute cytotoxicity assays after 72 h treatment

	AZD6738		Berzosertib	
	IC_{25}	IC_{50}	IC_{25}	IC_{50}
LN229	0.8 µM	1.6 µM	1 µM	2 µM
LNZ308	2.1 µM	4.7 µM	0.5 µM	1 µM
SMA560	0.38 µM	0.55 µM	0.005 µM	0.02 µM
GL261	0.5 µM	0.7 µM	0.25 µM	0.75 µM

Table 3: IC_{25}- and IC_{50}-values for clonogenic survival assays

	AZD6738		Berzosertib	
	IC_{25}	IC_{50}	IC_{25}	IC_{50}
LN229	125 nM	250 nM	62.5 nM	125 nM
LNZ308	250 nM	450 nM	62.5 nM	90 nM
SMA560	50 nM	125 nM	15.6 nM	31.25 nM
GL261	62.5 nM	125 nM	90 M	125

3.2.2.2 Analysis of apoptosis induction and cell cycle status upon ATR inhibition

To further elucidate the underlying mechanisms of ATRi in glioma, treatment dependent apoptosis induction and cell cycle status was evaluated. Koch et al. have shown apoptosis induction and cell cycle changes upon AZD6738 treatment in one glioma cell line [120]. In this project, the spectrum of cell lines was expanded to reflect the inter- and intratumoral heterogeneity of GB.

Induction of apoptosis was detected via flow cytometric analyses of Annexin V-PI stains (gating strategy can be found in **Appendix Figure 9**). All 4 cell lines show an accumulation of apoptotic cells

upon AZD6738 treatment (**Figure 21** A, **Appendix Figure 8** A). In the cell cycle analyses (gating strategy **Appendix Figure 3**), LN229 and GL261 cells displayed an S-phase arrest, while LNZ308 cells accumulated in G2-phase. No regulation of the cell cycle was detected in SMA560 cells (**Figure 21** B, **Appendix Figure 8** B).

As expected, a consistent anti-glioma efficacy of ATRi across different glioma long-term cell lines regarding cytotoxicity, reduction of clonogenic survival (**Figure 19**, **Figure 20**, **Appendix Figure 6**, **Appendix Figure 7**) and apoptosis induction (**Figure 21** A, **Appendix Figure 8** A) was seen. However, the accumulation of cells upon ATRi in different cell cycle phases (**Figure 21** B, **Appendix Figure 8** B) lead to the hypothesis of differing underlying molecular mechanisms.
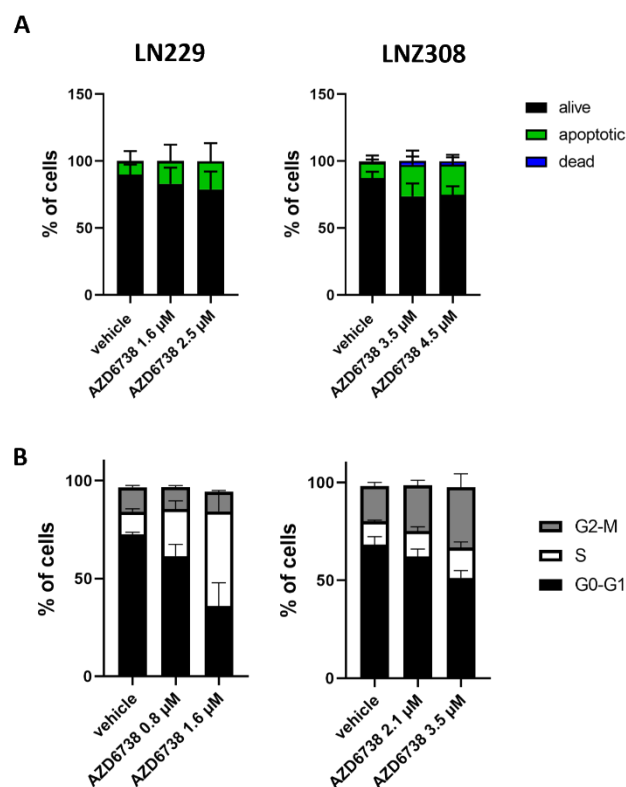
Figure 21: Flow cytometric analysis of apoptosis and cell cycle status of AZD6738 treated LN229 and LNZ308 cells A, Analysis of apoptosis induction in LN229 and LNZ308 cells upon AZD6738 treatment using Annexin V/PI staining evaluated by flow cytometry (n=3). B, Cell cycle analysis of LN229 and LNZ308 cells treated with AZD6738 in the indicated concentrations (n=3).

3.2.2.3 Transcriptome analysis of LN229 and LNZ308 cells treated with AZD6738

To acquire a more holistic picture of molecular pathways regulated upon ATRi in glioma cells, transcriptomic profiling of the glioma long-term cell lines LN229 and LNZ308 after AZD6738 treatment was conducted. Cells were treated with AZD6738 and respective vehicle control for 2 h, 24 h and 72 h.

RNA of the different conditions was extracted and sent for analysis. Resulting data was analyzed using the DESeq2 R package [177]. Initial analyses of transcriptomic data included principal component analyses (PCA) that showed that the strongest differentiator between all samples was the underlying cell line as all samples from one cell line clustered on the far left or far right of the plot. The second variable that differentiated the samples was treatment time, i.e., the longer the treatment duration, the stronger the differences compared to the control (**Appendix Figure 10** A). Volcano plots depicted in **Appendix Figure 10** B show graphically the up and downregulated genes after 72 h AZD6738 treatment per cell line. In the 72 h condition, we found 897 significantly up- and 151 significantly downregulated genes in LN229 cells and 1559 significantly up- and 842 significantly downregulated genes in LNZ308 cells compared to respective vehicle treatment conditions (**Appendix Table 3**, **Appendix Table 4**). These differentially expressed genes (DEG) were next analyzed for their overlap between the cell lines separated by up- and downregulation. 341 genes were upregulated in both LN229 and LNZ308 treated cells, while 22 overlapped for the downregulated genes (**Figure 22** A). The resulting list of overlapping genes was then analyzed for Kyoto encyclopedia of Genes and Genomes (KEGG) pathway affiliation [186]. Nine pathways were detected for the upregulated genes in the analysis of which three, namely Legionellosis, Amoebiasis and Hepatitis C, are not shown here as those are not biologically relevant to the research question and are most likely a result of the strong activation of the NF-kappa B signaling pathway (**Figure 22** B). For the downregulated genes only the Rap1 signaling pathway was detected.

To decipher molecular patterns that differ upon ATR inhibition the likelihood ratio test (LRT) was leveraged to determine which genes are significantly distinctly regulated between the cell lines. These hits were then re-aligned with their determined DEG score and split into up- and downregulated. Lastly, they were analyzed for KEGG pathway affiliation. Five upregulated and one downregulated pathways were detected in LN229 cells, for LNZ308 thirteen upregulated pathways were detected of which only the top six are displayed here (**Figure 22** C). No downregulated pathways in LNZ308 cells could be identified.

The three highest scoring pathways in the LRT analysis of LN229 cells are the MAPK pathway, the p53 pathway and the KEGG pathway "pathways in cancer". This last pathway entails, among others, cell cycle regulation and apoptosis pathways which are frequently dysregulated in cancer [186]. "Pathways in cancers" also scores in the LNZ308 LRT analysis significantly as seventh highest, however, due to the set cut-off it is not depicted in the graph. The pathway entails a large network of smaller pathways, this might be the reason why it was detected in both cell lines. In the LNZ308 background the three highest scoring pathways are focal adhesion, ECM-receptor interaction and
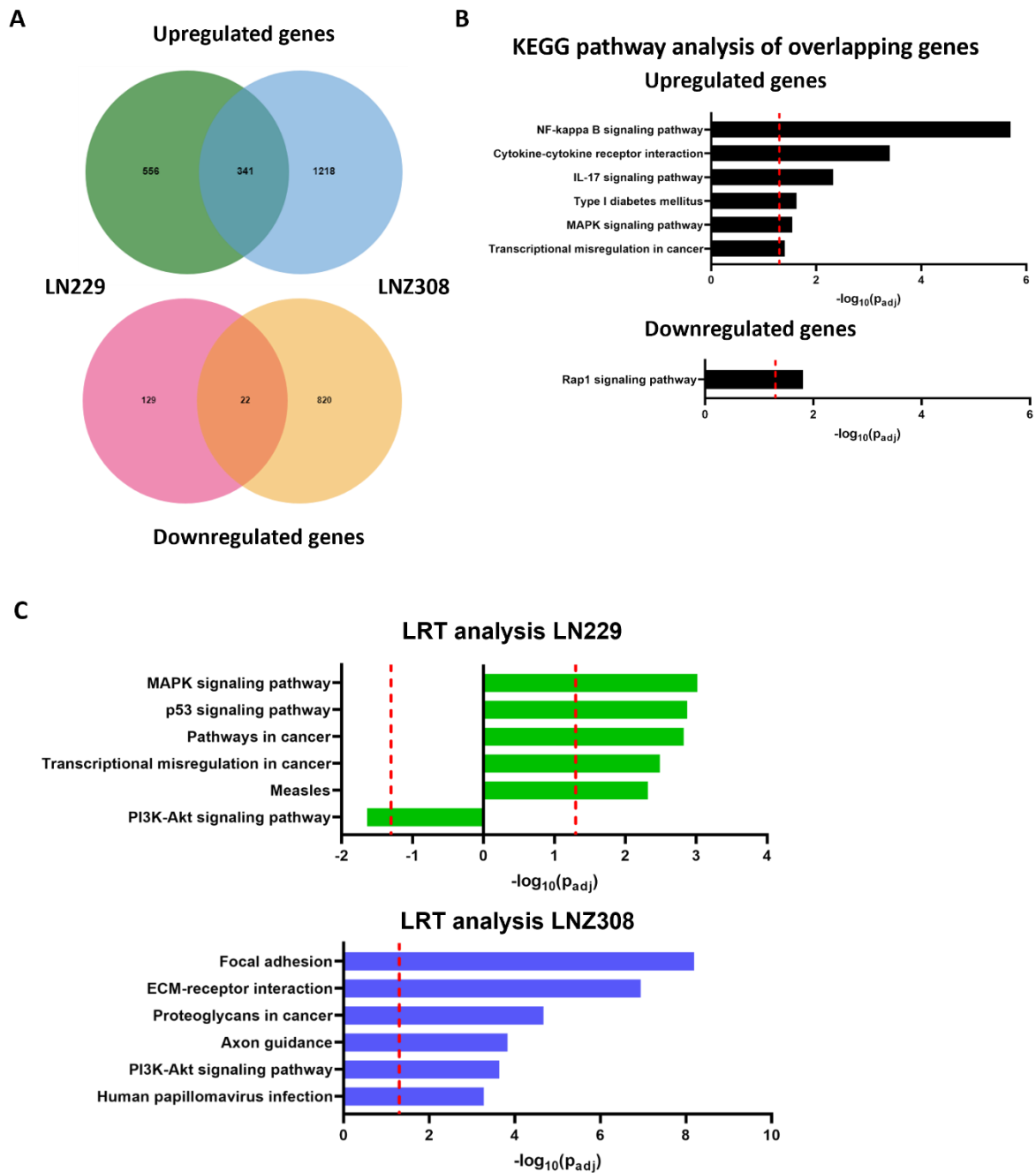
Figure 22: *Transcriptomic profiling of LN229 and LNZ308 cells treated with AZD6738 reveals commonly and distinctly regulated KEGG pathways*

***A**, Venn diagrams of differentially expressed genes (DEGs) in LN229 and LNZ308 cells treated with AZD6738 for 72 h. 341 upregulated genes and 22 downregulated genes are identified to overlap in both cell lines upon treatment. **B**, KEGG pathway analysis of identified overlapping genes. **C**, Based on the likelihood ratio test (LRT), genes identified to be significantly differentially expressed between the cell lines upon treatment are analyzed for KEGG pathway affiliation. p53 signaling is strongly upregulated in LN229 cells, PI3K-Akt signaling is opposingly regulated in the two cell lines.*

proteoglycans in cancer. Based on this, the activity of matrix metalloproteases was analyzed, but no significant difference between treated and untreated cells was seen (data not shown).

Of note, LNZ308 cells are p53[null] and therefore cannot activate the p53 pathway upon ATRi as LN229 cells. This might also explain the differing results in cell cycle analyses (**Figure 21** B) as ATR together with ATM are two of the main cell cycle checkpoint kinases in the DNA damage response for which p53 is an important part of the downstream signaling regarding cell cycle regulation [113, 187]. Strikingly, LN229 cells downregulate the PI3K-Akt signaling pathway which is upregulated in LNZ308 cells potentially providing a novel therapeutic window.

3.2.2.4 Proteomic profiling of LN229 and LNZ308 cells treated with AZD6738

To validate our transcriptomics data, DigiWest protein profiling analyses were performed. With this method 155 different antibodies were used to analyze the proteomic signature of LN229 and LNZ308 cells treated with AZD6738 analogously to the transcriptomic samples. Antibody selection was based on the transcriptomic findings and focused on cell cycle regulation, apoptosis, NF-kappa B and target engagement. The full list of antibodies can be found in **Appendix Table 5**. Similarly, to our previous findings, the proteomic signature revealed shared (**Figure 23** A) and distinctly regulated genes (**Figure 23** B). Among the shared significantly downregulated markers are pATR, a marker for target engagement, Chk2, involved in the cell cycle and ATR/ATM signaling, and Ku80, part of the DNA damage repair machinery. Examples for upregulated markers are NF-kappa B p100, in line with the transcriptomic data, cleaved PARP signal, an apoptosis marker, and pH2A.X also known as γH2A.X, a marker for DNA damage (**Figure 23** A).

In line with the transcriptomic data, p53 is upregulated in LN229 while a downregulation is measured in LNZ308, a similar pattern is seen for p21. Interestingly, different apoptosis markers, e.g., Bax, are distinctly regulated in the two cell lines as well, potentially pointing at distinct apoptotic signaling in between the cell lines. Furthermore, markers for the PI3K-Akt pathway, e.g., pAkt (S473), are downregulated in LN229 and tend to be up-regulated in LNZ308 (**Figure 23** B).

Taken together, the transcriptomic (**Figure 22**) and proteomic (**Figure 23**) data complement each other, proving shared and distinct signaling pathways in glioma long-term cell lines upon ATRi by AZD6738.

Figure 23*: Protein profiling using DigiWest analyses of LN229 and LNZ308 cells treated with AZD6738 confirm transcriptomic analyses*

*Based on the transcriptomic data, DigiWest protein profiling analyses were performed. Antibody panels covered markers for cell-cycle regulation, apoptosis, NF-κB, p53 signaling and DNA damage response. **A**, Heatmap depicting treatment specific effects across both cell lines confirming target engagement (pATR), apoptosis induction (cleaved PARP), NFκB activation (NF-κB p100) and cell-cycle regulation (Chk2). Statistical analysis of significance for heatmap using Wilcoxon test (non-parametric, p<0.05), for bar graphs Mann-Whitney test (non-parametric, rank comparison, p<0.05. DMSO (n=4) vs AZD6738 (n=4)). **B**, On the left heatmap depicting indicated analytes separated by cell line. On the right, bar graph depicting analytes differentially regulated in both cell lines*

68

upon treatment. In line with transcriptomic data, p53 is upregulated in LN229 cells while pAkt is downregulated in LN229 cells and trends towards upregulation in LNZ308 cells upon treatment.

3.2.3 Combining ATR inhibition with Temozolomide, Olaparib and PI3K/mTOR inhibitors

Firstly, ATRi was combined with Temozolomide which is the first-line treatment for concomitant and maintenance chemotherapy in GB [3]. In the previous study of the bHLH transcription factor family, the combination of ATRi and TMZ led to increased cytotoxicity [120].

Secondly, the combination of ATRi with PARP inhibition (PARPi) was investigated. This approach is based on the idea to pharmacologically mimic the synthetic lethal approach of BRCA1/2 deficient tumors treated with PARPi [99-101].

Thirdly, the combination of ATRi with PI3K/mTOR inhibitors Everolimus and Paxalisib was tested, based on the findings of the transcriptomic and DigiWest protein profiling. Due to the upregulation of the AKT pathway in LNZ308 cells upon ATRi a potential beneficial novel combination approach was hypothesized.

To determine synergistic capabilities of ATRi with a second therapy clonogenic survival assays were done and synergism evaluated by the Bliss Independence Criterion. Additionally, acute cytotoxicity assays were done and synergism evaluated using the ZIP synergy model.

3.2.3.1 ATR inhibition combined with Temozolomide

Combining AZD6738 or Berzosertib with Temozolomide treatment in clonogenic survival assays revealed a trend towards synergism in LN229 cells (**Figure 24** A, B left panel), while LNZ308 cells did not display this phenotype (**Figure 24** A, B right panel). In acute cytotoxicity assays this result was even more pronounced, showing very strong synergism results in LN229 with almost none in LNZ308 cells (**Figure 24** C, **Appendix Figure 11**). Analogous results were obtained using Berzosertib (**Figure 25**, **Appendix Figure 12**).
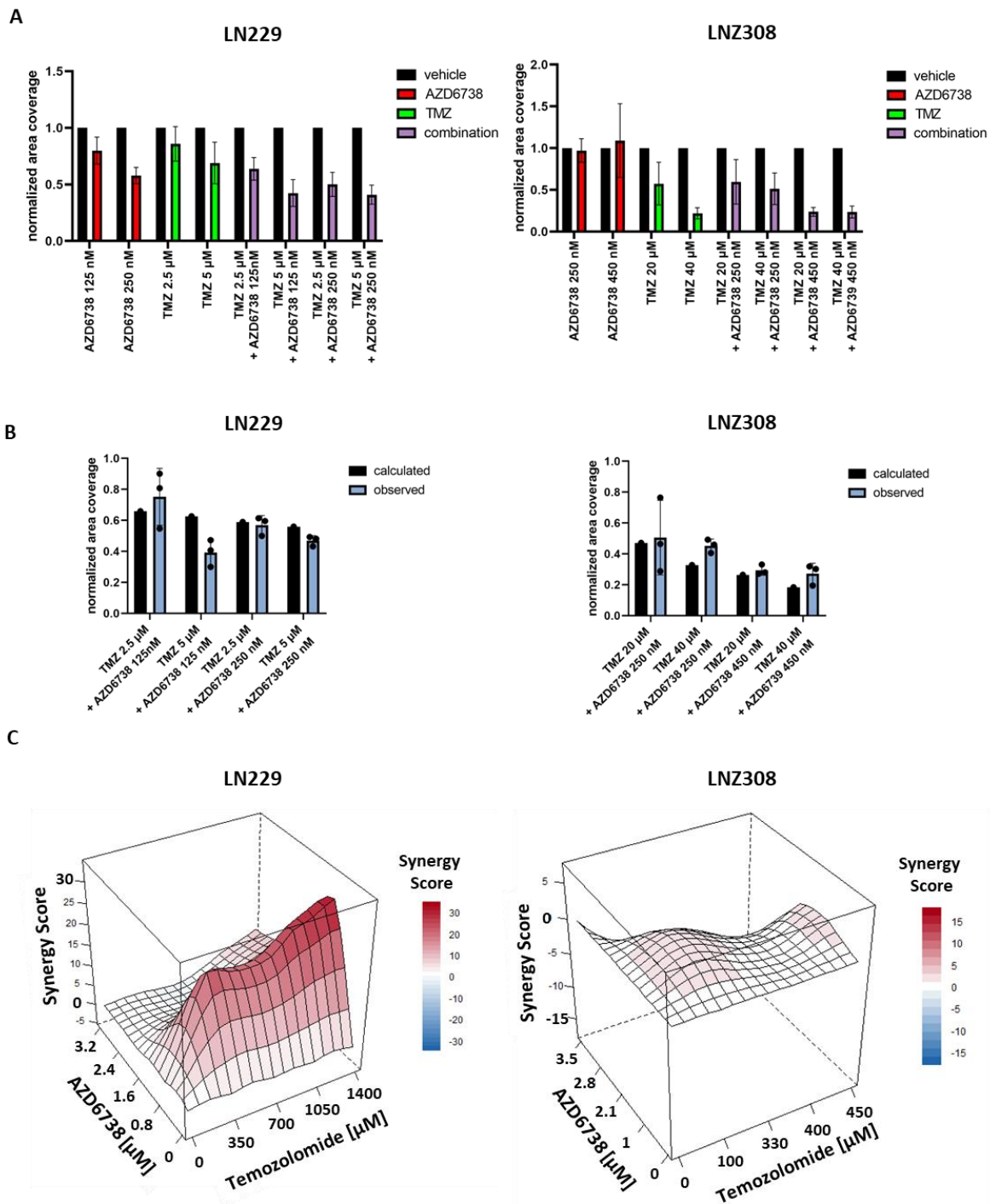
Figure 24: *Combining AZD6738 with Temozolomide shows synergistic effects in LN229 cells but not in LNZ308*

A*, Clonogenic survival assays for LN229, left, and LNZ308, right, cells treated with AZD6738 (red), Temozolomide (green) or a combination of both (purple) (n=3).* ***B****, Based on monotherapy effects measured in clonogenic survival assays, prediction for additive combination effects are calculated (black) based on the Bliss Independence Criterion and compared to observed (blue) measurements of combination treatment in clonogenic survival assays. Depicted is the evaluation of one representative run out of three (n=1).* ***C****, ZIP synergy read-out for cytotoxicity assays combining AZD6738 and Temozolomide in the indicated concentrations. Depicted is the evaluation of one representative run out of two (n=1).*
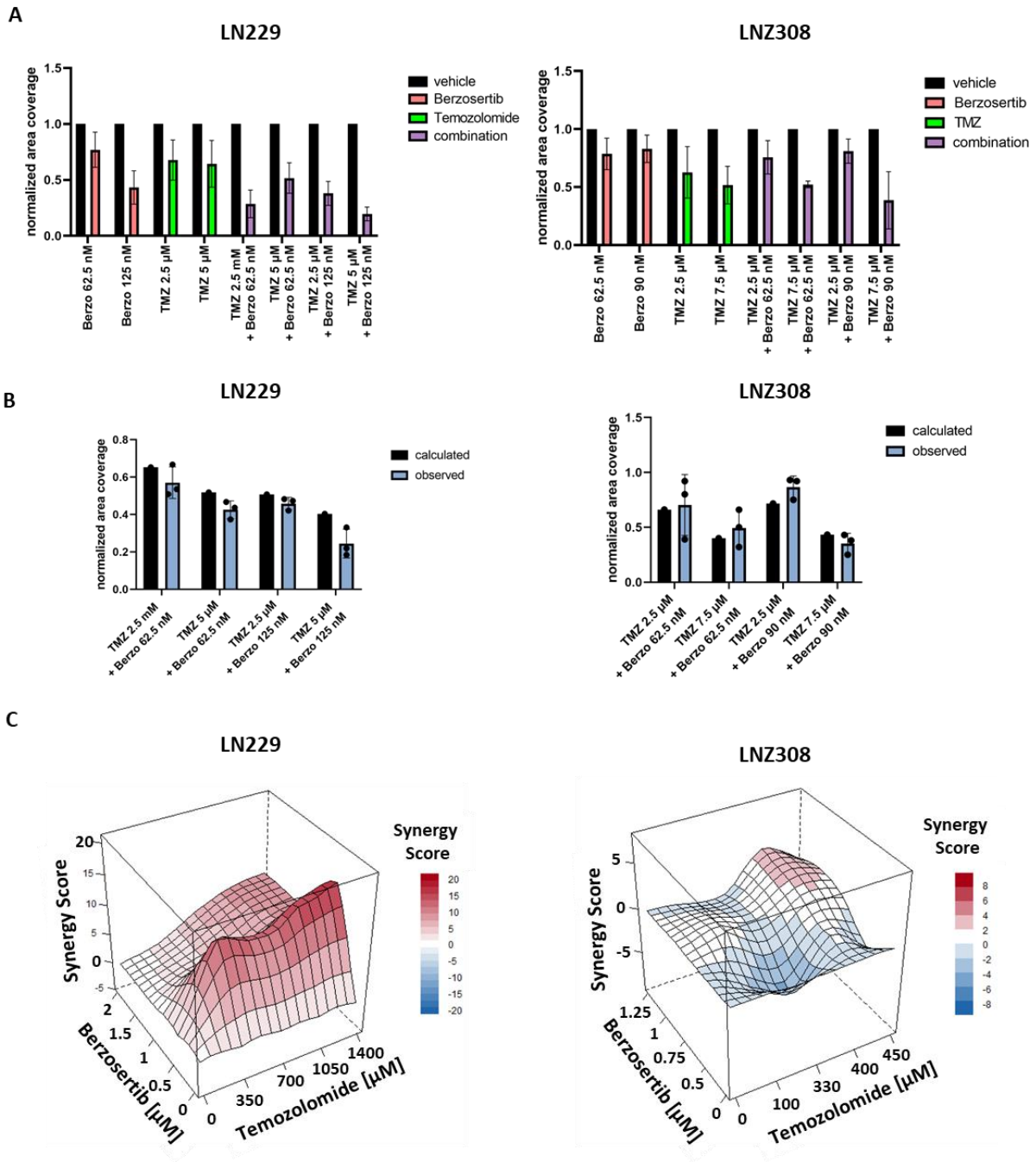
Figure 25: *Combining Berzosertib with Temozolomide shows synergistic effects in LN229 cells but not in LNZ308*

A, *Clonogenic survival assays for LN229, left, and LNZ308, right, cells treated with Berzosertib (pink), Temozolomide (green) or a combination of both (purple) (n=3). **B,** Based on monotherapy effects measured in clonogenic survival assays, prediction for additive combination effects are calculated (black) based on the Bliss Independence Criterion and compared to observed (blue) measurements of combination treatment in clonogenic survival assays. Depicted is the evaluation of one representative run out of three (n=1). **C,** ZIP synergy read-out for cytotoxicity assays combining AZD6738 and Temozolomide in the indicated concentrations. Depicted is the evaluation of one representative run out of two (n=1).*

3.2.3.2 ATR inhibition combined with Olaparib

AZD6738 in combination with Olaparib also lead to a trend towards synergism in LN229 cells regarding the clonogenic survival data, with a strong synergism signature in the acute cytotoxicity set-up (**Figure 26** left panel, **Appendix Figure 13** A). LNZ308 cells seem not to benefit from this combination (**Figure 26** right panel, **Appendix Figure 13** B). As depicted in **Figure 27**, in the proof of principle setting, using Berzosertib as ATR inhibitor, the same trend can be detected. Interestingly, in the LN229 cells the combination of Berzosertib with Olaparib lead to a more robust synergy signature than the combination of AZD6738 with Olaparib.

3.2.3.3 ATR inhibition combined with PI3K/mTOR inhibitors

The combination of ATRi with Paxalisib did not induce a synergistic read-out in LN229 cells. Neither clonogenic survival assays nor cytotoxicity synergy map analyses showed a positive synergistic signature (**Figure 28**, left). For LNZ308 cells a trend towards a synergistic read-out was detected in clonogenic survival assays and cytotoxicity synergy map analyses (**Figure 28**, right). However, in the synergy map analyses none of the tested combinations displayed a ZIP synergy score of higher than 6 (**Appendix Figure 14**).

In the clonogenic survival assays, LN229 cells treated with a combination of AZD6738 and Everolimus do not show a robust trend towards synergism. LNZ308 cells treated with this combination do show a more robust trend towards synergism (**Figure 29** A, B). Combining Everolimus with AZD6738 using cytotoxicity assays, displayed a trend towards synergism in LNZ308 cells as well (**Figure 29** C). Using 2.1 µM AZD6738 combined with any of the tested Everolimus concentrations ZIP synergy scores of above 8 were determined. However, the synergy scores did not reach higher than 9.5 (**Appendix Figure 15** B). LN229 cells treated with the AZD6738-Everolimus combination did not reach ZIP synergy scores above 6 in either of the two runs (**Figure 29** C, **Appendix Figure 15** A).
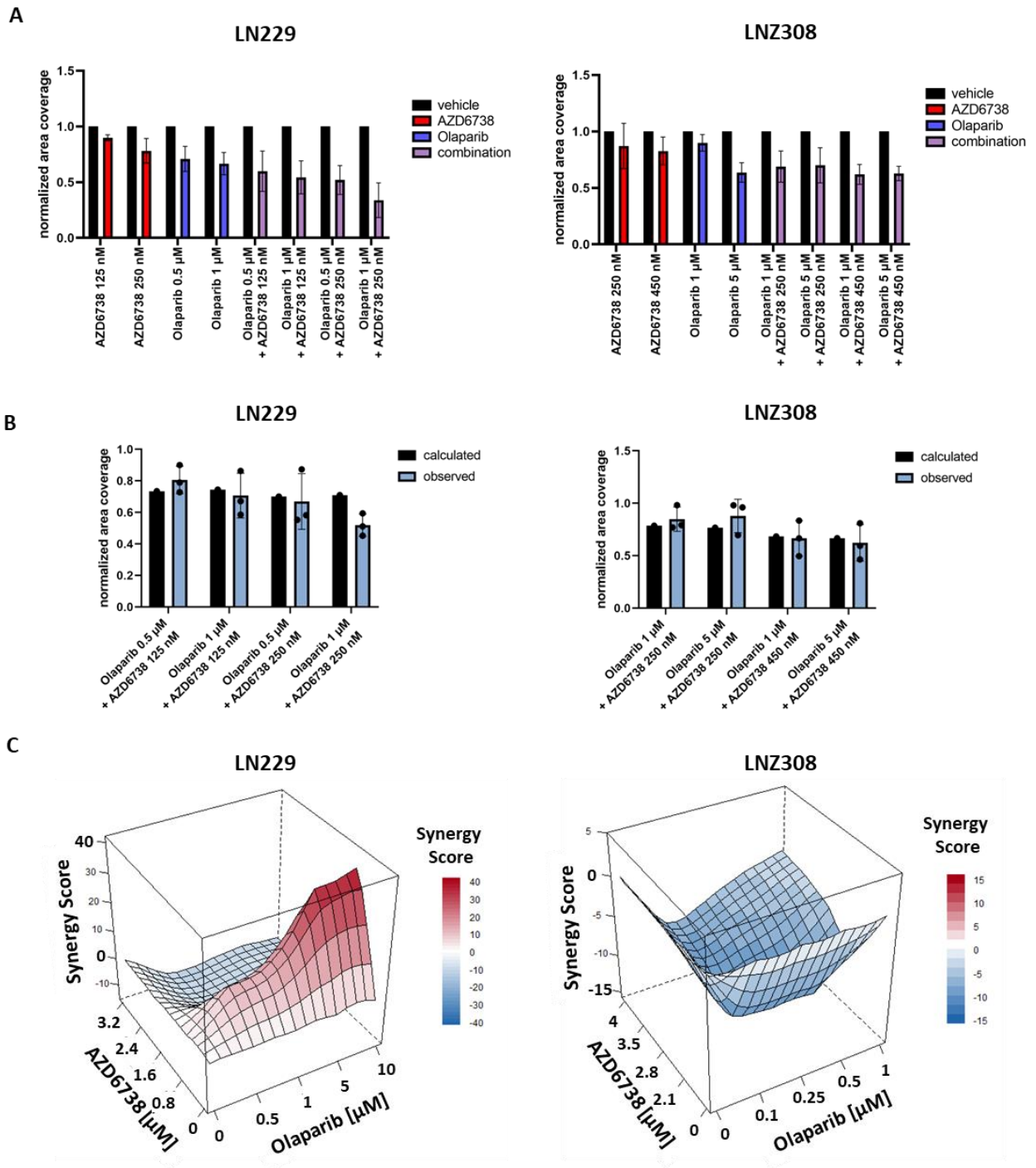
Figure 26: *Combining AZD6738 with Olaparib shows synergistic trends in LN229 cells but not in LNZ308 cells*
A, *Clonogenic survival assays for LN229, left, and LNZ308, right, cells treated with AZD6738 (red), Olaparib (blue) or a combination of both (purple) (n=3).* **B**, *Based on monotherapy effects measured in clonogenic survival assays, prediction for additive combination effects are calculated (black) based on the Bliss Independence Criterion and compared to observed (blue) measurements of combination treatment in clonogenic survival assays. Depicted is the evaluation of one representative run out of three (n=1).* **C**, *ZIP synergy read-out for cytotoxicity assays combining AZD6738 and Temozolomide in the indicated concentrations. Depicted is the evaluation of one representative run out of two (n=1).*

Figure 27: Combining Berzosertib with Olaparib shows synergistic effects in LN229 but not in LNZ308 cells
A, Clonogenic survival assays for LN229, left, and LNZ308, right, cells treated with AZD6738 (red), Olaparib (blue) or a combination of both (purple) (n=3). **B,** Based on monotherapy effects measured in clonogenic survival assays, prediction for additive combination effects are calculated (black) based on the Bliss Independence Criterion and compared to observed (blue) measurements of combination treatment in clonogenic survival assays. Depicted is the evaluation of one representative run out of three (n=1).
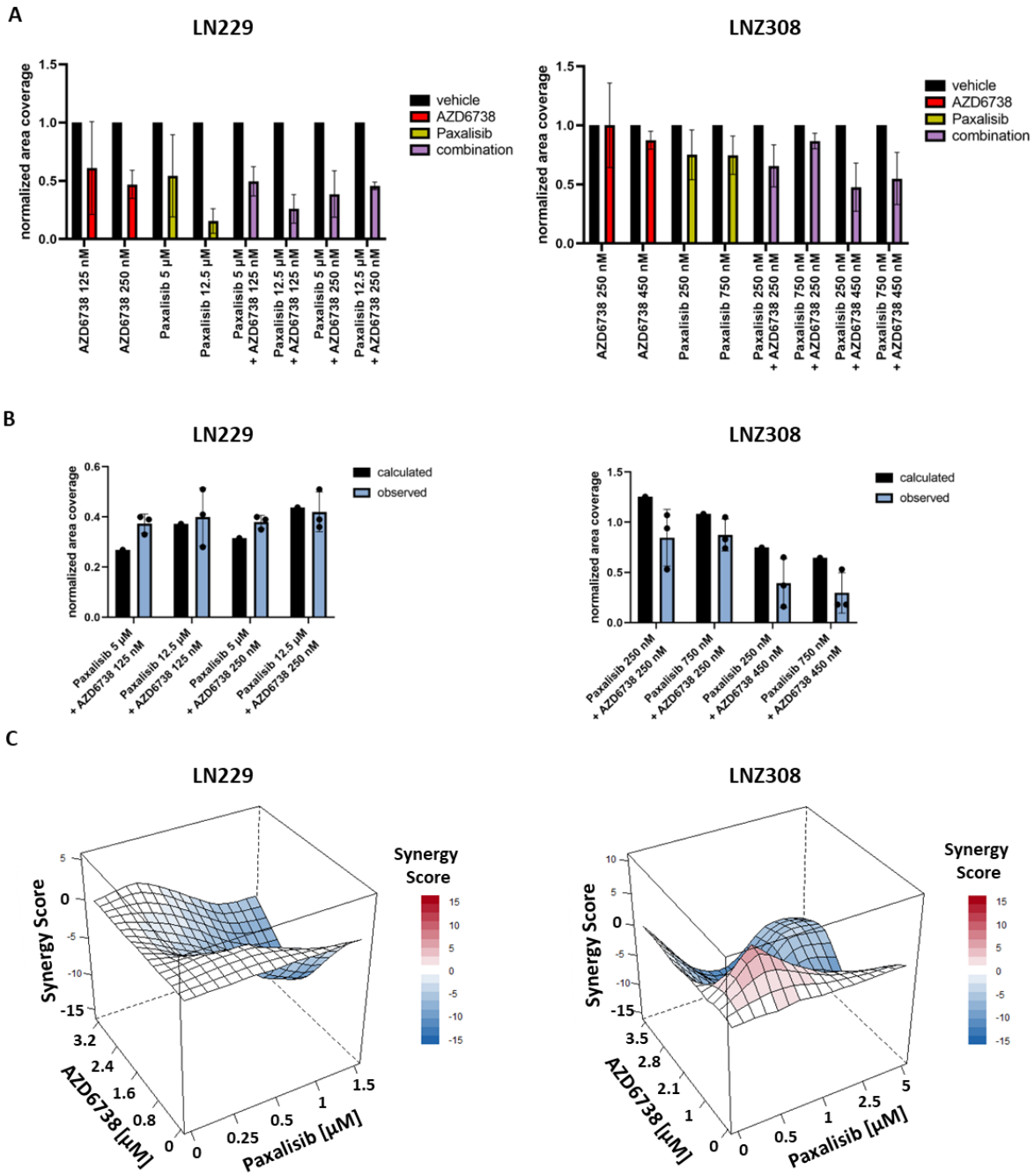
Figure 28*: Combining AZD6738 with Paxalisib displays no robust synergistic signature*

A, *Clonogenic survival assays for LN229, left, and LNZ308, right, cells treated with AZD6738 (red), Paxalisib (yellow) or a combination of both (purple) (n=3).* ***B,*** *Based on monotherapy effects measured in clonogenic survival assays, prediction for additive combination effects are calculated (black) based on the Bliss Independence Criterion and compared to observed (blue) measurements of combination treatment in clonogenic survival assays. Depicted is the evaluation of one representative run out of three (n=1).* ***C,*** *ZIP synergy read-out for cytotoxicity assays combining AZD6738 and Paxalisib in the indicated concentrations. Depicted is the evaluation of one representative run out of two (n=1).*
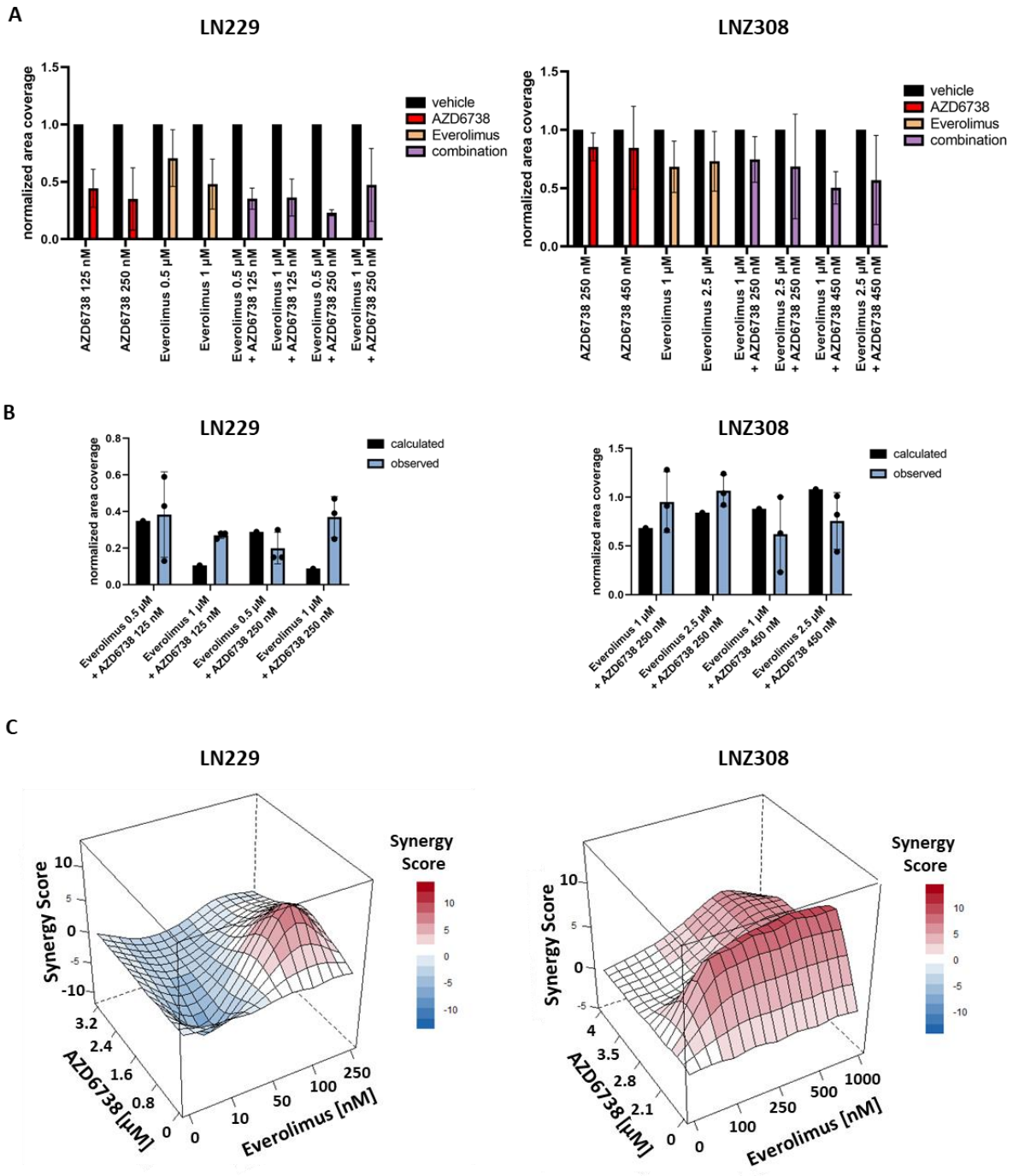
Figure 29: *Combining AZD6738 with Everolimus displays a trend towards synergism in LNZ308 cells*

A, Clonogenic survival assays for LN229, left, and LNZ308, right, cells treated with AZD6738 (red), Everolimus (orange) or a combination of both (purple) (n=3). ***B,*** *Based on monotherapy effects measured in clonogenic survival assays, prediction for additive combination effects are calculated (black) based on the Bliss Independence Criterion and compared to observed (blue) measurements of combination treatment in clonogenic survival assays. Depicted is the evaluation of one representative run out of three (n=1).* ***C,*** *ZIP synergy read-out for cytotoxicity assays combining AZD6738 and Everolimus in the indicated concentrations. Depicted is the evaluation of one representative run out of two (n=1).*

3.3 The role of the Fanconi anemia (FA) pathway in glioma

3.3.1 Molecular Tumor Board (MTB) Neurooncology cohort Tübingen

To determine potentially important genes for glioma development and/or treatment, an analysis of 586 patients of the Molecular Tumor Board (MTB) Neurooncology cohort Tübingen, diagnosed in the time between February 2016 and May 2020, was executed. Diagnoses in this cohort varied from primary central nervous system (CNS) tumors to brain metastases (**Figure 30** A). Of the 586 patients, 510 had a primary CNS tumor, the major subgroup consists of 216 diagnosed glioblastoma.

Up to now, glioblastoma has not been linked to any specific germline mutation. However, of the 586 patients included in this thesis, 60 carried germline mutations, i.e., 10% (**Figure 30** B, **Appendix Table 6**). Based on this data, an influence of the detected germline mutations was hypothesized. Hence, this project aimed to systematically assess the influence of the detected germline mutations in the MTB cohort on glioblastoma development, tumor propagation and therapy sensitivity.
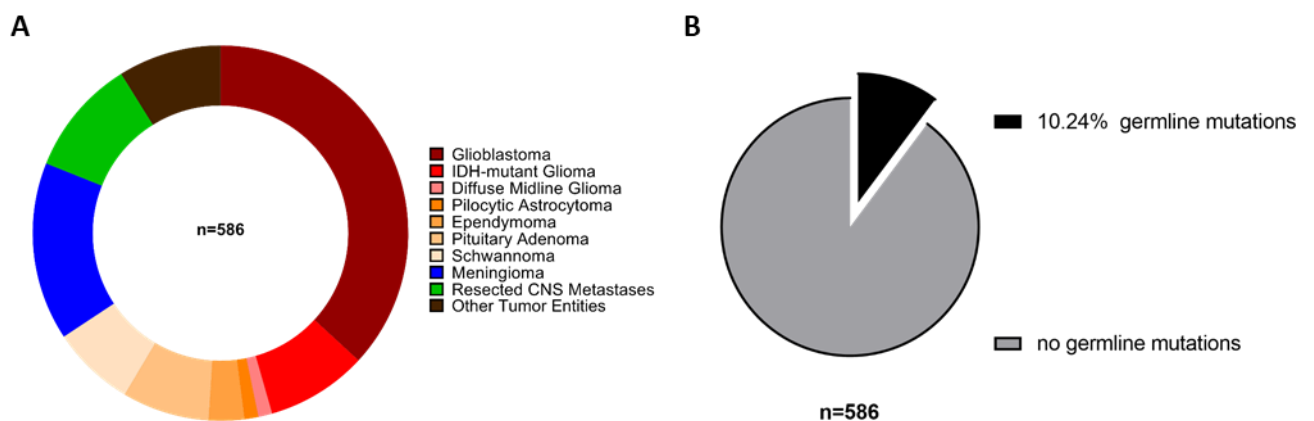
***Figure 30:** Characterization of the MTB Neurooncology Tübingen cohort*
***A,** Composition of the MTB Neurooncology Tübingen cohort (n=582). **B,** Analysis of germline mutation frequency in the MTB Neurooncology Tübingen cohort. Adapted from Renovanz et al. (under revision) [37]*

Of the 216 patients diagnosed with glioblastoma, 23 carried germline mutations (**Table 4**). Looking more closely into the germline mutations of IDH wt glioblastoma, an accumulation of mutations in the Fanconi anemia (FA) pathway was detected, i.e., 9 of the 23 detected germline mutations belonged to the FA pathway. Detected mutations of the FA pathway were in the BRCA1, FANCM, FANCA, BRCA2, PALB2, FANCC, XRCC2 and FANCD2 genes.

Table 4: Germline mutations in IDH wildtype glioblastoma patients in the MTB Neurooncology cohort Tübingen

MTB #	Gene	Functional class	Diagnosis	IDH status
TUE-0032	BRCA1	frameshift	Glioblastoma	wt
TUE-0035	DPYD	missense	Glioblastoma	wt
TUE-0044	FANCM	stop-gained	Glioblastoma	wt
TUE-0054	MAGI2	frameshift	Glioblastoma	wt
TUE-0065	FANCA	splice-region	Glioblastoma	wt
TUE-0071	BRCA2	missense	Glioblastoma	wt
TUE-0091	SDHD	missense	Glioblastoma	wt
TUE-0106	TP53	missense	Glioblastoma	wt
TUE-0114	PALB2	frameshift	Glioblastoma	wt
TUE-0152	FANCC	frameshift	Glioblastoma	wt
TUE-0180	MSH2	frameshift	Glioblastoma	wt
TUE-0428	FANCA	splice-region	Glioblastoma	wt
TUE-0440	ERCC3	frameshift	Glioblastoma	wt
TUE-0441	NF1	essential splice-site	Glioblastoma	wt
TUE-0474	XRCC2	stop-gained	Glioblastoma	wt
TUE-0484	DPYD	missense	Glioblastoma	wt
TUE-0488	MSH6	stop-gained	Glioblastoma	wt
TUE-0492	1) NBN 2) DPYD	1) frameshift 2) essential splice-site	Glioblastoma	wt
TUE-0503	DYPD	missense	Glioblastoma	wt
TUE-0504	UGT1A1	intronic	Glioblastoma	wt
TUE-0562	FANCD2	stop-gained	Glioblastoma	wt
TUE-0573	NRAS	missense	Glioblastoma	wt
TUE-0577	SBDS	splice-donor	Glioblastoma	wt

Abbreviations (alphabetical order): BRCA1, breast cancer 1; BRCA2, breast cancer 2; DPYD, dihydropyrimidine dehydrogenase; ERCC3, ERCC excision repair 3, TFIIH core complex helicase subunit; FANCA, Fanconi Anemia (FA) complementation group A; FANCC, FA complementation group C; FANCD2, FA complementation group D2; FANCM, FA complementation group M; MAGI2, membrane associated guanylate kinase; MSH2, mutS homolog 2; MSH6, mutS homolog 6; NBN, nibrin; NF1, neurofibromin 1; NRAS, neuroblastoma RAS viral oncogene; PALB2,

partner and localizer of BRCA2; SBDS, SBDS ribosome maturation factor; SDHD, succinate dehydrogenase; TP53, tumor protein P53; UGT1A1, UDP-glucuronosyltransferase 1A1; XRCC2, X-ray repair cross complementing 2

Next, the frequency of somatic FA protein family mutations in the patient cohort was determined. 9.7% of all MTB patients carried somatic FA mutations in any of the 22 known members of the FA pathway [123], this percentage increased to more than 11.1% when focusing on only glioblastoma patients (**Figure 31**).
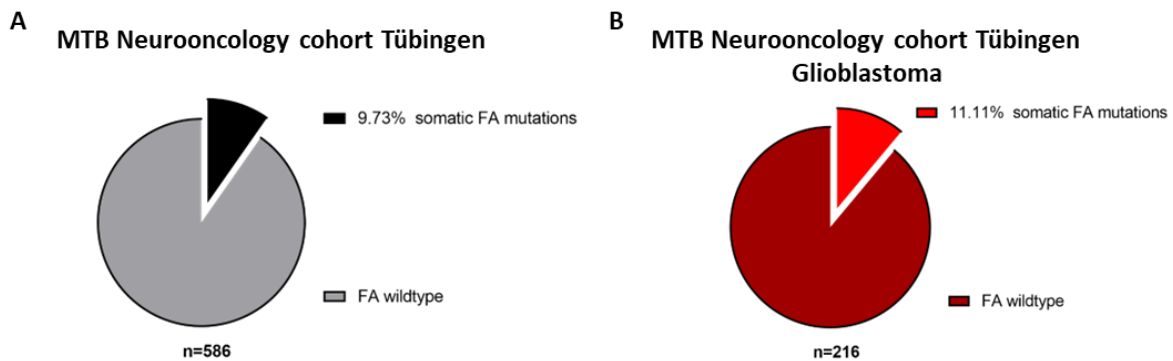
Figure 31: *Analysis of somatic mutations in the Fanconi Anemia (FA) pathway*
A, *Percentage of somatic FA mutations in the whole MTB Neurooncology cohort Tübingen.* ***B***, *Percentage of somatic FA mutation in glioblastoma patients in the MTB Neurooncology cohort Tübingen.*

3.3.2   Modeling FA mutations using the RCAS/tv-a mouse model

Based on the findings from the MTB patients, five FA genes were chosen to be modelled using the RCAS/tv-a system to deliver shRNAs into Nestin promoter expressing cells in the brains of 129S.Tg(NES-TVA)-Cdkn2a$^{-/-}$ mice. For shRNA expression the RCAS-Y DV vector was genetically engineered to express shRNAs with adjacent red fluorescence protein (RFP). RFP was then used as an expression control marker.

As a first step, two shRNAs per gene needed to be identified that specifically target the genes of interest leading to a sufficient knock-down of the expression of those. For this, NIH3T3 mouse fibroblasts expressing the tv-a receptor were used. The cells were infected with RCAS viruses carrying shRNAs targeting the genes of interest. For all five genes two shRNAs with a sufficient knock-down efficiency were identified using q-rtPCR (**Figure 32**).
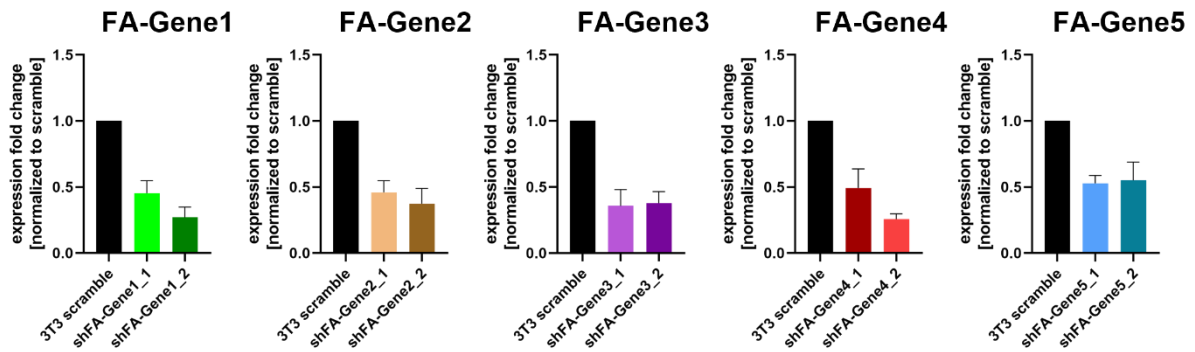
Figure 32: Knockdown efficiency for 5 Fanconi Anemia genes targeted by shRNAs expressed from RCAS viruses

129S.Tg(NES-TVA)-Cdkn2a$^{-/-}$ mice were intracranially injected with 25 000 DF-1 cells carrying RCAS viruses overexpressing PDGFB as a tumor driver and additionally 25 000 DF-1 cells carrying RCAS viruses expressing shRNAs specific for the target genes. Cells that were not used during the surgery were put back into cell culture flasks and RFP expression was validated again after surgery (**Appendix Figure 16**).

For each target gene plus a scramble control, six animals were transplanted with cells and monitored for onset of neurological symptoms upon which the animal was taken out and the brain was harvested for analysis. For all groups but the FA-Gene5 group at least five animals could be included into the subsequent analyses. In the FA-Gene5 group only two of the six animals displayed neurological symptoms and tumor development, hence, this group was excluded from further analyses (**Figure 33** A, blue survival curve).

Animals implanted with a mixture of cells overexpression PDGFB and shRNAs targeting FA-Gene1 had a median time until onset of neurological symptoms of 39.5 days, compared with 59.5 for scramble control animals. FA-Gene2, 3 and 4 developed symptoms in a comparable manner to scramble control animals. Median time until onset of neurological symptoms was 77.5 days in FA-Gene2, 87.5 days in FA-Gene3 and 60.5 days in the FA-Gene4 group (**Figure 33** A). Variability of survival times was lowest in FA-Gene1 groups with a median difference to scramble of 20 days with a span from 25 to 18 days reduction. For FA-Gene2 this span ranges from 8 days reduction to 40 days prolongation compared to scramble. FA-Gene3 displays 7 days reduction to 31 days prolongation. FA-Gene4 had a span from 5 days reduction to 41 days prolongation (**Figure 33** B).
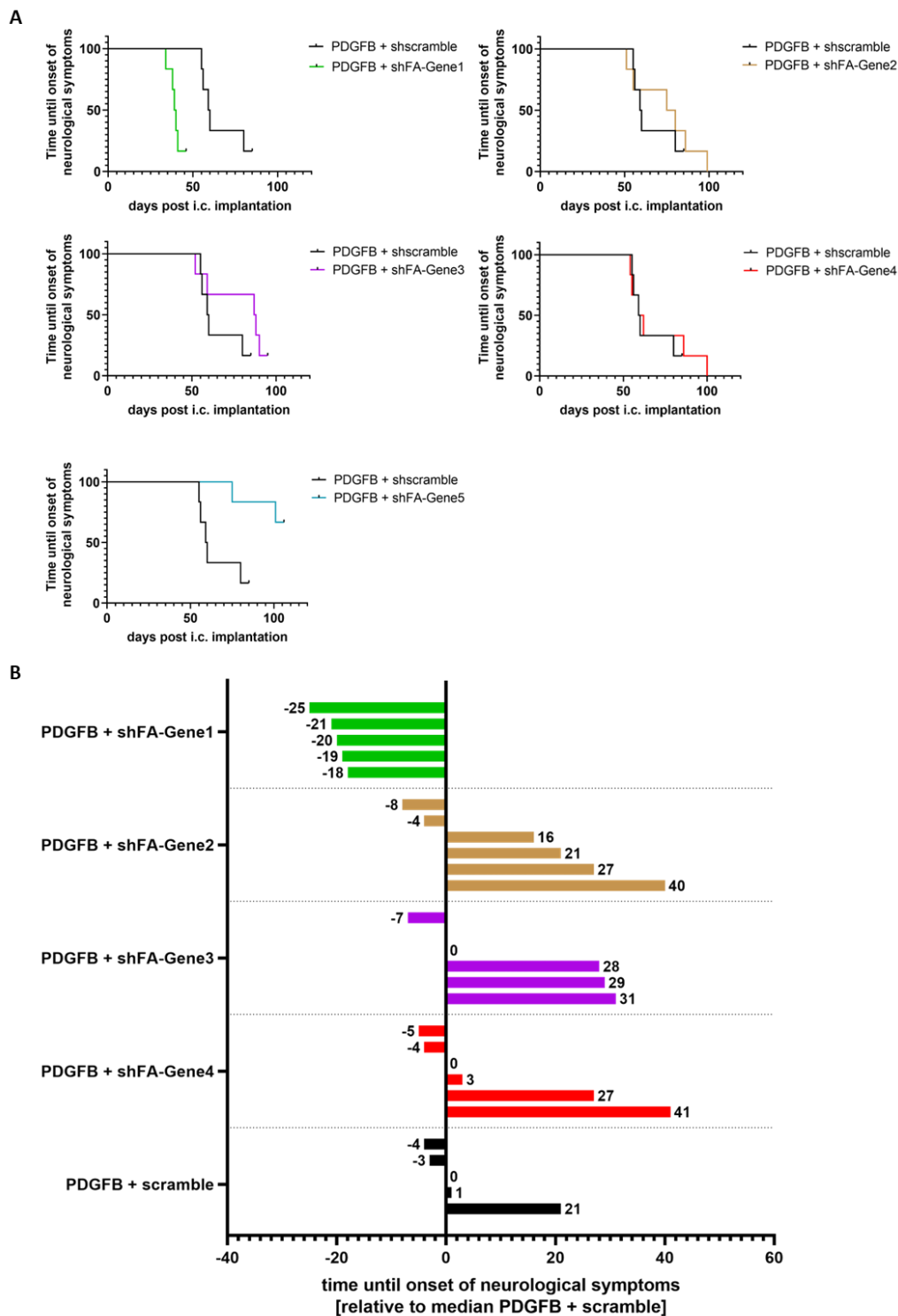
Figure 33: *Time until onset of neurological symptoms of FA gene knockdown together with PDGFB overexpression in XFM mice*

A, *Kaplan-Meier curves depicting the time until onset of neurological symptoms of FA gene knockdowns compared to scramble control group. FA-Gene1 knockdown leads to a shortened latency, only two animals can be included in the FA-Gene5 group.* **B**, *Waterfall plot depicting the time until onset of neurological symptoms relative to the median of PDGFB plus scramble group.*

Subsequently, histological analyses of the tumors resulting from PDGFB overexpression together with FA knockdown were performed (**Figure 34** A). The first row of the histological panel shows H&E stains. All groups show hypercellularity in the tumor area, however, the shFA-Gene1 group displays the highest cellular density compared to the other groups. The groups shFA-Gene2 and shFA-Gene3 show an intermediate level of cellular density, while shscramble and shFA-Gene4 display the lowest cellular density in this comparison. This additionally hints at a more malignant phenotype of the shFA-Gene1 group which also showed the shortest latency of symptom onset (**Figure 33**) compared to the other groups. Typical histological features of glioblastoma like pseudopallisading [12], could be detected in all FA knockdown tumors (H&E panel, examples in the shscramble, shFA-Gene1 and shFA-Gene2 group, **Figure 34** A). In the second row of **Figure 34** A, representative RFP stains are shown, which prove successful integration of RCAS virus carrying shRNA and furthermore retention of expression in established tumors. The level of neovascularization in the tumors was determined using the vascular marker CD31. Levels of neovascularization did not differ between the different groups as was determined by semi-automatic counting of vessel numbers (**Figure 34** A third row, B). Lastly, proliferation index was determined using Ki67 stains (**Figure 34** A, fourth row). In a quantitative analysis, a significantly higher proliferation index in tumors carrying a FA-Gene1 knockdown compared to the scramble group could be seen (**Figure 34** C). This fits to the findings of the shortened time until onset of neurological symptoms in this group (**Figure 33** 22).

Taken together, this data provides first evidence for a role of FA-genes in GB development *in vivo*. Especially shFA-Gene1 tumors displayed a shortened latency and histological markers of high grade glioma. Next, FA gene knockdowns *in vitro* were analyzed.

3.3.3 Modeling FA mutations *in vitro*

To further characterize the impact of FA mutations in glioma, the long-term glioma cell lines LN229 and LNZ308 were transduced with a pLKO1 vector carrying shRNAs targeting FA-GENE1 (shFA-GENE1_1, shFA-GENE1_2) and FA-GENE4 (shFA-GENE4_1, shFA-GENE1_2) which lead to a knockdown of at least 50% compared to cells carrying an shRNA targeting Luciferase (**Figure 35**).

3.3.3.1 Proliferative capabilities of FA knockdown cells

First, the influence of FA knockdown on proliferation was assessed. For this, every 24 h for up to 96 h cell numbers were determined. Neither knockdown of FA-GENE1 nor of FA-GENE4 led to a significant reduction or raise of proliferative capacity in LN229 or LNZ308 cells compared to shLuciferase control cells (**Figure 36**).
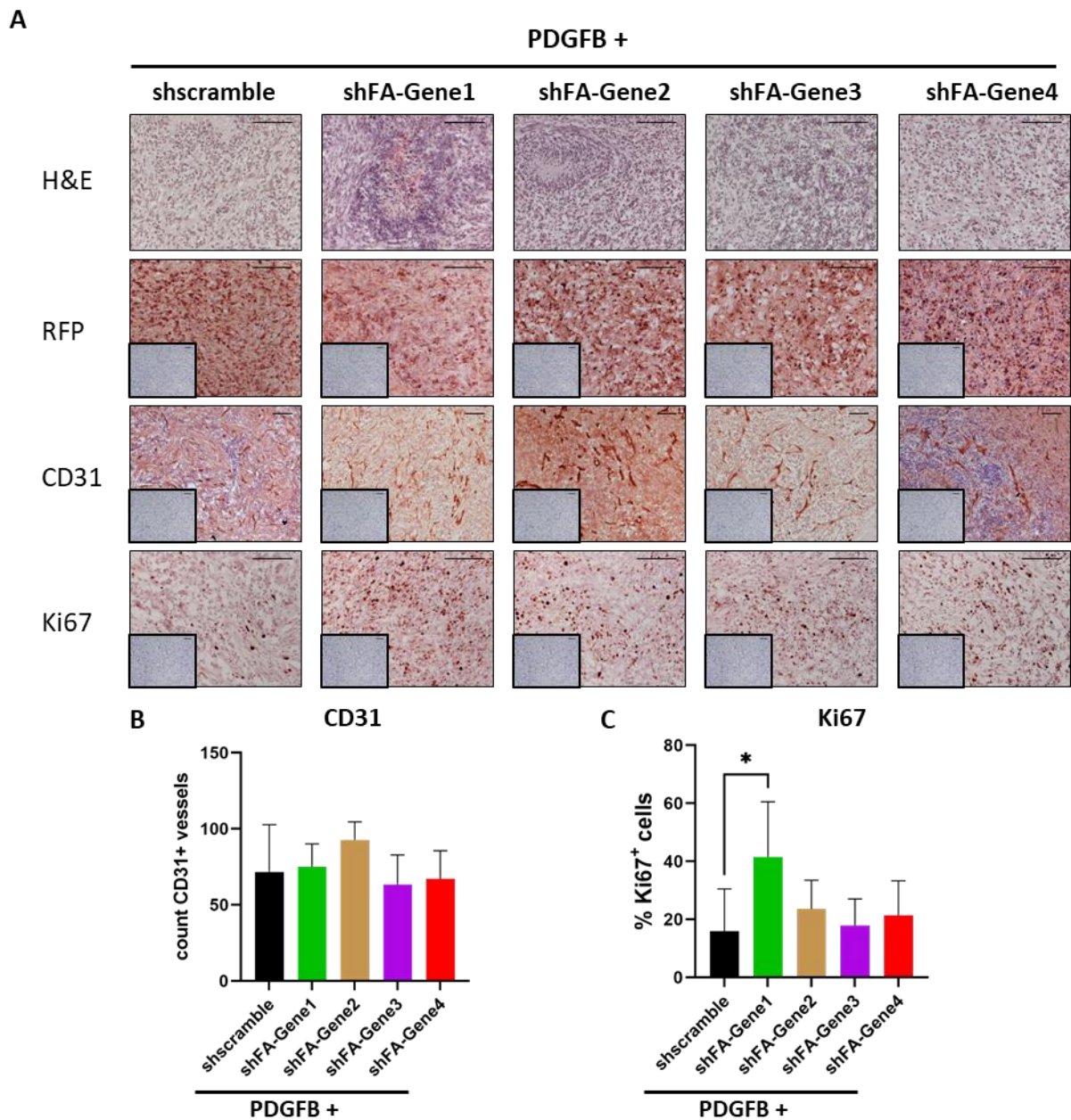
Figure 34: *Histological analysis of brain tumors carrying PDGFB overexpression and FA-gene knockdown*

*A, Histological panel depicting H&E, RFP, CD31 and Ki67 stains in PDGFB plus shscramble (control), shFA-Gene1, shFA-Gene2, shFA-Gene3, shFA-Gene4 tumors. Small inlays depict secondary antibody controls. Scale bars: 100 μm. **B**, Quantitative analysis of neovascularization levels by CD31 stain. **C**, Quantitative analysis of proliferation index by Ki67 stain. Statistical analysis using One-way ANOVA, p<0.05 considered significant.*
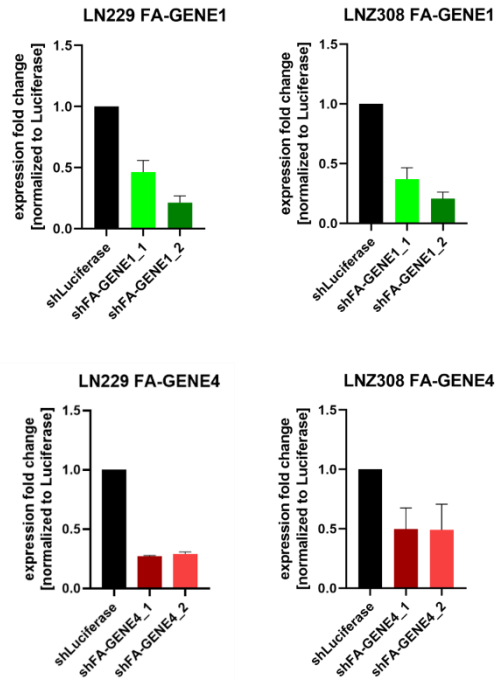
Figure 35: *Validation of knockdown by q-rtPCR of shRNAs targeting FA-GENE1 (green) and FA-GENE4 (red) in LN229 (left) and LNZ308 (right) cells (n=3).*
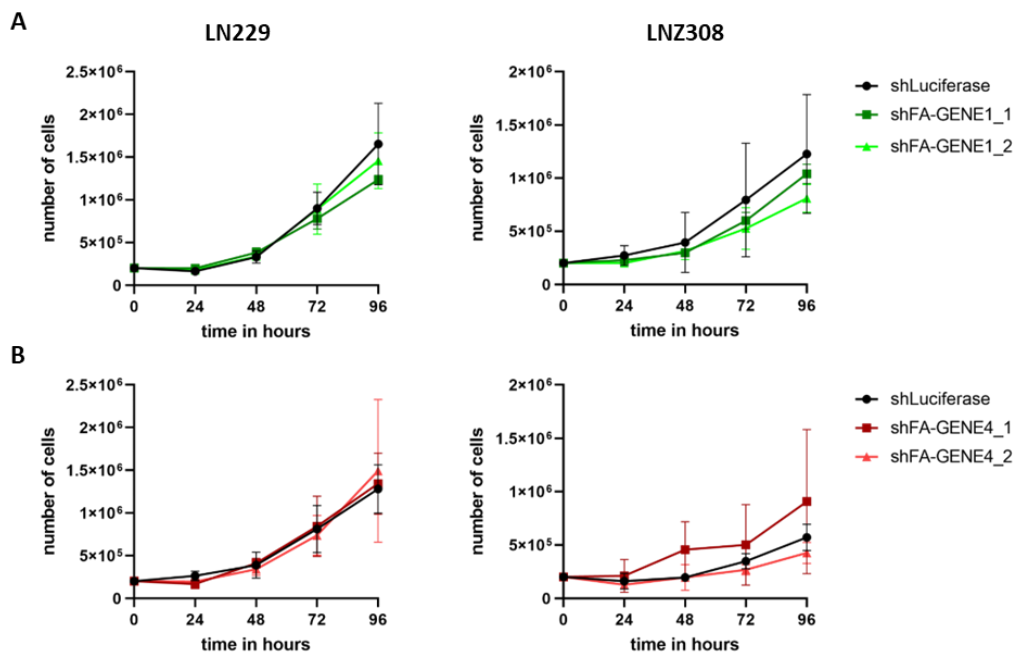
Figure 36: *Analysis of proliferative capacity of LN229 and LNZ308 cells upon FA-GENE1 or FA-GENE2 knockdown* ***A***, *Proliferation curves of LN229 and LNZ308 cells carrying shRNAs targeting Luciferase, shFA-GENE1_1 or shFA-GENE1_2 (n=3).* ***B***, *Proliferation curves of LN229 and LNZ308 cells carrying shRNAs targeting Luciferase, shFA-GENE4_1 or shFA-GENE4_2 (n=3). No significant differences detected using Two-way ANOVA.*

3.3.3.2 Plating efficiency of FA knockdown cells

Next, the plating efficiency (PE) of FA knockdown cells in clonogenic survival assays was determined to get an insight into the clone forming capabilities. In both cell lines, LN229 and LNZ308, the knockdown using shFA-GENE1_1 shows a tendency towards a lower PE compared to shLuciferase cells (**Figure 37** A), however, statistical significance was not reached. Interestingly, LN229 cells carrying knockdowns shFA-GENE4_1 and shFA-GENE4_2 showed significantly reduced PEs compared to corresponding shLuciferase cells (**Figure 37** B). LNZ308 cells carrying these shRNAs show a similar trend, but no significant difference could be detected (**Figure 37** B).
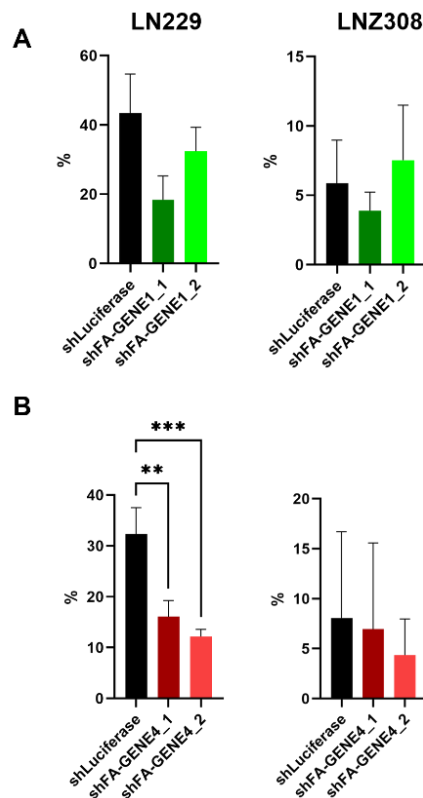
Figure 37: *Plating efficiency (PE) of LN229 and LNZ308 cells upon knockdown of FA-GENE1 and FA-GENE4*
*Bar graphs depicting plating efficiency of shFA-GENE1_1 and shFA-GENE1_2 (**A**) or shFA-GENE4_1 and shFA-GENE4_2 (**B**) compared to shLuciferase in LN229 (left) and LNZ308 (right) cells, respectively (n=3). shFA-GENE1_1 shows a tendency towards reduced PE. Significant reduction depicted in LN229 cells carrying shFA-GENE4_1 and shFA-GENE4-2 knockdown. Statistical analysis using One-way ANOVA, ** p<0.01, *** p<0.001.*

3.3.3.3 Sensitivity towards different treatment modalities of FA knockdown cells

To investigate the influence of FA mutation on treatment options, clonogenic survival assays to determine treatment sensitivity were conducted. Five different treatment modalities were leveraged, i.e., irradiation, Temozolomide, Lomustine, Olaparib and AZD6738 treatment. These treatment

modalities are either connected to standard of care for GB patients, i.e., irradiation, Temozolomide and Lomustine, or based on synthetic lethality approaches in line with BRCA2 mutated cancers [100], i.e., Olaparib and AZD6738.

Knockdown of FA-GENE1 did not change treatment sensitivity of LN229 or LNZ308 cells towards irradiation (**Figure 38** A). In neither knockdown nor cellular background a significant difference to shLuciferase cells could be detected. When looking at the chemotherapeutics both Temozolomide (TMZ) and Lomustine (CCNU) show sensitizing phenotypes in both cell backgrounds (**Figure 38** B, C). However, for LN229 only the knockdown using shFA-GENE1_1 leads to significant results compared to shLuciferase treatment sensitivity. For LNZ308 cells in both chemotherapies for both shRNAs a significant sensitization is detectable. Of note, in Temozolomide treated cells, again a slightly less sensitive phenotype can be detected for shFA-GENE1_2. Lomustine, on the other hand, very stably inhibited FA-GENE1 knockdown cells from forming colonies (**Figure 38** C). Targeted therapy against DNA damage response pathways using Olaparib (Olap) and AZD6738 (AZD) led to mixed results. In LN229 cells carrying shFA-GENE1_1 a significant sensitization towards Olaparib therapy was detected. shFA-GENE1_2 did not show this phenotype. No significant effects were detected in LNZ308 cells carrying those shRNAs (**Figure 38** D). For AZD6738 in neither cellular background nor shRNA a significant change in treatment sensitivity could be detected (**Figure 38** E).

For FA-GENE4 knockdowns, in line with FA-GENE1, no difference to shLuciferase could be detected when subjecting cells to irradiation treatment (**Figure 39** A). In the LN229 background cells, FA-GENE4 knockdown lead to a stable and consistent treatment sensitization towards Temozolomide (TMZ) treatment compared to shLuciferase cells in all tested treatment conditions. For LNZ308 cells in the highest applied Temozolomide concentration this sensitization is also detectable (**Figure 39** B). Lomustine (CCNU) did not show an equally robust sensitization, nevertheless, in both LN229 and LNZ308 cells carrying shRNAs targeting FA-GENE4 a treatment sensitization in both knockdown cell lines was measurable (**Figure 39** C). Olaparib (Olap) treatment did lead to a treatment sensitization in both lines. Opposed to FA-GENE1 knockdowns, also in the LNZ308 background a robust sensitization was detected (**Figure 39** D). Lastly, LN229 cells carrying shFA-GENE4_1 and shFAGENE4_2 did react more strongly towards AZD6738 (AZD) induced ATR inhibition than control shLuciferase cells in the 0.4 µM AZD6738 concentration. However, LNZ308 cells did not show this phenotype (**Figure 39** E).

Representative scans of clonogenic survival assay plates for the LN229 pLKO1 shLuciferase, shFA-GENE4_1 and shFA-GENE4_2 lines are shown in **Figure 40**. They highlight the visible difference between the three lines regarding PE, Temozolomide (TMZ), Lomustine (CCNU), Olaparib and AZD6738 treatment that lead to significant surviving fraction differences in the different conditions (**Figure 38**, **Figure 39**).

Taken together, these results might predict a differential treatment sensitivity profile for FA-gene mutated brain tumors. However, these findings need to be further validated *in vivo*.
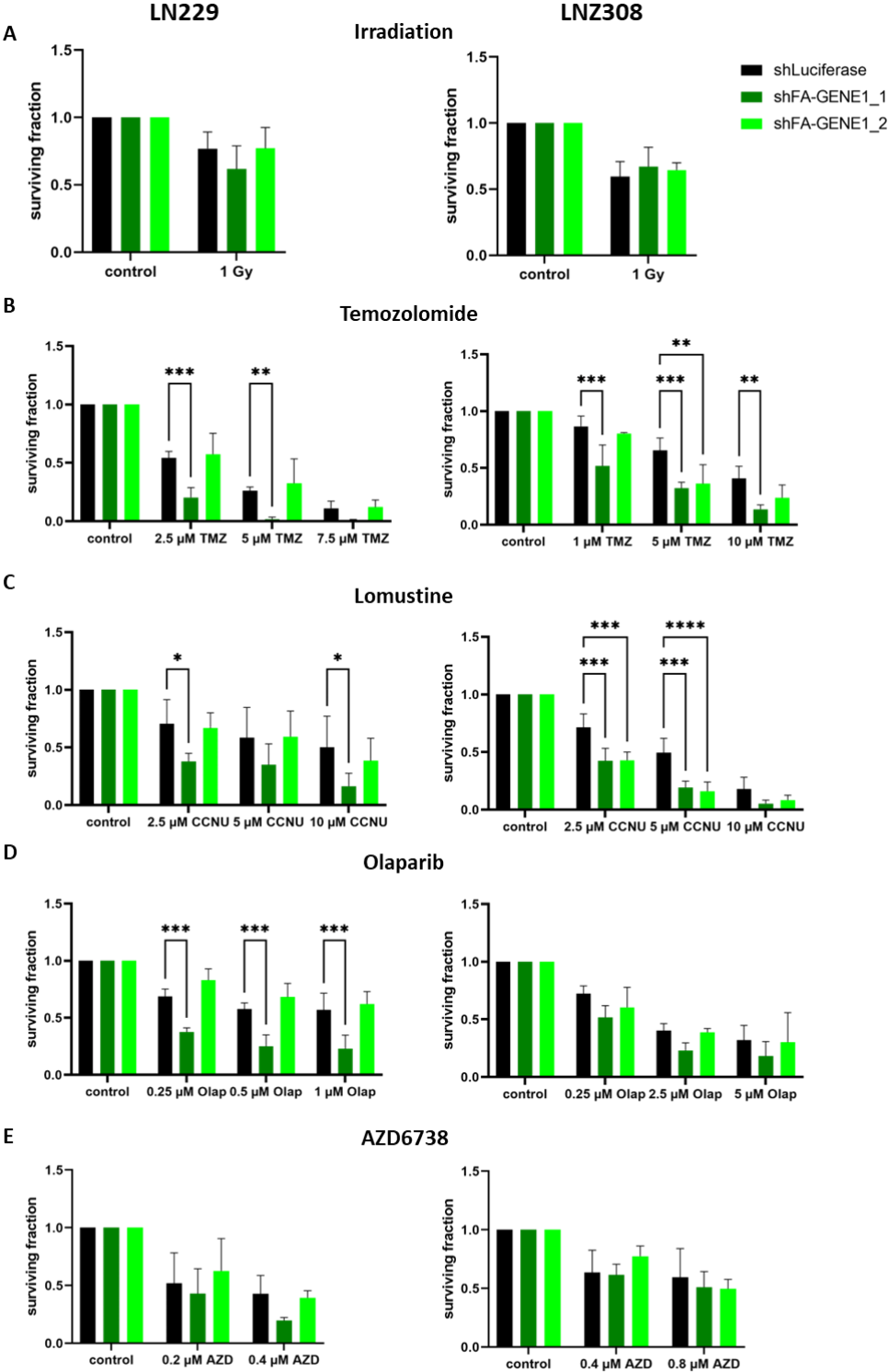
Figure 38: *Survival fractions of LN229 and LNZ308 cells carrying knockdowns for FA-GENE1 treated with irradiation, Temozolomide, Lomustine, olaparib and AZD6738*
*Bar graphs depicting surviving fractions of LN229 (left) and LNZ308 (right) cells carrying shLuciferase, shFA-GENE1_1 and shFA-GENE1_2 and treated with irradiation (**A**), Temozolomide (TMZ) (**B**), Lomustine (CCNU) (**C**),*

***Figure 39:** Survival fractions of LN229 and LNZ308 cells carrying FA-GENE4 knockdown cells treated with irradiation, Temozolomide, Lomustine, olaparib and AZD6738*

*Bar graphs depicting surviving fractions of LN229 (left) and LNZ308 (right) cells carrying shLuciferase, shFA-GENE4_1 and shFA-GENE4_2 and treated with irradiation (**A**), Temozolomide (TMZ) (**B**), Lomustine (CCNU) (**C**), Olaparib (Olap) (**D**) or AZD6738 (AZD) (**E**) (n=3). Statistical analysis using two-way ANOVA, * p<0.05, ** p<0.01*
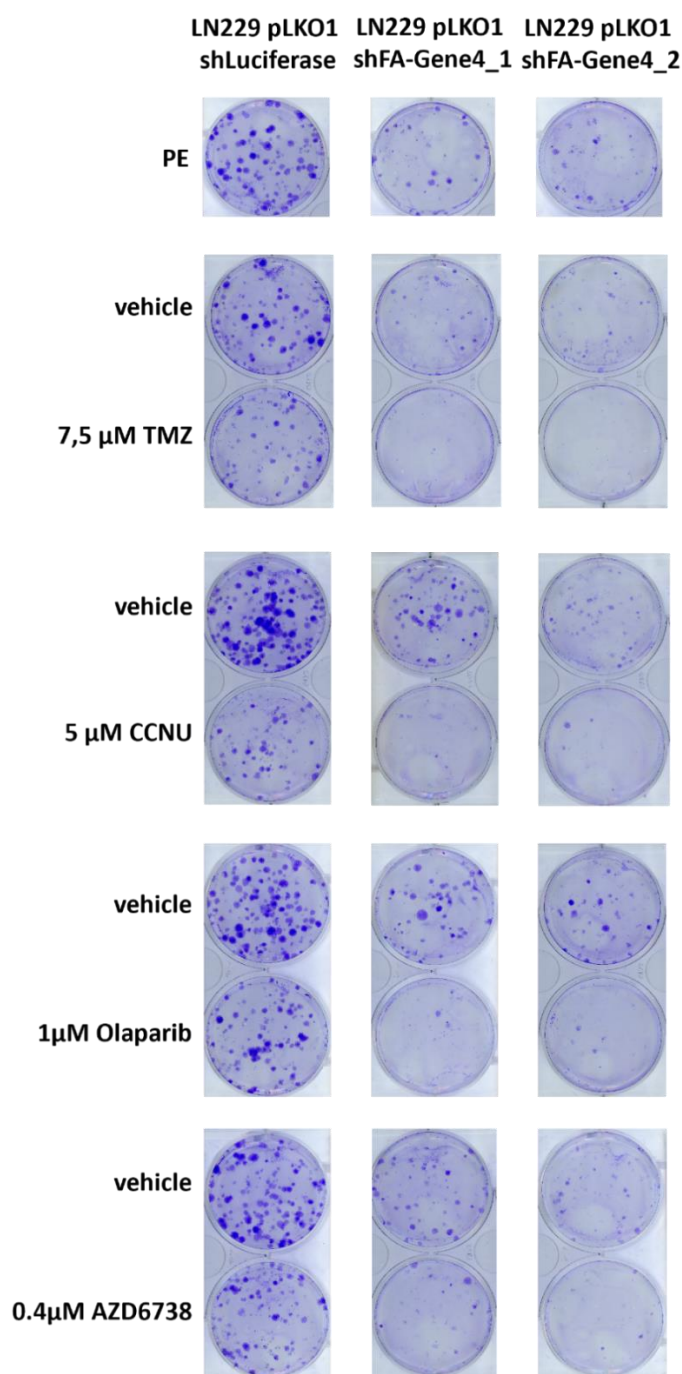
Figure 40: *Clonogenic survival assays of FA-GENE4 stained with Crystal Violet*

*Representative pictures of clonogenic survival assays plates of LN229 FA-GENE4 knockdown cells. Untreated wells are depicted in the first block. Blocks 2 to 5 depict treatment sensitivity in knockdown cells compared to shLuciferase control cells in indicated treatment conditions. The indicated treatments were found to be significantly more effective in knockdown cells compared to shLuciferase cells (**Figure 39**).*

4. Discussion

Despite multi-modal treatment approaches including maximal resection followed by radio-chemotherapy, the overall survival of patients suffering from glioblastoma (GB) remains in the range of 1.5 years [1, 2, 4]. Thus, novel treatment approaches are urgently needed.

In an attempt to improve patient care, extensive genetic analyses of GB patients have been conducted. Those unveiled three frequently altered pathways, namely the CDKN2A/CDKN2B/RB1 pathway that is mutated in 79% of all GB patients, alterations in the MAPK pathway and AKT pathway which are altered in 90% of all GB patients and 86% of all GB patients display alterations in the p53 pathway [25]. Furthermore, GB subtypes have been identified subdividing GB into classical, mesenchymal and proneural GBs, each with specific genetic signatures and prognosis regarding therapy sensitivity [27, 28]. Other studies showed that GB tumors usually do not display populations of only one cellular state, but usually harbor different ones [30, 31]. These cellular states remain plastic and can change in response to stimuli from their microenvironment [188]. This plasticity as well as heterogeneity is further highlighted by the fact that GB cells are highly infiltrative into the brain and lead to local as well as distant progression [189, 190], the latter have been shown to only minimally overlap genetically with the original tumor [191]. Almost all patients will suffer from progressive disease which is one of the main challenges regarding treatment of GB [2, 9], especially as those progressive tumors developed resistance towards therapy [192].

One of these resistance mechanisms against ,e.g., radio-therapy, is the upregulation of DNA damage response (DDR) pathways [109]. Targeting the DDR pathways has become a core topic of research in many cancer entities after the successful implementation of poly(ADP-ribose)-polymerase 1 (PARP1) inhibitors, i.e., Olaparib, in BRCA1 and BRCA2 mutant ovarian cancers [193]. In glioma different DDR pathways have been shown to play an important role, e.g., O^6-methylguanine-DNA-methyltransferase (MGMT) can directly repair O^6-methylguanine which can be induced by Temozolomide (TMZ) treatment leading to cell death. Functional MGMT thus renders cancer cells resistant towards TMZ therapy while cells harboring methylated, inactive MGMT promoters are sensitive towards TMZ therapy [20, 106]. Interestingly, it has been shown that in progressive GB the expression of mismatch repair (MMR) genes is reduced [107]. In glioma cell lines a downregulation of MMR genes leads to resistance towards alkylating therapy [108]. In a recent study by Koch et al. disruption of the basic helix loop helix (bHLH) transcription factor family that is frequently upregulated in glioma, revealed a treatment sensitivity of glioma cells towards ataxia telangiectasia and Rad3 related (ATR) inhibition [120]. Thus, targeting the DDR pathways is of high interest in glioma, however, clinical trials yet need to confirm its success [194].

Taken together, it remains a challenge to identify actionable tumor vulnerabilities in GB that can be successfully leveraged to stably inhibit tumor growth and prevent progressive disease. In this thesis, three different, novel approaches with the aim to understand, induce and exploit actionable tumor vulnerabilities in glioma are presented. The first approach shown, targets the cell cycle that is frequently perturbed in GB [25], effectively exploiting this tumor intrinsic vulnerability using Argyrin F. Secondly, the DDR is targeted by ATR inhibition based on the identified vulnerability of glioma by Koch et al. Thirdly, the landscape of germline mutations in the molecular tumor board (MTB) neuro-oncology cohort Tübingen was characterized to identify novel vulnerabilities that were then modelled and characterized *in vitro* and *in vivo*.

As has been mentioned, GB frequently harbor alterations in the Rb pathway which lead to a perturbation of cell cycle regulation in GB cells [25]. Treatment strategies inducing cell cycle-stabilization are thus considered to hold promising potential for novel therapeutic strategies. In the ongoing N2M2/NOA20 clinical trial (NCT03158389) Palbociclib, a cyclin dependent kinase (CDK) 4/6 inhibitor that has cell cycle-stabilizing capabilities [195], is combined with radiotherapy in CDKN2A/2B deleted GB [196]. Another approach to induce cell cycle control is to target the ubiquitin proteasome system. This system is strongly involved in the tight regulation of cell cycle regulators [197]. Marizomib and Bortezomib, both proteasome inhibitors, have been preclinically tested and successfully implemented into therapeutic strategies in several cancer entities, e.g., Bortezomib is approved as the first-line treatment in multiple myeloma [198-200]. In preclinical *in vivo* glioma models, Marizomib has been shown to induce cell death [47]. Its clinical development in glioma is in advanced stages with the phase III EORTC 1709 trial (NCT03345095) that investigates the addition of Marizomib to radiation therapy and TMZ postoperatively in newly diagnosed GB, however, overall survival and progression free survival did not improve with the addition of Marizomib compared to standard therapy [50].

In this thesis, stabilization of p27^{Kip1} was leveraged to infer cell cycle-stabilization in experimental glioma. The novel proteasome inhibitor Argyrin F, which is a cyclic peptide, has been shown to specifically inhibit the proteasomal degradation of p27^{Kip1} [5, 54]. Indeed, immunoblot analyses confirmed a stabilization of p27^{Kip1} and p21^{Cip1} by Argyrin F *in vitro* that was accompanied by a downregulation of Rb1 as well as pRb1 in glioma long-term cell lines (**Figure 12** A, B). Immunohistochemical analyses of post-treatment SMA560 glioma showed p27^{Kip1} accumulation *in vivo* upon Argyrin F treatment (**Figure 13**C). Thus, this is also suggestive for a successful crossing of the blood-brain barrier (BBB) in the experimental model. Consequently, cell cycle analyses by flow cytometry revealed an Argyrin F-induced G2/M accumulation (**Figure 12** C, D, **Appendix Figure 2**). Chen et al. have shown an accumulation of cells in G1 upon Argyrin F treatment [5], however, the

upregulation of p27^{Kip1} and p21^{Cip1} has also been reported to lead to an accumulation of cells in G2/M in, e.g., endometrial cancer [201]. Cytotoxicity and clonogenic survival assays in human and murine glioma long-term cell lines proved anti-glioma activity of Argyrin F treatment (**Figure 12** E-H, **Appendix Figure 2**).

As is shown in **Figure 13** B the SMA560/VM/Dk glioma model revealed a modest, but significant benefit for Argyrin F therapy compared to vehicle treated animals. In the subsequent histological analyses, the infiltration of T cells into SMA560 glioma upon Argyrin F treatment was quantified (**Figure 13** E). CD8$^+$ T cells increased 4.6-fold in the treatment group. In an attempt to more closely mimic the conditions of tumors in patients, an *ex vivo* GB model, using freshly resected tumor tissue, was established. Conventional tumor cell cultures cannot reflect the cellular heterogeneity of a tumor or its interaction with stromal and infiltrating cells, e.g., immune cells. From freshly resected tumor tissue, patient derived microtumors (PDMs) together with autologous tumor-infiltrated lymphocytes (TILs) were extracted and used for treatment studies (**Figure 14**, **Figure 16**). With this, anti-glioma effects and immune-mediated reactions could be investigated. First, dose finding experiments were done to determine IC$_{50}$-values (**Figure 14** C). Next, treatment-induced immunogenic effects in PDM/TIL co-cultures treated with Argyrin F were investigated. Indeed, already at very low concentrations a significant increase in cytotoxicity, that was not detected in PDMs alone treated with Argyrin F, was measured (**Figure 14** D, E), suggesting a pro-immunogenic effect of Argyrin F.

Based on these findings, the human leucocyte antigen (HLA) ligandome of Argyrin F- vs vehicle-treated LN229 and LNZ308 cells was analyzed (**Figure 15**, **Appendix Figure 4**). The aim was to further understand the underlying causes of Argyrin F-induced immunogenicity *ex vivo* and *in vivo* (**Figure 13**, **Figure 14**). Argyrin F treatment did induce up- and down-regulation as well as de novo presentation of peptides, however, the overall numbers of presented peptides did not change (**Figure 15**, **Appendix Figure 4, Table *1***). This is in line with a previous study that looked at the HLA peptidome of proteasome inhibitor treated cells using stable isotope labeling of amino acids (SILAC) [202]. Of note, the 20S proteasome, which is targeted by Argyrin F treatment, is heavily involved in the formation of the immunopeptidome and hence has a strong influence on presented major histocompatibility complex (MHC) peptides [203]. Several of the detected peptides upon Argyrin F treatment are derived from the protein Vimentin. This protein is a type III intermediate filament which is restrictively expressed in certain tissues in adults, e.g., specific brain cells or in cancer cells [204, 205]. Functions like migration, invasion and epithelial mesenchymal transition have been linked to Vimentin expression [206, 207]. SSVPGVRLL was one peptide that was significantly changed in LNZ308 cells treated with Argyrin F (**Figure 15** D). Interestingly, this peptide has been described to induce an interferon gamma (IFNγ) response upon presentation by Jarmalavicius et al. [180]. The presence of this peptide upon Argyrin F treatment might be one explanation for the observed immunogenic phenotype *in vivo*, i.e., influx of T

cells, (**Figure 13**) and *ex vivo*, i.e., increased cytotoxic read-out (**Figure 14**). Taking these results together, two conclusions are made: i) the treatment-induced changes to the HLA ligandome can be explained by the proteasome inhibitory function of Argyrin F and ii) combining Argyrin F with PD-1 blockade might enhance the efficacy of each monotherapy.

Consequently, the effect of Argyrin F plus anti PD-1 therapy, i.e., Nivolumab, in PDM/TILs co-cultures was tested in two models with different T cell contents *ex vivo* and compared to the respective monotherapies. In the PDM/TILs model with a high CD3$^+$ content (**Figure 16** A, B), a significant induction of cytotoxic read-out was detected together with an increase of intracellular tumor necrosis factor alpha (TNFα) levels in the CD8$^+$ T cell population. Opposed to this, the model with a low CD3$^+$ T cell content did not display a significant induction of cytotoxic read-out (**Figure 16** A, C). In the SMA560/VM/Dk model the novel combination of Argyrin F plus PD-1 blockade induced a further increased influx of T cells into SMA560 glioma and prolonged symptom-free survival of SMA560-bearing VM/Dk mice (**Figure 17**).

To conclude, Argyrin F therapy directly induces anti-glioma efficacy on tumor cells and increases treatment-induced immunogenicity. Consequently, a novel therapeutic window is opened and can be exploited by combination of Argyrin F with checkpoint inhibition. In light of the recently conducted clinical trials using checkpoint inhibition in GB that did not meet their primary study endpoints [80], the results presented in this thesis are of high relevance and provide a rationale for clinical translation. Moreover, preclinical toxicology studies of Argyrin F are in advanced stages, hence, this concept can be realized in an early phase clinical trial in the near future [51].

The next strategy to exploit actionable vulnerabilities in experimental glioma aimed to characterize the potential of targeting the DDR by use of ATR inhibition (ATRi). In a previous study, disruption of the bHLH network revealed a sensitivity of glioma which overexpress the bHLH transcription family towards ATR inhibition [120]. Based on this, an animal experiment testing the efficacy of AZD6738 *in vivo* was conducted and showed a significant delay of onset of neurological symptoms compared to vehicle control treated SMA560 bearing VM/Dk animals (**Figure 18**). Next, to provide a more comprehensive overview of ATRi efficacy in glioma AZD6738 and Berzosertib, another ATR inhibitor, were characterized in two human and two murine glioma long-term cell lines (**Figure 19**, **Figure 20**, **Appendix Figure 6**, **Appendix Figure 7**). Stable anti-glioma activity could be determined in all cell lines using both compounds. To further characterize the effects of ATRi on glioma cell lines, apoptosis induction and cell cycle status were analyzed as shown in **Figure 21** and **Appendix Figure 8**. Interestingly, LN229 and GL261 cells displayed S phase arrest while LNZ308 cells displayed G2-M accumulation and no regulation was detected in SMA560 cells. ATR together with its partner kinase

ataxia-telangiectasia mutated (ATM) are heavily associated with cell cycle control. ATM activation typically leads to G1 arrest, while ATR usually leads to intra S-arrest [110]. Classically, these two kinases have been viewed as the starting points of two separate pathways, however, evidence for a crosstalk between these pathways has been found [208]. Thus, ATM has been shown to also activate checkpoint-kinase 1 (Chk1), which classically is activated by ATR, and in turn might explain the detected S phase and G2 arrest [209, 210].

As AZD6738 was reported to cross the BBB more efficiently than Berzosertib [184, 185], the main focus in this thesis was on AZD6738 while Berzosertib served as a proof of principle compound. AZD6738 is tested in early clinical trials in patients with advanced solid tumors and displayed some anti-tumor efficacy but also some severe treatment-related adverse events which were managed using a 2-week-on, 2-week-off treatment schedule [211]. The *in vivo* data presented in **Figure 18** show a significant benefit of AZD6738 treatment compared to vehicle treated animals in experimental glioma, however, this benefit might be further improved by adding a second treatment compound. Furthermore, GB tumors are well known for their progressive capabilities which have been linked to resistance mechanisms [7, 109, 190]. Of note, targeting the DDR by PARP inhibitors in different cancer entities does lead to promising tumor responses, however, there is a distinct lack of regular and prolonged responses even in biomarker-selected populations either due to inherent or acquired resistance mechanisms [102]. Consequently, it was aimed to not only evaluate ATRi monotherapy, but also test combination approaches.

Intrigued by the differences in cell cycle status between LN229 and LNZ308 glioma cell lines and to acquire a more comprehensive picture of molecular mechanisms that might instruct novel combination therapy approaches, transcriptome analyses upon AZD6738 treatment were conducted. As is shown in **Figure 22**, overlapping and distinctly regulated genes were identified. The most strongly upregulated pathway upon treatment in both cell lines was the nuclear factor kappa-light-chain-enhancer of activated B-cells (NFκB) pathway. This upregulation could also be validated using DigiWest protein profiling (**Figure 23**). The NFκB family regulates a vast network of genes in the cells that are associated with inflammation, immunity, proliferation and cell death [212]. This might explain the detection of the "cytokine-cytokine receptor interaction", "IL-17 signaling" as well as the "type I diabetes mellitus" pathway which also were detected to be significantly upregulated in both cell lines upon ATRi. Interestingly, NFκB has also been found to be activated upon DNA double-strand breaks (DSB) by the ATM/ATR signaling pathways, functioning as an activator of pro-survival signals [95]. DigiWest protein profiling analyses revealed a significantly induced cleaved PARP (**Figure 23** A) signal and flow cytometry analyses displayed an increase in apoptotic cells upon treatment (**Figure 21** A, **Appendix Figure 8** A), both arguing for a pro-apoptotic signature. At the same time, in the DigiWest protein profiling analyses looking at several apoptosis signaling proteins a simultaneous regulation of

pro- and anti-apoptotic proteins, i.e., Survivin, Bax, pBad, could be seen (**Figure 23** B). The activation of NFκB signaling might be one underlying cause for the anti-apoptotic signals.

Looking at the results of the likelihood ratio test (LRT) that determines significantly distinct regulation between the cell lines upon treatment, two pathways are of great interest. On the one hand, a significant upregulation of the p53 signaling pathway is detected in LN229 cells in the LRT analysis and was validated in the DigiWest analysis (**Figure 22**C, **Figure 23** B). Interestingly, LNZ308 cells are p53^{null} and hence cannot regulate the p53 pathway [152]. The second pathway regulation to be pointed out is the downregulation of the phosphatidylinositol 3-kinase (PI3K)-Akt signaling pathway in LN229 cells while LNZ308 cells upregulate this pathway upon ATRi (**Figure 22** C). On the protein level a downregulation of pAkt was seen in LN229 cells (**Figure 23** B). Akt has been shown to suppress apoptosis in a PI3K-dependent manner [95], adding another level of apoptosis regulation to the molecular mechanisms in LNZ308 cells upon AZD6738 treatment. Differential genetic set-ups in the cells regarding phosphatase and tensin homolog (PTEN) which is the regulator of PI3K in cells [213] might be the explanation for the differential regulation. LN229 cells harbor a wildtype (wt) while LNZ308 cells harbor a mutated (mut) PTEN version [152]. Of note, mutations and alterations in the p53 and PTEN gene are quite frequent also in GB patients, i.e., 41% display PTEN mutations and 28% TP53 mutations [25]. Thus, these genetic differences between LN229 and LNZ308 cells do reflect the heterogeneity of patient tumors well and, according to these findings, seem to have important implications for treatment regimen of ATRi.

Combination therapies tested in this thesis were based on previous data in the literature and the molecular characterization presented here. The first combination that is looked at, combines ATRi with GB standard chemotherapeutic TMZ. Combination of chemotherapeutic agents, e.g., Carboplatin, with ATRi is leveraged frequently in other cancer entities, e.g., colorectal cancer, and has shown promising results [214-216]. This combination approach is additionally of special interest as preclinical and clinical data have shown that chemo-resistant cancers can be re-sensitized to chemotherapy using DDR inhibitors [114, 116]. In the GB context several studies have shown an important role of the ATM/ATR kinases in conferring resistance to TMZ treatment that can be overcome by ATRi [217, 218]. Koch et al. have shown a synergistic signature upon combination of AZD6378 with standard chemotherapeutic TMZ in LN229 cells [120]. Evaluation of LN229 and LNZ308 cells treated with AZD6738 or Berzosertib in combination with TMZ (**Figure 24**, **Figure 25**) revealed a stable synergistic signature for this combination in LN229 cells, but not in LNZ308 cells. Based on the molecular data collected in LN229 and LNZ308 cells, the differing p53 and PI3K signatures upon ATRi are hypothesized to be the underlying reason for the distinct synergy signatures.

Secondly, the combination of ATRi with PARP inhibition using Olaparib was studied. Cancer cells do depend differently on DDR pathways than healthy cells [102] and chemically inducing synthetic

lethality by inhibiting the PARP and ATR signaling axis is a widely used approach in several cancer entities, among them glioma [219-221]. First clinical trials in ovarian and advanced solid cancers showed a good safety-profile of the combined treatment, however, objective responses could not be detected so far [214, 222]. Similar to the previous results, LN229 cells display a positive synergistic signature in ATRi plus Olaparib treatments, that cannot be recapitulated in LNZ308 cells (**Figure 26**, **Figure 27**). The differing molecular mechanisms observed upon AZD6738 treatment in the transcriptomic and proteomic analyses might again be the underlying cause.

The third combinatorial approach looked into the combination of ATRi with inhibition of the PI3K-Akt pathway. Especially the LNZ308 cells which have shown no positive synergistic signatures with the combinations tested so far, were in the focus here. Based on the prominent upregulation upon AZD6738 treatment of the PI3K-Akt pathway (**Figure 22**) a positive synergistic outcome was hypothesized. Two compounds targeting PI3K and/or the downstream effector mechanistic target of Rapamycin (mTOR), Paxalisib and Everolimus, respectively, were used. Paxalisib is a dual inhibitor of PI3K and mTOR that recently underwent a phase II clinical trial in newly diagnosed GB, it was well tolerated and displayed preliminary anti-tumor activity [223]. Everolimus selectively inhibits mTOR and also underwent a phase II clinical trial in pediatric low-grade glioma. Similarly to Paxalisib the drug was well tolerated and is planned to be evaluated further in this patient population [224]. The combination of Paxalisib with AZD6738 did not show a strong synergistic signature in either of the two cell lines investigated (**Figure 28**). LNZ308 cells did display a trend towards synergism, however, not as strong as hypothesized based on the transcriptomic and proteomic data (**Figure 22**, **Figure 23**). Everolimus in combination with AZD6738 leads to a more stable trend towards synergism in LNZ308 cells but not in LN229 cells (**Figure 29**). Of note, although the PI3K-Akt pathway was identified to be significantly up-regulated in LNZ308 cells in the transcriptomic data set (**Figure 22**), neither PI3K nor mTOR themselves were actual hits. Also, the regulation of pAkt as shown in the DigiWest protein profiling analysis displayed a downregulation in LN229 cells but almost no regulation in LNZ308 cells (**Figure 23**). This might be one possible explanation for the suboptimal synergistic signatures measured in these experiments. As other parts of the pathway led to its identification, these might need to be targeted in order to fully exploit this identified vulnerability.

Taken together the data shown here provide novel insights into the mechanisms upon ATRi in experimental glioma. Novel combinatorial treatment approaches are evaluated and discussed. Targeting the DDR and especially ATR has become an intensively studied topic in the last couple of years in various cancer entities [225]. ATRi has not only been tested in mono-therapeutic settings but early on in combination approaches, too. These have been tested preclinically and in clinical trials [225, 226]. However, despite promising preclinical data, in clinical trials no objective response occurred [214, 222]. In a recent study testing AZD6738 in combination with Carboplatin, Irinotecan or Olaparib in

experimental breast cancer models, significant growth control could be achieved. However, the successful result strongly depended on the dosing schedule [227]. Taking this together with the variable synergism signatures described in this thesis, it becomes clear that an in depth understanding of the mechanism of ATRi is necessary to design successful clinical trials and leverage the optimal combination partners. Prospectively, preclinical analyses should be done in a larger cohort of cell lines to better reflect different genetic set-ups and potentially identify biomarkers that predict synergism signatures for different combination therapies. In the glioma setting leveraging GB-derived stem cell-enriched cultures (GS cells) should be considered [228]. In this regard it becomes also apparent that novel combination therapies need to be functionally guided. Hence, for a more holistic overview of potentially successful combination partners genome-wide clustered regularly interspaced short palindromic repeats (CRISPR)/Cas9 knockout or activation screens performed in cells treated with the inhibitor of choice might be of high value. Wang et al. have done something similar and identified RNASEH2 as a potential biomarker for ATR inhibitor sensitivity [229]. Applying CRISPR/Cas9 genome-wide screens to identify synergistic combination partners for ATR therapy is feasible and will be done in the future. It remains to be seen if a "one-fits-all" combination including ATRi can be identified in glioma or if a more personalized medicine approach stratifying patients according to biomarkers is necessary.

In the last part of this thesis, genetic data of patients is leveraged to identify and characterize potential novel tumor vulnerabilities. There are several cancer predisposition syndromes described, e.g., Li-Fraumeni caused by a pathogenic variant in the TP53 gene [230, 231] or hereditary breast and ovarian cancers (HBOC) mostly caused by hereditary BRCA1 or BRCA2 mutations [232]. GB does not have a strong link to any hereditary syndrome, however, e.g., in lynch syndrome, caused by mutations in the DDR, GB development has been described [233, 234]. Collection of patient data in the observational study "Molecular Tumor Board at the Center for Personalized Medicine Tübingen (MTB@ZPM)" (NCT03503149), makes genomic data of patients available to assessment. Interestingly, in the studied cohort of 586 patients included in the MTB neuro-oncology cohort Tübingen in this thesis, a germline mutation rate of 10% was detected (**Figure 30**). Further analyses revealed an accumulation of germline mutations in the Fanconi anemia (FA) pathway in GB patients (**Table 4**). The analysis of somatic mutations in the FA pathway revealed a 11.1% mutation rate in GB patients which was higher than the mutation rate of the whole cohort of below 10% (**Figure 31**). The FA pathway is a DDR pathway that is responsible for repairing interstrand cross-links [235]. Proteins get associated with this pathway by displaying symptoms of FA which include bone marrow failure, increased risk of cancer development and developmental abnormalities upon mutation [123]. FA is mainly associated with myelodysplastic

syndromes or acute myeloid leukemia [236], but also with solid tumor formation, e.g. breast, head and neck, or liver cancers [124, 237]. Especially BRCA1 and BRCA2, also known as FANCS and FANCD1, are associated with breast cancer risk [232]. However, FANCM mutations were described to lead to early-onset breast cancer as well [238, 239]. Literature on the influence of FA mutations on GB development is limited. One case report by Boukerroucha et al. looked into BRCA1 germline mutations of two patients that first developed breast cancer and later also GB. In these cases, they could not find any evidence for an influence of brain tumor development as BRCA1 expression was retained in the GB tissue [240]. Another study by Patil et al. found that FANCD2 is re-expressed in GB patient tissue which was correlated with tumor grade [130]. These reports were based on patient data but did not include experiments on modelling the mutations in an experimental set-up. Hence, based on the findings in the MTB neuro-oncology cohort, an influence of FA mutations on GB tumor development was still hypothesized.

The tumor forming capabilities of FA mutations in the glioma context was modeled using the replication competent avian leukosis and sarcoma virus/tumor virus a (RCAS/tv-a) system. A mixture of DF-1 cells producing RCAS virus either overexpressing platelet derived growth factor B (PDGFB) or shRNAs targeting one of five FA genes was implanted into mice (**Figure 32**, **Figure 33**). This system provides a platform that mimics tumor onset in patients very well due to i) the modification of intrinsic cells, ii) the immunocompetency of the model and iii) the low number of cells that are transformed to form tumors [149]. In the established experimental set-up using the RCAS/tv-a system 50 000 DF-1 cells carrying RCAS virus with a PDGFB overexpression are orthotopically injected into the brains of 129S.Tg(NES-TVA)-Cdkn2a$^{-/-}$ mice which leads to a latency of symptom onset of 39 days that is very stable across different experimental runs [145, 148].

In this thesis the experimental set-up was changed to transplanting 25 000 DF-1 cells carrying RCAS virus expressing PDGFB plus 25 000 DF-1 cell carrying RCAS virus expressing an shRNA. This led to a delay of approximately 20 days to a median of 59.5 days until development of neurological symptoms in the shscramble control group (**Figure 33**). Interestingly, in the group implanted with shFA-Gene1 a reduction of time until onset neurological symptom compared to the scramble control group was detected. The histological analysis of the mice in the shFA-Gene1 group displayed features of high-grade glioma that were not as pronounced in the scramble group or in any of the other FA groups. Additionally, a significantly higher amount of proliferating, Ki67$^+$ cells were detected (**Figure 33**, **Figure 34**). In the other groups, targeting FA-Gene2, FA-Gene3 and FA-Gene4, tumor formation was observed, however, the time until onset of neurological symptoms varied rather strong within each of these groups with a tendency to a prolonged latency especially in FA-Gene2 and 3. Interestingly, the shFA-Gene1 group recapitulates the latency of symptom onset of 39 days of the original set-up with a very low variability within the group. The variation of symptom onset within the other groups might be

explained by a varying composition of implanted cell mixtures or varying rates of successful infection leading to the variable tumor onset. There might also be a specific molecular mechanism in the infected cells that needs to be completed in order to form tumors in the PDGFB/FA-knockdown setting that changed the symptom onset in the other groups. Unfortunately, no longitudinal measurements of tumor development were possible which could shed some light on these open questions. Longitudinal measurements might have also provided insights into the mechanisms of FA-Gene5 knockdown in which only two animals displayed neurological symptoms and tumor development.

In a future experiment it is planned to more closely investigate the tumor onsetting capabilities of FA-Gene knockdown by using different compositions of DF-1 cells carrying PDGFB and shRNA up to only implanting DF-1 cells carrying shRNAs targeting FA genes. Novel techniques like spatial transcriptomics might also shed some more light on the molecular mechanisms underlying tumor formation in PDGFB/FA-Gene knockdown tumors and explain the different symptom onset phenotypes observed in this thesis. Another important experimental approach, that more closely reflects the germline mutations detected in the patient cohort, might be the usage of genetically engineered mice that carry FA germline mutations in order to determine the effect of developmental FA gene loss on brain tumor development.

Next, the influence of FA genes on cell biology in long-term glioma cell lines was evaluated with a special focus on therapeutic implications. No effects on proliferation capacity in long-term glioma cell lines LN229 and LNZ308 upon FA gene knockdown were detected (**Figure 36**). To test if FA knockdown has an influence on treatment sensitivity, five different treatment modalities were evaluated in clonogenic survival assays. Irradiation, Temozolomide and Lomustine (CCNU) are treatment modalities frequently used in GB treatment [3]. FA patients have been shown to be more radiosensitive than other patients [241, 242]. Preclinical studies proved a higher chemosensitivity of glioma cell lines upon FA inhibition [129, 130, 243]. However, in the LN229 and LNZ308 cells the knockdown of FA genes did not lead to a sensitization, compared to shLuciferase control cells (**Figure 38**, **Figure 39**). However, further investigation using different irradiation dosing regimens are necessary to assess potential sensitization processes that were not detected using only one irradiation dose. Using chemotherapeutics, on the other hand, a higher sensitivity of knockdown cells than shLuciferase cells could be recapitulated in this experimental set-up. For both TMZ and CCNU treatments treatment sensitization could be detected in both cellular backgrounds (**Figure 38**, **Figure 39**).

Targeted therapy leveraging potentially synthetic lethal approaches similar to BRCA1 or BRCA2 mutated breast cancer [193] are of increasing interest in an ever growing range of other cancer entities in particular with other FA germline mutations. For example, Horak et al. presented a case study on a PALB2 germline mutation in a prostate cancer patient that was treated with Olaparib which lead to disease stabilization [244]. Moreover, a phase II clinical trial using Talazoparib, another PARP inhibitor,

in solid tumors with mutations in the homologous recombination pathway other than BRCA1 and BRCA2 reported treatment efficacy in all patients with germline mutations in PALB2 [245]. In line, Olaparib treatment of FA knockdown cell lines of FA-GENE4 displayed higher sensitivity than in shLuciferase control cells. A similar trend was detected in FA-GENE1 knockdowns, however, only in the LN229 cellular background one shRNA knockdown significantly increased sensitivity, in LNZ308 cells none of the knockdowns displayed a significant difference. Similarly, using the ATR inhibitor AZD6738 LN229 cells carrying a knockdown of FA-GENE4 displayed a significantly more sensitive phenotype than shLuciferase control cells, however, none of the other knockdown cells could recapitulated this finding (**Figure 38**, **Figure 39**). Differences in therapy sensitivities upon FA gene knockdown might be due to differing underlying genetic backgrounds of the glioma long-term cell lines LN229 and LNZ308. As different genes and therefore different levels of the FA pathway were knocked down by the shRNAs, this might also have an influence on therapy sensitivity read-outs.

Importantly, these results together with reports in the literature do hint at differences in therapeutic sensitivities in tumors of germline mutated FA patients and might even have implications for patients with somatic FA mutations in the tumor. However, validation of these phenotypes in the RCAS/tv-a model *in vivo* is of utmost importance to acquire more profound insights. Of note, in FA patients who needed a hematopoietic stem cell transfer (HSCT) for which cyclophosphamide and radiotherapy pretreatment was necessary, an increased frequency of development of secondary solid tumors was described [237]. Hence, for a potential clinical translation this also needs to be considered in GB patients carrying FA germline mutations. In this regard it might be a valuable approach to identify additional targeted therapies, besides Olaparib and ATRi, that impose a lesser risk of secondary tumor development and still might improve therapeutic efficacy. Identification of novel therapeutic options could be done by genome-wide CRISPR/Cas9 dependency screens in FA knockdown cell lines.

Taken together, the data provided here include implications for a link of GB development to FA that has not been described before. Further experiments titrating the capability of FA knockdown alone to induce tumors need to be conducted to acquire a more holistic picture of this link. Furthermore, different treatment modalities have been tested to evaluate potential novel treatment options. Indeed, an influence of FA knockdown on treatment sensitivities could be detected, potentially identifying a novel actionable tumor vulnerability. However, further preclinical studies, including treatment studies to verify treatable variabilities are warranted.

To conclude, in this thesis three different approaches to understand, induce and exploit actionable tumor vulnerabilities are presented. First, Argyrin F which targets an intrinsic GB cancer vulnerability, i.e., inducing cell cycle-stabilization, is described. Upon anti-glioma activity analysis, it became

apparent that it additionally opens a novel, actionable therapeutic window by inducing an increased immunogenicity that can be targeted by checkpoint inhibition. Based on the identified vulnerability of glioma towards ATRi when overexpressing the bHLH transcription factor family, a thorough analysis of molecular mechanisms in experimental glioma was done that revealed the potential for novel combination therapies with ATRi. At the same time the data provided also highlight the importance of understanding the molecular mechanisms to accurately predict synergistic treatment effects. Further analyses leveraging for example genome wide CRISPR/Cas9 screens in a set-up designed to unravel potential synergistic therapies are needed to acquire a holistic picture and design novel functionally guided therapies that can be successfully translated into the clinic. Lastly, leveraging patient data to deduce so far unrecognized tumor vulnerabilities enables personalized medicine approaches that might even be translated to a larger patient population later-on. In this thesis the FA pathway has been identified and studied regarding its involvement in GB tumor onset as well as subsequent therapy implications. Further studies will help to better understand the molecular mechanisms and implications and might lead to novel therapy regimens.

This thesis shows that developing novel treatment strategies for GB is challenging, but with innovative approaches the identification, induction and exploitation of actionable tumor vulnerabilities is feasible and might lead to an improvement in GB patient care in the future.

5. References

1. Stupp R, Hegi ME, Mason WP, van den Bent MJ, Taphoorn MJB, Janzer RC, Ludwin SK, Allgeier A, Fisher B, Belanger K *et al*: **Effects of radiotherapy with concomitant and adjuvant temozolomide versus radiotherapy alone on survival in glioblastoma in a randomised phase III study: 5-year analysis of the EORTC-NCIC trial**. *The Lancet Oncology* 2009, **10**(5):459-466.
2. Stupp R, Taillibert S, Kanner A, Read W, Steinberg DM, Lhermitte B, Toms S, Idbaih A, Ahluwalia MS, Fink K *et al*: **Effect of Tumor-Treating Fields Plus Maintenance Temozolomide vs Maintenance Temozolomide Alone on Survival in Patients With Glioblastoma: A Randomized Clinical Trial**. *JAMA* 2017, **318**(23):2306-2316.
3. Weller M, van den Bent M, Preusser M, Le Rhun E, Tonn JC, Minniti G, Bendszus M, Balana C, Chinot O, Dirven L *et al*: **EANO guidelines on the diagnosis and treatment of diffuse gliomas of adulthood**. *Nature Reviews Clinical Oncology* 2021, **18**(3):170-186.
4. Stupp R, Mason WP, van den Bent MJ, Weller M, Fisher B, Taphoorn MJB, Belanger K, Brandes AA, Marosi C, Bogdahn U *et al*: **Radiotherapy plus Concomitant and Adjuvant Temozolomide for Glioblastoma**. *New England Journal of Medicine* 2005, **352**(10):987-996.
5. Chen X, Bui KC, Barat S, Thi Nguyen ML, Bozko P, Sipos B, Kalesse M, Malek NP, Plentz RR: **Therapeutic effects of Argyrin F in pancreatic adenocarcinoma**. *Cancer Letters* 2017, **399**:20-28.
6. Sung H, Ferlay J, Siegel RL, Laversanne M, Soerjomataram I, Jemal A, Bray F: **Global Cancer Statistics 2020: GLOBOCAN Estimates of Incidence and Mortality Worldwide for 36 Cancers in 185 Countries**. *CA: A Cancer Journal for Clinicians* 2021, **71**(3):209-249.
7. Ostrom QT, Cioffi G, Waite K, Kruchko C, Barnholtz-Sloan JS: **CBTRUS Statistical Report: Primary Brain and Other Central Nervous System Tumors Diagnosed in the United States in 2014–2018**. *Neuro-Oncology* 2021, **23**(Supplement_3):iii1-iii105.
8. Chinot OL, Wick W, Mason W, Henriksson R, Saran F, Nishikawa R, Carpentier AF, Hoang-Xuan K, Kavan P, Cernea D *et al*: **Bevacizumab plus Radiotherapy–Temozolomide for Newly Diagnosed Glioblastoma**. *New England Journal of Medicine* 2014, **370**(8):709-722.
9. Weller M, Cloughesy T, Perry JR, Wick W: **Standards of care for treatment of recurrent glioblastoma—are we there yet?** *Neuro-Oncology* 2012, **15**(1):4-27.
10. Louis DN, Ohgaki H, Wiestler OD, Cavenee WK, Burger PC, Jouvet A, Scheithauer BW, Kleihues P: **The 2007 WHO Classification of Tumours of the Central Nervous System**. *Acta Neuropathologica* 2007, **114**(2):97-109.
11. D'Alessio A, Proietti G, Sica G, Scicchitano BM: **Pathological and Molecular Features of Glioblastoma and Its Peritumoral Tissue**. *Cancers* 2019, **11**(4):469.
12. Rong Y, Durden DL, Van Meir EG, Brat DJ: **'Pseudopalisading' Necrosis in Glioblastoma: A Familiar Morphologic Feature That Links Vascular Pathology, Hypoxia, and Angiogenesis**. *Journal of Neuropathology & Experimental Neurology* 2006, **65**(6):529-539.
13. Horbinski C, Berger T, Packer RJ, Wen PY: **Clinical implications of the 2021 edition of the WHO classification of central nervous system tumours**. *Nature Reviews Neurology* 2022.
14. Louis DN, Perry A, Reifenberger G, von Deimling A, Figarella-Branger D, Cavenee WK, Ohgaki H, Wiestler OD, Kleihues P, Ellison DW: **The 2016 World Health Organization Classification of Tumors of the Central Nervous System: a summary**. *Acta Neuropathologica* 2016, **131**(6):803-820.
15. Board WCoTE: **World Health Organization Classification of Tumours of the Central Nervous System**, 5th edn: Lyon: International Agency for Research on Cancer; 2021.
16. Capper D, Jones DTW, Sill M, Hovestadt V, Schrimpf D, Sturm D, Koelsche C, Sahm F, Chavez L, Reuss DE *et al*: **DNA methylation-based classification of central nervous system tumours**. *Nature* 2018, **555**(7697):469-474.

17.   Louis DN, Perry A, Wesseling P, Brat DJ, Cree IA, Figarella-Branger D, Hawkins C, Ng HK, Pfister SM, Reifenberger G *et al*: **The 2021 WHO Classification of Tumors of the Central Nervous System: a summary**. *Neuro-Oncology* 2021, **23**(8):1231-1251.

18.   Becker AP, Sells BE, Haque SJ, Chakravarti A: **Tumor Heterogeneity in Glioblastomas: From Light Microscopy to Molecular Pathology**. *Cancers* 2021, **13**(4):761.

19.   Dunn GP, Rinne ML, Wykosky J, Genovese G, Quayle SN, Dunn IF, Agarwalla PK, Chheda MG, Campos B, Wang A *et al*: **Emerging insights into the molecular and cellular basis of glioblastoma**. *Genes & Development* 2012, **26**(8):756-784.

20.   Esteller M, Garcia-Foncillas J, Andion E, Goodman SN, Hidalgo OF, Vanaclocha V, Baylin SB, Herman JG: **Inactivation of the DNA-Repair Gene MGMT and the Clinical Response of Gliomas to Alkylating Agents**. *New England Journal of Medicine* 2000, **343**(19):1350-1354.

21.   Hegi ME, Diserens A-C, Gorlia T, Hamou M-F, de Tribolet N, Weller M, Kros JM, Hainfellner JA, Mason W, Mariani L *et al*: **MGMT Gene Silencing and Benefit from Temozolomide in Glioblastoma**. *New England Journal of Medicine* 2005, **352**(10):997-1003.

22.   Berger K, Turowski B, Felsberg J, Malzkorn B, Reifenberger G, Steiger H-J, Budach W, Haussmann J, Knipps J, Rapp M *et al*: **Age-stratified clinical performance and survival of patients with IDH-wildtype glioblastoma homogeneously treated by radiotherapy with concomitant and maintenance temozolomide**. *Journal of Cancer Research and Clinical Oncology* 2021, **147**(1):253-262.

23.   Reifenberger G, Hentschel B, Felsberg J, Schackert G, Simon M, Schnell O, Westphal M, Wick W, Pietsch T, Loeffler M *et al*: **Predictive impact of MGMT promoter methylation in glioblastoma of the elderly**. *International Journal of Cancer* 2012, **131**(6):1342-1350.

24.   Parsons DW, Jones S, Zhang X, Lin JC-H, Leary RJ, Angenendt P, Mankoo P, Carter H, Siu I-M, Gallia GL *et al*: **An Integrated Genomic Analysis of Human Glioblastoma Multiforme**. *Science* 2008, **321**(5897):1807-1812.

25.   Brennan Cameron W, Verhaak Roel GW, McKenna A, Campos B, Noushmehr H, Salama Sofie R, Zheng S, Chakravarty D, Sanborn JZ, Berman Samuel H *et al*: **The Somatic Genomic Landscape of Glioblastoma**. *Cell* 2013, **155**(2):462-477.

26.   Castle KD, Chen M, Wisdom AJ, Kirsch DGJTCR: **Genetically engineered mouse models for studying radiation biology**. *2017* 2017:S900-S913.

27.   Verhaak RGW, Hoadley KA, Purdom E, Wang V, Qi Y, Wilkerson MD, Miller CR, Ding L, Golub T, Mesirov JP *et al*: **Integrated Genomic Analysis Identifies Clinically Relevant Subtypes of Glioblastoma Characterized by Abnormalities in PDGFRA, IDH1, EGFR, and NF1**. *Cancer Cell* 2010, **17**(1):98-110.

28.   Wang Q, Hu B, Hu X, Kim H, Squatrito M, Scarpace L, deCarvalho AC, Lyu S, Li P, Li Y *et al*: **Tumor Evolution of Glioma-Intrinsic Gene Expression Subtypes Associates with Immunological Changes in the Microenvironment**. *Cancer Cell* 2017, **32**(1):42-56.e46.

29.   Ohba S, Mukherjee J, See WL, Pieper RO: **Mutant IDH1-Driven Cellular Transformation Increases RAD51-Mediated Homologous Recombination and Temozolomide Resistance**. *Cancer Research* 2014, **74**(17):4836-4844.

30.   Sottoriva A, Spiteri I, Piccirillo SGM, Touloumis A, Collins VP, Marioni JC, Curtis C, Watts C, Tavaré S: **Intratumor heterogeneity in human glioblastoma reflects cancer evolutionary dynamics**. *Proceedings of the National Academy of Sciences* 2013, **110**(10):4009-4014.

31.   Patel AP, Tirosh I, Trombetta JJ, Shalek AK, Gillespie SM, Wakimoto H, Cahill DP, Nahed BV, Curry WT, Martuza RL *et al*: **Single-cell RNA-seq highlights intratumoral heterogeneity in primary glioblastoma**. *Science* 2014, **344**(6190):1396-1401.

32.   Roth P, Kissel M, Herrmann C, Eisele G, Leban J, Weller M, Schmidt F: **SC68896, a Novel Small Molecule Proteasome Inhibitor, Exerts Antiglioma Activity In vitro and In vivo**. *Clinical Cancer Research* 2009, **15**(21):6609-6618.

33.   Le Tourneau C, Delord J-P, Gonçalves A, Gavoille C, Dubot C, Isambert N, Campone M, Trédan O, Massiani M-A, Mauborgne C *et al*: **Molecularly targeted therapy based on tumour molecular profiling versus conventional therapy for advanced cancer (SHIVA): a**

multicentre, open-label, proof-of-concept, randomised, controlled phase 2 trial. *The Lancet Oncology* 2015, **16**(13):1324-1334.

34. Massard C, Michiels S, Ferté C, Le Deley M-C, Lacroix L, Hollebecque A, Verlingue L, Ileana E, Rosellini S, Ammari S *et al*: **High-Throughput Genomics and Clinical Outcome in Hard-to-Treat Advanced Cancers: Results of the MOSCATO 01 Trial**. *Cancer Discovery* 2017, **7**(6):586-595.

35. Churko JM, Mantalas GL, Snyder MP, Wu JC: **Overview of High Throughput Sequencing Technologies to Elucidate Molecular Pathways in Cardiovascular Diseases**. *Circulation Research* 2013, **112**(12):1613-1623.

36. Demetri GD, von Mehren M, Blanke CD, Van den Abbeele AD, Eisenberg B, Roberts PJ, Heinrich MC, Tuveson DA, Singer S, Janicek M *et al*: **Efficacy and Safety of Imatinib Mesylate in Advanced Gastrointestinal Stromal Tumors**. *New England Journal of Medicine* 2002, **347**(7):472-480.

37. Renovanz M, Kurz SC, Rieger J: **Clinical outcome of biomarker-guided therapies in adult patients with tumors of the nervous system**. 2022 (under revision).

38. Weller M, Wick W, Aldape K, Brada M, Berger M, Pfister SM, Nishikawa R, Rosenthal M, Wen PY, Stupp R, Reifenberger G: **Glioma**. *Nature Reviews Disease Primers* 2015, **1**(1):15017.

39. Rechsteiner M, Realini C, Ustrell V: **The proteasome activator 11 S REG (PA28) and class I antigen presentation**. *Biochem J* 2000, **345 Pt 1**(Pt 1):1-15.

40. Kumar Deshmukh F, Yaffe D, Olshina MA, Ben-Nissan G, Sharon M: **The Contribution of the 20S Proteasome to Proteostasis**. *Biomolecules* 2019, **9**(5):190.

41. Reits E, Griekspoor A, Neijssen J, Groothuis T, Jalink K, van Veelen P, Janssen H, Calafat J, Drijfhout JW, Neefjes J: **Peptide Diffusion, Protection, and Degradation in Nuclear and Cytoplasmic Compartments before Antigen Presentation by MHC Class I**. *Immunity* 2003, **18**(1):97-108.

42. Reits E, Neijssen J, Herberts C, Benckhuijsen W, Janssen L, Drijfhout JW, Neefjes J: **A Major Role for TPPII in Trimming Proteasomal Degradation Products for MHC Class I Antigen Presentation**. *Immunity* 2004, **20**(4):495-506.

43. Teicher BA, Anderson KC: **CCR 20th Anniversary Commentary: In the Beginning, There Was PS-341**. *Clinical Cancer Research* 2015, **21**(5):939-941.

44. Adams J, Behnke M, Chen S, Cruickshank AA, Dick LR, Grenier L, Klunder JM, Ma Y-T, Plamondon L, Stein RL: **Potent and selective inhibitors of the proteasome: Dipeptidyl boronic acids**. *Bioorganic & Medicinal Chemistry Letters* 1998, **8**(4):333-338.

45. Teicher BA, Ara G, Herbst R, Palombella VJ, Adams J: **The proteasome inhibitor PS-341 in cancer therapy**. *Clin Cancer Res* 1999, **5**(9):2638-2645.

46. Groll M, Huber R, Potts BCM: **Crystal Structures of Salinosporamide A (NPI-0052) and B (NPI-0047) in Complex with the 20S Proteasome Reveal Important Consequences of β-Lactone Ring Opening and a Mechanism for Irreversible Binding**. *Journal of the American Chemical Society* 2006, **128**(15):5136-5141.

47. Manton CA, Johnson B, Singh M, Bailey CP, Bouchier-Hayes L, Chandra J: **Induction of cell death by the novel proteasome inhibitor marizomib in glioblastoma in vitro and in vivo**. *Scientific Reports* 2016, **6**(1):18953.

48. Di K, Lloyd GK, Abraham V, MacLaren A, Burrows FJ, Desjardins A, Trikha M, Bota DA: **Marizomib activity as a single agent in malignant gliomas: ability to cross the blood-brain barrier**. *Neuro-Oncology* 2015, **18**(6):840-848.

49. Bota DA, Mason W, Kesari S, Magge R, Winograd B, Elias I, Reich SD, Levin N, Trikha M, Desjardins A: **Marizomib alone or in combination with bevacizumab in patients with recurrent glioblastoma: Phase I/II clinical trial data**. *Neuro-Oncology Advances* 2021, **3**(1).

50. Roth P, Gorlia T, Reijneveld JC, Vos FYFLD, Idbaih A, Frenel J-S, Rhun EL, Sánchez JMS, Perry JR, Masucci L *et al*: **EORTC 1709/CCTG CE.8: A phase III trial of marizomib in combination with temozolomide-based radiochemotherapy versus temozolomide-based**

radiochemotherapy alone in patients with newly diagnosed glioblastoma**. *Journal of Clinical Oncology* 2021, **39**(15_suppl):2004-2004.

51. Walter B, Canjuga D, Yüz SG, Ghosh M, Bozko P, Przystal JM, Govindarajan P, Anderle N, Keller A-L, Tatagiba M *et al*: **Argyrin F Treatment-Induced Vulnerabilities Lead to a Novel Combination Therapy in Experimental Glioma**. *Advanced Therapeutics* 2021, **4**(9):2100078.

52. Choi J-S, Joo SH: **Recent Trends in Cyclic Peptides as Therapeutic Agents and Biochemical Tools**. *Biomolecules & Therapeutics* 2020, **28**(1):18-24.

53. Joo SH: **Cyclic Peptides as Therapeutic Agents and Biochemical Tools**. *Biomolecules & Therapeutics* 2012, **20**(1):19-26.

54. Nickeleit I, Zender S, Sasse F, Geffers R, Brandes G, Sörensen I, Steinmetz H, Kubicka S, Carlomagno T, Menche D *et al*: **Argyrin A Reveals a Critical Role for the Tumor Suppressor Protein p27kip1 in Mediating Antitumor Activities in Response to Proteasome Inhibition**. *Cancer Cell* 2008, **14**(1):23-35.

55. Abukhdeir AM, Park BH: **p21 and p27: roles in carcinogenesis and drug resistance**. *Expert Reviews in Molecular Medicine* 2008, **10**:e19.

56. Polyak K, Lee M-H, Erdjument-Bromage H, Koff A, Roberts JM, Tempst P, Massagué J: **Cloning of p27Kip1, a cyclin-dependent kinase inhibitor and a potential mediator of extracellular antimitogenic signals**. *Cell* 1994, **78**(1):59-66.

57. James MK, Ray A, Leznova D, Blain SW: **Differential Modification of p27Kip1 Controls Its Cyclin D-cdk4 Inhibitory Activity**. *Molecular and Cellular Biology* 2008, **28**(1):498-510.

58. Hnit SST, Xie C, Yao M, Holst J, Bensoussan A, De Souza P, Li Z, Dong Q: **p27Kip1 signaling: Transcriptional and post-translational regulation**. *The International Journal of Biochemistry & Cell Biology* 2015, **68**:9-14.

59. Bencivenga D, Caldarelli I, Stampone E, Mancini FP, Balestrieri ML, Della Ragione F, Borriello A: **p27Kip1 and human cancers: A reappraisal of a still enigmatic protein**. *Cancer Letters* 2017, **403**:354-365.

60. Bülow L, Nickeleit I, Girbig A-K, Brodmann T, Rentsch A, Eggert U, Sasse F, Steinmetz H, Frank R, Carlomagno T *et al*: **Synthesis and Biological Characterization of Argyrin F**. *ChemMedChem* 2010, **5**(6):832-836.

61. Bäcklund LM, Nilsson BR, Liu L, Ichimura K, Collins VP: **Mutations in Rb1 pathway-related genes are associated with poor prognosis in anaplastic astrocytomas**. *Br J Cancer* 2005, **93**(1):124-130.

62. Vesely MD, Kershaw MH, Schreiber RD, Smyth MJ: **Natural Innate and Adaptive Immunity to Cancer**. *Annual Review of Immunology* 2011, **29**(1):235-271.

63. Schreiber RD, Old LJ, Smyth MJ: **Cancer Immunoediting: Integrating Immunity's Roles in Cancer Suppression and Promotion**. *Science* 2011, **331**(6024):1565-1570.

64. Lipson EJ, Drake CG: **Ipilimumab: An Anti-CTLA-4 Antibody for Metastatic Melanoma**. *Clinical Cancer Research* 2011, **17**(22):6958-6962.

65. Thorsson V, Gibbs DL, Brown SD, Wolf D, Bortone DS, Ou Yang T-H, Porta-Pardo E, Gao GF, Plaisier CL, Eddy JA *et al*: **The Immune Landscape of Cancer**. *Immunity* 2018, **48**(4):812-830.e814.

66. Old LJ, Chen Y-T: **New Paths in Human Cancer Serology**. *Journal of Experimental Medicine* 1998, **187**(8):1163-1167.

67. Slamon DJ, Leyland-Jones B, Shak S, Fuchs H, Paton V, Bajamonde A, Fleming T, Eiermann W, Wolter J, Pegram M *et al*: **Use of Chemotherapy plus a Monoclonal Antibody against HER2 for Metastatic Breast Cancer That Overexpresses HER2**. *New England Journal of Medicine* 2001, **344**(11):783-792.

68. Yu S, Liu Q, Han X, Qin S, Zhao W, Li A, Wu K: **Development and clinical application of anti-HER2 monoclonal and bispecific antibodies for cancer treatment**. *Experimental Hematology & Oncology* 2017, **6**(1):31.

69. Theofilopoulos AN, Kono DH, Baccala R: **The multiple pathways to autoimmunity**. *Nature Immunology* 2017, **18**(7):716-724.

70. Mandelbrot DA, McAdam AJ, Sharpe AH: **B7-1 or B7-2 Is Required to Produce the Lymphoproliferative Phenotype in Mice Lacking Cytotoxic T Lymphocyte–associated Antigen 4 (CTLA-4)**. *Journal of Experimental Medicine* 1999, **189**(2):435-440.

71. Keir ME, Butte MJ, Freeman GJ, Sharpe AH: **PD-1 and Its Ligands in Tolerance and Immunity**. *Annual Review of Immunology* 2008, **26**(1):677-704.

72. Hodi FS, O'Day SJ, McDermott DF, Weber RW, Sosman JA, Haanen JB, Gonzalez R, Robert C, Schadendorf D, Hassel JC *et al*: **Improved Survival with Ipilimumab in Patients with Metastatic Melanoma**. *New England Journal of Medicine* 2010, **363**(8):711-723.

73. Larkin J, Chiarion-Sileni V, Gonzalez R, Grob J-J, Rutkowski P, Lao CD, Cowey CL, Schadendorf D, Wagstaff J, Dummer R *et al*: **Five-Year Survival with Combined Nivolumab and Ipilimumab in Advanced Melanoma**. *New England Journal of Medicine* 2019, **381**(16):1535-1546.

74. Sharon E, Streicher H, Goncalves P, Chen HX: **Immune checkpoint inhibitors in clinical trials**. *Chin J Cancer* 2014, **33**(9):434-444.

75. Dong H, Strome SE, Salomao DR, Tamura H, Hirano F, Flies DB, Roche PC, Lu J, Zhu G, Tamada K *et al*: **Tumor-associated B7-H1 promotes T-cell apoptosis: A potential mechanism of immune evasion**. *Nature Medicine* 2002, **8**(8):793-800.

76. Wilmotte R, Burkhardt K, Kindler V, Belkouch M-C, Dussex G, Tribolet Nd, Walker PR, Dietrich P-Y: **B7-homolog 1 expression by human glioma: a new mechanism of immune evasion**. *NeuroReport* 2005, **16**(10):1081-1085.

77. Berghoff AS, Kiesel B, Widhalm G, Rajky O, Ricken G, Wöhrer A, Dieckmann K, Filipits M, Brandstetter A, Weller M *et al*: **Programmed death ligand 1 expression and tumor-infiltrating lymphocytes in glioblastoma**. *Neuro-Oncology* 2014, **17**(8):1064-1075.

78. Wei B, Wang L, Zhao X, Du C, Guo Y, Sun Z: **The upregulation of programmed death 1 on peripheral blood T cells of glioma is correlated with disease progression**. *Tumor Biology* 2014, **35**(4):2923-2929.

79. Zeng J, See AP, Phallen J, Jackson CM, Belcaid Z, Ruzevick J, Durham N, Meyer C, Harris TJ, Albesiano E *et al*: **Anti-PD-1 Blockade and Stereotactic Radiation Produce Long-Term Survival in Mice With Intracranial Gliomas**. *International Journal of Radiation Oncology*Biology*Physics* 2013, **86**(2):343-349.

80. Reardon DA, Brandes AA, Omuro A, Mulholland P, Lim M, Wick A, Baehring J, Ahluwalia MS, Roth P, Bähr O *et al*: **Effect of Nivolumab vs Bevacizumab in Patients With Recurrent Glioblastoma: The CheckMate 143 Phase 3 Randomized Clinical Trial**. *JAMA Oncology* 2020, **6**(7):1003-1010.

81. Persico P, Lorenzi E, Dipasquale A, Pessina F, Navarria P, Politi LS, Santoro A, Simonelli M: **Checkpoint Inhibitors as High-Grade Gliomas Treatment: State of the Art and Future Perspectives**. *Journal of Clinical Medicine* 2021, **10**(7):1367.

82. Cristescu R, Mogg R, Ayers M, Albright A, Murphy E, Yearley J, Sher X, Liu XQ, Lu H, Nebozhyn M *et al*: **Pan-tumor genomic biomarkers for PD-1 checkpoint blockade–based immunotherapy**. *Science* 2018, **362**(6411):eaar3593.

83. Le DT, Durham JN, Smith KN, Wang H, Bartlett BR, Aulakh LK, Lu S, Kemberling H, Wilt C, Luber BS *et al*: **Mismatch repair deficiency predicts response of solid tumors to PD-1 blockade**. *Science* 2017, **357**(6349):409-413.

84. Zhang X, Zhu S, Li T, Liu Y-J, Chen W, Chen J: **Targeting immune checkpoints in malignant glioma**. *Oncotarget* 2016, **8**(4).

85. Lindahl T: **Instability and decay of the primary structure of DNA**. *Nature* 1993, **362**(6422):709-715.

86. O'Connor Mark J: **Targeting the DNA Damage Response in Cancer**. *Molecular Cell* 2015, **60**(4):547-560.

87.   Pearl LH, Schierz AC, Ward SE, Al-Lazikani B, Pearl FMG: **Therapeutic opportunities within the DNA damage response**. *Nature Reviews Cancer* 2015, **15**(3):166-180.

88.   Rodríguez A, D'Andrea A: **Fanconi anemia pathway**. *Current Biology* 2017, **27**(18):R986-R988.

89.   Jasin M, Rothstein R: **Repair of Strand Breaks by Homologous Recombination**. *Cold Spring Harbor Perspectives in Biology* 2013, **5**(11).

90.   Ceccaldi R, Rondinelli B, D'Andrea AD: **Repair Pathway Choices and Consequences at the Double-Strand Break**. *Trends in Cell Biology* 2016, **26**(1):52-64.

91.   Caldecott KW: **DNA single-strand break repair**. *Experimental Cell Research* 2014, **329**(1):2-8.

92.   Gillet LCJ, Schärer OD: **Molecular Mechanisms of Mammalian Global Genome Nucleotide Excision Repair**. *Chemical Reviews* 2006, **106**(2):253-276.

93.   Jiricny J: **The multifaceted mismatch-repair system**. *Nature Reviews Molecular Cell Biology* 2006, **7**(5):335-346.

94.   Margison GP, Santibáñez-Koref MF: **O6-alkylguanine-DNA alkyltransferase: Role in carcinogenesis and chemotherapy**. *BioEssays* 2002, **24**(3):255-266.

95.   Roos WP, Thomas AD, Kaina B: **DNA damage and the balance between survival and death in cancer biology**. *Nature Reviews Cancer* 2016, **16**(1):20-33.

96.   Hanahan D, Weinberg Robert A: **Hallmarks of Cancer: The Next Generation**. *Cell* 2011, **144**(5):646-674.

97.   Jackson SP, Bartek J: **The DNA-damage response in human biology and disease**. *Nature* 2009, **461**(7267):1071-1078.

98.   Dobzhansky T: **GENETICS OF NATURAL POPULATIONS. XIII. RECOMBINATION AND VARIABILITY IN POPULATIONS OF DROSOPHILA PSEUDOOBSCURA**. *Genetics* 1946, **31**(3):269-290.

99.   Bryant HE, Schultz N, Thomas HD, Parker KM, Flower D, Lopez E, Kyle S, Meuth M, Curtin NJ, Helleday T: **Specific killing of BRCA2-deficient tumours with inhibitors of poly(ADP-ribose) polymerase**. *Nature* 2005, **434**(7035):913-917.

100.   Fong PC, Boss DS, Yap TA, Tutt A, Wu P, Mergui-Roelvink M, Mortimer P, Swaisland H, Lau A, O'Connor MJ *et al*: **Inhibition of Poly(ADP-Ribose) Polymerase in Tumors from BRCA Mutation Carriers**. *New England Journal of Medicine* 2009, **361**(2):123-134.

101.   Ledermann J, Harter P, Gourley C, Friedlander M, Vergote I, Rustin G, Scott CL, Meier W, Shapira-Frommer R, Safra T *et al*: **Olaparib maintenance therapy in patients with platinum-sensitive relapsed serous ovarian cancer: a preplanned retrospective analysis of outcomes by BRCA status in a randomised phase 2 trial**. *The Lancet Oncology* 2014, **15**(8):852-861.

102.   Pilié PG, Tang C, Mills GB, Yap TA: **State-of-the-art strategies for targeting the DNA damage response in cancer**. *Nature Reviews Clinical Oncology* 2019, **16**(2):81-104.

103.   Kaufman B, Shapira-Frommer R, Schmutzler RK, Audeh MW, Friedlander M, Balmaña J, Mitchell G, Fried G, Stemmer SM, Hubert A *et al*: **Olaparib Monotherapy in Patients With Advanced Cancer and a Germline BRCA1/2 Mutation**. *Journal of Clinical Oncology* 2015, **33**(3):244-250.

104.   Fulton B, Short SC, James A, Nowicki S, McBain C, Jefferies S, Kelly C, Stobo J, Morris A, Williamson A, Chalmers AJ: **PARADIGM-2: Two parallel phase I studies of olaparib and radiotherapy or olaparib and radiotherapy plus temozolomide in patients with newly diagnosed glioblastoma, with treatment stratified by MGMT status**. *Clinical and Translational Radiation Oncology* 2018, **8**:12-16.

105.   Piotrowski A, Puduvalli V, Wen P, Campian J, Colman H, Pearlman M, Butowski N, Battiste J, Glass J, Cloughesy T *et al*: **ACTR-39. PAMIPARIB IN COMBINATION WITH RADIATION THERAPY (RT) AND/OR TEMOZOLOMIDE (TMZ) IN PATIENTS WITH NEWLY DIAGNOSED OR RECURRENT/REFRACTORY (R/R) GLIOBLASTOMA (GBM); PHASE 1B/2 STUDY UPDATE**. *Neuro Oncol* 2019, **21**(Suppl 6):vi21-22.

106.   Pegg AE: **Repair of O6-alkylguanine by alkyltransferases**. *Mutation Research/Reviews in Mutation Research* 2000, **462**(2):83-100.

107. Felsberg J, Thon N, Eigenbrod S, Hentschel B, Sabel MC, Westphal M, Schackert G, Kreth FW, Pietsch T, Löffler M *et al*: **Promoter methylation and expression of MGMT and the DNA mismatch repair genes MLH1, MSH2, MSH6 and PMS2 in paired primary and recurrent glioblastomas**. *International Journal of Cancer* 2011, **129**(3):659-670.

108. Yip S, Miao J, Cahill DP, Iafrate AJ, Aldape K, Nutt CL, Louis DN: **MSH6 Mutations Arise in Glioblastomas during Temozolomide Therapy and Mediate Temozolomide Resistance**. *Clinical Cancer Research* 2009, **15**(14):4622-4629.

109. Bao S, Wu Q, McLendon RE, Hao Y, Shi Q, Hjelmeland AB, Dewhirst MW, Bigner DD, Rich JN: **Glioma stem cells promote radioresistance by preferential activation of the DNA damage response**. *Nature* 2006, **444**(7120):756-760.

110. Abraham RT: **Cell cycle checkpoint signaling through the ATM and ATR kinases**. *Genes & Development* 2001, **15**(17):2177-2196.

111. Saldivar JC, Cortez D, Cimprich KA: **The essential kinase ATR: ensuring faithful duplication of a challenging genome**. *Nature Reviews Molecular Cell Biology* 2017, **18**(10):622-636.

112. Lavin MF: **Ataxia-telangiectasia: from a rare disorder to a paradigm for cell signalling and cancer**. *Nature Reviews Molecular Cell Biology* 2008, **9**(10):759-769.

113. Smith J, Mun Tho L, Xu N, A. Gillespie D: **Chapter 3 - The ATM–Chk2 and ATR–Chk1 Pathways in DNA Damage Signaling and Cancer**. In: *Advances in Cancer Research. Volume 108*, edn. Edited by Vande Woude GF, Klein G: Academic Press; 2010: 73-112.

114. Tentori L, Ricci-Vitiani L, Muzi A, Ciccarone F, Pelacchi F, Calabrese R, Runci D, Pallini R, Caiafa P, Graziani G: **Pharmacological inhibition of poly(ADP-ribose) polymerase-1 modulates resistance of human glioblastoma stem cells to temozolomide**. *BMC Cancer* 2014, **14**(1):151.

115. Yang L, Shen C, Pettit CJ, Li T, Hu AJ, Miller ED, Zhang J, Lin SH, Williams TM: **Wee1 Kinase Inhibitor AZD1775 Effectively Sensitizes Esophageal Cancer to Radiotherapy**. *Clinical Cancer Research* 2020, **26**(14):3740-3750.

116. Leijen S, Geel RMJMv, Sonke GS, Jong Dd, Rosenberg EH, Marchetti S, Pluim D, Werkhoven Ev, Rose S, Lee MA *et al*: **Phase II Study of WEE1 Inhibitor AZD1775 Plus Carboplatin in Patients With TP53-Mutated Ovarian Cancer Refractory or Resistant to First-Line Therapy Within 3 Months**. *Journal of Clinical Oncology* 2016, **34**(36):4354-4361.

117. Waqar SN, Robinson C, Olszanski AJ, Spira A, Hackmaster M, Lucas L, Sponton L, Jin H, Hering U, Cronier D *et al*: **Phase I trial of ATM inhibitor M3541 in combination with palliative radiotherapy in patients with solid tumors**. *Investigational New Drugs* 2022, **40**(3):596-605.

118. Middleton MR, Dean E, Evans TRJ, Shapiro GI, Pollard J, Hendriks BS, Falk M, Diaz-Padilla I, Plummer R: **Phase 1 study of the ATR inhibitor berzosertib (formerly M6620, VX-970) combined with gemcitabine ± cisplatin in patients with advanced solid tumours**. *British Journal of Cancer* 2021, **125**(4):510-519.

119. Kim R, Kwon M, An M, Kim ST, Smith SA, Loembé AB, Mortimer PGS, Armenia J, Lukashchuk N, Shah N *et al*: **Phase II study of ceralasertib (AZD6738) in combination with durvalumab in patients with advanced/metastatic melanoma who have failed prior anti-PD-1 therapy**. *Annals of Oncology* 2022, **33**(2):193-203.

120. Koch MS, Czemmel S, Lennartz F, Beyeler S, Rajaraman S, Przystal JM, Govindarajan P, Canjuga D, Neumann M, Rizzu P *et al*: **Experimental glioma with high bHLH expression harbor increased replicative stress and are sensitive toward ATR inhibition**. *Neuro-Oncology Advances* 2020, **2**(1).

121. Lobitz S, Velleuer E: **Guido Fanconi (1892–1979): a jack of all trades**. *Nature Reviews Cancer* 2006, **6**(11):893-898.

122. Bogliolo M, Surrallés J: **Fanconi anemia: a model disease for studies on human genetics and advanced therapeutics**. *Current Opinion in Genetics & Development* 2015, **33**:32-40.

123. Che R, Zhang J, Nepal M, Han B, Fei P: **Multifaceted Fanconi Anemia Signaling**. *Trends in Genetics* 2018, **34**(3):171-183.

124. Nepal M, Che R, Zhang J, Ma C, Fei P: **Fanconi Anemia Signaling and Cancer**. *Trends in Cancer* 2017, **3**(12):840-856.
125. Ling C, Huang J, Yan Z, Li Y, Ohzeki M, Ishiai M, Xu D, Takata M, Seidman M, Wang W: **Bloom syndrome complex promotes FANCM recruitment to stalled replication forks and facilitates both repair and traverse of DNA interstrand crosslinks**. *Cell Discovery* 2016, **2**(1):16047.
126. Rajendra E, Oestergaard Vibe H, Langevin F, Wang M, Dornan Gillian L, Patel Ketan J, Passmore Lori A: **The Genetic and Biochemical Basis of FANCD2 Monoubiquitination**. *Molecular Cell* 2014, **54**(5):858-869.
127. Panneerselvam J, Xie G, Che R, Su M, Zhang J, Jia W, Fei P: **Distinct Metabolic Signature of Human Bladder Cancer Cells Carrying an Impaired Fanconi Anemia Tumor-Suppressor Signaling Pathway**. *Journal of Proteome Research* 2016, **15**(4):1333-1341.
128. Root H, Larsen A, Komosa M, Al-Azri F, Li R, Bazett-Jones DP, Stephen Meyn M: **FANCD2 limits BLM-dependent telomere instability in the alternative lengthening of telomeres pathway**. *Human Molecular Genetics* 2016, **25**(15):3255-3268.
129. Chen CC, Taniguchi T, D'Andrea A: **The Fanconi anemia (FA) pathway confers glioma resistance to DNA alkylating agents**. *Journal of Molecular Medicine* 2007, **85**(5):497-509.
130. Patil AA, Sayal P, Depondt M-L, Beveridge RD, Roylance A, Kriplani DH, Myers KN, Cox A, Jellinek D, Fernando M *et al*: **FANCD2 re-expression is associated with glioma grade and chemical inhibition of the Fanconi Anaemia pathway sensitises gliomas to chemotherapeutic agents**. *Oncotarget* 2014, **5**(15).
131. Hicks WH, Bird CE, Traylor JI, Shi DD, El Ahmadieh TY, Richardson TE, McBrayer SK, Abdullah KG: **Contemporary Mouse Models in Glioma Research**. *Cells* 2021, **10**(3):712.
132. Jung J, Seol HS, Chang S: **The Generation and Application of Patient-Derived Xenograft Model for Cancer Research**. *Cancer Res Treat* 2018, **50**(1):1-10.
133. Sampson JH, Ashley DM, Archer GE, Fuchs HE, Dranoff G, Hale LP, Bigner DD: **Characterization of a spontaneous murine astrocytoma and abrogation of its tumorigenicity by cytokine secretion**. *Neurosurgery* 1997, **41**(6):1365-1372; discussion 1372-1363.
134. Serano RD, Pegram CN, Bigner DD: **Tumorigenic cell culture lines from a spontaneous VM/Dk murine astrocytoma (SMA)**. *Acta Neuropathologica* 1980, **51**(1):53-64.
135. Ausman JI, Shapiro WR, Rall DP: **Studies on the chemotherapy of experimental brain tumors: development of an experimental model**. *Cancer Res* 1970, **30**(9):2394-2400.
136. Holland EC, Hively WP, DePinho RA, Varmus HE: **A constitutively active epidermal growth factor receptor cooperates with disruption of G1 cell-cycle arrest pathways to induce glioma-like lesions in mice**. *Genes & Development* 1998, **12**(23):3675-3685.
137. Holland EC, Varmus HE: **Basic fibroblast growth factor induces cell migration and proliferation after glia-specific gene transfer in mice**. *Proceedings of the National Academy of Sciences* 1998, **95**(3):1218-1223.
138. Miller J, Eisele G, Tabatabai G, Aulwurm S, von Kürthy G, Stitz L, Roth P, Weller M: **Soluble CD70: a novel immunotherapeutic agent for experimental glioblastoma: Laboratory investigation**. *Journal of Neurosurgery JNS* 2010, **113**(2):280-285.
139. Przystal JM, Becker H, Canjuga D, Tsiami F, Anderle N, Keller A-L, Pohl A, Ries CH, Schmittnaegel M, Korinetska N *et al*: **Targeting CSF1R Alone or in Combination with PD1 in Experimental Glioma**. *Cancers* 2021, **13**(10):2400.
140. Learn CA, Grossi PM, Schmittling RJ, Xie W, Mitchell DA, Karikari I, Wei Z, Dressman H, Sampson JH: **Genetic analysis of intracranial tumors in a murine model of glioma demonstrate a shift in gene expression in response to host immunity**. *Journal of Neuroimmunology* 2007, **182**(1):63-72.
141. Oh T, Fakurnejad S, Sayegh ET, Clark AJ, Ivan ME, Sun MZ, Safaee M, Bloch O, James CD, Parsa AT: **Immunocompetent murine models for the study of glioblastoma immunotherapy**. *Journal of Translational Medicine* 2014, **12**(1):107.

142. Ahronian LG, Lewis BC: **Using the RCAS-TVA System to Model Human Cancer in Mice**. *Cold Spring Harbor Protocols* 2014, **2014**(11):pdb.top069831.

143. Lendahl U, Zimmerman LB, McKay RDG: **CNS stem cells express a new class of intermediate filament protein**. *Cell* 1990, **60**(4):585-595.

144. Fisher GH, Orsulic S, Holland E, Hively WP, Li Y, Lewis BC, Williams BO, Varmus HE: **Development of a flexible and specific gene delivery system for production of murine tumor models**. *Oncogene* 1999, **18**(38):5253-5260.

145. Hambardzumyan D, Amankulor NM, Helmy KY, Becher OJ, Holland EC: **Modeling Adult Gliomas Using RCAS/t-va Technology**. *Translational Oncology* 2009, **2**(2):89-IN86.

146. Dai C, Celestino JC, Okada Y, Louis DN, Fuller GN, Holland EC: **PDGF autocrine stimulation dedifferentiates cultured astrocytes and induces oligodendrogliomas and oligoastrocytomas from neural progenitors and astrocytes in vivo**. *Genes & Development* 2001, **15**(15):1913-1925.

147. Serrano M, Lee H-W, Chin L, Cordon-Cardo C, Beach D, DePinho RA: **Role of the INK4a Locus in Tumor Suppression and Cell Mortality**. *Cell* 1996, **85**(1):27-37.

148. Becker H, Castaneda-Vega S, Patzwaldt K, Przystal JM, Walter B, Michelotti FC, Canjuga D, Tatagiba M, Pichler B, Beck SC *et al*: **Multiparametric Longitudinal Profiling of RCAS-tva-Induced PDGFB-Driven Experimental Glioma**. *Brain Sciences* 2022, **12**(11):1426.

149. Kanvinde PP, Malla AP, Connolly NP, Szulzewsky F, Anastasiadis P, Ames HM, Kim AJ, Winkles JA, Holland EC, Woodworth GF: **Leveraging the replication-competent avian-like sarcoma virus/tumor virus receptor-A system for modeling human gliomas**. *Glia* 2021, **69**(9):2059-2076.

150. Le Rhun E, Preusser M, Roth P, Reardon DA, van den Bent M, Wen P, Reifenberger G, Weller M: **Molecular targeted therapy of glioblastoma**. *Cancer Treatment Reviews* 2019, **80**:101896.

151. Bonm A, Kesari S: **DNA Damage Response in Glioblastoma: Mechanism for Treatment Resistance and Emerging Therapeutic Strategies**. *The Cancer Journal* 2021, **27**(5):379-385.

152. Ishii N, Maier D, Merlo A, Tada M, Sawamura Y, Diserens A-C, Van Meir EG: **Frequent Co-Alterations of TP53, p16/CDKN2A, p14ARF, PTEN Tumor Suppressor Genes in Human Glioma Cell Lines**. *Brain Pathology* 1999, **9**(3):469-479.

153. Studer A, de Tribolet N, Diserens AC, Gaide AC, Matthieu JM, Carrel S, Stavrou D: **Characterization of four human malignant glioma cell lines**. *Acta Neuropathol* 1985, **66**(3):208-217.

154. Himly M, Foster DN, Bottoli I, Iacovoni JS, Vogt PK: **The DF-1 Chicken Fibroblast Cell Line: Transformation Induced by Diverse Oncogenes and Cell Death Resulting from Infection by Avian Leukosis Viruses**. *Virology* 1998, **248**(2):295-304.

155. Konermann S, Brigham MD, Trevino AE, Joung J, Abudayyeh OO, Barcena C, Hsu PD, Habib N, Gootenberg JS, Nishimasu H *et al*: **Genome-scale transcriptional activation by an engineered CRISPR-Cas9 complex**. *Nature* 2015, **517**(7536):583-588.

156. Sanjana NE, Shalem O, Zhang F: **Improved vectors and genome-wide libraries for CRISPR screening**. *Nature Methods* 2014, **11**(8):783-784.

157. STEWART SA, DYKXHOORN DM, PALLISER D, MIZUNO H, YU EY, AN DS, SABATINI DM, CHEN ISY, HAHN WC, SHARP PA *et al*: **Lentivirus-delivered stable gene silencing by RNAi in primary cells**. *RNA* 2003, **9**(4):493-501.

158. Aithal MGS, Rajeswari N: **Validation of Housekeeping Genes for Gene Expression Analysis in Glioblastoma Using Quantitative Real-Time Polymerase Chain Reaction**. *Brain Tumor Res Treat* 2015, **3**(1):24-29.

159. Silginer M, Burghardt I, Gramatzki D, Bunse L, Leske H, Rushing EJ, Hao N, Platten M, Weller M, Roth P: **The aryl hydrocarbon receptor links integrin signaling to the TGF-β pathway**. *Oncogene* 2016, **35**(25):3260-3271.

160. Han J, Ruan C, Huen MSY, Wang J, Xie A, Fu C, Liu T, Huang J: **BRCA2 antagonizes classical and alternative nonhomologous end-joining to prevent gross genomic instability**. *Nature Communications* 2017, **8**(1):1470.

161. Raudvere U, Kolberg L, Kuzmin I, Arak T, Adler P, Peterson H, Vilo J: **g:Profiler: a web server for functional enrichment analysis and conversions of gene lists (2019 update)**. *Nucleic Acids Research* 2019, **47**(W1):W191-W198.

162. Guzmán C, Bagga M, Kaur A, Westermarck J, Abankwa D: **ColonyArea: An ImageJ Plugin to Automatically Quantify Colony Formation in Clonogenic Assays**. *PLOS ONE* 2014, **9**(3):e92444.

163. Franken NAP, Rodermond HM, Stap J, Haveman J, van Bree C: **Clonogenic assay of cells in vitro**. *Nature Protocols* 2006, **1**(5):2315-2319.

164. Yan H, Zhang B, Li S, Zhao Q: **A formal model for analyzing drug combination effects and its application in TNF-α-induced NFκB pathway**. *BMC Systems Biology* 2010, **4**(1):50.

165. He L, Kulesskiy E, Saarela J, Turunen L, Wennerberg K, Aittokallio T, Tang J: **Methods for High-throughput Drug Combination Screening and Synergy Scoring**. In: *Cancer Systems Biology: Methods and Protocols.* edn. Edited by von Stechow L. New York, NY: Springer New York; 2018: 351-398.

166. Yadav B, Wennerberg K, Aittokallio T, Tang J: **Searching for Drug Synergy in Complex Dose–Response Landscapes Using an Interaction Potency Model**. *Computational and Structural Biotechnology Journal* 2015, **13**:504-513.

167. **pLKO.1 - TRC Cloning Vector** [http://www.addgene.org/protocols/plko/#I]

168. Loftus SK, Larson DM, Watkins-Chow D, Church DM, Pavan WJ: **Generation of RCAS Vectors Useful for Functional Genomic Analyses**. *DNA Research* 2001, **8**(5):221-226.

169. von Werder A, Seidler B, Schmid RM, Schneider G, Saur D: **Production of avian retroviruses and tissue-specific somatic retroviral gene transfer in vivo using the RCAS/TVA system**. *Nature Protocols* 2012, **7**(6):1167-1183.

170. Langford DJ, Bailey AL, Chanda ML, Clarke SE, Drummond TE, Echols S, Glick S, Ingrao J, Klassen-Ross T, LaCroix-Fralish ML *et al*: **Coding of facial expressions of pain in the laboratory mouse**. *Nature Methods* 2010, **7**(6):447-449.

171. Livak KJ, Schmittgen TD: **Analysis of Relative Gene Expression Data Using Real-Time Quantitative PCR and the 2−ΔΔCT Method**. *Methods* 2001, **25**(4):402-408.

172. Rajaraman S, Canjuga D, Ghosh M, Codrea MC, Sieger R, Wedekink F, Tatagiba M, Koch M, Lauer UM, Nahnsen S *et al*: **Measles Virus-Based Treatments Trigger a Pro-inflammatory Cascade and a Distinctive Immunopeptidome in Glioblastoma**. *Molecular Therapy - Oncolytics* 2019, **12**:147-161.

173. Kowalewski DJ, Stevanović S: **Biochemical Large-Scale Identification of MHC Class I Ligands**. In: *Antigen Processing: Methods and Protocols.* edn. Edited by van Endert P. Totowa, NJ: Humana Press; 2013: 145-157.

174. Kondo J, Endo H, Okuyama H, Ishikawa O, Iishi H, Tsujii M, Ohue M, Inoue M: **Retaining cell-cell contact enables preparation and culture of spheroids composed of pure primary cancer cells from colorectal cancer**. *Proceedings of the National Academy of Sciences* 2011, **108**(15):6235-6240.

175. Anderle N, Koch A, Gierke B, Keller A-L, Staebler A, Hartkopf A, Brucker SY, Pawlak M, Schenke-Layland K, Schmees C: **A Platform of Patient-Derived Microtumors Identifies Individual Treatment Responses and Therapeutic Vulnerabilities in Ovarian Cancer**. *Cancers* 2022, **14**(12):2895.

176. Jaime-Sanchez P, Uranga-Murillo I, Aguilo N, Khouili SC, Arias MA, Sancho D, Pardo J: **Cell death induced by cytotoxic CD8^{+} T cells is immunogenic and primes caspase-3–dependent spread immunity against endogenous tumor antigens**. *Journal for ImmunoTherapy of Cancer* 2020, **8**(1):e000528.

177. Love MI, Huber W, Anders S: **Moderated estimation of fold change and dispersion for RNA-seq data with DESeq2**. *Genome Biology* 2014, **15**(12):550.

178. Treindl F, Ruprecht B, Beiter Y, Schultz S, Döttinger A, Staebler A, Joos TO, Kling S, Poetz O, Fehm T *et al*: **A bead-based western for high-throughput cellular signal transduction analyses**. *Nature Communications* 2016, **7**(1):12852.

179. Saeed AI, Sharov V, White J, Li J, Liang W, Bhagabati N, Braisted J, Klapa M, Currier T, Thiagarajan M *et al*: **TM4: A Free, Open-Source System for Microarray Data Management and Analysis**. *BioTechniques* 2003, **34**(2):374-378.

180. Jarmalavicius S, Welte Y, Walden P: **High Immunogenicity of the Human Leukocyte Antigen Peptidomes of Melanoma Tumor Cells***. *Journal of Biological Chemistry* 2012, **287**(40):33401-33411.

181. Pritchard AL, Hastie ML, Neller M, Gorman JJ, Schmidt CW, Hayward NK: **Exploration of peptides bound to MHC class I molecules in melanoma**. *Pigment Cell & Melanoma Research* 2015, **28**(3):281-294.

182. Ternette N, Olde Nordkamp MJM, Müller J, Anderson AP, Nicastri A, Hill AVS, Kessler BM, Li D: **Immunopeptidomic Profiling of HLA-A2-Positive Triple Negative Breast Cancer Identifies Potential Immunotherapy Target Antigens**. *PROTEOMICS* 2018, **18**(12):1700465.

183. Walter B, Hirsch S, Kuhlburger L, Stahl A, Schnabel L, Wisser S, Haeusser LA, Tsiami F, Plöger S, Aghaallaei N *et al*: **Functionally-instructed modifiers of response to ATR inhibition in experimental glioma**. *Journal of Experimental & Clinical Cancer Research* 2024, **43**(1):77.

184. Fròsina G, Profumo A, Marubbi D, Marcello D, Ravetti JL, Daga A: **ATR kinase inhibitors NVP-BEZ235 and AZD6738 effectively penetrate the brain after systemic administration**. *Radiation Oncology* 2018, **13**(1):76.

185. Talele S, Zhang W, Burgenske DM, Kim M, Mohammad AS, Dragojevic S, Gupta SK, Bindra RS, Sarkaria JN, Elmquist WF: **Brain Distribution of Berzosertib: An Ataxia Telangiectasia and Rad3-Related Protein Inhibitor for the Treatment of Glioblastoma**. *Journal of Pharmacology and Experimental Therapeutics* 2021, **379**(3):343-357.

186. Kanehisa M, Furumichi M, Sato Y, Ishiguro-Watanabe M, Tanabe M: **KEGG: integrating viruses and cellular organisms**. *Nucleic Acids Research* 2020, **49**(D1):D545-D551.

187. Helleday T, Petermann E, Lundin C, Hodgson B, Sharma RA: **DNA repair pathways as targets for cancer therapy**. *Nature Reviews Cancer* 2008, **8**(3):193-204.

188. Neftel C, Laffy J, Filbin MG, Hara T, Shore ME, Rahme GJ, Richman AR, Silverbush D, Shaw ML, Hebert CM *et al*: **An Integrative Model of Cellular States, Plasticity, and Genetics for Glioblastoma**. *Cell* 2019, **178**(4):835-849.e821.

189. Cuddapah VA, Robel S, Watkins S, Sontheimer H: **A neurocentric perspective on glioma invasion**. *Nature Reviews Neuroscience* 2014, **15**(7):455-465.

190. Sahm F, Capper D, Jeibmann A, Habel A, Paulus W, Troost D, von Deimling A: **Addressing Diffuse Glioma as a Systemic Brain Disease With Single-Cell Analysis**. *Archives of Neurology* 2012, **69**(4):523-526.

191. Kim J, Lee I-H, Cho Hee J, Park C-K, Jung Y-S, Kim Y, Nam So H, Kim Byung S, Johnson Mark D, Kong D-S *et al*: **Spatiotemporal Evolution of the Primary Glioblastoma Genome**. *Cancer Cell* 2015, **28**(3):318-328.

192. Osuka S, Van Meir EG: **Overcoming therapeutic resistance in glioblastoma: the way forward**. *J Clin Invest* 2017, **127**(2):415-426.

193. Ledermann J, Harter P, Gourley C, Friedlander M, Vergote I, Rustin G, Scott C, Meier W, Shapira-Frommer R, Safra T *et al*: **Olaparib Maintenance Therapy in Platinum-Sensitive Relapsed Ovarian Cancer**. *New England Journal of Medicine* 2012, **366**(15):1382-1392.

194. Elmore KB, Schaff LR: **DNA Repair Mechanisms and Therapeutic Targets in Glioma**. In: *Curr Oncol Rep.* vol. 23; 2021: 87.

195. Liu M, Liu H, Chen J: **Mechanisms of the CDK4/6 inhibitor palbociclib (PD 0332991) and its future application in cancer treatment (Review)**. *Oncol Rep* 2018, **39**(3):901-911.

196. Alexander BM, Cloughesy TF: **Platform trials arrive on time for glioblastoma**. *Neuro-Oncology* 2018, **20**(6):723-725.

197. Bassermann F, Eichner R, Pagano M: **The ubiquitin proteasome system — Implications for cell cycle control and the targeted treatment of cancer**. *Biochimica et Biophysica Acta (BBA) - Molecular Cell Research* 2014, **1843**(1):150-162.

198. Naujokat C, Sezer O, Zinke H, Leclere A, Hauptmann S, Possinger K: **Proteasome inhibitors induce caspase-dependent apoptosis and accumulationof p21WAF1/Cip1 in human immatureleukemic cells**. *European Journal of Haematology* 2000, **65**(4):221-236.

199. Almond JB, Snowden RT, Hunter A, Dinsdale D, Cain K, Cohen GM: **Proteasome inhibitor-induced apoptosis of B-chronic lymphocytic leukaemia cells involves cytochrome c release and caspase activation, accompanied by formation of an ~700 kDa Apaf-1 containing apoptosome complex**. *Leukemia* 2001, **15**(9):1388-1397.

200. Fricker LD: **Proteasome Inhibitor Drugs**. *Annual Review of Pharmacology and Toxicology* 2020, **60**(1):457-476.

201. Zhou Y, Wang K, Zhen S, Wang R, Luo W: **Carfilzomib induces G2/M cell cycle arrest in human endometrial cancer cells via upregulation of p21Waf1/Cip1 and p27Kip1**. *Taiwanese Journal of Obstetrics and Gynecology* 2016, **55**(6):847-851.

202. Milner E, Gutter-Kapon L, Bassani-Strenberg M, Barnea E, Beer I, Admon A: **The effect of proteasome inhibition on the generation of the human leukocyte antigen (HLA) peptidome**. *Mol Cell Proteomics* 2013, **12**(7):1853-1864.

203. Sijts EJAM, Kloetzel PM: **The role of the proteasome in the generation of MHC class I ligands and immune responses**. *Cellular and Molecular Life Sciences* 2011, **68**(9):1491-1502.

204. Franke WW, Schmid E, Osborn M, Weber K: **Different intermediate-sized filaments distinguished by immunofluorescence microscopy**. *Proceedings of the National Academy of Sciences* 1978, **75**(10):5034-5038.

205. Kartenbeck J, Schwechheimer K, Moll R, Franke WW: **Attachment of vimentin filaments to desmosomal plaques in human meningiomal cells and arachnoidal tissue**. *Journal of Cell Biology* 1984, **98**(3):1072-1081.

206. Eckes B, Dogic D, Colucci-Guyon E, Wang N, Maniotis A, Ingber D, Merckling A, Langa F, Aumailley M, Delouvee A *et al*: **Impaired mechanical stability, migration and contractile capacity in vimentin-deficient fibroblasts**. *Journal of Cell Science* 1998, **111**(13):1897-1907.

207. Richardson AM, Havel LS, Koyen AE, Konen JM, Shupe J, Wiles WG, IV, Martin WD, Grossniklaus HE, Sica G, Gilbert-Ross M, Marcus AI: **Vimentin Is Required for Lung Adenocarcinoma Metastasis via Heterotypic Tumor Cell–Cancer-Associated Fibroblast Interactions during Collective Invasion**. *Clinical Cancer Research* 2018, **24**(2):420-432.

208. Bartek J, Lukas J: **Chk1 and Chk2 kinases in checkpoint control and cancer**. *Cancer Cell* 2003, **3**(5):421-429.

209. Gatei M, Sloper K, Sörensen C, Syljuäsen R, Falck J, Hobson K, Savage K, Lukas J, Zhou B-B, Bartek J, Khanna KK: **Ataxia-telangiectasia-mutated (ATM) and NBS1-dependent Phosphorylation of Chk1 on Ser-317 in Response to Ionizing Radiation***. *Journal of Biological Chemistry* 2003, **278**(17):14806-14811.

210. Sørensen CS, Syljuåsen RG, Falck J, Schroeder T, Rönnstrand L, Khanna KK, Zhou B-B, Bartek J, Lukas J: **Chk1 regulates the S phase checkpoint by coupling the physiological turnover and ionizing radiation-induced accelerated proteolysis of Cdc25A**. *Cancer Cell* 2003, **3**(3):247-258.

211. Dillon M, Guevara J, Mohammed K, Smith SA, Dean E, McLellan L, Boylan Z, Spicer J, Forster MD, Harrington KJ: **A phase I study of ATR inhibitor, AZD6738, as monotherapy in advanced solid tumours (PATRIOT part A, B)**. *Annals of Oncology* 2019, **30**:v165-v166.

212. Zinatizadeh MR, Schock B, Chalbatani GM, Zarandi PK, Jalali SA, Miri SR: **The Nuclear Factor Kappa B (NF-kB) signaling in cancer development and immune diseases**. *Genes & Diseases* 2021, **8**(3):287-297.

213. Chalhoub N, Baker SJ: **PTEN and the PI3-kinase pathway in cancer**. *Annu Rev Pathol* 2009, **4**:127-150.

214. Yap TA, Krebs MG, Postel-Vinay S, Bang YJ, El-Khoueiry A, Abida W, Harrington K, Sundar R, Carter L, Castanon-Alvarez E *et al*: **1LBA - Phase I modular study of AZD6738, a novel oral, potent and selective ataxia telangiectasia Rad3-related (ATR) inhibitor in combination (combo) with carboplatin, olaparib or durvalumab in patients (pts) with advanced cancers**. *European Journal of Cancer* 2016, **69**:S2.

215. Yap TA, Krebs MG, Postel-Vinay S, El-Khoueiry A, Soria J-C, Lopez J, Berges A, Cheung SYA, Irurzun-Arana I, Goldwin A *et al*: **Ceralasertib (AZD6738), an Oral ATR Kinase Inhibitor, in Combination with Carboplatin in Patients with Advanced Solid Tumors: A Phase I Study**. *Clinical Cancer Research* 2021, **27**(19):5213-5224.

216. Yap TA, O'Carrigan B, Penney MS, Lim JS, Brown JS, Luken MJdM, Tunariu N, Perez-Lopez R, Rodrigues DN, Riisnaes R *et al*: **Phase I Trial of First-in-Class ATR Inhibitor M6620 (VX-970) as Monotherapy or in Combination With Carboplatin in Patients With Advanced Solid Tumors**. *Journal of Clinical Oncology* 2020, **38**(27):3195-3204.

217. Eich M, Roos WP, Nikolova T, Kaina B: **Contribution of ATM and ATR to the Resistance of Glioblastoma and Malignant Melanoma Cells to the Methylating Anticancer Drug Temozolomide**. *Molecular Cancer Therapeutics* 2013, **12**(11):2529-2540.

218. El Touny LH, Hose C, Connelly J, Harris E, Monks A, Dull AB, Wilsker DF, Hollingshead MG, Gottholm-Ahalt M, Alcoser SY *et al*: **ATR inhibition reverses the resistance of homologous recombination deficient MGMT low /MMR proficient cancer cells to temozolomide**. *Oncotarget* 2021, **12**(21).

219. Kim H, Xu H, George E, Hallberg D, Kumar S, Jagannathan V, Medvedev S, Kinose Y, Devins K, Verma P *et al*: **Combining PARP with ATR inhibition overcomes PARP inhibitor and platinum resistance in ovarian cancer models**. *Nature Communications* 2020, **11**(1):3726.

220. Lloyd RL, Wijnhoven PWG, Ramos-Montoya A, Wilson Z, Illuzzi G, Falenta K, Jones GN, James N, Chabbert CD, Stott J *et al*: **Combined PARP and ATR inhibition potentiates genome instability and cell death in ATM-deficient cancer cells**. *Oncogene* 2020, **39**(25):4869-4883.

221. Sule A, Van Doorn J, Sundaram RK, Ganesa S, Vasquez Juan C, Bindra Ranjit S: **Targeting IDH1/2 mutant cancers with combinations of ATR and PARP inhibitors**. *NAR Cancer* 2021, **3**(2).

222. Shah PD, Wethington SL, Pagan C, Latif N, Tanyi J, Martin LP, Morgan M, Burger RA, Haggerty A, Zarrin H *et al*: **Combination ATR and PARP Inhibitor (CAPRI): A phase 2 study of ceralasertib plus olaparib in patients with recurrent, platinum-resistant epithelial ovarian cancer**. *Gynecologic Oncology* 2021, **163**(2):246-253.

223. Wen PY, Groot JFd, Battiste J, Goldlust SA, Garner JS, Friend J, Simpson JA, Damek D, Olivero A, Cloughesy TF: **Paxalisib in patients with newly diagnosed glioblastoma with unmethylated MGMT promoter status: Final phase 2 study results**. *Journal of Clinical Oncology* 2022, **40**(16_suppl):2047-2047.

224. Wright KD, Yao X, London WB, Kao P-C, Gore L, Hunger S, Geyer R, Cohen KJ, Allen JC, Katzenstein HM *et al*: **A POETIC Phase II study of continuous oral everolimus in recurrent, radiographically progressive pediatric low-grade glioma**. *Pediatric Blood & Cancer* 2021, **68**(2):e28787.

225. Sundar R, Brown J, Ingles Russo A, Yap TA: **Targeting ATR in cancer medicine**. *Current Problems in Cancer* 2017, **41**(4):302-315.

226. Wang L-W, Jiang S, Yuan Y-H, Duan J, Mao N-D, Hui Z, Bai R, Xie T, Ye X-Y: **Recent Advances in Synergistic Antitumor Effects Exploited from the Inhibition of Ataxia Telangiectasia and RAD3-Related Protein Kinase (ATR)**. *Molecules* 2022, **27**(8):2491.

227. Wilson Z, Odedra R, Wallez Y, Wijnhoven PWG, Hughes AM, Gerrard J, Jones GN, Bargh-Dawson H, Brown E, Young LA *et al*: **ATR Inhibitor AZD6738 (Ceralasertib) Exerts Antitumor Activity as a Monotherapy and in Combination with Chemotherapy and the PARP Inhibitor Olaparib**. *Cancer Research* 2022, **82**(6):1140-1152.

228. Günther HS, Schmidt NO, Phillips HS, Kemming D, Kharbanda S, Soriano R, Modrusan Z, Meissner H, Westphal M, Lamszus K: **Glioblastoma-derived stem cell-enriched cultures form**

distinct subgroups according to molecular and phenotypic criteria. *Oncogene* 2008, **27**(20):2897-2909.

229. Wang C, Wang G, Feng X, Shepherd P, Zhang J, Tang M, Chen Z, Srivastava M, McLaughlin ME, Navone NM *et al*: **Genome-wide CRISPR screens reveal synthetic lethality of RNASEH2 deficiency and ATR inhibition**. *Oncogene* 2019, **38**(14):2451-2463.

230. Li FP: **Soft-Tissue Sarcomas, Breast Cancer, and Other Neoplasms**. *Annals of Internal Medicine* 1969, **71**(4):747-752.

231. Gargallo P, Yáñez Y, Segura V, Juan A, Torres B, Balaguer J, Oltra S, Castel V, Cañete A: **Li–Fraumeni syndrome heterogeneity**. *Clinical and Translational Oncology* 2020, **22**(7):978-988.

232. Yoshida R: **Hereditary breast and ovarian cancer (HBOC): review of its molecular characteristics, screening, treatment, and prognosis**. *Breast Cancer* 2021, **28**(6):1167-1180.

233. Idos G, Valle L: **Lynch Syndrome**. In: *GeneReviews(®).* edn. Edited by Adam MP, Everman DB, Mirzaa GM, Pagon RA, Wallace SE, Bean LJH, Gripp KW, Amemiya A. Seattle (WA): University of Washington, Seattle

Copyright © 1993-2022, University of Washington, Seattle. GeneReviews is a registered trademark of the University of Washington, Seattle. All rights reserved.; 1993.

234. Menahem B, Alves A, Regimbeau JM, Sabbagh C: **Lynch Syndrome: Current management In 2019**. *Journal of Visceral Surgery* 2019, **156**(6):507-514.

235. Kee Y, D'Andrea AD: **Expanded roles of the Fanconi anemia pathway in preserving genomic stability**. *Genes & Development* 2010, **24**(16):1680-1694.

236. Alter BP: **Fanconi anemia and the development of leukemia**. *Best Practice & Research Clinical Haematology* 2014, **27**(3):214-221.

237. Peake JD, Noguchi E: **Fanconi anemia: current insights regarding epidemiology, cancer, and DNA repair**. *Human Genetics* 2022.

238. Bogliolo M, Bluteau D, Lespinasse J, Pujol R, Vasquez N, d'Enghien CD, Stoppa-Lyonnet D, Leblanc T, Soulier J, Surrallés J: **Biallelic truncating FANCM mutations cause early-onset cancer but not Fanconi anemia**. *Genetics in Medicine* 2018, **20**(4):458-463.

239. Catucci I, Osorio A, Arver B, Neidhardt G, Bogliolo M, Zanardi F, Riboni M, Minardi S, Pujol R, Azzollini J *et al*: **Individuals with FANCM biallelic mutations do not develop Fanconi anemia, but show risk for breast cancer, chemotherapy toxicity and may display chromosome fragility**. *Genetics in Medicine* 2018, **20**(4):452-457.

240. Boukerroucha M, Josse C, Segers K, El-Guendi S, Frères P, Jerusalem G, Bours V: **BRCA1 germline mutation and glioblastoma development: report of cases**. *BMC Cancer* 2015, **15**:181.

241. Gluckman E, Devergie A, Dutreix J: **Radiosensitivity in Fanconi anaemia: application to the conditioning regimen for bone marrow transplantation**. *British Journal of Haematology* 1983, **54**(3):431-440.

242. Birkeland AC, Auerbach AD, Sanborn E, Parashar B, Kuhel WI, Chandrasekharappa SC, Smogorzewska A, Kutler DI: **Postoperative Clinical Radiosensitivity in Patients With Fanconi Anemia and Head and Neck Squamous Cell Carcinoma**. *Archives of Otolaryngology–Head & Neck Surgery* 2011, **137**(9):930-934.

243. Kondo N, Takahashi A, Mori E, Noda T, Zdzienicka MZ, Thompson LH, Helleday T, Suzuki M, Kinashi Y, Masunaga S *et al*: **Correction: FANCD1/BRCA2 Plays Predominant Role in the Repair of DNA Damage Induced by ACNU or TMZ**. *PLOS ONE* 2011, **6**(6):10.1371/annotation/c1376be1324d1371-bc1323-1343b1374-ae1301-b1386dad174069.

244. Horak P, Weischenfeldt J, von Amsberg G, Beyer B, Schütte A, Uhrig S, Gieldon L, Klink B, Feuerbach L, Hübschmann D *et al*: **Response to olaparib in a PALB2 germline mutated prostate cancer and genetic events associated with resistance**. *Molecular Case Studies* 2019, **5**(2).

245. Gruber JJ, Afghahi A, Timms K, DeWees A, Gross W, Aushev VN, Wu H-T, Balcioglu M, Sethi H, Scott D *et al*: **A phase II study of talazoparib monotherapy in patients with wild-type BRCA1**

and BRCA2 with a mutation in other homologous recombination genes. *Nature Cancer* 2022, **3**(10):1181-1191.

6. Statement of contributions

The thesis was designed, supervised and mentored by Prof. Dr. Dr. Ghazaleh Tabatabai, Department of Neurology & Neuro-Oncology at the Hertie Institute for Clinical Brain Research in the research group "Laboratory for Clinical and Experimental Neurooncology". Dr. Susanne Beck was the scientific coordinator and responsible for writing of the animal licenses after critical discussions about the scientific approaches orchestrated by Prof. Tabatabai an me personally.

Throughout all discussed experiments in this thesis, the candidate was greatly supported by Sarah Hendel, Heike Pfrommer and Yeliz Donat, in regards of cell culture, animal maintenance, histological workups and patient samples.

6.1 Argyrin F Treatment-Induced Vulnerabilities Lead to a Novel Combination Therapy in Experimental Glioma

In this project the anti-glioma activity of Argyrin F was characterized and an immunogenic potential evaluated. To evaluate the immunogenic potential patient derived microtumors were used, established and analyzed at the NMI in Reutlingen and the immunopeptidome analyzed by the Immunology Department at the University of Tübingen.

In detail:

Western immunoblot analyses, assessment of cell cycle status, cytotoxicity and clonogenic survival assays as presented in **Figure 12** and **Appendix Figure 1** and **Appendix Figure 2** were collected by the candidate under the supervision of Sarah Hendel and Heike Pfrommer. The applicant established the protocol for cell cycle measurement by flow cytometry herself (**Appendix Figure 3**).

In the animal experiment presented in **Figure 13** the candidate was mentored and instructed by Prof. Dr. Dr. Ghazaleh Tabatabai, Dr. Justyna Przystal and Dr. Parameswari Govindarajan regarding the surgical procedure, animal treatment afterwards and animal monitoring. Upon reaching the endpoints the candidate preserved study material supervised by Dr. Justyna Przystal. Subsequent histological analysis was done by the candidate under the supervision of Heike Pfrommer. Dr. Hannes Becker provided the semi-quantitative workflow for ImageJ that was used to quantify T cell numbers in histological stains (2.2.2.3).

The animal experiment depicted in **Figure 17** was done by the candidate together with Lara Häußer, Dr. Sophie Hirsch and Heike Pfrommer. Treatments as indicated and animal monitoring was done by the candidate together with Heike Pfrommer.

All experiments presented in this thesis connected to patient derived microtumors (PDMs) (**Figure 14**, **Figure 16**) were conducted at the NMI Reutlingen in the group of Dr. Christian Schmees. The main

researchers doing the experiments were Dr. Simge Yüz, Nicole Anderle and Anna-Lena Keller. The scientific approach was based on planning of Prof. Tabatabai and the candidate, subsequent planning of the experiments was done by all researchers involved. The candidate prepared the final presentation of data.

For the HLA ligandome analysis (**Figure 15**) Dr. Denis Canjuga prepared the cells, Dr. Michael Ghosh then conducted the experiments at the Immunology Department at the University Tübingen in the laboratory of Prof. Dr. Hans-Georg Rammensee and Prof. Dr. Stefan Stevanovic. Final presentation of data was done by the candidate.

Lydia Noch was mentored by the applicant and conducted cytotoxicity and clonogenic survival assays using Argyrin F.

6.2 ATR inhibition in experimental glioma

In this project the anti-glioma activity of ATR inhibition was evaluated. Furthermore, combination therapy approaches were tested based on the molecular analyses (RNASeq, DigiWest protein profiling) conducted at the Human Genetics Department and the NMI in Reutlingen.

In detail:
For the animal experiment presented in the ATR project (**Figure *18***), the candidate conducted the surgery together with Lara Häußer, Foteini Tsiami and Heike Pfrommer. Subsequent treatment, animal monitoring and sample collection was done by the candidate.

Cytotoxicity, clonogenic survival assays, cell cycle analysis and apoptosis assays were conducted by Dr. Sophie Hirsch, Leonard Schnabel and the candidate, supported by Sarah Hendel (**Figure 19**, **Figure 20**, **Figure 21**, **Figure 24**, **Figure 26**, **Figure 27**, **Figure 28**, **Figure 29**, **Appendix Figure 6-9, Appendix Figure 11-15**). The candidate established the apoptosis evaluation by flow cytometry. Final evaluation and visualization of all data sets mentioned was done by the candidate.

The samples for RNA sequencing analysis were prepared and extracted by Dr. Sophie Hirsch, initial analysis of transcriptomic data was done by Dr. Daniel Merk (**Figure 22**, **Appendix Figure 10, Appendix Table 3**, **Appendix Table 4**). Visualization and final evaluation of data was done by the candidate supervised by Dr. Daniel Merk. Subsequent DigiWest protein profiling analyses were conducted at the NMI in the lab of Dr. Markus Templin by Aaron Stahl (**Figure 23**). The candidate prepared the samples and decided on which analytes to assess using DigiWest together with Prof. Dr. Dr. Ghazaleh Tabatabai. Visualization was done by Aaron Stahl in consultation with the candidate.

6.3 The role of the Fanconi anemia pathway in glioma

In this project patient data of the Molecular Tumor Board in Tübingen was evaluated for germline mutations. Based on the findings the Fanconi anemia pathway was studied in depth regarding its tumor onsetting abilities as well as potential influences on therapy sensitivity.

In detail:

Patient data from the MTB neuro-oncology cohort Tübingen as shown in **Figure 30**, **Figure 31**, *Table 4* and **Appendix Table 6** in this thesis were collected and sorted by PD Dr. Mirjam Renovanz, Hanni Hille and the candidate. The candidate visualized the data and based on the findings outlined together with Prof. Dr. Dr. Ghazaleh Tabatabai the subsequent project plan.

The workflow concerning RCAS-Y DV cloning, DF-1 cell infection and knockdown efficiency validation as outlined in 2.2.1.8 was developed in the laboratory of Prof. Dr. Dr. Eric Holland. The candidate was mentored by Dr. Frank Szulzewsky during her visit in Seattle. Subsequent cloning and knockdown evaluation was done by the candidate (**Figure 32**).

Surgical procedures done for this project (**Figure 33**) were done by the applicant together with Lara Häußer, Foteini Tsiami and Heike Pfrommer. Animal monitoring, sample collection and histological workup was done by the candidate supported by Heike Pfrommer (**Figure 34**).

The candidate evaluated knockdown efficiencies as outlined in **Figure 35** and planned the subsequent proliferation and clonogenic survival assays in consultation with Prof. Dr. Dr. Ghazaleh Tabatabai. First trial runs and establishment of the system was done by the candidate. Sarah Hendel conducted a substantial amount of proliferation and clonogenic survival assays connected to this project supervised by the candidate (**Figure 36**, **Figure 37**, **Figure 38**, **Figure 39**, **Figure 40**).

Foteini Tsiami and Munira Maklouf were mentored by the candidate and did cloning of single pLKO1 vectors, subsequent knockdown evaluation in cell lines, first proliferation and clonogenic survival assays of knockdown cells compared to Luciferase control cells.

7. Publications

Parts of this thesis have been published in the following publications (all as Bianca Walter):

Walter, B., Canjuga, D., Yüz, S.G., Ghosh, M., Bozko, P., Przystal, J.M., Govindarajan, P., Anderle, N., Keller, A.-L., Tatagiba, M., Schenke-Layland, K., Rammensee, H.-G., Stevanovic, S., Malek, N.P., Schmees, C. and Tabatabai, G. (2021), Argyrin F Treatment-Induced Vulnerabilities Lead to a Novel Combination Therapy in Experimental Glioma. Adv. Therap., 4: 2100078. https://doi.org/10.1002/adtp.202100078

Walter, B., Hirsch, S., Kuhlburger, L., Stahl, A., Schnabel, L., Wisser, S., Haeusser, L. A., Tsiami, F., Plöger, S., Aghaallaei, N., Dick, A. M., Skokowa, J., Schmees, C., Templin, M., Schenke-Layland, K., Tatagiba, M., Nahnsen, S., Merk, D. J., and Tabatabai, G. (2024), Functionally-instructed modifiers of response to ATR inhibition in experimental glioma. Journal of experimental & clinical cancer research: CR, 43(1), 77. https://doi.org/10.1186/s13046-024-02995-z

Further publications and invention reports are currently in preparation.

8. Acknowledgements

Furthermore, I want to thank Dr. Frank Szulzewsky and Prof. Dr. Dr. Eric Holland for the opportunity to visit the Fred Hutch Cancer Center in Seattle and the introduction to the cloning strategy for the RCAS vector.

I also want to thank Dr. Mathias Jucker and Dr. Angelos Skodras for the introduction to the AxioFluor Microscope as well as giving me permission to use it.

I would like to thank Prof. Dr. Julia Skokowa and Dr. Jonas Neher for their support during my PhD, taking the time to be part of my Advisory Board. I valued your scientific input a lot and am very grateful for your support.

Lastly, thank you to Anne Griesshammer for the support and discussions. Thank you to Benedikt Armbruster and my whole family for the never-ending support during my PhD time. I could not have done this without you.

APPENDIX

Figures

Tables

Appendix Figure 1

Appendix Figure 1: *Immunoblots of Argyrin F treated LN229 and LNZ308 cells*

Depicted are full immunoblot pictures of p27, p21, pRb1, Rb1 and GAPDH of LN229 (A) and LNZ308 (B) cells treated with Argyrin F in indicated concentrations for 48 h.
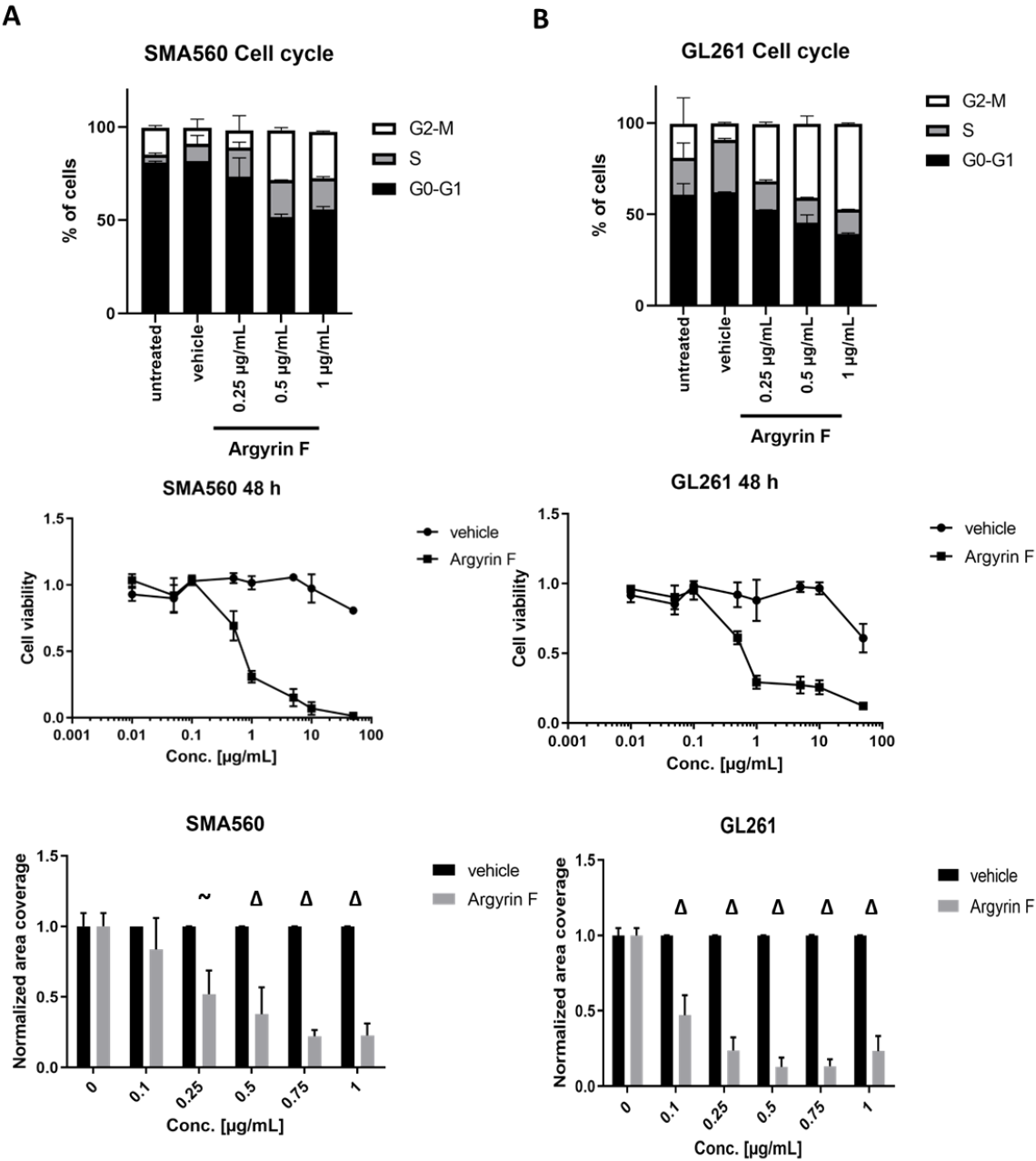
Appendix Figure 2: Anti-glioma efficacy of Argyrin F in murine glioma cells

*Cell cycle (first row), cytotoxicity (second row) and clonogenic survival (third row) of SMA560 (A) and GL261 (B) murine glioma cells treated with Argyrin F in indicated concentrations. Shown are mean ± SD, normalized to untreated cells. Statistical testing using multiple T-tests with the Holm-Sidak method. * p<0.05, ~ p<0.005, Δ p<0.0000001*

Appendix Figure 3
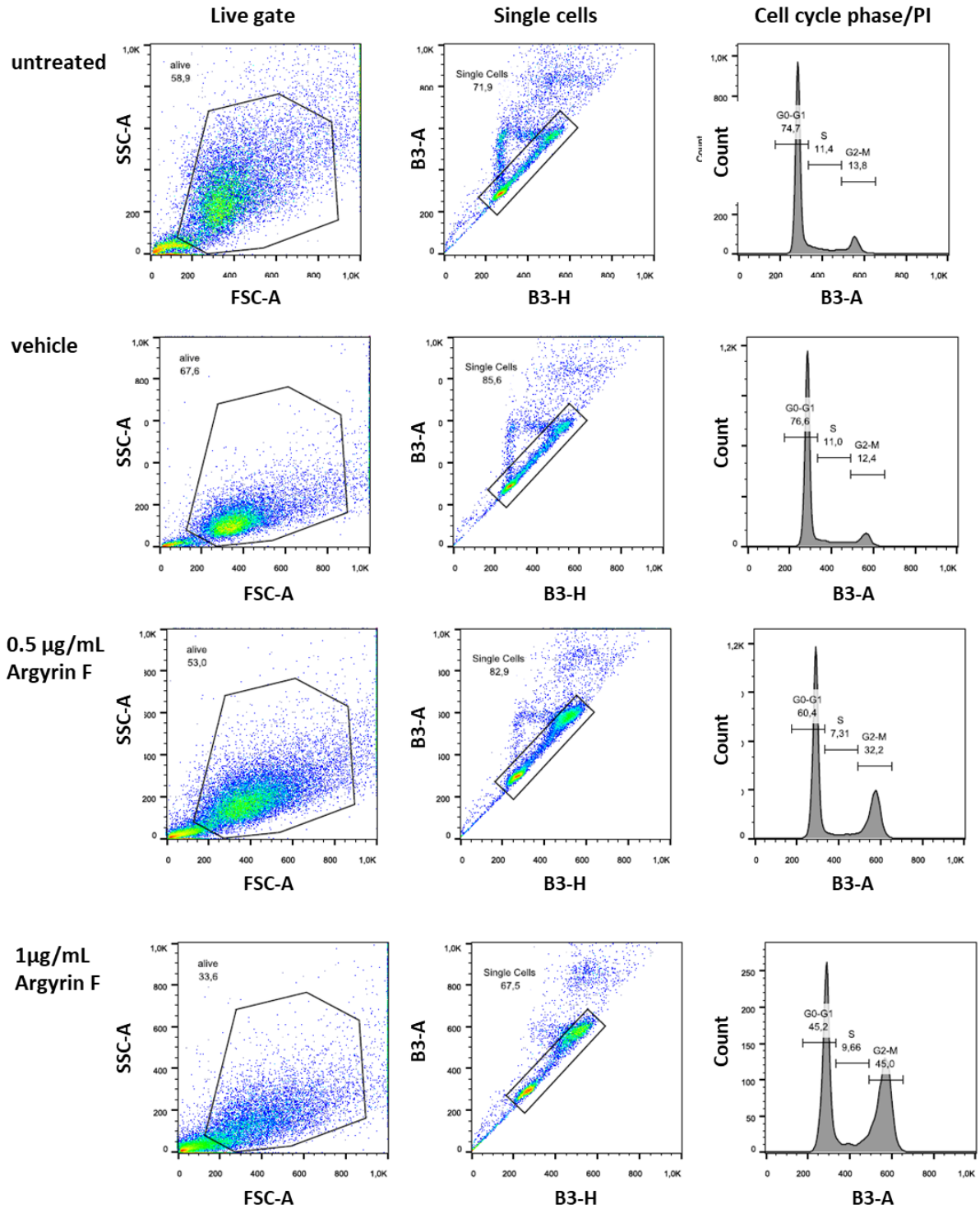
LN229

Appendix Figure 3: *Gating strategy for cell cycle analysis*

Exemplary gating strategy for LN229 cells treated with Argyrin F as indicated. First cells passed through a light scatter and single cells are determined. Cell cycle phase is determined in th B3-A channel as indicated in the right panel.

Appendix Figure 4

A

Number of peptides

B

Peptide overlap

C
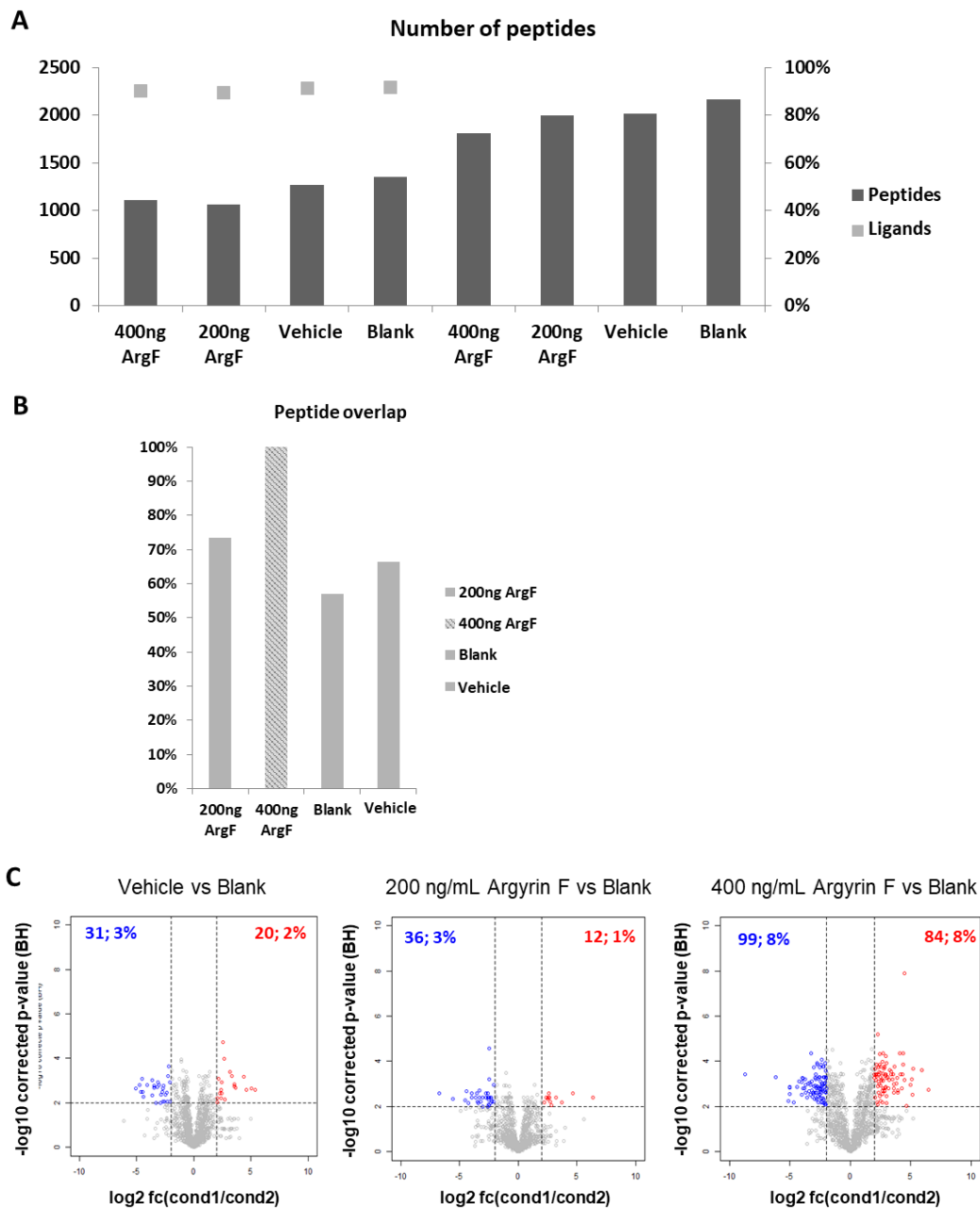
Appendix Figure 4 *HLA ligandome displays up- and downmodulated peptides upon Argyrin F treatment in LN229 cells*

***A**, Number of presented peptides divided in class I and II peptides of LN229 cells treated with Argyrin F. **B**, Overlap of peptides comparing 400 ng/mL Argyrin F with all other treatment conditions. **C**, Volcano blots depicting detected peptides in vehicle, 200 ng/mL Argyrin F and 400 ng/mL Argyrin F compared to blank condition. Treatment conditions show up- (red) and down- (blue) modulated peptides upon Argyrin F treatment.*

Appendix Figure 5
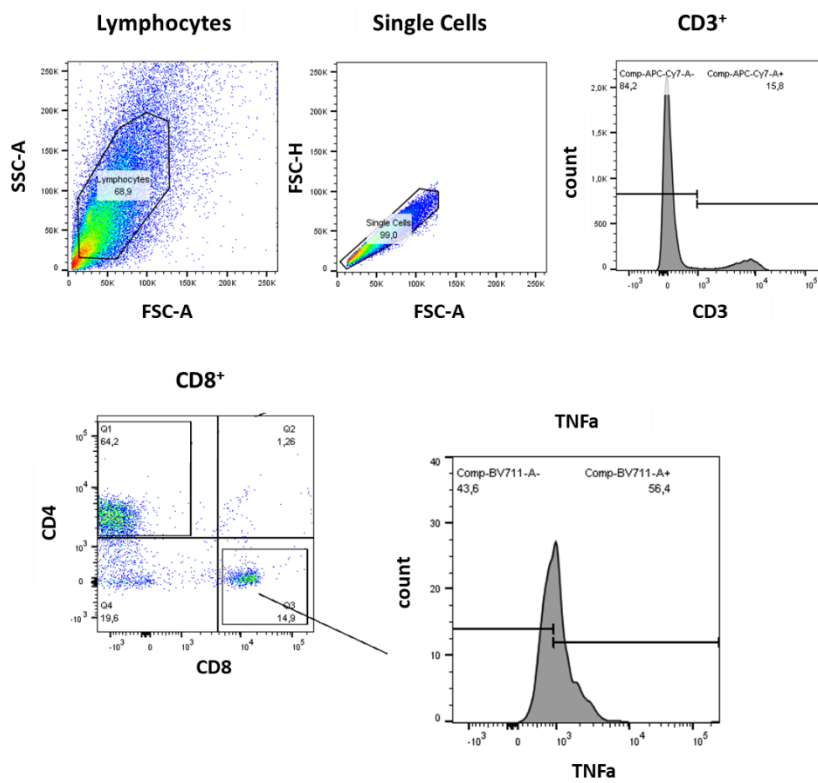
Appendix Figure 5*: Gating strategy for CD8+ TNFα+ TIL sub-populations*

First the cells pass through a light-scatter and single cells are selected. Next CD3+ cells are selected and further subdivided into CD4+ and CD8+. Lastly, the amount of TNFα is determined.

Appendix Figure 6
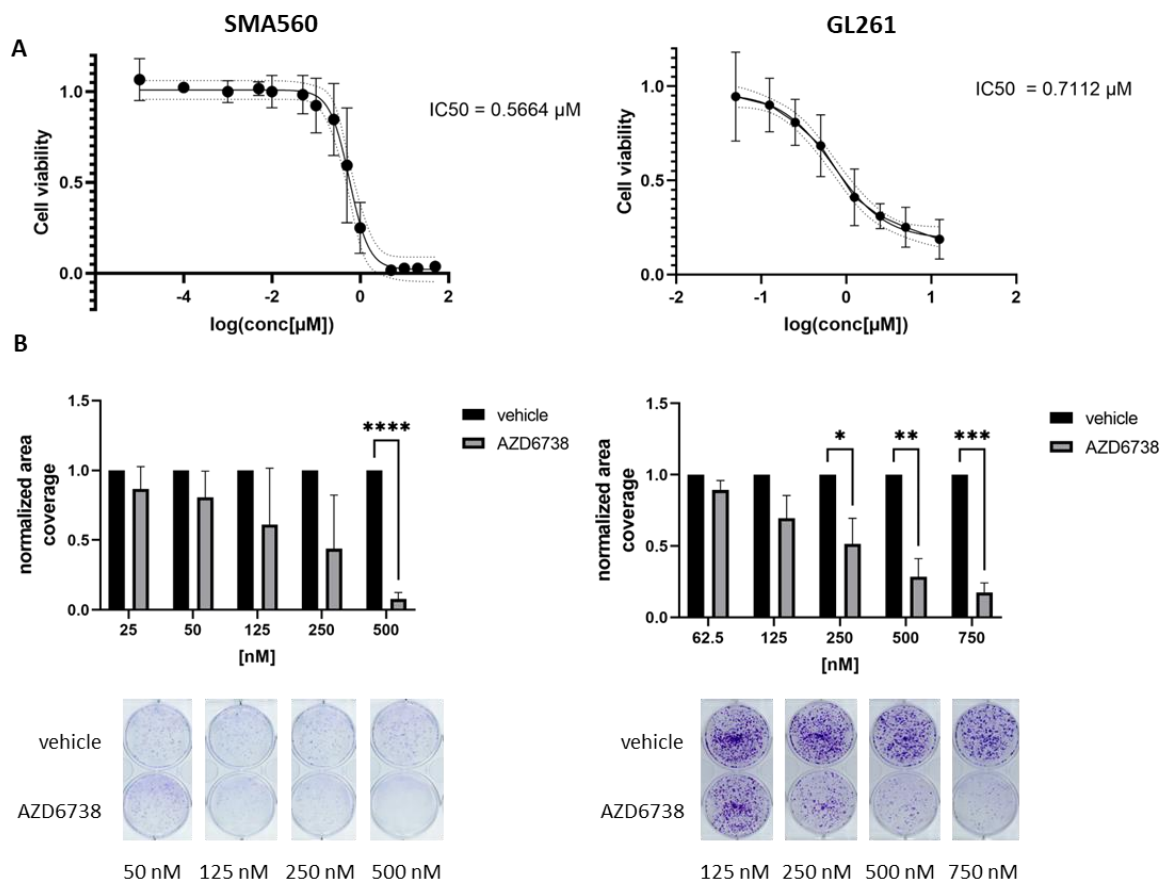
Appendix Figure 6: Acute cytotoxicity and clonogenic survival assays in SMA560 and GL261 cells treated with AZD6738

*A, Dose dependent reduction of cell viability in SMA560 and GL261 cell upon AZD6738 treatment. IC_{50}-values for each cell line are also indicated in the graph. **B,** Bar graphs depicting dose dependent reduction of clonogenic survival in SMA560 and GL261 cells treated with AZD6738. Lower panel shows exemplary pictures of cells treated in indicated concentrations and stained with Crystal Violet. Statistical analysis was done using multiple t-tests with the Holm-Sidak method. * $p < 0.05$, ** $p < 0.01$, *** $p < 0.001$, **** $p < 0.0001$.*

Appendix Figure 7
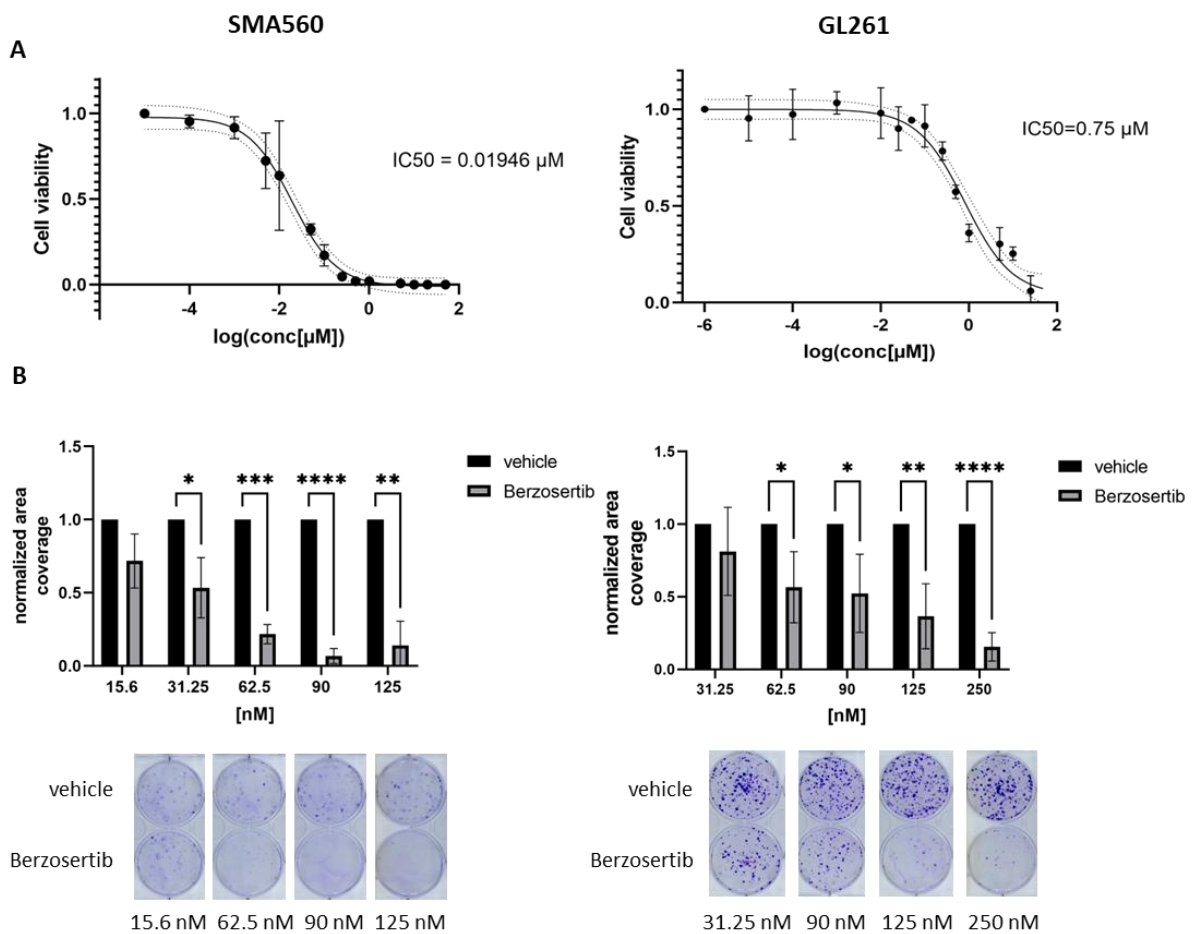
Appendix Figure 7: Acute cytotoxicity and clonogenic survival assays in SMA560 and GL261 cells treated with Berzosertib

*A, Dose dependent reduction of cell viability in SMA560 and GL261 cell upon Berzosertib treatment. IC$_{50}$-values for each cell line are also indicated in the graph. B, Bar graphs depicting dose dependent reduction of clonogenic survival in SMA560 and GL261 cells treated with Berzosertib. Lower panel shows exemplary pictures of cells treated in indicated concentrations and stained with Crystal Violet. Statistical analysis was done using multiple t-tests with the Holm-Sidak method. * p < 0.05, ** p < 0.01, *** p < 0.001, **** p < 0.0001.*

Appendix Figure 8
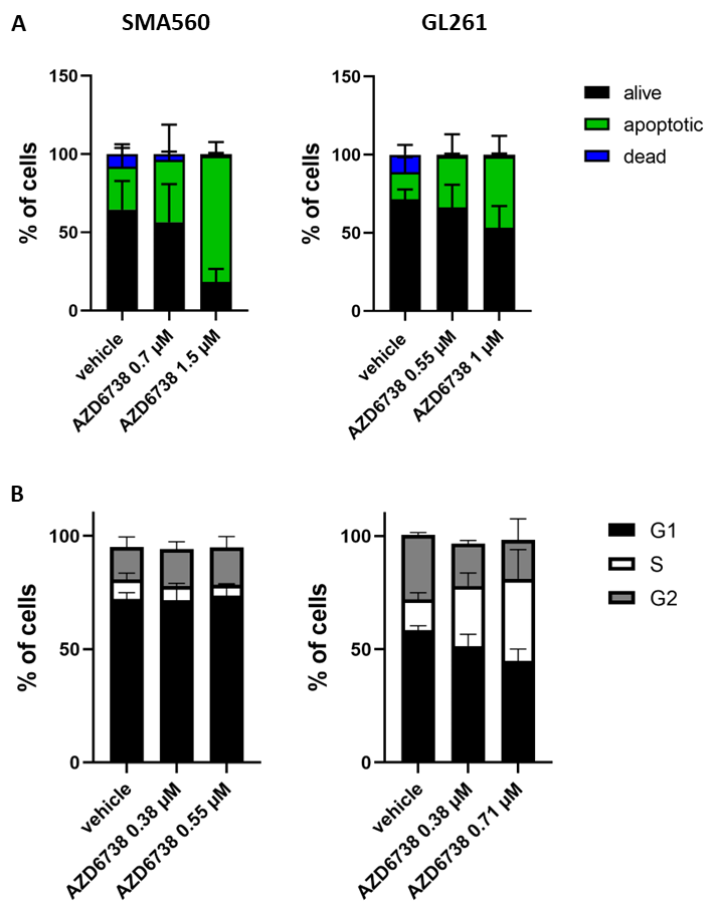
Appendix Figure 8: *Flow cytometric analysis of apoptosis and cell cycle status of AZD6738 treated SMA560 and GL261 cells*

A, Analysis of apoptosis induction in SMA560 and GL261 cells upon AZD6738 treatment using Annexin V/PI staining evaluated by flow cytometry. (n=3) B, Cell cycle analysis of SMA560 and GL261 cells treated with AZD6738 in the indicated concentrations. (n=3)

Appendix Figure 9

LNZ308
vehicle
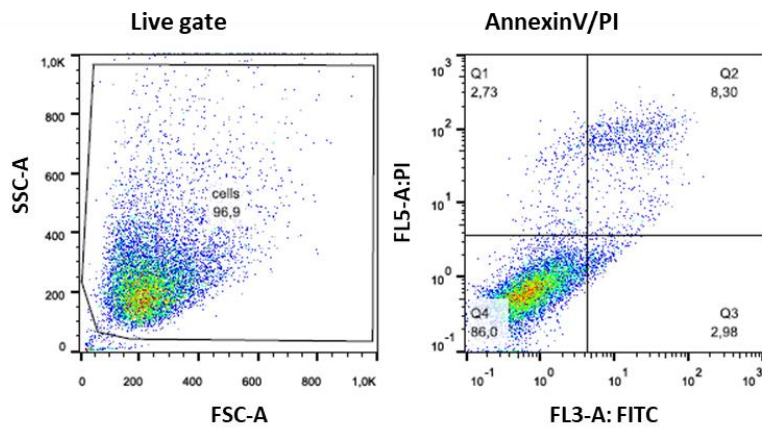
LNZ308
3.5 µM AZD6738
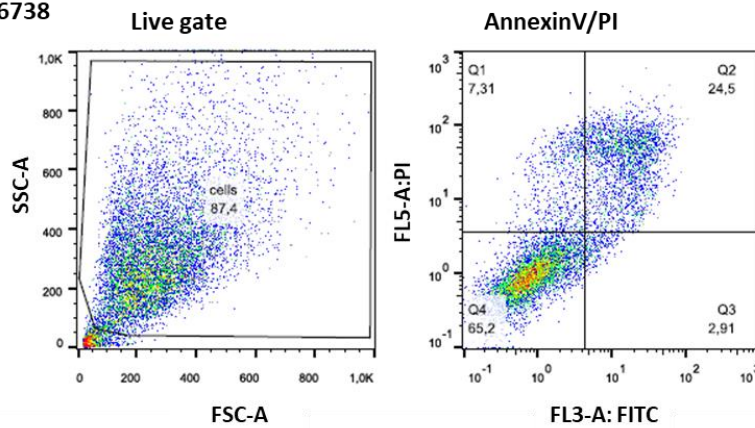
Appendix Figure 9: Gating strategy for Annexin V/PI stains to determine apoptotic cell populations

First the cells pass through a light-scatter. Next Measured cells are divided into Annexin V/PI negative (Q4), Annexin-V positive/PI negative (Q3), Annexin V and PI positive (Q2) and PI positive cells (Q1). Cells detected in Q4 comprise "alive" population, Q2 and Q3 together make up "apoptotic" population and Q1 entails "dead" population.

Appendix Figure 10
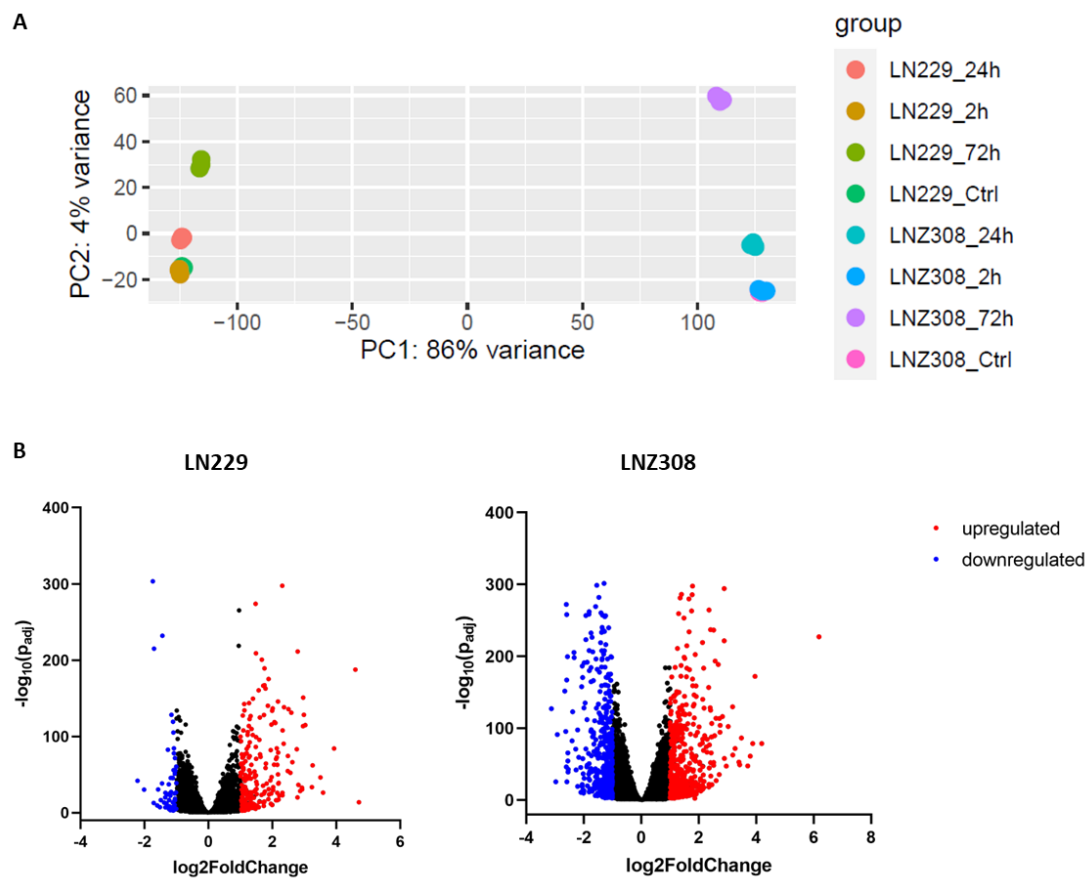
Appendix Figure 10: Initial analyses of transcriptomic data from LN229 and LNZ308 cells treated with AZD6738 A, Principal component analysis of LN229 and LNZ308 cells treated with AZD6738 for 2h, 24h and 72h, respectively. Replicates cluster together, biggest difference to control within each cell line is at 72h (x-axis). Strongest dividing component is the cellular background itself (y-axis), LN229 samples all on the left, LNZ308 samples all on the right side of the blot. B, Volcano blots depicting the log2FoldChange vs. the associated - $log_{10}(p_{adj})$ of LN229 (left) and LNZ308 (right) cells treated with AZD6738 for 72h. Highlighted are down- (blue) and upregulated genes (red) with a log2FoldChange > |1|.

Appendix Figure 11
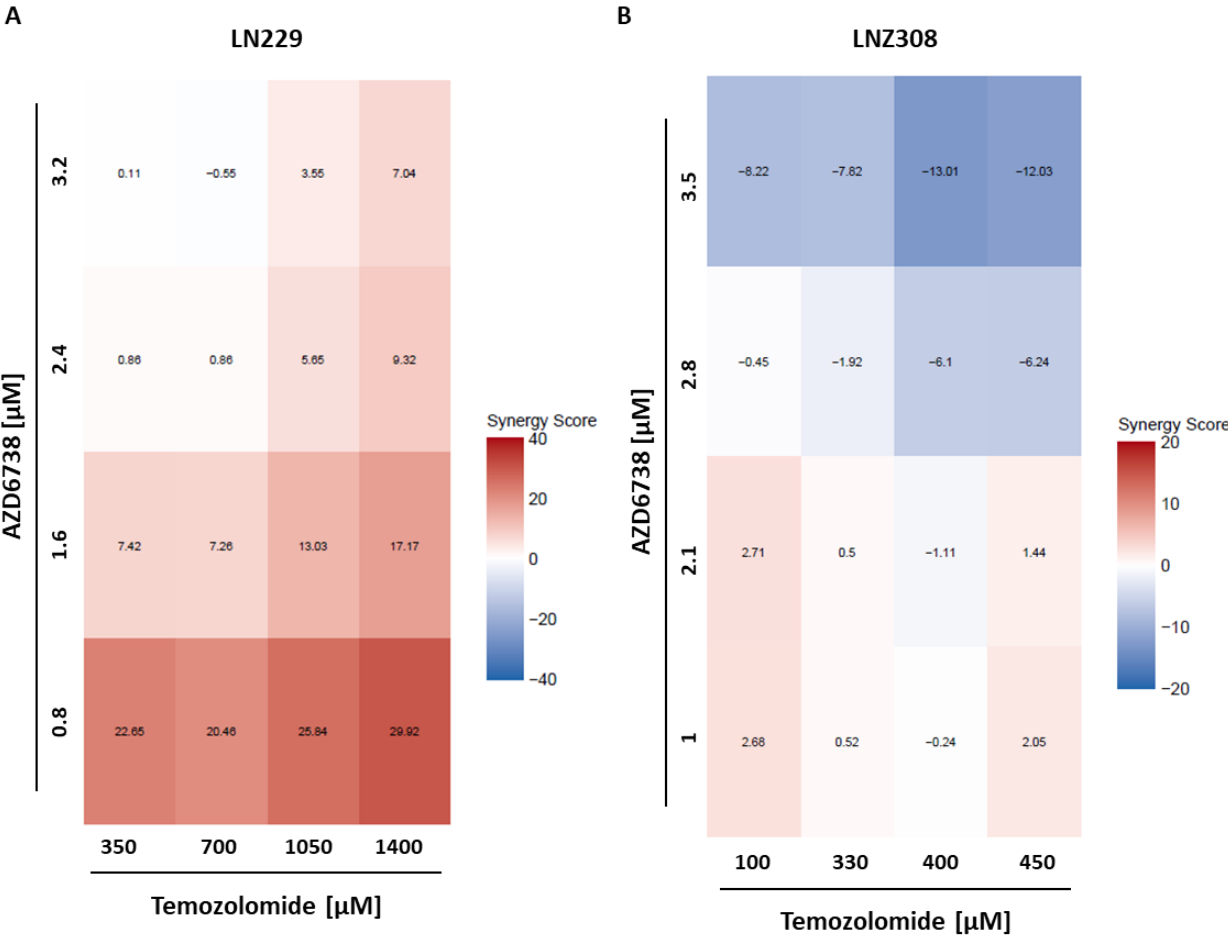
Appendix Figure 11: Heatmap of ZIP synergy scores of LN229 and LNZ308 cells treated with AZD6738 combined with Temozolomide in indicated concentrations
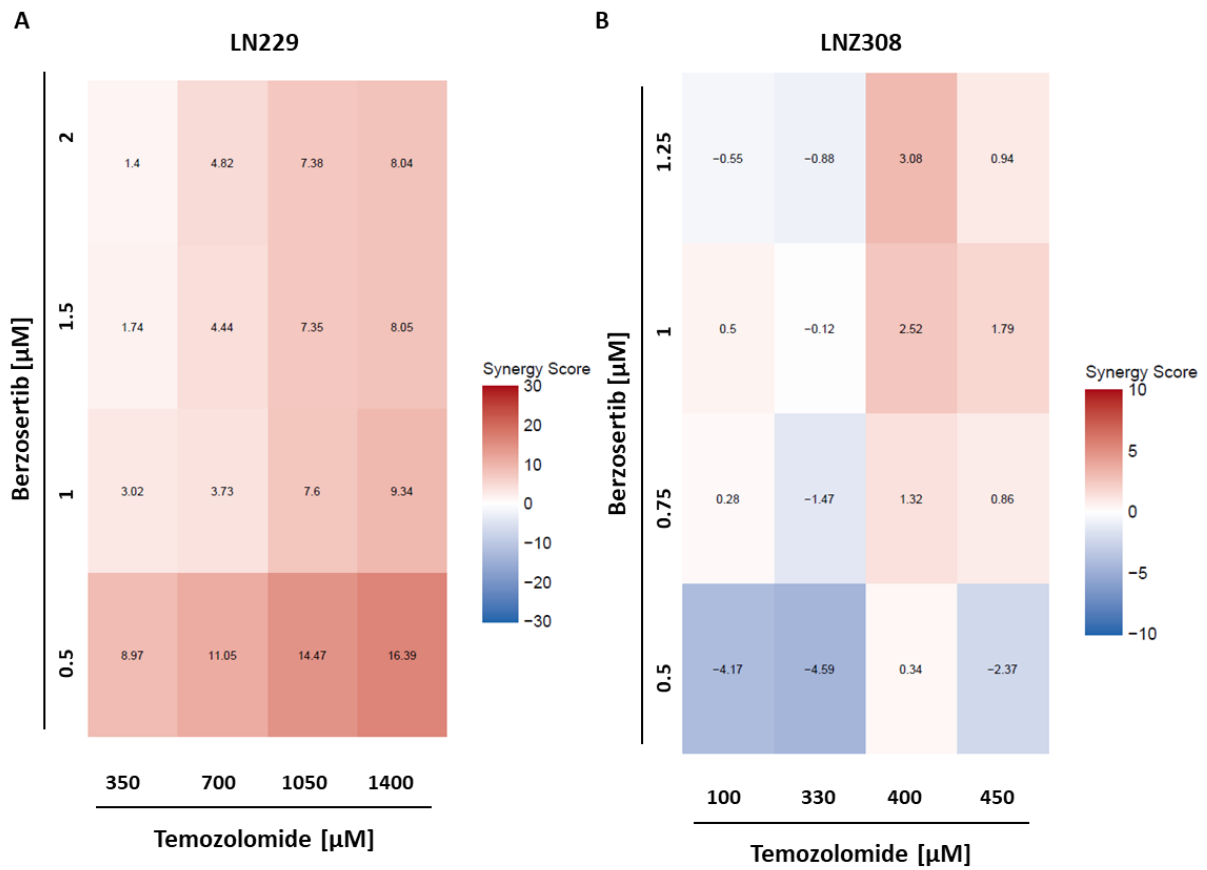
Appendix Figure 12

Appendix Figure 12: Heatmap of ZIP synergy scores of LN229 and LNZ308 cells treated with Berzosertib combined with Temozolomide in indicated concentrations
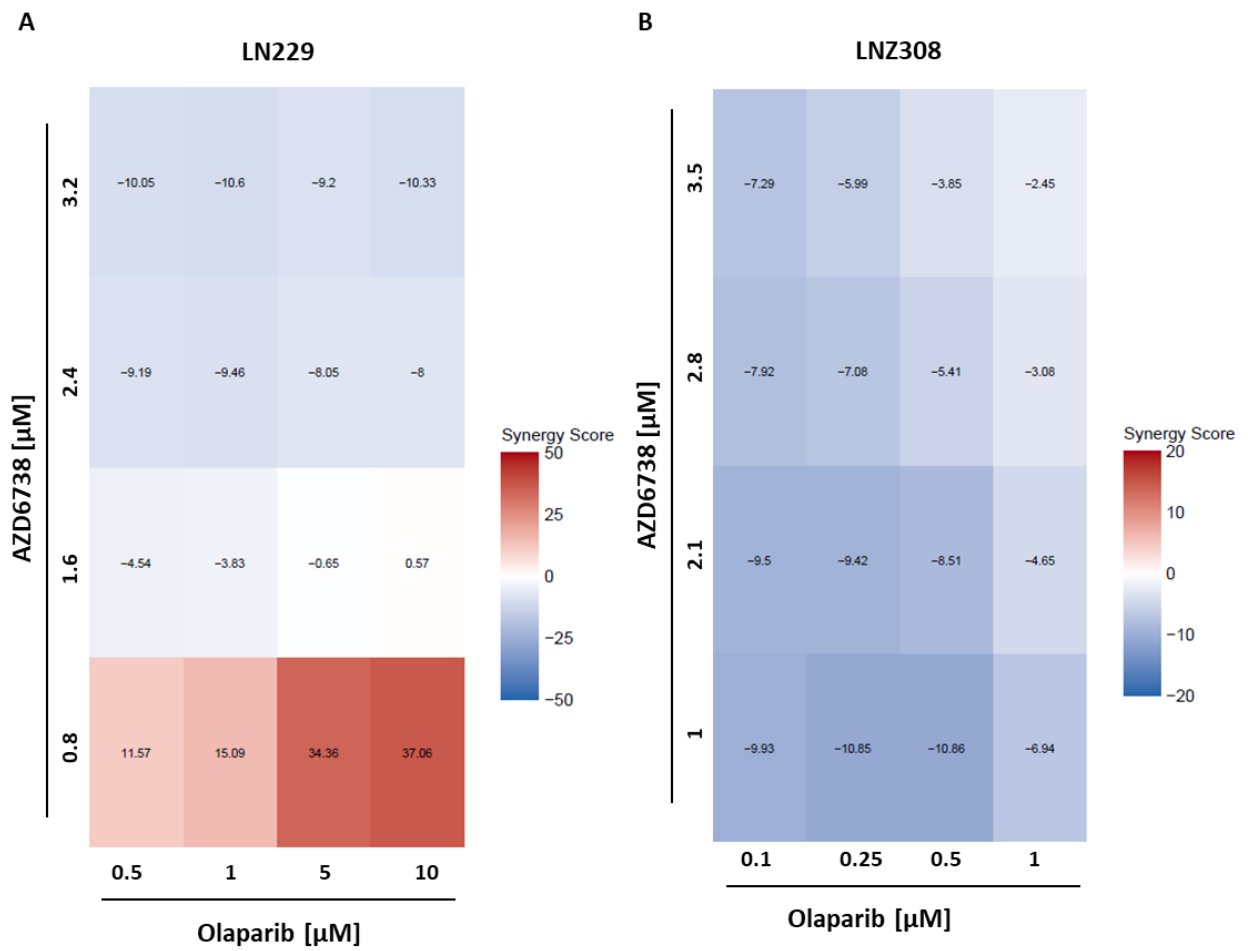
Appendix Figure 13

Appendix Figure 13: Heatmap of ZIP synergy scores of LN229 and LNZ308 cells treated with AZD6738 combined with Olaparib in indicated concentrations
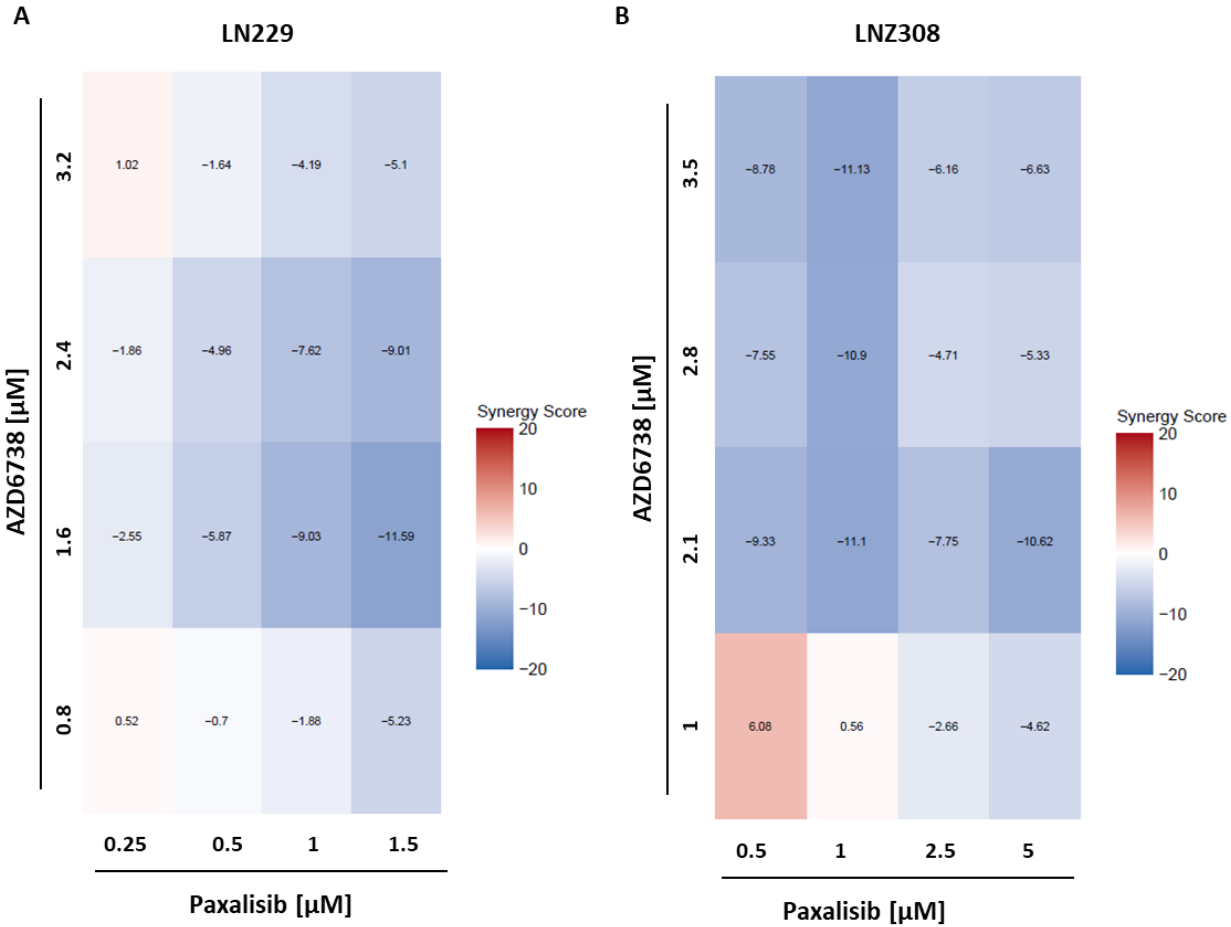
Appendix Figure 14

Appendix Figure 14: Heatmap of ZIP synergy scores of LN229 and LNZ308 cells treated with AZD6738 combined with Paxalisib in indicated concentrations
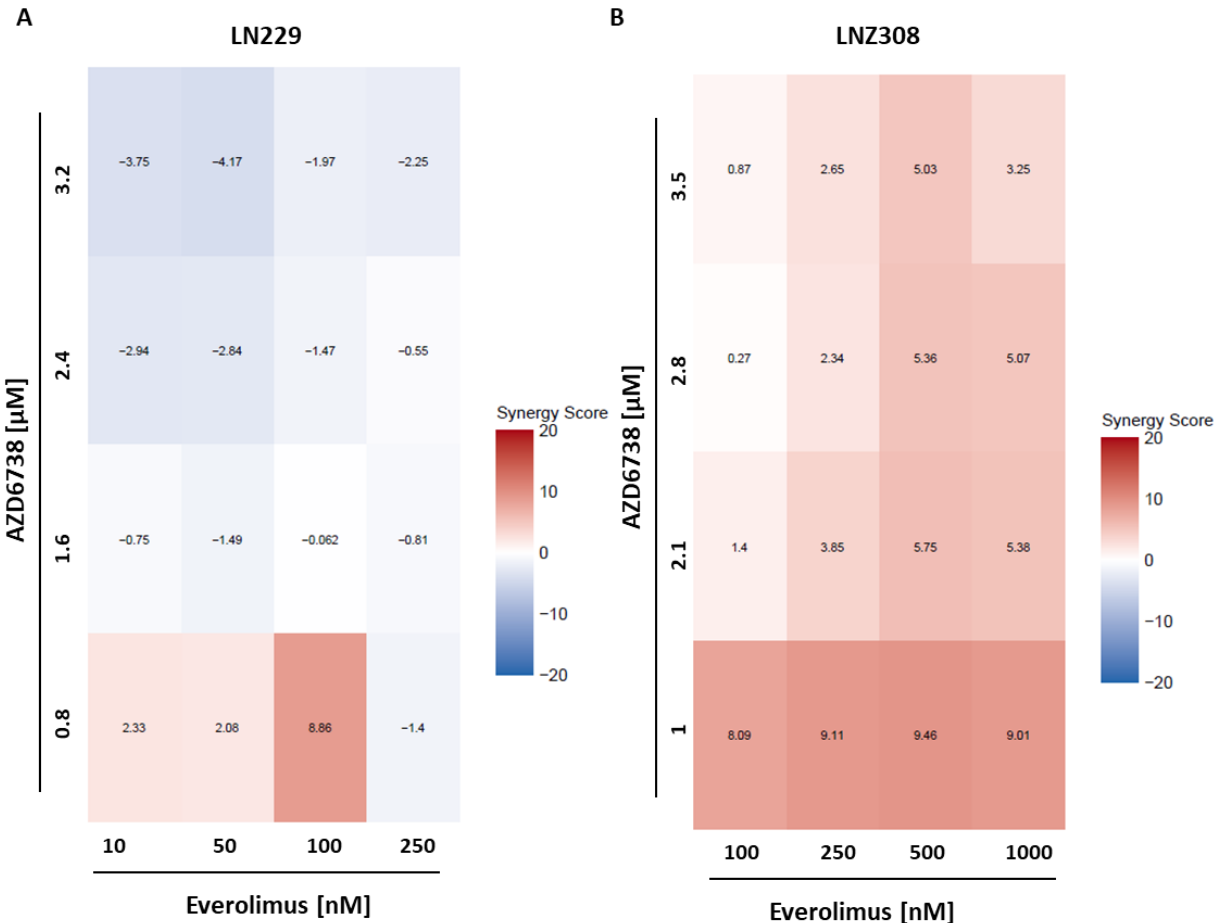
Appendix Figure 15

Appendix Figure 15: *Heatmap of ZIP synergy scores of LN229 and LNZ308 cells treated with AZD6738 combined with Temozolomide in indicated concentrations*
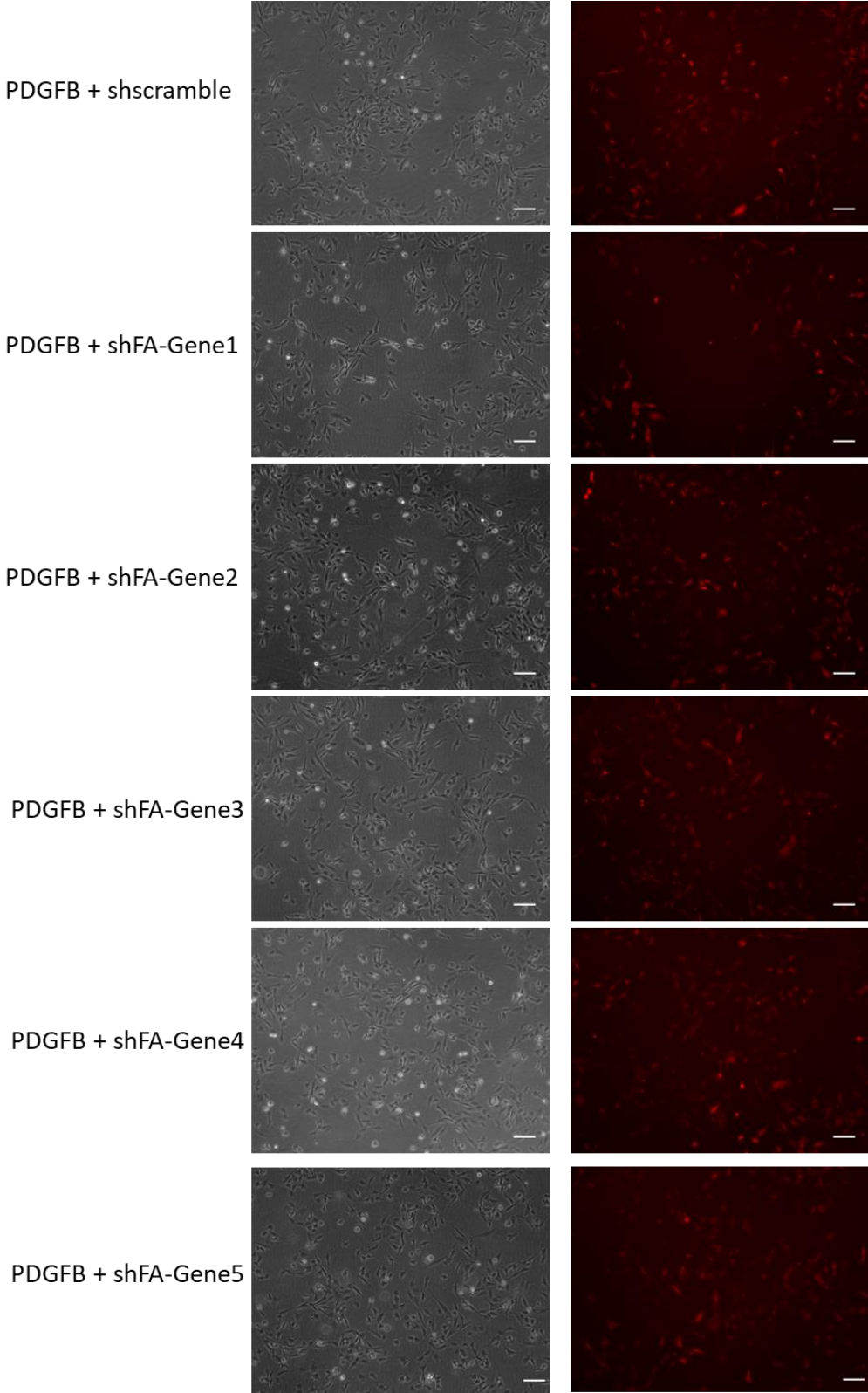
Appendix Figure 16

Appendix Figure 16: DF-1 cells one day after surgery

Left panel depicts bright field right panel the RFP expression of the cells of the respective groups. Scale bar:
100 μm.

Appendix Table 1: Score sheet for animal experiment 1: Argyrin F monotherapy in SMA560/VM-Dk mice*

Parameter	Phenotype	Score
Weight loss (A)	0	0
	10-14%	1
	maximal 15%	2
	maximal 20%	3
General appearance (B)	Clean skin and orifices, no pain	0
	Slight eye or nose discharge, slight pain	1
	Sticky eyes, moderate pain	2
	Cramps, dehydration, strong pain	3
Behavior and posture (C)	Normal spontaneous-explorative behavior, normal posture	0
	Reduced spontaneous-explorative behavior, slightly hunched back	1
	Strongly reduced spontaneous-explorative behavior, moderately hunched back	2
	Total inactivity, strongly hunched back	3
Neurological symptoms (D) Pen test, grid, left paw paralysis	None	0
	Slight loss-of-balance, occasionally missed steps, slight paralysis	1
	Moderate loss-of-balance, every third step missed, moderate paralysis	2
	Strong loss-of-balance, total inactivity, strong paralysis	3
Endpoint	1) 3x Score 1 + 1x Score2	
	2) 2x Score 2	
	3) 1x Score 3	

Further details are outlined in Material & Methods.

Appendix Table 2: Score sheet animal experiment 2: Argyrin F in combination with PD-1 blockade in SMA560/VM-Dk mice*

1	general appearance		
a	state of care	clean, shiny, smooth fur	0
		no fur grooming, dull fur	1
		no fur grooming, dirty	2
		no fur grooming, dirty, piloerection	4
b	Eyes	normal	0
		subtly sunk in, swollen	1
		lids closed	2
		strongly sunken in, lids closed, sticky	4
c	Posture	normal	0
		slightly bent	1
		strongly bent	2
		strongly bent, paws under the body	4
d	Breathing	regular	0
		regular, slightly enhanced	1
		strongly enhanced	2
		difficulty breathing, pumping	4
e	behavior/activity	normal	0
		slightly changed	1
		reduced spontaneous-explorative behavior, isolated	2
		apathic, inactivity	4
2	nutritional status		
a	Bodycondition score	vertebrae and pelvic bones only palpable when slightly pressed	0

		vertebrae and pelvic bones easily palpable, abdominal retraction detectable from the side	1
		vertebrae visible, pelvic bones palpable	2
		vertebrae, pelvic bones and rips visible	4
b	Weight	normal, continuous increase (±5%)	0
	calculated from original weight, corrected for expected weight gain of healthy animals	weight loss 5-10%	1
		weight loss >10 bis <20%	2
		weight loss max. 20%	**end point**
3	**experiment associated: tumor growth**		
a	Neurological symptoms: pen test, grid, lef paw paralysis	none	0
		slight loss-of-balance, occasionally missed steps, slight paralysis	1
		Moderate loss-of-balance, every third step missed, moderate paralysis	2
		Strong loss-of-balance, total inactivity, strong paralysis	**end point**
b	Grimace Scale	normal	0
		less than 5 pain scores 1, slight pain	1
		all categories of pain (#1 to #5) equal slight (1), moderate pain	2
		all categories of pain (#1 to #5) equal strong (2), strong pain	**end point**
end points	0 -2 points	Normal	

	3 -8 points	daily scoring/weight control, might talk to veterinarians (pain killers, wet food)
	9 and more points	**end point**
	4 points in experiment associated criteria	**end point**
exceptional measures	weight loss 20%	
	neurological symptoms with strong loss-of-balance, total inactivity and strong paralysis	
	strong pain (compare "Grimace Scale")	
	1x Score 4	

*Further details are outlined in Material & Methods.

In all experiments pain evaluation according to Langford et al. [1]

_____

1.   Langford DJ, Bailey AL, Chanda ML, Clarke SE, Drummond TE, Echols S, Glick S, Ingrao J, Klassen-Ross T, LaCroix-Fralish ML *et al*: **Coding of facial expressions of pain in the laboratory mouse**. *Nature Methods* 2010, **7**(6):447-449.

Appendix Table 3: List of significantly differentially expressed genes (DEG) in LN229 cells treated with 1.6 µM AZD6738 for 72h

Gene	log2(FoldChange)	p$_{adj}$	-log$_{10}$(p$_{adj}$)
MDFI	-3.053030277	1.78E-07	6.748854352
NTF3	-2.604227721	0.001376561	2.861204571
AL050327.1	-2.403334988	0.006805085	2.167166456
MYCNOS	-2.287931815	0.001929122	2.714640414
GGACT	-2.282662778	0.002157536	2.666041952
GFRA2	-2.222185521	1.83E-42	41.73846642
AC095057.3	-2.169375566	0.00642184	2.1923405
MYCN	-2.084904614	7.39E-83	82.13119405
H19_1	-2.018267653	0.001037099	2.984179957
CPVL	-2.01422664	1.34E-30	29.87409378
AL645608.3	-1.988038916	0.000253415	3.596167926
BANCR	-1.953108606	3.20E-09	8.494707623
RAET1E-AS1	-1.905373677	0.000963329	3.016225175
PERM1	-1.843892021	0.001176299	2.929482133
PRIMA1	-1.831346143	1.06E-71	70.97392652
RIPOR2	-1.780757118	0.001275484	2.894325037
TRIL	-1.75466518	2.32E-85	84.63533326
ITGA9	-1.743906634	3.33E-304	303.4769137
H19	-1.725364745	7.49E-55	54.12524406
EFHD1	-1.715536003	2.52E-13	12.59900604
KIF26B	-1.705484063	1.13E-215	214.9452342
PRH1	-1.682383508	0.005248932	2.279929043
KCNJ10	-1.675692259	4.70E-53	52.32767124
PODXL	-1.652173441	0	0
AC020763.4	-1.613489138	0.000651994	3.185756339
GPC3	-1.611346804	2.50E-26	25.60214624
HPGD	-1.600666004	4.82E-10	9.317309692
WFDC1	-1.596509452	1.40E-05	4.854171095
SOCS2-AS1	-1.575869014	4.26E-31	30.37024068
SEPT4-AS1	-1.572416057	0.00324447	2.488856222
KCNA2	-1.569504664	1.64E-119	118.7860811
UG0898H09	-1.523533767	1.06E-18	17.97379339
LINC00639	-1.518023211	8.02E-08	7.095643962
COL9A1	-1.509699071	1.36E-36	35.86489159
PRDM16	-1.490792931	8.11E-17	16.09090036
MTSS1	-1.463609472	6.47E-06	5.188877122
AC005746.2	-1.458817618	1.55E-08	7.808427966
TLX1	-1.454383437	4.20E-64	63.37681854
NOVA2	-1.450148507	6.00E-39	38.22166411
COL15A1	-1.44126318	2.17E-234	233.6630836
CHST9	-1.43932772	9.44E-16	15.02491493
ANKRD45	-1.414009578	0.002476531	2.606156252
SERPINF1	-1.40895008	6.85E-05	4.164340063

Gene	log2(FoldChange)	p_{adj}	$-\log_{10}(p_{adj})$
SCARA5	-1.404556848	3.84E-40	39.41557844
FRMPD3	-1.395284429	0.001061149	2.974223658
PPP1R1B	-1.392828413	0.002699863	2.568658209
KIT	-1.386443098	7.90E-14	13.10224853
EFS	-1.384273792	0.000239999	3.619789816
PCDHGC4	-1.380283936	3.62E-14	13.4411141
TMEM178B	-1.364859812	4.17E-20	19.37959632
DCT	-1.362953668	1.27E-08	7.89721598
ICOSLG	-1.357227054	0.00056837	3.245368771
VASH2	-1.352757751	1.96E-20	19.70844114
FRMD4B	-1.347465342	1.23E-26	25.90952392
PLCB2	-1.345671833	1.68E-07	6.775074326
XKR5	-1.344559689	1.54E-12	11.81123441
FXYD7	-1.33568599	3.15E-12	11.50209085
AC005972.4	-1.33538645	0.009818411	2.007958803
AF287957.1	-1.320892884	0.006902304	2.16100591
AC091563.1	-1.320524118	0.003067195	2.513258572
NMU	-1.315451833	1.21E-12	11.91841744
MYB	-1.296265024	0.000106804	3.971413832
SLITRK3	-1.292637596	3.62E-10	9.441565029
HEY2	-1.289811657	1.21E-22	21.91797923
Sep 04	-1.281679392	1.37E-24	23.86206163
NFIA	-1.279095293	1.17E-17	16.93321739
STXBP6	-1.277002934	4.16E-69	68.38054549
EFR3B	-1.26720553	1.97E-83	82.70652731
FAM69B	-1.266687898	5.11E-18	17.29180879
ARHGAP20	-1.265177428	5.91E-08	7.22876096
AGT	-1.261121806	0.000477783	3.320769239
APCDD1	-1.259134094	1.11E-24	23.95287889
SERPINA3	-1.242482015	8.20E-10	9.086208701
MAP2K6	-1.242445986	1.72E-37	36.76437521
RGS4	-1.240946442	7.01E-55	54.1542202
COL8A2	-1.238357046	1.65E-05	4.782838461
MOB3B	-1.234349002	0.001961972	2.707307261
NCKAP5	-1.229810903	3.93E-17	16.40532255
PCDHB3	-1.225225607	8.43E-09	8.074412063
GNG7	-1.221878261	1.29E-125	124.8903434
RAB17	-1.220102986	1.37E-25	24.86401252
ZNF385B	-1.207178518	0.00853748	2.068670282
NEURL1B	-1.205525019	1.69E-60	59.77261656
PCDHGA9	-1.194894495	3.46E-05	4.461153366
METTL7A	-1.190609985	5.30E-23	22.27544244
LINC01546	-1.19039883	0.00071771	3.144051261
ERBB4	-1.183969984	7.82E-05	4.106598645
SPC24	-1.178148147	1.80E-45	44.74469863
PRRX2	-1.176376491	0.000600838	3.221242631

Gene	log2(FoldChange)	p_{adj}	$-\log_{10}(p_{adj})$
CCR1	-1.17165335	0.00025395	3.595251438
RAPGEF4	-1.169480687	6.17E-28	27.20989489
C4orf19	-1.167935663	3.97E-38	37.40164921
RHBDL3	-1.165543808	3.58E-06	5.446053578
AC069499.1	-1.159376062	0.000661455	3.179499623
GRIK3	-1.157799165	1.71E-43	42.76641126
MEF2C	-1.157476121	1.06E-129	128.9740778
SMAD6	-1.122971135	4.40E-46	45.35688922
PCSK6	-1.117593413	2.08E-05	4.682673274
ZNF704	-1.117449183	4.73E-37	36.32523145
SCIN	-1.114463338	3.11E-33	32.50781937
NAV2	-1.112949431	4.45E-45	44.35191975
PALM	-1.11251274	3.82E-14	13.41848291
IGSF3	-1.107023952	7.04E-120	119.1524762
FLRT1	-1.105372493	3.21E-08	7.493626452
NR5A2	-1.101969902	1.27E-05	4.895963948
PCDHGA3	-1.10041835	0.002161948	2.665154768
LDLRAD4	-1.10002721	2.86E-16	15.5435442
DUSP5P1	-1.09978372	0.00181276	2.741659694
LMNB1	-1.099757652	4.16E-105	104.3805415
ATOH8	-1.092639114	2.93E-44	43.53263039
RBMS3	-1.092476848	2.91E-56	55.53591754
SBK1	-1.083978915	3.62E-07	6.441364678
ACADL	-1.080943742	0.002497981	2.602410875
TNS2	-1.080286655	7.84E-79	78.10567005
HPN-AS1	-1.079508276	1.13E-30	29.94570296
TBC1D4	-1.078547442	1.35E-84	83.86931117
ADORA1	-1.075941765	7.00E-09	8.15468122
AC004925.1	-1.074758941	0.000390056	3.408872684
AC117500.6	-1.07177495	7.57E-20	19.12088353
ROPN1B	-1.071147486	5.03E-16	15.29804083
ELN	-1.068922633	0.006019618	2.220431061
EPHB1	-1.06620727	0.001570706	2.803905082
LINC01505	-1.06494385	1.60E-16	15.79470549
AC093535.2	-1.06472191	1.09E-07	6.960970731
HAS2	-1.058890019	7.08E-26	25.15002609
DCHS2	-1.056087293	4.25E-14	13.37189163
AR	-1.055707187	6.42E-11	10.19258262
SOCS2	-1.055489869	1.58E-51	50.80052147
STAC2	-1.053264309	2.39E-05	4.621680424
FBLN1	-1.046172126	4.00E-19	18.39794407
SAPCD2	-1.046067012	6.32E-72	71.19908029
NRROS	-1.045329852	1.41E-06	5.851475086
AC009041.2	-1.04499135	2.28E-16	15.64264062
BEND5	-1.043243697	0.000163533	3.786394502
ABCA6	-1.042756512	6.52E-53	52.18575553

Gene	log2(FoldChange)	p_{adj}	$-\log_{10}(p_{adj})$
PPP1R14C	-1.038734651	1.08E-56	55.9667403
EBF3	-1.031092637	2.41E-43	42.61749898
FAM135B	-1.025768156	6.86E-09	8.163619532
STARD8	-1.025676733	8.40E-13	12.07591644
PIANP	-1.023304712	0.003171854	2.498686818
ZNF710-AS1	-1.021776844	1.10E-05	4.957654676
PIF1	-1.014677933	5.12E-27	26.29102964
NKAIN3	-1.009958414	1.10E-07	6.957316295
DPF3	-1.009833016	1.13E-05	4.948367091
TP63	-1.008086241	0.004517681	2.345084438
KIF15	-1.005951903	8.96E-61	60.04753782
DTWD2	-1.004298031	1.37E-39	38.86172842
GJA5	-1.004272334	2.26E-10	9.646132122
SHC3	-1.00321749	3.67E-05	4.435475634
PCDHGC5	-1.002636519	4.95E-07	6.305355239
AL390115.1	-1.001928944	1.71E-06	5.766904633
DDB2	1.001617399	5.57E-101	100.2539426
GABARAPL1	1.003615782	4.26E-49	48.37071074
NGFR	1.008930362	4.86E-52	51.31322646
DEPDC7	1.017346801	2.29E-64	63.6409121
PML	1.020218945	2.02E-94	93.69538897
ZNF844	1.022884463	7.46E-17	16.12740888
HOXB4	1.02382098	0.0027244	2.564729101
TAP1	1.0314321	9.49E-63	62.02278409
ZNF442	1.033892997	1.49E-05	4.827094161
AC009404.1	1.034941273	0.000181702	3.740639312
ACTA2	1.037797969	7.48E-31	30.1258141
ABCC3	1.03927546	9.16E-37	36.03818601
KCNE4	1.041409344	1.86E-14	13.7300412
AL590326.2	1.042679879	0.003614702	2.441927448
CBX4	1.043660927	4.53E-76	75.3440707
OSGIN1	1.045715463	5.34E-53	52.27222215
SNAPC1	1.045769492	6.17E-37	36.20953244
AC109347.1	1.04637425	0.00638246	2.195011885
HIST1H2AG	1.047259732	3.42E-10	9.466439632
RSRP1	1.04787677	1.79E-21	20.74669785
NBPF25P	1.048040782	7.62E-05	4.118206103
SLC17A7	1.049317859	0.003801225	2.420076372
TSPAN11	1.050333434	3.32E-109	108.479034
AP001453.2	1.051032382	1.38E-10	9.859750764
AC016027.1	1.05174122	0.00021575	3.666049383
MT-TI	1.054120847	0.000118333	3.926892697
RPS10	1.05467428	0.000298001	3.525782315
AC072061.1	1.056814908	5.59E-06	5.252834025
NKX3-1	1.057042253	5.41E-16	15.26700809
AC004477.1	1.058189046	3.52E-08	7.45286283

Gene	log2(FoldChange)	p_{adj}	$-log_{10}(p_{adj})$
AL355488.1	1.060832374	0.006697907	2.174060908
ZNF622	1.06305363	1.54E-72	71.81319721
NEXN	1.066665132	1.43E-20	19.84508214
RELB	1.067312251	3.57E-26	25.44753888
CLK1	1.070309739	5.03E-58	57.29801515
NXF1	1.072512629	1.78E-129	128.7501563
COL5A3	1.073544261	6.85E-25	24.16461569
AC079305.1	1.073620336	0.001564671	2.805576899
LINC00324	1.073920346	1.72E-08	7.765591195
GIPR	1.07999335	4.08E-06	5.38977554
FES	1.08168436	0.003999419	2.398003092
LAG3	1.082692976	1.46E-06	5.837126803
DUSP8	1.083239018	2.02E-14	13.6946315
TXNIP	1.089701101	2.83E-58	57.54828994
MICA	1.090084584	2.09E-59	58.67995715
ZNF385A	1.090200195	3.44E-74	73.46357906
OLFML2A	1.090740692	3.60E-65	64.44404333
AKNAD1	1.092761483	0.000811725	3.09059093
RDH5	1.092873469	0.005573895	2.253841244
NT5E	1.092927105	1.87E-108	107.7278659
AL121772.1	1.094379704	2.52E-10	9.598414379
CH25H	1.094547878	0.001258031	2.900308616
ZNF28	1.094643826	4.06E-57	56.3912972
SPINT1	1.09466508	3.77E-10	9.423423814
AL354740.1	1.095452298	1.30E-06	5.887519551
UNC13D	1.096443526	0.000355718	3.448894531
FILIP1L	1.097130706	7.44E-31	30.1285655
ADM2	1.097438924	1.17E-09	8.933484489
DTX3L	1.103123067	7.52E-44	43.1238826
CYB5R2	1.106507357	2.11E-34	33.67546068
AC062017.1	1.107521023	0.008973462	2.047039988
TRIM21	1.109413464	5.65E-31	30.2477008
FGF10	1.114886385	0.003243014	2.489051178
LY6K	1.11594664	0.000665653	3.17675221
FTL	1.118150072	1.23E-142	141.9106088
AC009118.2	1.118524338	0.001106379	2.956096011
ZNF702P	1.11858338	3.15E-25	24.50144982
RASL11A	1.118978717	2.72E-09	8.564689997
GATA3	1.121762539	1.09E-09	8.96105508
TCAP	1.123006266	0.002047979	2.688674595
RPS27L	1.123774854	2.92E-136	135.5350494
AC073548.1	1.124032723	0.00229617	2.638995927
AC016597.1	1.127273788	0.000463543	3.333909703
AC239868.1	1.129106833	2.57E-25	24.59078559
LINC00115	1.130412881	0.000862819	3.064080524
CXCL1	1.133396427	2.67E-11	10.57419305

Gene	log2(FoldChange)	p_{adj}	$-\log_{10}(p_{adj})$
STXBP2	1.13409642	1.85E-07	6.733057172
LINC01004	1.136379334	2.93E-07	6.533262042
B3GALT5	1.13776166	0.000477946	3.320621392
IFIT2	1.138957717	1.50E-13	12.82400012
L1CAM	1.141267753	1.80E-42	41.7441116
HSD17B14	1.141473193	0.0044879	2.34795683
AP001273.1	1.142361463	0.001805301	2.743450318
BNIPL	1.145340356	0.003299718	2.481523125
FAS	1.148032898	2.59E-34	33.5874194
AC092117.1	1.148921842	6.71E-10	9.173319311
MORF4L2-AS1	1.149246813	0.005817994	2.235226765
CHGB	1.149693101	0.001098261	2.959294614
RGS2	1.150952621	7.44E-35	34.12864921
RIPK4	1.152721205	9.60E-07	6.017849293
ANGPTL4	1.152766415	0.00369743	2.432100076
ADAMTS7	1.152772729	1.91E-49	48.71825917
HEXIM1	1.152779168	5.68E-76	75.2456894
PARP10	1.155589311	1.68E-47	46.7739024
CD70	1.156521466	2.42E-25	24.61535562
PHPT1	1.156764678	2.21E-66	65.65654218
UXT-AS1	1.160710796	0.000400076	3.397857864
COL7A1	1.16276895	1.51E-16	15.82010763
GAS6-AS2	1.163341869	0.000899722	3.045891486
SLC37A1	1.164298928	0.007228282	2.140964887
HIST1H2BN	1.167435986	6.70E-09	8.173791287
BRWD1-AS2	1.167591833	0.008484229	2.071387595
TMCC3	1.176590965	4.10E-05	4.387584734
EGLN3	1.177206418	5.75E-06	5.24054148
AC012181.3	1.178172482	0.00986311	2.005986114
AC079305.3	1.178474597	0.001515846	2.81934503
PLK3	1.180277162	2.31E-30	29.63577162
NUTM2E	1.180655241	0.002234219	2.650874222
FLJ20021	1.181705495	4.07E-08	7.39051681
PLEKHA7	1.185054746	7.71E-05	4.113100421
SLC37A2	1.187642162	9.67E-11	10.01444429
CEBPB-AS1	1.191734367	1.00E-08	7.999853405
ADAMTS16	1.193593812	5.75E-09	8.240576735
PARP14	1.195463618	7.39E-24	23.13135787
MT-RNR1	1.196811755	1.47E-82	81.8321636
TRIM3	1.197595565	6.17E-78	77.20950685
SIK1	1.203701144	2.84E-19	18.54695947
ZNF425	1.20474635	5.61E-28	27.25126983
AC087741.3	1.209480663	3.21E-07	6.494004477
TRAPPC5	1.210669158	2.35E-06	5.628723553
HLA-J	1.213082226	0.002119868	2.673691277
AP003108.2	1.216948689	0.002486654	2.604384595

Gene	log2(FoldChange)	p_{adj}	$-log_{10}(p_{adj})$
ZNF114	1.218368788	0.00011659	3.933337313
IFI35	1.22233118	4.57E-45	44.33981149
DNAJB4	1.222361009	1.94E-44	43.71269426
KLF4	1.223852144	7.61E-105	104.1185452
C7orf57	1.227393379	0.002491039	2.603619499
LAMA2	1.229335358	1.21E-06	5.916365681
VEGFA	1.229450489	1.36E-106	105.8654236
ZNF703	1.233084567	4.47E-27	26.35014312
LINC02119	1.244729356	9.34E-19	18.02968801
OSR2	1.245676477	9.33E-12	11.03011393
AEN	1.246780793	4.18E-86	85.37864381
UCN2	1.247356465	6.18E-13	12.20929971
TRANK1	1.250565364	1.01E-21	20.99519728
BX537318.1	1.251532079	0.000167383	3.776289079
AC144831.1	1.251808752	5.42E-05	4.266336143
PARP9	1.253322478	6.74E-20	19.17141952
GGN	1.258187931	0.000878381	3.056317301
LAMC3	1.259629633	0.003638073	2.43912859
MGAM2	1.261663752	3.20E-09	8.494757749
GEM	1.26188574	1.08E-72	71.96763408
PMAIP1	1.264662322	5.40E-114	113.2673526
DDX60L	1.264897021	8.02E-48	47.09572892
HERPUD1	1.270070441	4.63E-146	145.3344244
AC079145.1	1.272616193	0.006933274	2.159061667
FDXR	1.274303586	9.06E-56	55.04267373
ULBP2	1.274356899	1.05E-22	21.9806828
AL355472.1	1.275675977	2.32E-08	7.634224779
AC253536.6	1.281151542	0.002258269	2.646224245
SNAI1	1.285579579	8.66E-123	122.062555
CFL1P1	1.286685719	0.000852793	3.069156223
TYRP1	1.289299238	0.00033133	3.479739193
CLU	1.289767206	2.88E-93	92.54009657
CYP51A1-AS1	1.291994212	0.001115699	2.952452906
NFKBIA	1.292987157	8.01E-75	74.09620868
TPPP	1.298533776	0.007842828	2.105527324
WDR66	1.298627701	1.62E-06	5.790109686
CEACAM19	1.300669262	0.002292662	2.639660006
HIST1H2BE	1.302937834	9.67E-09	8.014367812
CD274	1.307251419	1.83E-13	12.73742743
ADRB2	1.307433436	7.04E-07	6.152635276
VGF	1.308410159	5.95E-31	30.22551024
MIR222HG	1.308534412	1.04E-10	9.984860037
MYH3	1.308635017	0.00222553	2.652566614
CCDC62	1.310694166	0.000153913	3.812725062
HIST2H2BE	1.313012462	1.44E-51	50.8421797
LINC00910	1.314720162	1.97E-12	11.70473513

Gene	log2(FoldChange)	p_{adj}	$-log_{10}(p_{adj})$
CYP1B1	1.316875566	2.50E-17	16.60219606
JMJD1C-AS1	1.317644381	0.001674257	2.776177822
AL031587.3	1.31893895	0.008159974	2.088311199
MED26	1.319184951	3.35E-27	26.47538953
CASZ1	1.319216624	2.13E-12	11.67206018
RRM2B	1.319217263	6.27E-126	125.2026418
KBTBD8	1.31952214	4.71E-13	12.32707222
TIGAR	1.322296816	7.87E-45	44.10393466
THEMIS2	1.324302596	4.59E-08	7.338048247
KCNJ2-AS1	1.324500649	0.007908004	2.101933141
AC010654.1	1.325440495	0.006883048	2.162219173
PICART1	1.32984687	0.003796854	2.420576081
LINC01060	1.330471762	0.00882087	2.05448857
RTP4	1.330778721	2.57E-09	8.590257311
EDA2R	1.333572961	4.68E-37	36.32974113
STAT1	1.340402137	2.15E-63	62.66810032
FAM83G	1.343889439	2.23E-23	22.6521405
HSPB8	1.344192804	2.99E-38	37.52455897
SNHG1	1.344449255	2.64E-109	108.5788177
AL035681.1	1.35046507	0.004270406	2.369530793
AL391069.2	1.352004742	3.59E-07	6.444681256
VWCE	1.354377434	0.000392299	3.406382597
LGALS9	1.361013599	0.000617262	3.209530514
RTL5	1.362743625	1.59E-05	4.797623901
MYLK2	1.362921092	0.005844252	2.233271031
CNN1	1.365004715	8.68E-10	9.061479969
PTPN22	1.368166375	0.000173619	3.760403575
SNHG9	1.372044233	1.21E-12	11.91735005
TMEM27	1.372457742	0.008059217	2.093707136
AC090192.2	1.376853267	0.005218419	2.282461092
UNC79	1.376876479	0.003662095	2.43627037
CYBA	1.378969731	0.00976113	2.010499922
CDKN1C	1.381961288	3.79E-08	7.421398793
AP002990.1	1.387008706	0.008974728	2.0469787
KITLG	1.38868154	4.28E-102	101.3686595
FOSL1	1.390548645	1.87E-148	147.7280409
EDN1	1.396239265	0.004468129	2.349874279
ZFHX2	1.402561078	0.009693848	2.013503797
PTPN6	1.403347385	0.006264608	2.203106124
AL365203.1	1.407406499	0.001245386	2.9046959
CDH15	1.413180481	0.000619976	3.20762523
LINC01023	1.418388644	1.51E-05	4.822293599
ITGB2-AS1	1.418444733	0.001398694	2.854277303
AL138966.2	1.419798445	0.005250631	2.279788492
IFIH1	1.419892525	2.81E-40	39.55055836
BST2	1.41994439	9.80E-32	31.00885699

Gene	log2(FoldChange)	p_{adj}	$-log_{10}(p_{adj})$
AL365181.2	1.422014198	0.000154517	3.811023647
AOC2	1.42209241	5.70E-12	11.24425284
MAMDC4	1.426799948	1.93E-21	20.71384309
CATSPERG	1.430640575	9.59E-05	4.018301459
VAMP8	1.436484173	0.001213245	2.916051602
AL137077.2	1.442005561	8.79E-07	6.056146462
GREB1	1.443434565	1.03E-53	52.98823596
DDN-AS1	1.444349968	1.64E-06	5.786202008
FOXQ1	1.446168166	3.57E-05	4.447343103
AC004854.2	1.446647532	2.83E-08	7.548765679
SAMD9	1.447033164	2.82E-47	46.54941006
ASGR1	1.4504905	0.007272218	2.138333121
ZNF763	1.450841244	0.001920922	2.716490256
AC217777.1	1.450869526	0.003534659	2.451652479
AC108673.2	1.450890353	0.006941457	2.158549337
CDC42BPG	1.454765678	2.47E-09	8.607288627
MIR22HG	1.457213836	2.49E-49	48.60412782
PLAC8L1	1.459213903	0.003884736	2.410638495
MIR34AHG	1.461242442	2.91E-17	16.53679918
CSAG4	1.46251474	1.98E-06	5.70293168
ARRDC4	1.472853155	8.51E-13	12.07001429
GATA2	1.474633859	1.29E-30	29.88850631
HIST2H2AC	1.476290425	1.16E-05	4.933853065
HIST1H2BO	1.476564826	0.004664859	2.331161439
DNAJB1	1.477566166	8.32E-277	276.0796607
MXD1	1.481066719	1.41E-87	86.85232235
KRT6B	1.482467881	0.002642443	2.577994293
FSTL5	1.483927803	1.25E-29	28.90391785
HSPH1	1.484440956	5.83E-209	208.2339867
PTCHD4	1.485861145	4.05E-26	25.39299006
ITIH5	1.487706754	8.46E-50	49.07242102
BEX2	1.489968872	5.91E-07	6.228074996
IL15RA	1.490207687	0.000349352	3.456736298
HIST1H2AC	1.491254306	4.03E-71	70.39430165
TRIM22	1.492477792	4.19E-98	97.3781217
SLC15A3	1.49303853	3.82E-10	9.417930317
MSX1	1.496441998	1.27E-40	39.89558112
AP001596.1	1.496968837	0.000479351	3.319346498
ARL4D	1.500927193	5.58E-31	30.25308158
OAS3	1.506176165	5.88E-25	24.23053782
HIST1H2BC	1.511682963	9.14E-10	9.038830759
AL442663.3	1.512152853	0.001074021	2.968987311
BCL2L15	1.512648717	0.003031185	2.518387596
LINC00685	1.514325639	0.000473295	3.324867724
SAMD9L	1.516414841	9.00E-38	37.04552154
SNORD14A	1.517589838	0.005575375	2.253725911

Gene	log2(FoldChange)	p_{adj}	$-log_{10}(p_{adj})$
MIR616	1.52004063	0.000101185	3.994885853
HUS1B	1.523809612	0.007595445	2.119446786
AL354718.3	1.525078098	0.004167629	2.380110954
LAPTM5	1.525265121	2.12E-05	4.673708097
POU6F2-AS2	1.530346211	0.004055726	2.391931409
TMEM88	1.532265201	0.005351525	2.27152241
ELFN2	1.53541022	0.001155572	2.937203102
CARD9	1.539745369	0.005878635	2.230723521
AC016586.1	1.561198249	0.00892814	2.049239015
CARNS1	1.562977462	4.78E-08	7.320342557
RTL9	1.568836007	7.16E-08	7.14534657
SLC30A1	1.569984654	2.50E-159	158.6028704
AL356512.1	1.572981677	1.58E-05	4.802626972
AC073611.1	1.575767883	6.58E-08	7.181662441
AC007250.1	1.581801324	0.004015971	2.396209385
DUSP5	1.59008275	2.73E-95	94.5644131
GCNA	1.592696783	1.08E-14	13.96767716
CLDN4	1.594742534	0.000185648	3.731308696
AC132192.2	1.596425465	6.32E-15	14.19899826
ACHE	1.600803288	0.000168976	3.772173873
HMOX1	1.608142668	1.45E-126	125.838466
SLFN5	1.611676868	3.44E-77	76.46406423
CPA4	1.617345334	5.12E-17	16.29036318
RASAL1	1.619394335	0.000451574	3.34527082
AC115284.2	1.622999072	8.38E-05	4.076539423
AP003071.5	1.625952301	0.004249494	2.371662794
TNFSF4	1.629373815	0.002239921	2.649767376
AL023806.1	1.630256327	0.008884144	2.051384402
SNHG12	1.631991871	1.32E-73	72.87972208
BOLA2-SMG1P6	1.634016928	0.004329099	2.363602502
AL161431.1	1.640212195	7.74E-08	7.11137567
AC084824.1	1.640990441	7.66E-06	5.115924491
AP000844.2	1.652296739	1.53E-05	4.815871413
SLC3A2	1.65343467	0	#ZAHL!
AC021242.3	1.654551553	0.000122518	3.911800416
S100A2	1.656328667	1.25E-23	22.90466144
WNT9A	1.65853472	2.20E-05	4.658082096
AC087752.3	1.659404914	9.20E-05	4.036321258
BST1	1.660638894	0.003576638	2.446525013
AC016831.1	1.661446359	1.50E-07	6.824179984
PLAU	1.665821838	0.002738407	2.562502072
AC131212.3	1.666583177	2.33E-05	4.633452183
SESN2	1.669344708	1.61E-204	203.7936285
ACRBP	1.670079086	0.00859918	2.065542954
ASPRV1	1.671138348	0.002185305	2.66048792

Gene	log2(FoldChange)	p_{adj}	$-log_{10}(p_{adj})$
AC116407.2	1.671872852	8.04E-05	4.094552249
DIRC3-AS1	1.672205053	0.00911589	2.040200941
RPL13AP20	1.67227445	0.00071881	3.143385957
CISH	1.675018169	8.57E-06	5.066912628
C1orf61	1.684692851	0.002323516	2.633854366
SNHG25	1.687002247	5.63E-05	4.249856983
C1orf116	1.687321844	0.000782965	3.106257848
AL451042.2	1.690909829	0.007561953	2.121366051
MYPN	1.691038276	2.09E-12	11.68023493
LINC01191	1.691949354	0.007848386	2.105219629
ICAM4	1.696215986	0.001924096	2.715773267
KIAA1161	1.707192486	2.25E-14	13.64857945
HIST1H4H	1.711048085	2.80E-35	34.55291061
TSPYL2	1.711811578	6.20E-165	164.2074506
PINLYP	1.717170842	1.22E-05	4.913917376
XDH	1.717594006	0.000471207	3.326788519
ASNS	1.73210869	2.10E-25	24.67857265
AL031728.1	1.732324284	0.006603197	2.180245733
AC009831.1	1.732621623	2.39E-09	8.620825354
MIR3189	1.73272246	0.003566952	2.447702743
LAYN	1.734278661	0.008623019	2.064340632
RASL12	1.735250748	0.008467958	2.072221299
ADM	1.735921072	1.65E-127	126.7831074
AURKC	1.737341612	0.003091974	2.509764178
PPP5D1	1.73828475	0.006907072	2.160706004
AC116407.1	1.739465141	0.006181197	2.208927427
COL6A3	1.743408089	2.59E-14	13.58694299
KIAA1683	1.744720943	3.49E-15	14.457739
KRT8P33	1.745273796	7.73E-07	6.111675636
ARHGAP9	1.745821768	2.21E-06	5.654755466
CYP4F11	1.748681741	0.000834388	3.078632095
DDIT3	1.750603138	1.28E-167	166.8921905
AL031710.2	1.754843401	0.009298008	2.031610084
ARRDC3	1.755214217	4.44E-189	188.3523673
IFIT3	1.761535846	2.06E-28	27.68604289
AC007663.3	1.769433307	0.008433266	2.074004212
NHLH1	1.769889922	5.23E-05	4.281453473
AC009570.1	1.779751744	0.004927834	2.307343916
AC007032.1	1.783175833	1.02E-06	5.99015568
ZNF468	1.783814137	1.13E-163	162.9480956
HERC6	1.787185517	1.21E-57	56.91769592
CYP1A1	1.792300324	1.64E-12	11.78458537
AL451050.2	1.792647869	0.001748689	2.757287309
ZC3H12A	1.794831247	6.19E-64	63.20860163
AC005785.1	1.796411595	0.008256246	2.083217397
AL157756.1	1.798579496	0.000165085	3.782292611

Gene	log2(FoldChange)	p_{adj}	$-log_{10}(p_{adj})$
LINC01588	1.805183462	5.07E-06	5.294936901
MUC12	1.807771257	0.00049462	3.305728476
SPDYA	1.809372317	0.001449459	2.838794036
KCNJ11	1.809766676	0.0047501	2.323297268
NPTX1	1.813108799	1.85E-31	30.73323614
ZG16B	1.814608535	0.000183572	3.73619285
RINL	1.817331122	0.00024741	3.60658284
AC084880.1	1.818644232	0.001252226	2.902317243
CRISPLD2	1.820975254	6.94E-38	37.15845438
ZP1	1.831771233	8.37E-05	4.07739243
SPOCD1	1.835352179	2.81E-10	9.550543083
DHDH	1.838583875	0.00298802	2.524616469
AMPD3	1.839345112	0.001808673	2.742639895
LINC01186	1.841262611	0.006511241	2.186336257
IL12A	1.841977455	6.88E-07	6.162180193
AL390067.1	1.854681664	0.00225498	2.646857286
QPCT	1.856172115	1.68E-05	4.775521037
ZFAND2A	1.856866826	2.41E-141	140.6179911
KRT15	1.857010541	0.000288647	3.539633338
CALB2	1.85995461	8.04E-07	6.094846342
TINCR	1.86243364	5.59E-06	5.252399873
HPX	1.871908193	5.71E-06	5.243351162
FOSB	1.877081566	2.19E-18	17.65892731
C2	1.880183089	0.000110532	3.956513075
TUFT1	1.883338349	1.35E-177	176.8708926
AC107959.1	1.888707776	3.08E-31	30.51130837
PPP1R15A	1.891387039	0	#ZAHL!
CRABP2	1.895940325	8.29E-24	23.08157239
HIST1H2BJ	1.899217028	1.99E-24	23.70126633
SNORA72	1.900246318	9.54E-06	5.020240981
AC104971.2	1.904628574	1.12E-06	5.951846875
ABCC2	1.911174883	2.87E-07	6.542485411
CACNA1G	1.913478878	0.00210712	2.676310681
AC084018.2	1.922202353	8.81E-10	9.05486073
AC009063.2	1.932356054	0.004362548	2.360259814
DHX58	1.934509555	2.74E-41	40.56150286
AC243772.2	1.943290178	0.000787031	3.10400798
KRT17	1.943819242	2.27E-07	6.643824018
SLC14A1	1.944455713	7.12E-81	80.14764354
AC020765.2	1.945149519	1.20E-05	4.921372199
U1	1.94746128	1.20E-05	4.920357759
ADAMTSL4-AS1	1.947608827	1.88E-08	7.724872143
LINC00525	1.947793295	0.003009312	2.521532835
HIST1H2BH	1.953247008	2.48E-12	11.60498824
PMP2	1.955835208	8.48E-32	31.07149389

Gene	log2(FoldChange)	p_{adj}	$-\log_{10}(p_{adj})$
PLA2G12AP1	1.960046023	0.004111479	2.386001883
AL365181.3	1.963174193	1.43E-25	24.84506995
BIRC3	1.967454586	1.09E-21	20.96360367
SULT6B1	1.968451189	0.000419514	3.377253808
SERTAD1	1.969770933	4.77E-113	112.321703
KRT8P36	1.97104395	0.003398867	2.468665773
AP000553.4	1.971921069	0.003085817	2.51062979
USP18	1.972250281	1.39E-45	44.85751787
GABRR2	1.972754949	0.003316889	2.479269017
PDE2A	1.985228852	6.23E-05	4.205275406
PTGES2-AS1	1.988939577	9.38E-06	5.027774386
C10orf111	1.98928043	0.003830599	2.416733323
BATF2	1.990743297	9.08E-16	15.04210792
HIST1H2BK	1.991365934	4.42E-133	132.3541044
AL360270.2	1.992285	1.29E-10	9.888648914
CMPK2	1.994033747	2.29E-15	14.63927662
TNXB	1.995621209	9.27E-11	10.03276677
CSRNP1	2.007803762	8.14E-134	133.0894007
MFNG	2.007827769	3.86E-06	5.412868646
HIST1H2AK	2.007828874	4.08E-06	5.38977554
TIGD3	2.011958446	3.91E-09	8.408285093
AL139288.1	2.015131308	0.001255543	2.901168285
ITIH3	2.018070028	0.000654268	3.184244207
OVGP1	2.018974343	1.91E-07	6.718995017
PTHLH	2.022457859	1.07E-29	28.97170984
PCSK1N	2.023730993	0.004053193	2.392202712
IGDCC4	2.02501212	5.17E-34	33.28672606
ETV7	2.030042372	4.21E-11	10.37586632
SNORA3B	2.031399716	0.009848686	2.006621713
EID3	2.047529747	0.006728547	2.172078711
BAG3	2.054045294	0	#ZAHL!
KRT80	2.054342684	7.04E-64	63.15251768
AC093525.8	2.057576226	2.72E-08	7.565271085
AL590666.2	2.061688638	7.85E-10	9.104987519
DEDD2	2.061968293	5.30E-117	116.2754692
SNORA14B	2.06201634	0.008546667	2.068203192
DCAF4L1	2.062931652	4.97E-06	5.303555708
CASS4	2.07562413	0.000124843	3.903634987
PTPRN	2.085776196	0.002406817	2.618556866
PRKCH	2.086294719	1.35E-08	7.869357852
IDI2-AS1	2.086563096	7.83E-05	4.106293042
DKK1	2.09022391	2.58E-118	117.5878319
EFCAB12	2.095629767	0.004013913	2.396432079
HIST1H2AI	2.106930336	0.000249161	3.603519788
FAM167A	2.111091507	0.000256055	3.591666866
BBC3	2.112547602	1.11E-69	68.95345526

Gene	log2(FoldChange)	p_{adj}	$-log_{10}(p_{adj})$
LUCAT1	2.113576976	7.03E-17	16.15318961
AC044849.2	2.13037979	5.34E-05	4.27215477
BTG2	2.131379716	4.48E-101	100.3489789
LGALS8-AS1	2.13589799	0.008514828	2.069824133
TNFAIP3	2.136333697	1.74E-84	83.76047689
CDKN1A	2.13663657	0	#ZAHL!
IFI44	2.13856277	5.60E-102	101.2514457
ANKRD1	2.140571525	0.008432176	2.074060348
RGS8	2.140867393	2.53E-07	6.59718717
AC026124.2	2.145199732	0.000289992	3.537613364
ABCA12	2.147211388	1.64E-18	17.78581084
HIST1H2AE	2.149406509	2.12E-06	5.673553149
HIST1H2BD	2.150924069	1.94E-62	61.7132042
HSPA1L	2.151094954	1.12E-26	25.94889275
CD79A	2.153282965	0.000698594	3.155774863
MYH15	2.15854037	8.52E-05	4.0694132
SNORD104	2.161004228	1.30E-16	15.88448259
LINC02078	2.164128097	0.001436384	2.842729478
AC012360.1	2.169618395	0.001452487	2.83788762
EGR4	2.172355705	0.003308943	2.480310774
PTP4A1	2.174242897	0.000342186	3.465738372
HELZ2	2.175408443	8.29E-51	50.08143677
HIST1H1C	2.177273752	1.02E-144	143.9898145
TNFSF9	2.178845168	3.47E-77	76.45971911
AC022154.1	2.182587388	0.008541912	2.068444902
AOX1	2.186270963	7.70E-08	7.113581164
AL390719.1	2.187202625	1.36E-06	5.864957393
DDX58	2.188264131	7.97E-39	38.09828179
HIST2H2BF	2.189289596	1.00E-17	16.99961709
SERPINF2	2.190527342	0.001155572	2.937203102
TSPAN1	2.196481919	3.96E-05	4.402304778
LAMC2	2.197231819	1.28E-07	6.891771122
GAS6-AS1	2.198391064	1.51E-38	37.81975711
GJB3	2.201646232	2.71E-05	4.567665897
LURAP1L	2.214427665	5.09E-23	22.29314643
HIST2H4A	2.215497289	3.14E-08	7.503249097
AC002378.1	2.21923165	0.005489198	2.260491136
AC120024.1	2.222164835	6.79E-05	4.168237681
AC004264.1	2.225616469	6.29E-09	8.201422831
AL390755.1	2.226797782	2.95E-14	13.5305106
BAIAP2L2	2.228814318	0.001348732	2.870074476
AC010999.2	2.232950877	0.004405988	2.355956711
BAAT	2.236700534	0.001471815	2.832146689
GRIP2	2.23694623	0.001106379	2.956096011
PDE6G	2.237657367	0.000544161	3.264272853
CFAP54	2.246694065	0.007595445	2.119446786

Gene	log2(FoldChange)	p_{adj}	$-\log_{10}(p_{adj})$
ZNF296	2.260591127	9.31E-07	6.031211923
RPL4P6	2.265910735	1.04E-05	4.983881715
PTGER1	2.267990815	0.004545834	2.342386468
KCTD14	2.277412782	0.003949855	2.403418811
AC008429.1	2.284288771	4.97E-06	5.303681419
AC046176.1	2.287414711	0.002249503	2.647913349
MMRN2	2.295123563	3.20E-07	6.494242374
GADD45A	2.307985498	2.59E-293	292.5872199
KCNJ2	2.312938589	1.63E-23	22.78674744
IL7R	2.31304548	8.53E-27	26.06927505
MYO15A	2.313091705	0.000869052	3.06095433
STC2	2.317331578	9.80E-109	108.0085844
TKTL1	2.319324096	0.000943132	3.025427715
HLA-V	2.332072348	0.007719419	2.112415383
AC098818.2	2.332811129	0.000265855	3.575355047
PPIEL	2.332857185	3.27E-09	8.48501135
NRARP	2.334607102	0.000357153	3.447145866
AL356356.1	2.338755211	1.47E-05	4.833951974
GRB7	2.347867221	0.003781664	2.422317101
KRT7	2.351121856	2.64E-13	12.57872915
AL118516.1	2.351948783	5.18E-90	89.28574888
ID2	2.361449458	2.09E-136	135.6795449
IL1A	2.363951548	0.000119826	3.921449215
PAPPA	2.377086487	5.65E-57	56.24769795
CXCL3	2.377506753	8.93E-09	8.049326085
ACTA1	2.380235162	1.07E-05	4.96869556
BASP1	2.380260752	0.000799977	3.096922633
MYH16	2.380300402	0.004817177	2.317207357
PPL	2.392167819	6.46E-12	11.18982398
TTN	2.418914771	0.001379112	2.860400371
IFITM1	2.421035185	2.45E-18	17.61008625
AC100800.1	2.421312845	0.000566113	3.247097124
C9orf24	2.423237954	0.004965876	2.304004088
RYR1	2.426813539	0.007832626	2.10609261
BCAS1	2.429694041	1.11E-14	13.95560739
FILIP1	2.430249131	7.66E-07	6.115588218
SLC22A20	2.431579216	0.000230654	3.637039585
C1orf228	2.433649922	9.83E-05	4.007273669
GTF2IRD2P1	2.453922979	0.002525402	2.597669459
MB21D1	2.460838293	0.00558887	2.25267601
RASGRP2	2.461818039	0.00535716	2.271065351
HSPA7	2.467329539	1.74E-05	4.759404453
AL359853.2	2.467795786	2.74E-05	4.562481842
NMRAL2P	2.470039973	1.84E-19	18.73610192
KIAA1324	2.471950252	7.95E-13	12.09962497
SNORA65	2.478755099	0.003266202	2.48595702

Gene	log2(FoldChange)	p_{adj}	$-log_{10}(p_{adj})$
METTL12	2.478872626	7.44E-55	54.12855728
IRF7	2.485451444	4.63E-75	74.33465208
PACRG-AS1	2.487491181	0.007914509	2.101576003
DRC7	2.502228657	0.006959305	2.157434104
GDF15	2.502417407	2.03E-136	135.6930376
SOSTDC1	2.509242293	0.001201686	2.920208913
HIST1H2BF	2.510735857	2.86E-09	8.543022536
AC108134.2	2.513258716	0.009169307	2.037663483
SLC18A1	2.521513166	7.32E-08	7.135277446
AOC3	2.531048277	1.49E-12	11.82740404
AC013400.1	2.532804626	0.000176717	3.752721573
LINC00589	2.559825087	6.36E-13	12.19662263
IFI6	2.56303178	7.04E-53	52.15222047
AC087239.1	2.570800286	1.95E-07	6.710173332
ACTG2	2.5776673	0.003178575	2.497767494
HIST1H3A	2.581956411	0.000268296	3.571385391
HIST1H1B	2.588528885	2.50E-06	5.602688698
CLCF1	2.590951021	2.93E-132	131.5330824
COL20A1	2.603506389	0.00436153	2.360361152
SLC8A2	2.612853135	0.009944415	2.002420752
LINC01021	2.617810243	1.75E-83	82.75738943
TMPRSS9	2.6199271	1.19E-07	6.923408622
TUBA4A	2.623178285	1.99E-66	65.7005794
AL136126.1	2.626047344	0.007271714	2.138363214
AP002364.1	2.627863006	1.84E-06	5.735299029
AC012313.8	2.633552985	0.003896277	2.409350127
AC093635.1	2.63785201	7.39E-05	4.131569771
SNORD14E	2.639691305	2.26E-10	9.646463251
RAB33A	2.639739789	0.00067712	3.169334184
HIST1H2BG	2.660239173	6.85E-28	27.16448505
RPSAP52	2.663222406	4.79E-22	21.31936811
AL109614.1	2.673137309	6.12E-05	4.213241338
MRGPRX4	2.67350443	0.000288572	3.53974648
NECAB2	2.675435132	0.000621789	3.206356965
FAM177B	2.680440156	0.004192391	2.377538247
AL021578.1	2.681813023	4.17E-06	5.379763429
KRT86	2.684817996	0.001894234	2.722566469
PLCH2	2.685123313	0.00821427	2.085431003
AL138828.1	2.690232109	0.00138779	2.85767633
AC107959.2	2.692508699	0.000408724	3.388569741
NEXN-AS1	2.696609649	8.64E-07	6.06359092
SERINC4	2.70476248	3.62E-08	7.441784506
ALOXE3	2.713992096	2.22E-05	4.653739052
OAS1	2.715379197	3.18E-10	9.49729991
ADPRHL1	2.732788509	1.20E-13	12.92048748
GABPB2	2.735018777	0.001682351	2.774083497

Gene	log2(FoldChange)	p_{adj}	$-log_{10}(p_{adj})$
IER5	2.748387489	0	#ZAHL!
EPPK1	2.753572082	0.001384522	2.858700245
PTPRR	2.754315669	0.006557004	2.183294543
MX2	2.761019688	4.27E-06	5.369384672
KRT81	2.763918728	1.11E-09	8.952797232
VASN	2.766311366	7.13E-84	83.14715081
LURAP1L-AS1	2.768568188	0.000136258	3.865639348
EPSTI1	2.776834112	2.28E-33	32.64142382
KRT18P31	2.785242755	0.000626916	3.202790814
XAF1	2.788809893	1.12E-20	19.94965041
IL11	2.791929816	2.63E-211	210.5798351
TCTEX1D4	2.802241977	0.002474618	2.606491865
AC009908.1	2.804091229	0.006822694	2.166044085
HIST1H3H	2.807298051	1.53E-24	23.81546007
LINC00475	2.813364695	3.06E-36	35.51442999
INPP5D	2.817853753	0.0024508	2.610692208
TMEM40	2.84011544	5.80E-06	5.236208199
SOX15	2.843292559	0.007968421	2.098627711
ARL14EPL	2.853689743	2.98E-05	4.526057424
PLEKHA6	2.863508395	3.95E-19	18.40305208
AC007728.2	2.86516172	0.000683894	3.165011179
AC026367.1	2.865531087	0.009352081	2.029091729
PLCXD2	2.866794993	1.52E-28	27.81860682
HIST1H3D	2.8714144	1.83E-09	8.73730508
AF129075.2	2.873876964	8.39E-05	4.076339125
JUP	2.877364847	0.003954883	2.402866367
AC022217.1	2.8777194	0.005132308	2.289687323
DCDC2B	2.878067009	0.005929293	2.226997075
AC090559.1	2.878340585	0.009966509	2.001456944
CATIP	2.88287349	5.02E-11	10.29912768
AC005899.8	2.882965484	0.003645469	2.438246546
AL606760.3	2.902294127	0.00790142	2.102294829
AC005532.1	2.909414293	0.000217708	3.662125635
LSMEM1	2.922361279	3.30E-33	32.48196687
AL021453.1	2.92823173	6.70E-31	30.1742024
POU2F2	2.92962294	5.80E-09	8.236444282
HIST1H1E	2.933292654	4.33E-13	12.3631378
AC116366.1	2.94121479	0.001721562	2.76407731
MIR320A	2.946288501	0.00600212	2.221695341
NCBP2-AS1	2.949587457	2.78E-05	4.555452808
CLDN6	2.950206061	2.58E-08	7.58768105
KIF1A	2.955316091	0.000152346	3.817168937
DLX2	2.960920382	1.45E-113	112.8395627
CXCL8	2.964386038	1.83E-151	150.738286
DLL1	2.976991989	1.86E-06	5.729994138
C5AR1	2.977653509	1.94E-11	10.71174274

Gene	log2(FoldChange)	p_{adj}	$-\log_{10}(p_{adj})$
SLAMF7	2.982654157	2.93E-05	4.533816983
AL031777.1	2.984321574	0.001609302	2.793362524
SERPINE1	2.986139036	1.27E-128	127.8952301
RPS29P16	3.001274656	0.00455349	2.341655577
AC007952.4	3.015583416	0.000796469	3.098831212
AP003419.4	3.017736805	3.36E-07	6.473038999
HIST1H2AH	3.01974617	2.70E-05	4.568112688
CHAC1	3.032272686	1.69E-115	114.7717926
AKR1B10	3.043004031	6.87E-12	11.16322597
BMP7	3.047619175	0.001928459	2.714789641
AC005593.1	3.049695906	3.86E-05	4.413395783
RPLP0P2	3.059108283	0.00109425	2.960883396
HIST2H3D	3.08719439	1.80E-07	6.745751188
PPP1R27	3.088968258	0.001162339	2.934667327
NAT16	3.089037759	2.06E-05	4.687148816
TNNC1	3.099077972	0.001567437	2.804809917
GCM1	3.10646643	0.002213335	2.654952763
AC105233.5	3.116070791	0.003578447	2.44630536
FAM83E	3.121836468	3.02E-10	9.520021585
HIST1H3I	3.123608303	6.17E-05	4.209886815
TRIML2	3.124012797	0.000101659	3.992855921
HIST1H4E	3.139088074	1.65E-21	20.78290108
RN7SL473P	3.144667158	0.007596733	2.119373118
AC015912.3	3.145311821	1.34E-28	27.87339688
AL591846.2	3.168956116	9.48E-09	8.023349184
AC117382.2	3.183469785	3.92E-05	4.406648629
HIST1H4C	3.185452399	7.06E-09	8.151473704
DLGAP1	3.20120457	0.008938334	2.048743407
AC097059.2	3.232291764	0.005005875	2.300519976
PKD1L1	3.237402988	8.84E-34	33.0536291
LINC01468	3.239560609	0.006584581	2.18147183
AC084346.2	3.252123	0.004667833	2.330884726
SOCS1	3.257153927	1.06E-62	61.97414646
S100A14	3.263343886	1.07E-08	7.972130652
ELAVL3	3.30150526	0.001865873	2.729117827
GRM2	3.306165092	0.004307849	2.365739491
AP001160.1	3.306244023	1.36E-08	7.867058937
LCK	3.308906744	0.009734966	2.011665576
RSAD2	3.318820762	2.44E-17	16.61239527
SLC2A9	3.329365029	0.00578163	2.237949724
RHOV	3.331586322	0.000145161	3.83814989
GADD45B	3.33979178	0	#ZAHL!
ITGAM	3.346487737	0.000244206	3.612244265
SBSN	3.362657262	0.000661455	3.179499623
DNAH3	3.371595032	0.000429922	3.366610835
ATF3	3.37361259	0	#ZAHL!

Gene	log2(FoldChange)	p_{adj}	$-log_{10}(p_{adj})$
AC131009.4	3.376636714	0.000933146	3.030050567
HIST1H1D	3.421252472	0.001206897	2.918329811
PTGER3	3.458973297	8.15E-09	8.088899578
HBEGF	3.464411668	0	#ZAHL!
AC013565.3	3.465309824	0.000277788	3.556286269
AC068580.2	3.468393351	0.003402651	2.468182599
AC113410.3	3.46955258	3.17E-06	5.499421273
CACNA1H	3.469725489	0.005907118	2.228624334
AC109326.1	3.47244834	9.96E-34	33.00154034
ISG15	3.502662604	5.73E-47	46.2414895
SNORD3A	3.514726177	1.57E-13	12.80291219
GUCA1B	3.515801022	0.008588365	2.066089518
CYP4F3	3.517854309	0.000954288	3.020320522
NUP210L	3.531587565	0.007273495	2.138256856
ALPL	3.549160591	1.20E-05	4.920368141
IFI27	3.570378286	6.45E-28	27.19029932
HIST1H4J	3.579625656	1.65E-08	7.783442695
LINC01554	3.583160777	0.005628933	2.249573909
IFIT1	3.583337933	5.80E-27	26.23649405
KCNH2	3.585447502	0.00960307	2.017589884
AL731571.1	3.592316568	2.01E-14	13.6958131
NPIPB2	3.595810188	0.003843931	2.415224413
CCDC163	3.601659664	1.53E-05	4.815336347
HIST1H4K	3.607301343	2.37E-07	6.625424761
MAFA	3.628069806	5.08E-17	16.29401821
CD14	3.66770748	1.02E-14	13.99248313
CRACR2B	3.675919667	0.009735573	2.011638488
AC092117.2	3.676640322	0.000888009	3.051582548
PCNPP3	3.69020606	0.000695374	3.157781581
KCNF1	3.712196095	0.002437079	2.613130465
AKR1C7P	3.723070548	0.00505598	2.29619464
AP003680.1	3.735277815	0.005664777	2.246817168
AL121983.1	3.743300088	3.65E-05	4.438018108
GRIN2C	3.758066049	0.008998264	2.045841287
DHRS2	3.779730375	2.31E-23	22.63610849
C1orf162	3.80519838	8.67E-10	9.061956403
FLNC	3.813572467	5.14E-05	4.288908119
HIST1H4D	3.8731084	6.27E-10	9.203039239
AL645608.1	3.900133496	0.007469907	2.126684822
WNT7B	3.904816073	0.007077856	2.150098275
FGF9	3.90590579	0.007341563	2.134211457
PEAR1	3.90754106	0.005811874	2.235683839
KRT3	3.911183231	0.007468055	2.126792488
AC011591.2	3.912444471	0.005674482	2.246073799
RASD1	3.929684131	8.69E-85	84.06092144
ZSCAN10	3.94175526	0.001165355	2.933541814

Gene	log2(FoldChange)	p_{adj}	$-log_{10}(p_{adj})$
HSPA1A	3.949067098	0	#ZAHL!
LTA	3.99282286	0.000378596	3.421824508
TNFRSF9	4.002195318	0.000692156	3.15979621
CNGB1	4.010971163	0.004249193	2.371693513
AC012462.3	4.015259157	0.008985513	2.046457137
PCDH8	4.015843055	0.000269145	3.570013043
LINC01115	4.023960112	0.007585192	2.120033419
AC012557.3	4.032357888	0.00010201	3.991356517
MYO5B	4.040326195	0.001527094	2.816134344
VWA5B2	4.04716681	1.27E-05	4.895963948
RUNX1T1	4.054456292	0.004588483	2.338330873
AL137793.1	4.055476292	0.004588827	2.3382983
SLC1A7	4.055552969	0.004492673	2.347495164
AC012435.1	4.066646067	8.32E-05	4.079763212
SGCG	4.068796479	0.006113778	2.2136903
LINC00880	4.073404565	0.001580133	2.801306492
HIST1H4B	4.084195015	1.30E-05	4.887443955
HCG9	4.096235072	0.007868424	2.104112245
ELF3	4.163478573	0.002453073	2.610289483
GREM1	4.179985395	0.007987162	2.097607484
AL022313.2	4.188826442	0.00324537	2.488735846
AP000695.2	4.191049908	0.006713712	2.173037319
ABCA4	4.192209201	0.004715454	2.326476456
ESM1	4.192875322	0.002997595	2.523227082
IL32	4.20060263	5.24E-06	5.280652525
KCNQ2	4.206817695	0.004909802	2.308936036
CCM2L	4.21419739	0.006747453	2.170860133
OASL	4.222381951	1.72E-20	19.76372137
NECTIN4	4.225560279	5.21E-18	17.28350147
AC095031.1	4.228275379	0.005668333	2.246544616
SLC17A9	4.230657495	0.001901214	2.720969097
DLL4	4.283655505	0.00074261	3.129239486
GALR2	4.289021284	2.89E-21	20.53842492
RN7SL146P	4.298040707	0.009565322	2.019300416
HTATIP2	4.318309262	0.002021343	2.694359882
GCGR	4.319828667	0.002160015	2.665543223
LINC02240	4.325383175	0.008154907	2.088581011
CCL26	4.335597636	0.000154879	3.810007425
AC026803.2	4.33673605	8.50E-13	12.07067906
AC008403.2	4.348412851	0.005517426	2.258263512
AC015936.1	4.352690286	0.007116874	2.147710722
IGFL2-AS1	4.357097265	0.001273769	2.89490916
RNU5D-1	4.365340027	0.003781243	2.422365366
AP005432.2	4.378364819	0.000314788	3.501982224
ARL4AP5	4.380894689	0.008832617	2.053910592
RFPL3S	4.388429311	6.35E-07	6.196915045

Gene	log2(FoldChange)	p_{adj}	$-\log_{10}(p_{adj})$
AC005921.3	4.404984201	0.007143342	2.146098527
OAS2	4.413323166	1.78E-14	13.74952974
SOST	4.416442583	0.001077435	2.967608849
CCNA1	4.422018883	0.001994315	2.700206158
MYL9	4.434738203	0.001385897	2.85826916
CD4	4.437830076	0.007056518	2.151409575
AC093799.2	4.444495433	0.002686257	2.570852372
SSBP3-AS1	4.452049295	0.008770544	2.056973492
SP6	4.453045896	1.49E-05	4.826001553
INSM1	4.503773555	0.004813273	2.317559518
AC092120.3	4.510994415	0.007163321	2.14488559
PYGM	4.528448688	8.55E-28	27.06825922
ZBTB7C	4.541195825	0.000969668	3.013377004
AL513318.1	4.56119703	0.006377129	2.195374824
MTUS2-AS1	4.578380829	0.003034879	2.517858672
C19orf38	4.579058487	0.001396378	2.854997017
ARC	4.598701631	1.18E-184	183.9278551
SLC6A13	4.610236689	0.006022292	2.220238163
TBC1D3B	4.622617179	0.007497743	2.12506945
AEBP1	4.641823344	0.000761078	3.118570977
HSPA1B	4.647944004	0	#ZAHL!
LINC01647	4.666166215	1.11E-05	4.95441475
RND1	4.674838355	6.78E-47	46.16847051
TSSK4	4.681951138	0.009839109	2.007044216
RNU1-2	4.686452632	0.001303493	2.884891442
CNTFR	4.687885857	0.005171702	2.286366522
IFI44L	4.710250209	2.40E-14	13.62054689
ANPEP	4.718933008	0.006889065	2.161839743
PIK3AP1	4.729578524	0.001112894	2.95354634
AADACP1	4.735838719	0.000523319	3.281233292
IDI2	4.758266991	0.001196665	2.922027505
AC104046.1	4.764640905	0.005372666	2.269810147
PECAM1	4.771124003	0.000570534	3.243718725
MIR3190	4.771493414	0.002467184	2.607798389
AC092718.1	4.789815097	0.003549563	2.449825067
TG	4.807647331	0.000918335	3.036998692
AC007106.1	4.824361153	0.001082986	2.965377278
SCRT1	4.833408405	0.002904347	2.536951461
HIST1H4L	4.833753145	0.002415587	2.616977265
AL365436.2	4.85050409	0.000775937	3.110173563
HMCN2	4.858707716	0.000243636	3.613258851
FAM209A	4.864091926	0.000173637	3.760358035
FNDC7	4.873085637	0.00119437	2.922861108
KRT16	4.881884479	0.000452456	3.344424052
FSTL4	4.901021557	0.000211498	3.674694559
IQCA1L	4.907094815	0.001672154	2.776723646

Gene	log2(FoldChange)	p_{adj}	$-log_{10}(p_{adj})$
TNFSF15	4.907334061	0.000318678	3.496648348
AC011481.3	4.909717176	0.003751229	2.425826394
CHMP4BP1	4.955527958	6.97E-07	6.1565748
PLVAP	4.977179472	0.001743913	2.758475089
CALB1	4.984680026	0.000428056	3.368499895
RNU1-1	4.98542623	0.000879903	3.055565142
TCERG1L-AS1	4.989409635	0.000277569	3.556628543
TPO	5.010086197	0.000224817	3.648171689
MYO1A	5.033017814	0.002326612	2.63327596
C9orf152	5.035664041	0.001825002	2.738736685
PCDH19	5.039434658	0.00097661	3.010279041
TRIM29	5.046956631	0.001917579	2.717246812
NEFH	5.050261316	0.001212211	2.916421912
MUC19	5.056080939	0.000161865	3.790847096
AC073263.2	5.066832786	0.001173575	2.930489174
PRKCG	5.089297522	0.000851688	3.069719316
LCN2	5.094900784	0.000139387	3.85577708
AC016700.3	5.124018753	0.00089072	3.050258893
PCK1	5.135594046	0.000269808	3.568944387
RAB25	5.158065379	0.002859375	2.54372887
AC004241.2	5.164361299	0.00065005	3.1870534
MOBP	5.167997727	0.002182634	2.661019111
B3GALT4	5.174966814	0.00011258	3.948540282
RNF225	5.189048797	0.000391445	3.407329314
AC018639.1	5.190328102	0.001509105	2.82128066
CSF3	5.200093127	0.003866679	2.412661933
IL1RL1	5.227097756	2.36E-05	4.626277026
GADD45G	5.245126502	0.000297441	3.526599305
AC004835.1	5.277675698	0.003262314	2.48647421
NPHS1	5.282330734	0.002142514	2.669076309
AC093001.1	5.293845415	0.006254188	2.203829061
KLKP1	5.309894026	0.000807075	3.093085952
MAP7D2	5.314375302	0.000219242	3.659075803
NLRC4	5.328108356	0.001652807	2.781777948
FBLL1	5.328184237	0.000966968	3.014587753
ARHGAP30	5.329492372	5.61E-05	4.251385143
GZMM	5.343498469	0.0002218	3.65403778
LINC00452	5.416930125	0.000172121	3.764166392
BTLA	5.421878137	0.000279161	3.554146015
INHBE	5.434421483	3.67E-05	4.435567893
GAL	5.437729589	0.000274153	3.562007504
KRTAP5-AS1	5.442006143	8.66E-05	4.062325839
HSPA6	5.4429299	0	#ZAHL!
CCDC168	5.470570512	0.000135026	3.8695825
KRT8P11	5.481813234	0.001169837	2.931874781
SORCS2	5.485320272	0.001566373	2.8051049

Gene	log2(FoldChange)	p_adj	-log$_{10}$(p_adj)
GAL3ST1	5.498640031	0.000274682	3.561170402
NPC1L1	5.517124693	2.26E-08	7.646629925
SLC34A2	5.568922012	0.002704638	2.567890866
TRIM72	5.587813715	0.000218474	3.660600893
CCR4	5.668466432	9.27E-05	4.032853497
MMP25	5.675173636	4.43E-09	8.353491334
AC097478.1	5.687846939	0.000132431	3.878010233
RRAD	5.710529357	1.80E-31	30.74422798
BEST2	5.722113754	0.000145673	3.836620239
CRYBA4	5.74676117	0.000381188	3.418860431
AL122018.1	5.766346762	0.001286667	2.890533796
AC090673.2	5.801261423	0.000154043	3.812358908
EREG	5.842779368	3.91E-05	4.407920778
PNLDC1	5.845763343	2.25E-06	5.647226898
LINC01164	5.87243542	2.05E-31	30.68740494
IMPDH1P10	5.883503936	2.54E-05	4.595018801
TRPC7-AS1	5.890785901	0.000202359	3.693876777
MUC5AC	6.053480136	3.34E-08	7.476751649
PIWIL2	6.152189686	6.16E-06	5.210105857
LINC00973	6.186368812	2.67E-06	5.573814769
C6orf222	6.188911259	0.000228866	3.64041904
SNORD3B-1	6.224520554	1.52E-06	5.816809062
FRG2C	6.338295253	1.50E-05	4.824698598
MIR3648-1	6.378797492	0.000110977	3.954765224
DIO3	6.418565128	9.82E-05	4.007759658
ZNF280A	6.50149771	1.41E-05	4.851317194
RFPL4AL1	6.504815627	0.00018054	3.743427376
IGF2-AS	6.565433529	1.08E-06	5.96651033
MAFB	6.614643123	2.64E-07	6.578689944
FRG2B	6.675861233	4.32E-06	5.364469529
KLHDC7B	6.687855362	1.29E-07	6.88959675
AC108134.1	6.792243203	6.25E-07	6.204153826
POU3F1	6.818342874	1.72E-07	6.763326466
AC017104.2	6.822078732	2.31E-06	5.635548449
TNF	6.832145326	1.60E-06	5.795556778
IL24	6.932782223	3.69E-10	9.432981261
AP001189.5	6.984894291	2.47E-07	6.606464385
CHRNA2	7.061993809	4.96E-06	5.304340719
RFPL4A	7.174845206	2.07E-07	6.683773122
CENPV	7.463795045	2.98E-09	8.525266548
XIRP1	8.216179646	5.91E-11	10.22833474

Appendix Table 4: List of significantly differentially expressed genes (DEG) in LNZ308 cells treated with 3.5 μM AZD6738 for 72h

Gene	log2(FoldChange)	p_adj	-log₁₀(p_adj)
BPIFB2	-6.420312736	7.44E-06	5.128206442
ELANE	-5.827326891	3.28E-05	4.484681341
SULT2B1	-5.250210084	0.000112964	3.947059882
PLD5	-5.106713577	0.001089309	2.962848831
AC114803.1	-4.932859093	0.006780839	2.168716584
PHOSPHO1	-4.799358949	2.25E-116	115.6478606
BSPH1	-4.670861552	4.58E-24	23.33870538
SCN1A	-4.641055875	3.18E-12	11.49769066
HOXD4	-4.550610077	0.000809386	3.091844419
AL138962.1	-4.450614339	0.006708658	2.173364362
FP565260.3	-4.424368029	0.004604357	2.336831021
AC004936.1	-4.401918054	3.62E-05	4.441761164
AL157395.1	-4.390536337	0.006261967	2.203289227
BCAS1	-4.345004522	2.20E-82	81.65805647
AC093609.1	-4.309655658	0.007539474	2.122658947
CABP5	-4.251971638	6.95E-121	120.1582219
AC026469.1	-4.234198179	0.009906217	2.004092179
PCP4L1	-4.205127086	0	0
MPZ	-4.155842069	0	0
CLDN22	-4.033411559	6.73E-67	66.17217638
SEMA5B	-3.944525705	2.59E-16	15.58739631
BBOX1-AS1	-3.844587962	0.009667249	2.014697088
ERMN	-3.81202032	0.001793184	2.746375138
MMP28	-3.779472875	8.04E-36	35.09494167
TMC1	-3.775901789	6.85E-10	9.164533061
STOML3	-3.759042022	3.20E-12	11.49519304
PDZRN4	-3.613810341	4.30E-32	31.3660779
SORCS3	-3.61095473	1.62E-127	126.7899066
PAXX	-3.58206944	7.72E-06	5.11229484
CDH23	-3.540413963	2.34E-18	17.63061916
AC108748.1	-3.513017496	0.000294311	3.531193059
KLHDC7A	-3.429901597	5.52E-25	24.25808527
PTPRD	-3.276795757	7.38E-10	9.131956288
SBSPON	-3.22422586	7.70E-28	27.11353175
PRTN3	-3.197709406	8.89E-05	4.050874062
MME	-3.19477661	0	#ZAHL!
KRT13	-3.179013767	9.94E-05	4.002629432
CEACAM20	-3.173991731	3.95E-14	13.40297188
PLEKHS1	-3.16982689	0	#ZAHL!
TDRD9	-3.127788046	1.98E-79	78.70265655
PPFIA4	-3.127156451	7.96E-128	127.0989375
ESPNP	-3.116919678	6.93E-06	5.159274511
AL359502.1	-3.110699114	2.17E-07	6.663717374

Gene	log2(FoldChange)	p_{adj}	$-\log_{10}(p_{adj})$
MATN2	-3.100817586	0	#ZAHL!
NRIP2	-3.076240149	0.000576502	3.239199391
GLYATL2	-3.073494127	3.32E-06	5.478959232
PDCD1	-3.021181659	1.43E-39	38.84408815
HHIPL2	-2.982172159	5.70E-65	64.24435911
RPRM	-2.980451034	0	#ZAHL!
LINC00639	-2.973417685	6.35E-26	25.1973213
NR1I3	-2.968710559	0.001860758	2.730310096
FOXJ1	-2.964973619	2.04E-10	9.690964668
CFAP126	-2.95292187	6.65E-05	4.177326853
KCNN1	-2.949537973	6.34E-13	12.19776367
DLEC1	-2.94648601	3.29E-77	76.48307353
IBSP	-2.943087492	1.99E-86	85.70163825
FABP7	-2.934603693	0.002513935	2.599645929
SMPDL3B	-2.930907033	6.34E-07	6.198123077
WNT4	-2.920905509	3.86E-32	31.41294306
NFASC	-2.92068249	1.11E-91	90.95298986
RTP5	-2.920254796	0.003148717	2.501866382
RGMA	-2.91089397	2.84E-09	8.546972144
FREM1	-2.89712241	0	#ZAHL!
VWA5B2	-2.873538837	0	#ZAHL!
CLCNKA	-2.872659637	1.19E-37	36.92327816
BPIFB4	-2.869550415	6.45E-23	22.19046754
LINC00092	-2.857914391	2.35E-23	22.62840826
ELSPBP1	-2.843938992	0	#ZAHL!
CDH10	-2.836401294	1.39E-63	62.85693777
MOB3B	-2.811155599	2.58E-164	163.5889584
RGS6	-2.805471147	5.05E-23	22.29647265
CFI	-2.803675697	0.000845127	3.073078067
CLIC5	-2.784714684	0	#ZAHL!
AC244502.1	-2.774717111	3.99E-32	31.39948749
AC093620.1	-2.760347696	0.008063552	2.093473598
PRELP	-2.750838156	0.001137684	2.943978256
ERP27	-2.745784818	1.83E-11	10.73703461
TRDC	-2.745414613	8.09E-16	15.09206709
ABCA12	-2.71947056	0.000459987	3.337253999
AC079466.1	-2.71528469	9.66E-13	12.01507952
WDR86-AS1	-2.682347113	0.000105629	3.976215777
PTPRN2	-2.662348152	2.11E-151	150.6754287
AC011504.1	-2.635919404	2.54E-20	19.5957921
TLE2	-2.631211631	5.81E-96	95.23586256
FGD3	-2.627231775	4.26E-06	5.370784297
CER1	-2.622876458	4.66E-05	4.332008701
ZNF536	-2.612216889	1.52E-275	274.8186049
TF	-2.608474481	1.16E-46	45.9358787
ENPP2	-2.601590226	0	#ZAHL!

Gene	log2(FoldChange)	p_{adj}	$-\log_{10}(p_{adj})$
SOX2-OT	-2.598549203	5.39E-258	257.2684663
RGS9	-2.594739565	1.11E-167	166.9533834
HMGB1P1	-2.592749271	2.05E-15	14.68880019
TPD52L1	-2.591849114	1.61E-25	24.79188325
IGF1	-2.58487546	2.86E-22	21.54398952
SMAD9	-2.584158545	3.27E-130	129.4853503
MMP23A	-2.570358083	0.005057471	2.296066588
AC068473.3	-2.569370212	3.39E-96	95.47001963
SLC29A4	-2.567783486	0	#ZAHL!
ACADL	-2.567066173	4.81E-60	59.31767658
ADAMTS8	-2.565367898	3.01E-59	58.52084507
AC116345.1	-2.564012635	6.76E-08	7.169930949
TMPRSS5	-2.557491121	3.23E-65	64.49059238
TCAF2	-2.554735738	1.09E-54	53.96134429
AL159166.1	-2.554677526	1.97E-06	5.704554104
PPFIBP2	-2.547495297	1.71E-39	38.76664206
APOD	-2.545473264	3.72E-43	42.42980801
ANOS1	-2.523911517	2.32E-45	44.63490091
AL390778.2	-2.516225346	0.000128758	3.890224749
MYO16	-2.511813015	1.27E-33	32.89681813
LINC00482	-2.51082708	0.00059767	3.223538444
SOWAHA	-2.499828411	2.05E-07	6.689136542
PRKCB	-2.489904026	0	#ZAHL!
MEPE	-2.483243174	6.30E-12	11.20035193
ALPL	-2.477990701	0	#ZAHL!
LCNL1	-2.4765901	1.21E-05	4.91893968
TFF2	-2.466654936	1.77E-07	6.751637498
CA9	-2.463262532	7.45E-35	34.12786671
AC093642.1	-2.455674669	1.22E-14	13.91187302
C2orf70	-2.450336716	0.001252208	2.902323659
TPO	-2.437525848	1.16E-06	5.935952548
TNNC1	-2.43521572	3.33E-179	178.4781508
AC099548.2	-2.420941584	1.32E-11	10.88080678
DLX6	-2.407445102	1.66E-82	81.78073659
CP	-2.389628694	6.64E-120	119.1780373
COL21A1	-2.379691193	1.29E-51	50.89097404
NRG4	-2.379516881	5.88E-05	4.230327855
STK32A	-2.356800901	1.88E-11	10.72526202
NKAIN2	-2.351999815	0.004013096	2.396520444
COL23A1	-2.345352503	2.01E-47	46.6961255
ITGB4	-2.341064448	1.68E-200	199.7744669
AL121759.2	-2.340681218	5.94E-25	24.2262013
ARHGEF6	-2.335943933	1.49E-199	198.8264824
AC092376.2	-2.322538907	9.70E-05	4.01305136
ABLIM1	-2.322345983	0	#ZAHL!
AL133325.2	-2.319477512	0.002995898	2.523472934

Gene	log2(FoldChange)	p_{adj}	$-\log_{10}(p_{adj})$
AC117500.6	-2.318843671	0.002987248	2.524728785
ANGPTL1	-2.316951083	0.00035245	3.452902499
GPC5	-2.315775916	7.63E-05	4.117674389
ALDH1A1	-2.313598615	0.000550886	3.258938345
SOSTDC1	-2.308087641	0	#ZAHL!
TMEM51-AS1	-2.307203183	6.98E-32	31.15611712
STON2	-2.299254348	1.42E-35	34.84753841
PRR15	-2.294382769	1.89E-27	26.72440151
PLEKHB1	-2.292259033	1.36E-19	18.86765119
TAGAP	-2.291635277	2.00E-265	264.6996256
MLC1	-2.283098034	4.49E-41	40.34751229
ST6GALNAC2	-2.281593099	3.70E-71	70.43207999
RALGPS1	-2.267804598	5.73E-42	41.24167476
NEBL	-2.263048163	2.93E-252	251.5326225
NTAN1P3	-2.248758323	0.002925697	2.533770666
GALNT6	-2.243658719	1.59E-51	50.79950632
GALNT13	-2.232871291	0.000638266	3.194998179
STRC	-2.220686586	0.001522097	2.817557689
SLC4A8	-2.218064155	9.16E-99	98.03801903
ABCA2	-2.217868629	0	#ZAHL!
RAPGEF4	-2.214901174	1.61E-19	18.79276136
LIN7A	-2.214857486	3.08E-14	13.51084165
SLC14A2	-2.208167412	0.000202567	3.693431711
APELA	-2.207265851	5.16E-78	77.28702655
ATP13A5	-2.205429886	1.86E-127	126.7296176
AL133304.2	-2.19994717	4.69E-05	4.329056992
DEGS2	-2.196689275	5.51E-23	22.25858742
ZBTB7C	-2.188546208	0	#ZAHL!
ARHGEF37	-2.174256338	3.06E-60	59.51483786
PDCL3P4	-2.167699275	0.007980174	2.097987662
HOXD-AS2	-2.167078023	0.000497317	3.303366483
GPC3	-2.165666378	5.67E-07	6.246666745
SLC7A10	-2.162615969	0.002915371	2.535306206
PALMD	-2.157944393	0.001377614	2.86087242
SP7	-2.157078394	1.61E-14	13.79331173
SPON1	-2.150814409	1.41E-06	5.850130675
WDR86	-2.150680625	1.16E-26	25.93691056
AC078883.1	-2.146213572	9.55E-21	20.01987028
DUSP5P1	-2.141980198	2.20E-08	7.657193045
AC048382.5	-2.123122698	0.000427375	3.369191018
AP001062.1	-2.112049807	1.02E-44	43.99234618
SELL	-2.10766383	1.70E-14	13.76933233
AL513534.1	-2.103886113	5.39E-11	10.26850521
PCDHGB6	-2.102454867	3.73E-09	8.428634245
AL355803.1	-2.099225029	1.47E-65	64.83165816
PTGDS	-2.086291687	6.65E-05	4.177297242

Gene	log2(FoldChange)	p_{adj}	$-log_{10}(p_{adj})$
PIGZ	-2.083572962	0.000866286	3.06233858
RANBP3L	-2.077762322	4.62E-05	4.335218967
GPM6B	-2.077601741	7.19E-159	158.1430574
LCTL	-2.056529104	3.34E-22	21.47635486
GLTP	-2.055822021	0	#ZAHL!
DLX5	-2.05420906	7.01E-189	188.1543325
ACAN	-2.053717425	2.90E-19	18.53722831
C3orf33	-2.047610152	1.65E-05	4.782928277
VSX1	-2.047369476	3.73E-07	6.428594253
GPR160	-2.047056532	5.13E-13	12.29015017
FAM162A	-2.046413843	1.60E-169	168.7964456
TYRP1	-2.042632808	1.16E-24	23.93396579
LINC00303	-2.037822897	0.000199445	3.700176552
MIR210HG	-2.034106462	6.04E-58	57.2191849
DOK5	-2.033734297	4.03E-07	6.394873267
AC068896.1	-2.029650915	1.22E-05	4.912873247
DPEP1	-2.024931479	2.84E-62	61.54728948
TMCC3	-2.022915127	4.03E-37	36.39420325
NOXA1	-2.0129142	6.30E-10	9.200347641
FER1L6	-2.004284704	4.05E-15	14.39221712
AL157932.1	-2.002018443	0.003440073	2.463432388
RASGRP2	-1.999535836	1.50E-246	245.8238886
AC116351.1	-1.998798459	1.02E-13	12.99351488
SCN9A	-1.99820961	7.23E-128	127.1409529
PPP1R3G	-1.998048635	5.91E-11	10.22870024
MYH7B	-1.994246914	8.69E-07	6.060980865
SLC9A9	-1.992438263	3.76E-30	29.42468587
PDK1	-1.99061977	1.86E-192	191.7312191
AC007255.1	-1.975550572	2.19E-05	4.658968876
ZNF395	-1.959501599	1.24E-136	135.906506
KRT86	-1.952323	5.83E-151	150.234334
AC012501.2	-1.948710556	9.72E-05	4.012464646
ACKR3	-1.940135146	0	#ZAHL!
SLC27A6	-1.937628309	1.16E-60	59.93648848
SELENBP1	-1.934127875	3.11E-12	11.50698202
AL772337.1	-1.933462817	2.30E-10	9.637915754
SLC25A10	-1.931993107	3.26E-71	70.48644643
LINC02466	-1.928517375	9.76E-06	5.010683629
OLFM1	-1.92828355	7.87E-226	225.103928
FBN2	-1.928206193	1.70E-251	250.7689905
C1QTNF1-AS1	-1.925494678	1.42E-05	4.846974789
TCAF2P1	-1.925425233	0.000549959	3.259669848
IGSF3	-1.919413385	0	#ZAHL!
PGM1	-1.911186955	0	#ZAHL!
MMP11	-1.909462413	0	#ZAHL!
TMEM26	-1.908405983	0.000383296	3.416466167

Gene	log2(FoldChange)	p_{adj}	$-log_{10}(p_{adj})$
AL391834.2	-1.901906043	0.001605572	2.79437029
CIB2	-1.898634522	3.65E-46	45.43720759
EGLN1	-1.892759588	2.64E-110	109.5780722
MEF2C	-1.891307229	0	#ZAHL!
TLL1	-1.889553047	1.25E-09	8.90230565
AL035681.1	-1.886758148	7.67E-17	16.11502075
DYNC1I1	-1.884246335	3.02E-195	194.5193898
TSPAN7	-1.880383353	1.23E-48	47.90921293
HOXD8	-1.879975596	0.000125022	3.903012856
TFCP2L1	-1.878875168	5.36E-71	70.27094971
DLX6-AS1	-1.878176685	3.27E-20	19.48598818
GRIA1	-1.872070468	4.71E-06	5.326990622
DNAAF3	-1.870047469	0.005883563	2.230359564
ACSL6	-1.863450612	0.003733351	2.427901182
LINC00957	-1.858410874	3.36E-07	6.4738416
ACSS2	-1.852516626	0	#ZAHL!
HMCN2	-1.851557175	8.01E-69	68.09629396
AC078883.3	-1.844578764	0.000604905	3.218313111
MUC1	-1.83764547	1.04E-64	63.98325744
RAB40B	-1.83036815	4.17E-30	29.37935356
TNFRSF18	-1.830304631	0.000722738	3.141019311
GPR146	-1.827154331	3.61E-36	35.44281223
HDAC4	-1.820693006	1.52E-261	260.8187389
NLGN4X	-1.819486345	6.45E-211	210.1902412
ENPP5	-1.8184916	1.01E-11	10.99568743
MYCL	-1.817254164	3.73E-50	49.42849866
LINC00662	-1.815960071	3.58E-260	259.4465645
PTCSC2	-1.815346872	1.14E-07	6.942783995
KIAA0040	-1.81152575	2.01E-179	178.6978653
DTWD2	-1.801923264	7.60E-39	38.11936075
AC007405.3	-1.800110239	0.002229935	2.65170785
DCN	-1.798492907	3.33E-16	15.47812055
VWF	-1.798267889	3.35E-28	27.47489149
AL160276.1	-1.798187865	1.49E-25	24.82768219
FGL1	-1.792091986	0.008438365	2.07374167
CHRFAM7A	-1.787779249	4.37E-07	6.359214559
CEP112	-1.78707356	9.92E-41	40.00335324
DNAH11	-1.777989823	1.22E-17	16.91269374
FOXE1	-1.775066358	1.17E-197	196.9310878
APOL4	-1.774140544	1.41E-08	7.849907923
NLGN1	-1.769730782	1.27E-05	4.895508094
PRAMEF20	-1.769415106	0.000213766	3.670060706
MAP6D1	-1.767462845	3.36E-07	6.47428018
LPAR3	-1.762994474	0.006523685	2.185507003
CAPS2	-1.762016329	3.73E-07	6.428241174
CBR3	-1.75941542	2.03E-96	95.69324309

Gene	log2(FoldChange)	p_{adj}	$-log_{10}(p_{adj})$
BNIP3	-1.750664239	1.30E-231	230.8852291
TMEM51	-1.749686701	3.85E-165	164.414286
DDIT4	-1.749072964	1.16E-181	180.9346163
KLF2	-1.748594814	2.51E-44	43.60054241
XPA	-1.746499575	6.59E-99	98.18099388
AC018470.1	-1.738740912	0.00229873	2.638512055
PROC	-1.734366904	1.67E-08	7.776622719
ITIH5	-1.733452469	1.59E-62	61.79977168
LINC01836	-1.731684423	9.19E-142	141.0368725
TMEM191B	-1.726158014	0.006764993	2.169732643
TFF3	-1.724607167	1.19E-76	75.92330151
RNASE4	-1.721488391	0.008560666	2.067492431
LINC01505	-1.720026912	7.84E-40	39.10576302
SLC26A2	-1.719924657	8.84E-224	223.0535519
AL354861.3	-1.715784973	2.37E-23	22.6254878
PKP2	-1.714728023	7.26E-97	96.13933903
PRUNE2	-1.708167131	6.92E-15	14.15976706
PRELID2	-1.707828767	8.27E-13	12.08249495
C19orf71	-1.703995472	6.87E-05	4.162793242
AC008035.1	-1.701865429	0.008413092	2.075044366
AC008708.1	-1.699710963	5.93E-11	10.22665274
MIR99AHG	-1.69788232	0.000599432	3.222260164
ZNF883	-1.695719527	0.000751145	3.124276277
H3F3AP6	-1.695463345	0.007443081	2.128247231
NWD1	-1.695285833	0.003092737	2.509657023
PLCL2	-1.694817328	1.58E-88	87.80053917
PLA2G3	-1.694677758	2.31E-08	7.636067354
SERPINI1	-1.689972894	1.52E-205	204.8179138
AC025183.1	-1.685381152	0.001073035	2.969386143
FGF10	-1.683692884	6.78E-06	5.168484521
WFDC1	-1.680523145	1.99E-23	22.70223054
TRIM16L	-1.676379693	2.50E-88	87.60216189
AC145124.1	-1.672494605	0.002702874	2.568174208
FER1L4	-1.672192933	1.42E-16	15.84866138
PDIA5	-1.67178994	1.48E-169	168.8308893
CEND1	-1.664084571	2.82E-92	91.54972698
ARL10	-1.660670612	1.19E-92	91.92495231
AC064875.1	-1.656664677	1.11E-07	6.954516584
ZSCAN31	-1.652600899	3.16E-68	67.50047567
C1QTNF1	-1.648051744	2.78E-76	75.55518845
AC091563.1	-1.646138404	7.00E-05	4.154994306
SEMA3G	-1.636767493	4.00E-22	21.3976659
AC244021.1	-1.624893864	4.82E-23	22.31683543
NRN1	-1.622663703	4.13E-111	110.3838809
LKAAEAR1	-1.620537317	0.000291894	3.53477418
BMP3	-1.619725397	0.000414448	3.38253046

Gene	log2(FoldChange)	p_{adj}	$-log_{10}(p_{adj})$
LRRC75B	-1.618125313	2.86E-08	7.543110588
LINC02211	-1.615503037	0.007731633	2.111728761
ZNF488	-1.614878811	3.70E-30	29.43175379
PHACTR3	-1.612355082	1.20E-06	5.921888735
METTL7A	-1.607105939	7.01E-41	40.15423431
NKX2-8	-1.606464091	1.85E-15	14.7323613
PCDHGA3	-1.606287661	1.26E-06	5.898165915
TMEM150C	-1.604040732	2.72E-27	26.56534805
ATP8A2	-1.601061529	0.002491754	2.603494901
HRASLS	-1.598951758	7.22E-43	42.14132819
AP003068.3	-1.598493289	3.24E-05	4.489438721
AC079414.3	-1.594205566	0.004610685	2.33623454
PIK3CD-AS2	-1.593688692	1.20E-16	15.91950838
HS6ST1	-1.591917761	4.47E-271	270.3496023
SLC18B1	-1.589444427	7.23E-33	32.14110402
HS6ST1P1	-1.587196882	0.004048585	2.392696728
SAMD12	-1.587183694	1.13E-25	24.9471215
GFRA1	-1.585997962	0	#ZAHL!
GRHL1	-1.582899109	6.97E-85	84.15696343
CYP39A1	-1.581724619	1.62E-19	18.78986723
LARGE1	-1.575606437	1.18E-198	197.9294727
ABCA7	-1.571912577	4.92E-61	60.30834828
SNTG2	-1.569791368	1.76E-28	27.75395272
AC104692.1	-1.567193885	0.000137892	3.860459786
SH3PXD2A	-1.566359557	2.01E-66	65.69674848
GSTM4	-1.565456569	7.19E-128	127.1433294
LRRC10B	-1.560586823	2.03E-06	5.692814352
RAB33A	-1.558467762	4.01E-22	21.39725232
FAT3	-1.555523144	7.32E-08	7.135576656
NPY4R	-1.553995093	0.009131218	2.039471304
RCAN2	-1.55170666	3.29E-35	34.48221302
AC127502.1	-1.549653039	2.16E-05	4.665851607
WWOX	-1.548278545	3.73E-32	31.42841443
MAP2K6	-1.547913499	1.31E-64	63.88414896
TIAM1	-1.547181715	0	#ZAHL!
C16orf54	-1.546313812	4.25E-19	18.37180757
TM7SF2	-1.544609115	9.01E-71	70.04529074
CNFN	-1.542019444	0.000353825	3.45121201
ERC2	-1.541270477	3.20E-11	10.49529323
AC136475.2	-1.539179323	0.001726521	2.762828167
PROS1	-1.534876289	7.70E-184	183.1134093
FOXP2	-1.534411581	7.08E-47	46.14971698
DCLK1	-1.528080747	1.06E-45	44.97572904
GLDC	-1.527290351	8.54E-10	9.068315354
SLC25A20	-1.524659284	7.00E-72	71.15471657
AC005520.2	-1.523966911	1.51E-06	5.820621338

Gene	log2(FoldChange)	p_{adj}	$-\log_{10}(p_{adj})$
ADGRV1	-1.50905327	8.23E-121	120.084509
SLC29A2	-1.505752144	1.42E-41	40.8463443
PCDHB4	-1.504040103	0.000666362	3.176289534
HCN3	-1.503664952	1.53E-58	57.8144324
CCDC69	-1.497998514	8.09E-05	4.091851185
TCEA2	-1.495752231	2.44E-131	130.6117225
RASSF7	-1.493842642	5.42E-62	61.26631293
MINDY1	-1.493141033	3.77E-135	134.4237423
MGST2	-1.491434533	1.87E-27	26.72829649
TFAP2A-AS1	-1.490872077	3.77E-10	9.423263565
SLC40A1	-1.489012897	3.31E-16	15.48045056
HCK	-1.488502383	2.02E-09	8.695651328
FBXO44	-1.480647977	2.66E-17	16.57592138
DLEU2L	-1.480255543	0.002433405	2.613785526
TBC1D1	-1.478326344	2.66E-285	284.5747899
RNF144B	-1.474744159	2.95E-08	7.530089376
AC135983.2	-1.473337279	7.54E-08	7.122748481
SRRM3	-1.47302445	5.73E-120	119.2418671
ARHGAP9	-1.472001278	4.09E-147	146.3887851
FLJ22447	-1.471721716	5.22E-15	14.28268988
B3GALT4	-1.471075097	7.11E-05	4.148422272
TSPAN32	-1.470117921	6.92E-06	5.160082087
KIAA1614	-1.468779121	2.90E-28	27.53710113
LAMA4	-1.468488477	1.97E-65	64.70520257
F11R	-1.460038859	4.63E-22	21.33426556
MAPK10	-1.459489291	2.67E-109	108.5732949
AMOT	-1.458280984	2.19E-180	179.6598953
AC005944.1	-1.457248171	0.007425043	2.129301039
IL7	-1.456348229	7.67E-09	8.115268896
SIMC1	-1.454249515	0.002362733	2.626585271
BAALC	-1.453358697	1.98E-06	5.703605868
Sep 01	-1.450781764	2.63E-12	11.57984672
ASS1	-1.450458877	8.71E-34	33.06012408
AC078942.1	-1.448351958	2.47E-15	14.60729077
FNDC1	-1.447897934	2.36E-19	18.62724326
A4GALT	-1.445099313	1.70E-193	192.7701938
LYNX1	-1.444116417	3.43E-75	74.46424093
KIAA1324	-1.443653771	8.55E-16	15.06816125
TMEM176A	-1.442398364	2.16E-19	18.66605288
EGLN3	-1.441595382	2.30E-12	11.63734485
ADCY7	-1.43557466	4.43E-151	150.3536367
DPYSL4	-1.43432002	1.47E-39	38.83414539
TSPAN18	-1.433518215	1.20E-90	89.92131231
CATSPER2	-1.433222794	1.46E-07	6.836785546
EDARADD	-1.432488005	0.000397049	3.401155498
DDIT4-AS1	-1.432241722	0.004519523	2.344907359

Gene	log2(FoldChange)	p_{adj}	$-\log_{10}(p_{adj})$
SP9	-1.428107493	2.72E-38	37.56539823
PRKX	-1.425608122	7.77E-120	119.1094885
ADGRB1	-1.423099913	3.21E-71	70.49383498
PDE4A	-1.419468392	1.59E-87	86.79911497
DDN-AS1	-1.416158996	7.33E-16	15.13481793
HMGCS1	-1.415150443	1.68E-218	217.77511
AL356235.1	-1.411739773	0.009162979	2.037963329
ATP13A4	-1.406564277	3.35E-05	4.4754668
TCN2	-1.404824517	8.61E-18	17.06491264
AC103760.1	-1.403381624	1.86E-05	4.730117772
MAP3K20	-1.402225302	1.08E-263	262.9651007
HHIP-AS1	-1.40221785	1.75E-80	79.7573294
PCDHGA7	-1.401820736	4.38E-05	4.358866413
FAM53B	-1.40032266	5.09E-113	112.2935422
AP005433.1	-1.399171517	0.000255256	3.593024178
PCDHGB3	-1.398169163	1.15E-06	5.940498784
HFE	-1.395598327	1.66E-59	58.77972172
IL18R1	-1.394610833	0.003321814	2.478624743
CPXM2	-1.394137199	3.23E-24	23.49044651
GPRC5C	-1.393845898	1.37E-189	188.8632147
ERG	-1.389492021	4.68E-57	56.32939659
ZNF385B	-1.389364863	0.000103075	3.986846902
RCAN3	-1.387084083	1.56E-96	95.8074369
PFKL	-1.386173841	2.99E-185	184.5249787
AC068631.3	-1.385655107	0.00495819	2.304676794
HIP1R	-1.383059897	1.35E-158	157.8683812
KIAA1456	-1.382871791	0.001534489	2.814036143
COLEC12	-1.381065263	0	#ZAHL!
MFSD6	-1.381044031	3.80E-240	239.4198575
PCDHGA5	-1.374696927	1.19E-05	4.924868706
LDHA	-1.3740725	1.93E-207	206.7137454
EP300-AS1	-1.374049599	5.42E-08	7.266371758
DHRS13	-1.371777197	1.26E-28	27.89951308
GOLGA8H	-1.370611294	0.000323555	3.490051748
PDE6A	-1.370448212	2.78E-06	5.556329953
ARHGEF10L	-1.369874257	0.003811784	2.418871694
STAP2	-1.368399247	8.60E-05	4.065638468
MAP4K2	-1.368027874	4.24E-197	196.3724468
C9	-1.367812153	3.75E-09	8.425937577
BOK	-1.364973236	2.72E-197	196.5653491
AC061992.1	-1.363119432	3.53E-05	4.452291297
CHRM3	-1.362507971	1.80E-09	8.744558954
PTCH1	-1.360844595	3.05E-241	240.5154666
AIF1L	-1.360577912	2.99E-09	8.523629833
LRP1B	-1.35835028	4.43E-28	27.35320325
PCDHGA4	-1.356694546	3.54E-18	17.45144779

Gene	log2(FoldChange)	p_{adj}	$-log_{10}(p_{adj})$
APLP1	-1.355667596	4.02E-113	112.3958429
CFD	-1.355649897	5.75E-23	22.24062924
AP003068.4	-1.352585625	7.10E-05	4.148460099
CCDC184	-1.350920505	1.05E-25	24.97925604
MRAS	-1.350822742	6.31E-261	260.2000782
CEBPA	-1.348706187	9.35E-95	94.02925919
PATJ	-1.348596258	1.40E-38	37.85510353
SOX18	-1.344996331	1.47E-31	30.83123055
NIPAL3	-1.344784509	6.88E-108	107.162418
NOTUM	-1.344364911	3.72E-57	56.42968571
AC067930.4	-1.341954001	0.002398761	2.620012971
VAV3	-1.341414118	1.12E-98	97.95089264
AGAP2-AS1	-1.34038436	1.98E-239	238.7031376
KAT2B	-1.337414416	1.41E-77	76.84971216
NKD2	-1.332707349	7.60E-45	44.11922643
RUNX3	-1.328439537	0	#ZAHL!
PIR	-1.327779726	3.83E-95	94.41635154
FGFBP2	-1.326800411	5.90E-06	5.22886113
ASAP3	-1.324977193	1.54E-130	129.8124963
NDUFA4L2	-1.32488556	3.19E-10	9.495555556
COMTD1	-1.322476696	1.41E-38	37.85109792
ANG	-1.322317105	7.39E-25	24.13158553
LHPP	-1.321668696	3.43E-42	41.46464672
SLC37A1	-1.320550962	0.00038298	3.416824064
PLCD1	-1.317215852	1.11E-59	58.95374572
TMEM176B	-1.316042029	1.11E-21	20.95305726
GTF2IP4	-1.315607807	5.21E-115	114.2828555
AC015802.6	-1.315507546	9.64E-08	7.015814511
ADAMTS15	-1.314409372	6.35E-37	36.19737338
F13A1	-1.313926934	1.06E-20	19.97385675
CASP5	-1.312291524	0.004823735	2.316616578
ISPD	-1.311366829	9.15E-13	12.03875861
PSPHP1	-1.311149385	1.55E-56	55.81080761
PLCB4	-1.310286877	1.13E-10	9.948175696
GSN	-1.307723364	4.85E-204	203.3144074
TLE6	-1.301659495	1.34E-05	4.8740641
THBS4	-1.301494543	1.32E-05	4.879193802
AC106795.1	-1.30046337	9.74E-42	41.01137506
ACADSB	-1.298576227	8.43E-48	47.07419563
RN7SL689P	-1.29815604	0.003223231	2.491708515
PLEKHA2	-1.297662954	5.15E-90	89.28819567
RAB37	-1.294943616	1.22E-43	42.91395202
CARMIL1	-1.294525656	3.82E-65	64.41811617
S100A4	-1.293619266	1.79E-28	27.74834046
SCUBE3	-1.293444527	0	#ZAHL!
NT5M	-1.292848793	3.09E-18	17.51016662

Gene	log2(FoldChange)	p_{adj}	$-\log_{10}(p_{adj})$
ATP1A2	-1.291663466	7.40E-08	7.130951345
PLCE1	-1.291295408	3.72E-46	45.42925694
TNFSF12	-1.290330978	1.35E-09	8.870769731
KRT4	-1.289057022	0.00156206	2.806302211
CTDSPL	-1.286607665	4.57E-242	241.3399894
TLR3	-1.285239735	2.73E-34	33.56430961
ITGA8	-1.284166774	2.09E-87	86.68025595
C1RL	-1.283005782	1.98E-83	82.70325318
HYKK	-1.282370214	0.000147234	3.83199173
MAMDC4	-1.282263279	9.68E-16	15.01415958
SERGEF	-1.28211247	6.35E-31	30.19701483
LSS	-1.280972718	7.52E-209	208.1237714
PKDCC	-1.280886333	1.08E-92	91.96820147
ALKAL1	-1.279508625	3.84E-11	10.41591852
KRT3	-1.278659229	4.55E-07	6.3416416
C11orf96	-1.27725099	3.18E-43	42.49709691
PDLIM3	-1.276946954	5.42E-100	99.26589683
CD163	-1.275628194	0.000105371	3.977279648
PRR18	-1.273258821	8.17E-46	45.08765975
WDR31	-1.271875	0.000229502	3.63921318
SLC12A7	-1.271147298	6.08E-139	138.2157413
ZBED3	-1.27094515	1.12E-63	62.95053687
HUNK	-1.266947309	1.15E-162	161.9388798
NCAM1	-1.266851095	1.57E-264	263.804571
BACE1-AS	-1.266644385	2.51E-22	21.60008619
NTN1	-1.265978267	9.08E-128	127.0420792
CDKN2AIP	-1.262821751	3.36E-188	187.4733723
TCEA1P2	-1.262408703	0.001210678	2.916971334
GIPR	-1.260042586	8.35E-21	20.07812816
CXCL16	-1.259864367	5.38E-37	36.26917551
C4orf33	-1.25828599	9.68E-27	26.01394281
ANKZF1	-1.257172464	6.12E-86	85.21305431
MORN3	-1.257068773	0.004435732	2.353034732
EFNA3	-1.256861755	3.05E-06	5.515533158
TRIM7	-1.25626238	1.04E-41	40.9813004
CORO7	-1.255073635	7.04E-11	10.15224617
FRK	-1.255066752	7.84E-07	6.105787945
IGSF1	-1.254687526	1.61E-29	28.79359202
AC156455.1	-1.254498653	0.001192207	2.923648212
OLFML2B	-1.253713087	1.27E-27	26.89466085
PCSK9	-1.250896674	3.77E-56	55.42330596
AC233266.2	-1.250430152	0.009730679	2.011856849
TOMM40L	-1.249893642	3.81E-82	81.41869326
RGS19	-1.249081616	5.45E-133	132.2639152
CDH5	-1.248962771	1.94E-09	8.71284599
RAB20	-1.247915559	1.41E-15	14.84987742

Gene	log2(FoldChange)	p_{adj}	$-log_{10}(p_{adj})$
MISP3	-1.247629925	6.68E-05	4.175537981
SPG20-AS1	-1.246809522	0.00152826	2.81580279
DDIT4L	-1.245650221	4.77E-17	16.32134502
TP53INP1	-1.243730824	1.80E-117	116.7438392
ADD2	-1.242721225	1.36E-12	11.8677975
ACAT2	-1.241705712	2.43E-262	261.6136391
COL14A1	-1.241491955	3.90E-57	56.4091206
C3orf58	-1.240880145	7.33E-106	105.1350208
ARPIN	-1.240451271	7.09E-10	9.149650501
CHRNA7	-1.238500625	0.000182067	3.739769413
HHIP	-1.238198818	3.33E-221	220.4778763
TENM2	-1.238004907	6.02E-176	175.2205035
CHCHD10	-1.235814694	8.60E-72	71.0654172
GPR55	-1.23557546	7.23E-68	67.14065676
SYNPO	-1.234903862	1.82E-161	160.740549
TMEM53	-1.234111179	6.11E-33	32.21429882
MDFI	-1.233613039	1.95E-40	39.71044078
EFHD1	-1.232783872	6.83E-104	103.1656854
ACOT11	-1.231211238	0.003417684	2.46626804
TACC2	-1.230394208	2.43E-32	31.6142593
DAPK1	-1.229917472	4.47E-14	13.34953423
COL9A3	-1.22848141	1.30E-07	6.88683796
PYGL	-1.228286806	1.46E-150	149.836864
AC024230.1	-1.226458129	6.51E-05	4.186226722
GCNT1	-1.225803796	3.29E-17	16.4831008
LMNTD2	-1.225651795	1.83E-06	5.736828393
MBOAT1	-1.223783843	2.13E-48	47.67135484
LINC02506	-1.223335478	1.14E-11	10.94353957
KIZ	-1.222755935	3.87E-61	60.41187736
NID2	-1.221883761	6.70E-133	132.174243
SHROOM1	-1.221418947	9.97E-85	84.00151814
GPR1	-1.22139987	8.17E-50	49.08760721
CA5B	-1.221397425	2.91E-175	174.5356032
NINL	-1.221322958	4.26E-82	81.37038769
GPM6A	-1.220224022	0.007682902	2.114474716
NPAS3	-1.218402421	8.47E-11	10.07189626
CGN	-1.217038042	4.98E-56	55.30282424
PKIA	-1.215987229	0.002824158	2.549111
SLC29A3	-1.215391769	6.67E-15	14.17582829
MCC	-1.21419853	4.73E-124	123.3248759
TPI1P1	-1.213595258	9.65E-07	6.015674725
CEBPA-AS1	-1.213589363	0.00382309	2.417585524
SYT17	-1.210493756	3.06E-05	4.514964516
TMEM94	-1.207356374	5.08E-124	123.2942159
ZNF219	-1.206645595	1.23E-51	50.90837956
RBP1	-1.206251011	4.06E-37	36.39114804

Gene	log2(FoldChange)	p$_{adj}$	-log$_{10}$(p$_{adj}$)
SLC4A11	-1.205740726	2.00E-50	49.69981591
BANK1	-1.204618009	1.77E-05	4.752307751
TESK2	-1.204186277	1.77E-16	15.75140229
TEX22	-1.203885014	1.15E-14	13.9391837
THOC3	-1.203883864	1.28E-39	38.89411814
HS3ST5	-1.203449296	2.78E-27	26.55546085
ARHGAP26	-1.202251406	3.37E-134	133.4719425
CHN2	-1.201517858	1.84E-06	5.73596701
ANGPTL2	-1.20148267	1.38E-26	25.86012592
SAP30	-1.200438505	4.76E-62	61.32221148
LINC00266-1	-1.20018487	1.06E-10	9.975963328
PIPOX	-1.198922128	1.69E-05	4.771914413
TRPV4	-1.198378002	2.64E-53	52.5787879
AC114947.2	-1.197641101	0.004448575	2.351779131
AC008738.5	-1.196983257	0.00293463	2.532446617
TMCC2	-1.195036657	4.29E-43	42.36804703
AC009061.2	-1.191206237	0.0008751	3.057942107
IMPA2	-1.190574444	1.28E-20	19.89441552
AC131392.1	-1.190366683	0.000350953	3.45475148
CHST8	-1.188912925	3.35E-26	25.47512064
INHBE	-1.187343545	1.57E-105	104.8044261
SOX21-AS1	-1.184928814	7.30E-08	7.136896755
LINC01914	-1.184279582	6.67E-11	10.17582579
THRB	-1.184136501	1.19E-35	34.92579475
CRYZ	-1.184090426	7.03E-115	114.1531181
PEX11A	-1.183484622	1.36E-08	7.867405236
PXMP4	-1.183423058	1.70E-23	22.76930211
APOC1	-1.182380145	0.000395569	3.402777758
DLL1	-1.182244825	1.16E-36	35.93614192
PTPRB	-1.179611567	6.81E-121	120.1666155
PGK1	-1.179312943	7.79E-198	197.1084415
LINC01833	-1.178339315	0.005342378	2.272265352
TCHP	-1.177172101	1.37E-88	87.86484103
ZHX2	-1.177080043	3.83E-103	102.4163553
OPRL1	-1.176093175	1.15E-23	22.94001435
SNED1	-1.175944036	2.79E-172	171.5540784
ZDHHC1	-1.175376271	0.00903305	2.044165573
APBA1	-1.175062401	1.55E-92	91.81035155
NUDT18	-1.174727531	1.33E-31	30.87668125
RAC3	-1.174420317	2.09E-20	19.6804607
ZDHHC23	-1.17322573	7.35E-22	21.13386917
AC016708.1	-1.172652018	0.000549627	3.259932135
TMCO4	-1.171136447	6.17E-71	70.20938668
AC126768.2	-1.170794377	1.03E-07	6.988684725
AC008464.1	-1.167651097	4.58E-07	6.338709586
ASB15	-1.167468411	0.007807458	2.107490357

Gene	log2(FoldChange)	p_{adj}	$-\log_{10}(p_{adj})$
C7orf31	-1.166343458	7.22E-19	18.1415996
TRIB2	-1.159251741	2.75E-160	159.5605301
ADGRG6	-1.15898542	1.27E-24	23.89716312
MYOM1	-1.158783395	4.91E-06	5.308932157
AC009005.1	-1.158769643	0.000299513	3.52358431
TMEM17	-1.157916692	1.44E-12	11.84018646
NUDT14	-1.157089961	1.43E-67	66.84487718
RPS10P7	-1.156666423	2.92E-06	5.534039082
PCDHB5	-1.154894128	2.19E-10	9.659546479
C14orf159	-1.154808176	2.92E-32	31.53468748
SLC25A35	-1.152913193	3.97E-22	21.40110549
GTF2IP1	-1.151359051	1.98E-29	28.70310746
PARD6A	-1.149140783	0.001392033	2.85635037
EPB41L4A	-1.146925331	5.71E-05	4.243326445
PRADC1	-1.146800064	1.32E-35	34.87935275
IKZF2	-1.144825173	5.51E-07	6.25876191
MAB21L1	-1.144076964	0.000496129	3.304405812
NAGS	-1.143735267	1.55E-06	5.809895097
AL357054.2	-1.142832343	0.000708222	3.1498303
NDFIP1	-1.142659067	1.74E-108	107.7591968
CDK3	-1.142636999	0.009772302	2.01000314
TNN	-1.141729949	0.005382598	2.269008031
SMPD1	-1.141633141	3.70E-178	177.4322184
CD24	-1.141076253	1.23E-174	173.9097759
DMTN	-1.140824324	7.93E-05	4.100891234
FYB1	-1.140250266	5.48E-175	174.2611962
HMX1	-1.138242935	1.65E-69	68.78242453
AL162431.2	-1.135847506	8.42E-05	4.074904881
IDH1	-1.135451492	4.17E-247	246.379702
PARD6G	-1.133920067	2.08E-41	40.68197999
NKX6-2	-1.133899917	1.14E-19	18.9443722
PRICKLE1	-1.133282257	2.29E-23	22.64060397
DOCK11	-1.131832315	1.45E-132	131.8399182
RAB26	-1.131112286	1.06E-10	9.974744889
AC073323.1	-1.131039841	7.63E-93	92.11763653
ECH1	-1.13075083	5.45E-91	90.26386135
PLCH1	-1.130224819	1.22E-14	13.9151735
PLXNC1	-1.129978134	6.23E-17	16.20581361
TIPARP	-1.128181832	1.46E-138	137.8360174
AL365295.1	-1.12709124	0.000513086	3.289810217
TRIM6	-1.124677347	0.000179042	3.747046123
JAKMIP2	-1.123925482	6.94E-83	82.15868426
SPAG4	-1.123483797	1.80E-07	6.745165511
NOD1	-1.121900388	4.31E-22	21.36555163
CRACR2A	-1.12063593	0.000512121	3.290627247
GYG2	-1.120000378	5.81E-13	12.23597324

Gene	log2(FoldChange)	p_{adj}	$-\log_{10}(p_{adj})$
LGR4	-1.119816543	7.19E-150	149.1432433
ZNF436	-1.119780055	2.13E-156	155.6721815
FAM228B	-1.118423032	2.90E-10	9.537434185
KDM4B	-1.116773496	2.16E-82	81.66538262
PTPRU	-1.11545104	3.81E-31	30.41898018
CXCL14	-1.114632459	0.00199908	2.699169894
HNRNPLP2	-1.114545786	0.002478746	2.605767946
NFATC1	-1.11254722	1.87E-93	92.72794419
AC127502.2	-1.112505969	2.85E-05	4.544534843
AL645608.1	-1.112098777	8.09E-09	8.092213435
SPATA24	-1.111580319	8.76E-06	5.057427036
LINC00237	-1.10893938	0.002184856	2.66057723
CPE	-1.108501858	4.25E-46	45.3712395
ACADS	-1.107769053	8.73E-17	16.05917465
RASSF4	-1.105759372	2.94E-78	77.5316294
PARD3B	-1.104835682	7.07E-25	24.15050997
PDK3	-1.104283614	7.02E-39	38.15360466
DARS-AS1	-1.103383066	5.46E-06	5.262694323
NMRK1	-1.101611344	4.07E-17	16.39054791
CPED1	-1.099549826	1.27E-91	90.89620941
SECTM1	-1.099147333	2.78E-06	5.556145371
NEO1	-1.098620633	7.73E-150	149.1119484
ASXL3	-1.097012222	3.15E-29	28.50232928
LRBA	-1.095415734	6.13E-69	68.2127183
RNF122	-1.094866956	3.72E-06	5.429684696
ELOVL6	-1.094064976	8.81E-68	67.05523751
FAM3A	-1.093674262	3.75E-70	69.42548392
JAZF1	-1.093570366	2.49E-60	59.60367798
AK4	-1.092114796	0.000770039	3.113487135
ASRGL1	-1.091986838	2.44E-29	28.61342559
IFI27L2	-1.090526775	3.83E-15	14.41687542
HMGN5	-1.089733071	1.64E-13	12.78496302
LNPK	-1.087787347	3.27E-83	82.48579492
NUPR1	-1.087207538	6.62E-50	49.17885656
GSE1	-1.086021092	3.74E-88	87.42702834
TMEM100	-1.084967158	6.65E-17	16.17701442
FARP1	-1.084639637	5.55E-147	146.256091
PCBP4	-1.083354925	1.09E-109	108.9625441
ALDH2	-1.083241911	8.03E-62	61.09511223
CNGB1	-1.081699025	0.001533636	2.81427773
ISOC2	-1.081350007	8.76E-91	90.05728481
MROH8	-1.080938927	0.001032344	2.986175576
HOXA13	-1.079078106	0.000409242	3.388019625
SLC44A3	-1.078954133	5.90E-05	4.229131904
VLDLR	-1.078516151	3.81E-46	45.41945482
LAMP3	-1.078379994	2.32E-14	13.63495231

Gene	log2(FoldChange)	p_{adj}	$-log_{10}(p_{adj})$
ZFHX4-AS1	-1.077788463	4.44E-09	8.352588903
FAM229B	-1.076734331	4.72E-15	14.32641309
GABRA3	-1.073682933	8.83E-09	8.054049814
AC000403.1	-1.072872853	0.008626787	2.064150911
MSRA	-1.072600239	2.09E-40	39.67884975
GATS	-1.071254659	2.52E-25	24.59857679
PPIP5K1	-1.070356971	3.85E-42	41.41445317
PPP1R13B	-1.070319726	4.96E-70	69.30416566
ACBD4	-1.070162334	2.26E-06	5.646178036
MARCH2	-1.069883078	2.70E-28	27.56880582
TGFA	-1.06818661	1.41E-67	66.85092849
OXTR	-1.067121644	5.65E-40	39.24810371
TPI1	-1.066678832	1.30E-177	176.887319
RAI14	-1.065387493	1.08E-168	167.965286
IL11RA	-1.065203327	2.99E-06	5.524864173
PSAT1	-1.064244143	3.54E-138	137.451042
AC098934.1	-1.0640472	0.007243301	2.140063481
CLGN	-1.061557234	5.46E-35	34.26309421
PLCB2	-1.060820213	2.79E-09	8.55413311
GALNT11	-1.058483164	1.41E-149	148.84941
LIMCH1	-1.058204861	2.42E-205	204.616396
CPZ	-1.057674474	1.01E-28	27.9972222
AL355916.1	-1.056315511	0.009441576	2.024955487
RBMS3	-1.055979007	3.45E-36	35.46209237
KCNAB1	-1.055704096	0.001057543	2.9757021
EXD3	-1.055655981	4.19E-27	26.37820623
AL138900.3	-1.054743132	4.15E-16	15.38230859
PCDHGA2	-1.05429746	1.52E-06	5.817925781
STX8	-1.053839962	2.76E-31	30.55913228
PLEKHA7	-1.052423764	3.35E-75	74.47534091
MPC1	-1.051611138	2.12E-118	117.6726481
CHRNB1	-1.050932392	9.08E-10	9.042046128
SESN3	-1.048346663	3.85E-53	52.41509824
AC097534.2	-1.047933782	3.70E-07	6.432047476
CRACR2B	-1.047073469	2.83E-07	6.547917499
PPP1R16B	-1.04684684	4.33E-08	7.363164327
RGS7BP	-1.046092628	4.16E-14	13.38070461
CCNG1	-1.04418456	3.99E-57	56.39911332
RCOR2	-1.043809147	1.18E-17	16.92852094
SOCS1	-1.043542445	1.62E-45	44.78963519
RGS14	-1.043472347	6.16E-16	15.21070776
GMDS-AS1	-1.043069403	2.28E-05	4.641422208
GMDS	-1.042665815	8.11E-40	39.09102651
AGXT	-1.040451394	3.30E-07	6.481801793
ANK2	-1.039862018	5.21E-11	10.28344227
SETBP1	-1.039739563	2.66E-84	83.5752605

Gene	log2(FoldChange)	p_{adj}	$-\log_{10}(p_{adj})$
USP43	-1.038997639	8.45E-08	7.072895191
PCDHA10	-1.038652733	5.55E-12	11.25541485
AC021106.1	-1.037401584	0.000637748	3.19535117
COL11A1	-1.036973285	2.90E-202	201.5381202
NNMT	-1.036748992	1.68E-48	47.77401601
TARID	-1.036714807	1.23E-05	4.910986824
DOK6	-1.036333791	2.34E-39	38.63024303
NBPF2P	-1.036015279	2.16E-05	4.664748806
EFEMP1	-1.035397639	2.58E-116	115.5886697
IRAK1BP1	-1.035229837	7.46E-11	10.12723454
GPR155	-1.03519359	1.51E-38	37.82226896
MYT1	-1.033036394	5.84E-05	4.233265263
GPR63	-1.032045055	9.64E-13	12.01595115
BDH2	-1.031813525	5.07E-32	31.2952493
CACFD1	-1.031248543	1.93E-23	22.71420385
TMEM106C	-1.030806006	1.56E-90	89.80704958
ARMCX4	-1.027642792	1.28E-70	69.89394836
CFH	-1.027043955	4.67E-49	48.33038926
KIAA1671	-1.02570689	1.34E-08	7.874027969
C10orf10	-1.025658532	1.88E-52	51.72545069
DIS3L	-1.025475515	3.47E-37	36.45947968
INSIG2	-1.024944226	7.47E-63	62.12649023
APBB1	-1.024804564	2.57E-95	94.59084282
STON1	-1.023224227	4.13E-30	29.38413311
PRKAG2-AS1	-1.019801603	2.15E-07	6.668349946
RAB17	-1.019659702	9.94E-05	4.00253178
FBXL7	-1.019448489	1.83E-53	52.73715932
CADPS2	-1.019350402	1.85E-88	87.73210141
SVBP	-1.01888136	4.92E-18	17.30807142
ZNF358	-1.018280972	1.62E-74	73.78931637
BOK-AS1	-1.018182285	2.14E-06	5.669622729
AL590399.4	-1.017957716	0.003519868	2.453473621
CC2D2A	-1.017885629	2.13E-25	24.67215585
TRANK1	-1.017729147	8.97E-14	13.04738575
LINC00261	-1.017352558	1.16E-121	120.9340493
AGO4	-1.016954438	4.51E-51	50.34604815
NHS	-1.016540667	2.25E-66	65.64829407
ABHD8	-1.015754618	2.99E-20	19.52490897
MFSD2A	-1.01511281	1.59E-42	41.79967502
RGL1	-1.015023562	3.26E-125	124.4864133
LINC00476	-1.014804176	2.88E-33	32.54065688
STPG1	-1.014706436	7.06E-17	16.15119481
AES	-1.014702717	2.29E-98	97.63937806
NRL	-1.014061405	5.70E-05	4.24395969
RXRA	-1.012106712	7.17E-80	79.14456749
ATP6V0E2	-1.011638587	7.97E-53	52.09876972

Gene	log2(FoldChange)	p_{adj}	$-log_{10}(p_{adj})$
PNCK	-1.011223272	0.001672838	2.776546206
SLC25A36	-1.011195855	9.86E-73	72.0060185
BLVRB	-1.010717961	1.81E-55	54.74341476
SOX21	-1.010459689	3.58E-05	4.446076212
Sep 06	-1.010324925	3.51E-51	50.45470286
SLC1A7	-1.010219124	2.19E-64	63.65867501
TMEM8B	-1.010142173	1.45E-22	21.83935071
PDGFRA	-1.009892954	3.57E-28	27.44673522
AL451085.2	-1.008589206	7.22E-05	4.141283428
PROB1	-1.008232056	0.000586719	3.231569821
PSMB8-AS1	-1.00816876	1.40E-06	5.854327081
RASL11A	-1.006257304	3.57E-07	6.447798708
ADCK2	-1.004969843	6.36E-36	35.19681178
SYCP2	-1.003679108	1.66E-09	8.780462354
ARHGAP18	-1.003200926	1.28E-75	74.89302674
EVI5L	-1.001964899	2.17E-25	24.66421407
PPP1R9A	-1.001734525	2.42E-06	5.616926664
KCNH3	1.000102279	0.000122207	3.91290544
ZC3H12A	1.001361045	1.00E-31	30.9995701
ADCY1	1.002368953	1.04E-106	105.9824886
GAS5	1.003621931	1.89E-100	99.72455158
MT-TI	1.00405733	0.001151864	2.938598717
RAPGEF3	1.004696581	6.83E-06	5.165550141
NF2	1.005171033	1.59E-109	108.79818
URB1-AS1	1.006470397	3.97E-05	4.401341848
CMTM3	1.006635933	1.60E-138	137.7963935
SDC1	1.007200714	1.31E-97	96.88146956
IGF1R	1.007901072	5.47E-111	110.262026
EPSTI1	1.009827425	2.72E-23	22.56587196
BYSL	1.010061998	6.02E-53	52.22014218
ABCC3	1.010581298	1.31E-35	34.88357614
NTM	1.010624815	1.18E-34	33.92780342
IFI6	1.011303462	4.08E-09	8.389501066
RPL22L1	1.011848763	3.43E-18	17.46532553
ITPR1	1.012997517	4.75E-11	10.32332092
STK17A	1.013351883	5.90E-64	63.22947521
TNFRSF25	1.013490665	0.000214305	3.668968204
MEIS2	1.013666132	2.84E-09	8.547350274
CAPRIN2	1.015742331	8.43E-35	34.07414739
ARNTL2	1.016693417	9.14E-40	39.03927043
TMPPE	1.01749036	9.04E-06	5.043625059
CD55	1.022757489	3.55E-122	121.4503213
GPR137B	1.023233925	3.67E-07	6.435228163
NFKBIA	1.024408789	7.55E-47	46.12207919
ADGRA3	1.025017101	1.52E-67	66.8169558
GRPR	1.026876825	4.95E-06	5.304966057

Gene	log2(FoldChange)	p_{adj}	$-log_{10}(p_{adj})$
COL1A1	1.027006664	5.40E-142	141.2678865
HIST3H2A	1.028306112	8.50E-17	16.07041067
SPSB1	1.0287442	4.37E-83	82.35934271
S100A3	1.029499612	7.35E-12	11.13344152
RBM24	1.030394271	1.34E-06	5.87249012
CCL26	1.030463153	4.67E-21	20.33069673
TFPI	1.030699256	3.48E-67	66.45808427
S1PR1	1.030714937	0.0056231	2.25002418
AL391121.1	1.032296347	0.009839163	2.007041841
AC239868.2	1.033763036	3.83E-35	34.41653372
CDH2	1.034407886	1.55E-124	123.8098922
KCNG1	1.035188473	2.18E-60	59.66072642
AC023355.1	1.03529215	0.004200138	2.376736476
AC145285.7	1.036048109	0.000175501	3.755720008
FAM46C	1.036470835	9.75E-23	22.01092225
AC020571.1	1.036547395	0.000890772	3.050233376
AC131212.3	1.03938415	0.001182512	2.927194278
FGD4	1.04009117	2.77E-56	55.55779888
CALCA	1.041181513	0.001792138	2.746628487
ERO1B	1.041810647	2.40E-08	7.619126121
SCN1B	1.043659854	3.55E-16	15.44986766
AC134312.5	1.044167566	4.46E-27	26.35097582
AL078621.3	1.044275041	2.72E-06	5.56532603
IGDCC4	1.045043217	4.31E-20	19.36542896
MYEOV	1.0472822	5.03E-50	49.2983939
ADAMTSL4	1.048026773	0.002988038	2.524613885
PRRX2	1.048255667	0.002222068	2.653242737
AC254633.1	1.050499982	7.70E-08	7.11328805
SULT1C4	1.05106739	2.29E-09	8.641035826
MIR100HG	1.052969521	2.61E-36	35.58318894
HPCAL1	1.053015682	2.46E-78	77.60836311
ITGB3	1.054120306	1.85E-90	89.7325988
CTSB	1.054379984	7.56E-174	173.1216927
C10orf25	1.054534666	0.000655705	3.183291534
IL6	1.057088712	9.78E-07	6.009715055
AC093525.8	1.058383774	0.005130499	2.28984043
AL021453.1	1.059391776	2.13E-06	5.670808558
LTBP2	1.059622837	1.41E-67	66.85092849
SNHG15	1.05994429	3.64E-21	20.43942835
AL117336.3	1.061035105	0.006028094	2.21981995
PLD6	1.065111456	2.15E-12	11.6685036
EFR3B	1.068170023	7.57E-23	22.12069315
IL17D	1.068471193	6.89E-17	16.16189992
PCOTH	1.069022692	0.002841497	2.546452831
ZNF121	1.070919471	1.65E-54	53.78268003
IFFO2	1.071218632	9.03E-44	43.0442443

Gene	log2(FoldChange)	p_{adj}	$-\log_{10}(p_{adj})$
ZNF674-AS1	1.071541314	3.32E-09	8.479507657
CEACAM19	1.073428542	5.43E-11	10.26480258
IFITM1	1.076276401	0.003028681	2.518746463
STEAP1	1.076353597	3.43E-19	18.46529242
ABL2	1.077385582	1.01E-60	59.9942561
NOP16	1.079971423	2.87E-51	50.54157385
KSR1	1.081002898	1.25E-06	5.90368217
LTBP3	1.083467321	1.29E-91	90.89057789
NR2F1-AS1	1.083864793	3.25E-30	29.48815181
PRAG1	1.085684923	4.61E-07	6.336600742
AL137793.1	1.086859611	5.43E-17	16.26535919
PLXNA4	1.088185093	1.24E-10	9.907278111
ERFE	1.089064856	1.22E-31	30.91219347
GPX3	1.090231377	0.00011057	3.95636318
AC135506.1	1.090976497	0.009329802	2.030127576
NR1D1	1.092204767	3.50E-55	54.45582408
NKX1-2	1.093869179	1.86E-06	5.729392071
FAM107B	1.094246709	6.92E-91	90.16012495
KLF10	1.095022667	7.83E-19	18.10619105
FLJ27354	1.097093518	9.09E-05	4.041299123
NRIP1	1.097215289	8.09E-99	98.09206737
SNHG10	1.098950031	2.22E-13	12.65427849
ITPRIP	1.099546993	3.49E-88	87.45776746
ZNF267	1.099598387	5.24E-21	20.28073627
TAF1D	1.101941121	3.28E-53	52.4841092
IGF2BP1	1.103774351	7.00E-62	61.15510049
MYLK	1.105819044	1.17E-28	27.93187767
AL161421.1	1.106248155	1.44E-06	5.840797466
AL359921.2	1.106609843	0.003801712	2.420020833
BPGM	1.108252472	1.44E-96	95.84285064
ST7-AS1	1.111912318	2.18E-16	15.66084031
LETM2	1.113251505	1.41E-05	4.85099789
EPB41L4A-AS1	1.113442675	4.25E-26	25.37155765
GABRQ	1.113525622	0.00701308	2.154091236
CKLF	1.113546316	3.18E-08	7.498252242
AP000525.1	1.113828675	4.75E-05	4.323077397
ZNF469	1.115033224	1.31E-53	52.88226245
LINC00342	1.115908992	1.03E-11	10.98570681
SP2-AS1	1.117370387	0.00949821	2.022358218
NPW	1.117445285	0.000997094	3.001263786
MGP	1.118543642	1.06E-09	8.973267563
DIEXF	1.119381015	3.15E-80	79.50180919
SPRY2	1.121123035	3.43E-148	147.4649956
CDC42EP1	1.121578947	1.15E-70	69.93934109
AL391244.3	1.12201161	8.75E-12	11.05778873
UBE2V1	1.123092352	1.46E-10	9.83630678

Gene	log2(FoldChange)	p_{adj}	$-log_{10}(p_{adj})$
AC008764.6	1.124546057	0.000561039	3.25100668
GPR3	1.125364354	2.14E-19	18.66966678
ADAMTS6	1.127332778	1.22E-27	26.91240817
CCNO	1.127444443	6.41E-12	11.19336226
AC010331.1	1.127655477	0.003201805	2.494605079
IRX5	1.127833676	5.23E-20	19.28151109
PNP	1.128615886	1.47E-55	54.83181931
AC124016.1	1.129241611	0.00185425	2.731831665
ISM1	1.132676008	0.002184153	2.66071689
IL32	1.132995257	6.17E-46	45.2099976
AL441883.1	1.133645604	0.005250274	2.279818036
GCC2-AS1	1.134491865	0.000749952	3.12496669
RASD2	1.135412449	0.005648196	2.248090218
AC092807.3	1.136835279	5.53E-05	4.257137973
MECOM	1.136837887	2.84E-19	18.54618192
KCNQ1OT1	1.137855803	3.75E-08	7.42568325
HIST1H2BN	1.138082914	1.20E-08	7.921303488
IDO1	1.139254746	0.00280404	2.552215738
SLC22A23	1.140310419	6.42E-63	62.19242404
CLU	1.142345436	8.52E-75	74.06980127
BASP1	1.14257142	5.42E-97	96.26608717
ENC1	1.142612686	3.73E-146	145.4283023
GPR19	1.142974298	0.008945212	2.04840938
SIM2	1.144183663	5.00E-75	74.30125589
NOP2	1.147083752	3.02E-05	4.520556865
CCDC62	1.147918211	2.22E-05	4.654224226
AC116667.1	1.148427104	0.004552594	2.341741038
CACNG4	1.148885152	2.94E-36	35.5312336
MAFK	1.149307949	4.77E-71	70.32155875
COL16A1	1.150067405	2.20E-29	28.65834858
NT5E	1.150297421	1.08E-101	100.9670704
ZBTB10	1.15069681	2.53E-48	47.59723061
HEXIM1	1.151810956	8.02E-68	67.09566567
NR5A2	1.153093811	1.81E-05	4.743175149
AC090409.1	1.153265962	1.29E-10	9.88945573
B4GALNT3	1.154801869	1.17E-13	12.93176264
CAVIN1	1.155622902	7.51E-146	145.1241887
AL662797.2	1.155770952	0.002660924	2.574967524
ZSWIM4	1.157395108	6.34E-80	79.19788754
DDI2	1.15769219	2.62E-91	90.58142753
AP000844.2	1.158207089	0.000115229	3.938438259
NETO2	1.159313947	6.87E-84	83.16289867
IER5L	1.159554413	1.21E-22	21.91860612
WEE1	1.159580864	1.85E-104	103.731678
SLC30A3	1.159891999	0.002415184	2.617049842
RAB3IL1	1.160214679	2.86E-06	5.543364596

Gene	log2(FoldChange)	p_{adj}	$-\log_{10}(p_{adj})$
AC023908.3	1.160590064	0.001356411	2.867608693
DNMT3B	1.16156598	9.62E-21	20.01690421
AKNAD1	1.162201188	0.004865321	2.312888513
SMIM3	1.163659243	6.95E-25	24.15806914
FAM167B	1.164270491	8.16E-11	10.08846246
TLN2	1.165350464	2.23E-55	54.65087032
IGFBPL1	1.169410676	1.98E-10	9.703637769
ROBO3	1.170016284	4.49E-08	7.34751809
EVA1A	1.172256834	1.94E-24	23.71231074
AL590326.2	1.173722498	0.003461127	2.460782507
SVIL	1.173783416	2.22E-139	138.6538111
FOXQ1	1.17386066	7.73E-15	14.11188069
TSPAN10	1.173898393	0.000766504	3.115485612
COTL1	1.174929489	7.46E-187	186.1273753
ANKRD18A	1.177380608	0.005211878	2.283005746
HMGA2	1.177798164	8.76E-91	90.05728481
EEF1A1P5	1.179003903	5.59E-08	7.252682009
TRIM9	1.182374749	0.007503747	2.124721792
MUC5AC	1.182817627	2.12E-26	25.67462303
KANK4	1.183035707	8.21E-15	14.08553955
AL355472.1	1.185543006	1.32E-05	4.878462544
BMP8B	1.185573272	0.001512817	2.820213605
TNFRSF11B	1.186284805	6.68E-31	30.17499763
KIF5A	1.187443711	6.06E-27	26.21766145
AC011468.5	1.189958948	2.08E-05	4.68189316
RASEF	1.191527155	6.04E-53	52.21916866
SYPL2	1.191567981	2.62E-05	4.58203149
ANKLE1	1.191692906	2.10E-05	4.678636441
MAP3K14	1.192316147	1.36E-21	20.86648441
NAV2	1.193197104	3.75E-55	54.42637102
DUSP7	1.195272164	9.11E-43	42.04034979
PHF21B	1.196364529	0.002602868	2.584547826
MPP3	1.19799598	1.39E-35	34.85817841
AC239798.4	1.198565979	3.86E-12	11.4136269
FRMD5	1.198640792	2.73E-106	105.5633655
AC083880.1	1.199316738	0.000285589	3.544258367
LINC00115	1.201370597	0.000162295	3.789694851
TNNT1	1.205875089	3.10E-07	6.509167723
ZDHHC11	1.206161211	0.000132515	3.877733457
AL137003.2	1.206975373	3.38E-07	6.471681945
ARHGAP29	1.207295147	1.96E-106	105.7074583
PIK3CD	1.208242572	8.30E-57	56.08079929
FMNL2	1.208251984	0.000209153	3.679536055
COL3A1	1.209133567	0.007357422	2.133274305
ITGB5	1.210493933	2.78E-147	146.5566307
NFKB2	1.211355281	1.77E-96	95.75257209

Gene	log2(FoldChange)	p_{adj}	$-log_{10}(p_{adj})$
EFNA2	1.213259914	0.002290788	2.640015148
BACH1	1.215591257	1.26E-82	81.89874528
MYLIP	1.216272198	1.58E-18	17.80230854
ATP2A1	1.216576561	0.001102134	2.957765538
BOC	1.218262055	1.33E-14	13.87471391
ZNF408	1.220997557	1.79E-49	48.74611017
P2RX6	1.22165689	0.007357422	2.133274305
SRRM2-AS1	1.221849722	0.000272713	3.5642946
HIST1H2AG	1.227197098	2.14E-05	4.670534925
EML1	1.227221957	1.38E-111	110.8591118
MAP2K3	1.228309458	2.36E-154	153.6266266
PRDM8	1.229304132	1.72E-05	4.765007374
ARSG	1.231704802	2.48E-06	5.605572104
AL355388.2	1.233642178	0.002022922	2.694020781
AL031432.4	1.236251664	0.000287915	3.540736096
GALNT10	1.236855742	5.46E-20	19.2625217
MET	1.237667848	1.93E-83	82.71539883
HIC1	1.23817215	2.46E-29	28.60975159
AL512408.1	1.23892218	0.002367088	2.625785514
AC072061.1	1.240265707	1.21E-05	4.917091524
CPM	1.241285028	1.84E-18	17.73481357
N4BP2L1	1.242645944	3.48E-06	5.459010554
WHRN	1.244188249	2.12E-18	17.67362636
AL139089.1	1.244249945	0.004402011	2.356348849
ITGA2	1.246079686	3.79E-100	99.42155699
VGLL3	1.247936751	1.10E-26	25.95761792
SNHG4	1.251128842	8.08E-18	17.09241344
NFYC-AS1	1.251751736	1.04E-09	8.982274559
CKLF-CMTM1	1.252824972	4.76E-07	6.322058129
AEBP1	1.252919399	2.34E-10	9.630717483
C1S	1.254690332	1.28E-32	31.89290017
BMF	1.254734881	1.55E-215	214.810144
IPO4	1.254737308	9.73E-05	4.011961962
AC012531.1	1.254940079	0.00106449	2.972858581
SPANXB1	1.257294123	3.93E-14	13.4053044
SPANXC	1.259015506	2.15E-07	6.66794258
AL354740.1	1.261045235	1.38E-09	8.861356834
CMTM1	1.261249778	1.84E-28	27.73514436
MTCL1	1.261619644	1.99E-91	90.70185719
AC080080.1	1.262385473	0.000838759	3.076362713
C15orf65	1.26423544	0.000307428	3.51225666
CLCF1	1.264468416	7.24E-49	48.14035493
SNHG8	1.265336216	9.32E-41	40.03077733
AC245060.4	1.266934028	0.005962534	2.224569101
VASH1	1.267398875	0.002847864	2.545480774
PMAIP1	1.269979523	7.87E-122	121.1042964

Gene	log2(FoldChange)	p_{adj}	$-log_{10}(p_{adj})$
AC006538.1	1.271627217	3.55E-06	5.449291694
AC007066.2	1.271778078	1.15E-08	7.939342868
AC009303.4	1.271808141	3.37E-06	5.472596065
Metazoa_SRP	1.271939582	0.001150515	2.939107565
AC004477.1	1.272123294	2.57E-07	6.59035198
TWNK	1.273681801	1.16E-91	90.93421187
ONECUT2	1.274216385	7.66E-08	7.115636631
AP005233.2	1.276991807	2.20E-08	7.658154542
UBE2FP1	1.282350302	1.21E-06	5.916028048
SLC35F2	1.285136001	5.09E-56	55.2935419
CCNA1	1.285875263	0.002520141	2.598575236
AC246787.1	1.287206036	0.005406995	2.267044015
PIP5KL1	1.287492432	0.000160726	3.793912679
Sep 03	1.288926203	0.00035987	3.443853919
REPS2	1.288929341	8.45E-11	10.07327049
HTR1D	1.289991826	1.87E-14	13.72728882
AL138724.1	1.2910354	5.12E-08	7.290507261
AL161772.1	1.292134696	3.62E-36	35.44098559
MFAP4	1.294388731	0.007877573	2.103607567
DPF3	1.294698338	1.49E-09	8.828156179
BISPR	1.294922222	0.002656806	2.575640115
PPM1H	1.295258615	3.51E-05	4.454745607
AC009118.2	1.29584876	0.001445303	2.840041139
PMP22	1.296809938	8.39E-265	264.076323
SPP1	1.297655535	1.95E-119	118.7092469
MAMLD1	1.297912213	3.17E-43	42.49898347
LINC01126	1.299868213	0.005336169	2.272770458
CSGALNACT2	1.300029416	2.96E-115	114.5285511
PSORS1C1	1.304525879	1.40E-05	4.854111814
GLIPR1	1.304695636	3.13E-97	96.50417596
RAG1	1.304848376	0.000389677	3.409295679
NANOS1	1.309086578	2.28E-22	21.6428228
IL15RA	1.309193611	1.11E-20	19.95345964
AP001453.2	1.310024471	7.99E-13	12.09722882
SMTN	1.310115636	1.45E-150	149.8395141
BAIAP2L1	1.310806955	6.89E-42	41.16154946
AL121832.3	1.311174214	2.12E-05	4.672981239
AL133346.1	1.311198586	3.47E-06	5.46015083
PGM2L1	1.313540073	3.34E-85	84.47676331
AP003469.4	1.315860317	2.97E-05	4.526739383
RENBP	1.317326437	9.60E-05	4.017531743
AC036108.2	1.317584513	0.000258415	3.587682359
PTPRM	1.318709043	2.13E-29	28.67210045
AC009404.1	1.320191958	1.42E-06	5.848364668
CNNM4	1.320894962	3.49E-131	130.4568324
ADAM11	1.321884158	0.000809412	3.091830549

Gene	log2(FoldChange)	p_{adj}	$-\log_{10}(p_{adj})$
TSPYL2	1.322452124	1.40E-97	96.85378679
FJX1	1.323396685	7.99E-73	72.09747134
CAPN10-AS1	1.323861878	9.17E-14	13.03772111
TGM1	1.324409351	0.001919239	2.716870833
JUN	1.325045477	1.40E-36	35.85422633
DFFBP1	1.329366035	0.005310319	2.274879362
SAMD14	1.332742417	0.001713583	2.766094897
HIST1H2BE	1.333104854	6.92E-13	12.15963068
AC025470.2	1.333738773	0.008608481	2.065073476
TNXB	1.333788989	8.84E-07	6.053615836
LINC02454	1.334003861	0.000141434	3.849445945
AC009078.3	1.334971506	0.001809614	2.742414092
EFCAB12	1.337794328	0.001932861	2.713799347
ISG15	1.337966051	3.46E-08	7.460644863
AC010168.2	1.338195061	0.000318753	3.496545444
DUXAP9	1.338738328	4.52E-16	15.34522083
AP003071.5	1.340098714	0.00010146	3.993705334
EFNB1	1.34069079	1.26E-39	38.89915816
AL132639.2	1.341976931	0.001050198	2.978728672
DUXAP8	1.341990639	2.95E-114	113.5305833
SLC20A1	1.342666129	4.17E-125	124.3797781
HIST1H4H	1.343707871	7.11E-27	26.14807566
CDC37L1-AS1	1.344660163	0.008470957	2.072067521
AC108673.2	1.344972928	0.00032338	3.490287185
PDE4B	1.347966634	0.00014487	3.839022038
IFIT2	1.348086286	3.44E-19	18.46315128
HELZ2	1.349129648	2.50E-20	19.60261633
STAM-AS1	1.349513722	0.000309901	3.508777147
MCF2L	1.350031402	0.000363144	3.439920949
KIF5C	1.35086475	1.85E-19	18.73235158
GJA1	1.351073716	5.09E-288	287.2931104
LINC02057	1.352958283	0.005498436	2.259760826
AC010359.1	1.354939447	0.007080822	2.14991631
AOC2	1.355978073	3.92E-17	16.40723393
AC145098.2	1.35658166	7.80E-06	5.107767608
AC008567.3	1.358183684	0.00012615	3.89911445
CREB5	1.360313554	6.65E-43	42.17736417
AC062029.1	1.362208599	2.66E-05	4.575227509
MEIS1	1.363553726	6.79E-08	7.168409158
EFNA5	1.364863748	4.78E-60	59.32077898
SH2B3	1.36565219	1.29E-103	102.8894286
AC015909.1	1.365946317	0.000485535	3.313779497
ARID5A	1.366505493	4.22E-96	95.37473519
SAXO2	1.367026396	0.001271002	2.895853832
DVL1	1.367302168	5.19E-99	98.28505574
LY96	1.368849735	0.000284606	3.545755527

Gene	log2(FoldChange)	p_{adj}	$-\log_{10}(p_{adj})$
WNT2B	1.369551548	3.10E-09	8.509186316
RELB	1.36975695	7.97E-53	52.09876972
NKX2-1	1.371713313	0.000215303	3.666950409
AP001992.1	1.371904518	1.42E-05	4.846825923
MAFF	1.374427269	1.30E-93	92.8875389
CSRNP1	1.374982051	2.64E-61	60.57793858
TMEM156	1.375146994	2.08E-166	165.6821421
TNFSF9	1.37626806	9.16E-09	8.037894457
ITGA5	1.376810168	0	#ZAHL!
RPL4P6	1.377049105	0.003656532	2.436930673
MYC	1.377159216	2.64E-175	174.5791704
AL604028.2	1.377596079	0.004830772	2.315983433
FRMD6-AS1	1.377974347	0.000173738	3.760105988
RGCC	1.381269721	9.66E-32	31.01494841
CAV1	1.383280869	2.82E-187	186.5502389
LINC00958	1.383457663	0.000114996	3.939317819
AL512353.1	1.384298698	2.04E-07	6.691096375
C11orf91	1.38667779	0.007980732	2.097957274
SLC9A7	1.387766605	3.76E-26	25.42477872
ZNF697	1.389328177	2.53E-81	80.59633495
MYH15	1.392200091	0.006910928	2.160463654
LINC01004	1.392265182	1.94E-07	6.711657966
MAFB	1.394249566	6.11E-06	5.213787858
PPP1R15A	1.395714803	1.66E-292	291.7805972
AL163051.1	1.397638536	0.001756915	2.755249344
NGF	1.398363491	7.82E-10	9.106673128
AC239868.1	1.399601746	4.35E-41	40.36106717
MCTP1	1.399651942	7.50E-55	54.12469524
SNHG12	1.39985974	5.39E-55	54.26815854
AC022916.1	1.400796172	0.000835875	3.077858691
LINC01311	1.40094464	5.40E-06	5.267384452
C3orf52	1.404773095	1.97E-42	41.70444244
PRSS35	1.412479967	0.002526579	2.597467049
SUGCT	1.414117306	3.71E-21	20.43085682
BRWD1-AS2	1.414193334	0.009073159	2.042241481
ANKRD24	1.415354744	3.49E-05	4.456804981
CHRM4	1.416736826	0.00015032	3.822983926
ID2	1.418700877	5.14E-40	39.2893761
UNC13D	1.418778381	0.000136518	3.864809377
AC008741.2	1.422631493	9.94E-10	9.002455709
PTPRE	1.422998449	6.08E-21	20.21625806
HOXA5	1.424165471	0.000240067	3.619667577
AL390067.1	1.428701704	0.001124078	2.949203544
HIST1H4C	1.429139968	0.002661854	2.574815776
EHD3	1.429338973	7.18E-126	125.1438181
HIST1H2AC	1.429701312	1.87E-92	91.72881711

Gene	log2(FoldChange)	p_{adj}	$-\log_{10}(p_{adj})$
ARRDC3	1.430118027	9.64E-132	131.0160584
DSEL	1.432039055	1.53E-98	97.81460305
ANKRD36C	1.433106683	1.90E-15	14.72088075
AL645608.8	1.434489813	1.46E-05	4.834318883
KDR	1.435628409	4.52E-34	33.34454224
BTG2	1.439819556	0.000206145	3.685827172
LRRC8C	1.439887368	1.60E-85	84.79662158
CDK5R1	1.440371572	5.77E-17	16.23847346
SEMA4D	1.440415592	3.55E-05	4.449380821
AL021807.1	1.442030194	0.001558772	2.807217335
RAB9B	1.442511956	3.30E-10	9.481588115
PLK3	1.442824632	4.32E-60	59.36435635
F2RL2	1.444548721	0.003876561	2.411553379
KLF4	1.445512108	1.25E-56	55.90154399
RAB3B	1.445693653	3.62E-30	29.44163637
IRS2	1.446459873	2.34E-118	117.6307147
AP001273.1	1.447462505	3.78E-05	4.422320549
NECTIN1	1.448264559	1.74E-09	8.759074641
KCNN3	1.449649984	0.001011252	2.995140616
HIST1H3H	1.450188296	0.002517506	2.599029459
PHLDA1	1.450929243	0	#ZAHL!
AXL	1.452173666	0	#ZAHL!
P2RY1	1.452496425	1.01E-22	21.99767382
RAET1G	1.453997866	0.005574603	2.253786066
AC002456.1	1.454338094	3.57E-06	5.446857872
GREB1	1.454865882	6.02E-08	7.220133873
KRT8P46	1.455153093	0.000410605	3.386575818
AL118516.1	1.45529201	2.55E-29	28.59262847
TTC28	1.455450512	4.93E-05	4.307101872
C7orf57	1.458433714	2.79E-08	7.554243641
AC027117.1	1.458734119	0.000148518	3.82821995
FXYD5	1.458853994	4.49E-58	57.34785332
SNORD3B-1	1.461045182	8.53E-15	14.06899165
KCNC4	1.46106628	0.007730671	2.111782803
FAM117A	1.461283122	3.63E-05	4.440382306
SSSCA1-AS1	1.466073777	1.42E-05	4.848181898
AC131009.4	1.466080494	0.001970521	2.705418891
CARD10	1.466087776	5.53E-79	78.25709678
PAN3-AS1	1.467140712	1.43E-05	4.843297586
CARMN	1.46756453	2.32E-29	28.6350123
KLRD1	1.467585264	8.88E-05	4.051511583
AP000873.2	1.468548793	1.21E-06	5.917677759
AC132872.1	1.475948391	6.50E-12	11.18734761
AC103706.1	1.477162034	4.30E-05	4.366572158
AC006449.5	1.477717391	2.87E-05	4.54147003
GZMA	1.477856465	2.69E-05	4.570188417

Gene	log2(FoldChange)	p_{adj}	$-log_{10}(p_{adj})$
ATP2B1-AS1	1.478626786	4.57E-12	11.34036843
GPR176	1.48036502	3.41E-259	258.4676662
AC005224.4	1.48055475	1.06E-07	6.973282461
AC090192.2	1.480987437	2.79E-10	9.554917731
AC025594.2	1.482041779	5.22E-15	14.28229076
RNU5A-1	1.482757879	1.76E-08	7.753768682
PFKFB4	1.483843735	1.00E-101	100.9984347
NDRG4	1.487035427	8.22E-09	8.085118522
SPANXD	1.488701659	8.18E-12	11.08700113
HIST1H2BK	1.489379376	3.31E-67	66.48048083
ARL13A	1.490403795	0.007677175	2.114798569
PVR	1.491107483	1.53E-199	198.8160943
ITGA7	1.491294371	9.16E-09	8.037870408
GBX2	1.492026853	8.21E-28	27.08568845
EPHA5	1.493272605	1.93E-32	31.71434803
FOXA3	1.494000573	6.23E-05	4.205697094
NEXN-AS1	1.497308038	1.04E-05	4.98395083
AL357054.4	1.498004032	0.002967111	2.527666257
ARHGAP5-AS1	1.501053344	2.36E-20	19.62678086
AC103740.2	1.501232186	0.000279501	3.553616611
NEXN	1.502441331	1.47E-143	142.8324367
AC009093.1	1.502893143	1.33E-35	34.87756652
SNHG3	1.503572423	3.65E-100	99.4378249
ARC	1.504984842	4.59E-19	18.33852948
DLG2	1.505962302	0.006527901	2.18522646
AC099522.2	1.507093816	0.003460422	2.46087094
NRIP3	1.507531973	4.86E-78	77.31307365
AC068205.2	1.507816023	0.000276667	3.55804299
IGFBP3	1.512501847	1.23E-201	200.9091131
PHKA1	1.513207074	0.003324189	2.478314296
TOLLIP-AS1	1.514759617	0.001049335	2.979085654
GLB1L3	1.515737679	3.16E-08	7.500922865
AC106881.1	1.517196882	2.28E-06	5.643016271
BX255923.1	1.517659614	0.005431535	2.265077384
CD163L1	1.518697888	3.38E-18	17.47071164
DCBLD2	1.518772829	0	#ZAHL!
AL442128.2	1.521602833	0.007526133	2.123428133
RIPK2	1.522278304	1.63E-121	120.7869165
NDUFV2	1.522935004	2.97E-08	7.526539639
DUSP6	1.523220058	1.04E-117	116.9846235
FAM27E3	1.524054383	0.000965516	3.015240527
AC133552.2	1.524668436	0.003155145	2.500980718
RASA4B	1.526619111	0.002742545	2.561846231
HIST1H1E	1.526909858	0.00016103	3.793092683
HIST2H4A	1.52991489	9.28E-05	4.032354805
AC089983.1	1.534449894	0.002869703	2.542163111

Gene	log2(FoldChange)	p_{adj}	$-\log_{10}(p_{adj})$
HIST3H2BB	1.534649763	2.02E-06	5.695406829
MAPK8IP1	1.536311074	5.04E-24	23.29736824
CD14	1.539078718	8.33E-05	4.079386074
GATA6-AS1	1.542274887	0.000152159	3.817700959
AC009570.1	1.542352887	0.003786133	2.421804117
AL121672.2	1.546054131	0.004352819	2.361229383
AC023157.3	1.54962653	5.97E-07	6.224343829
REP15	1.550653202	0.000841248	3.075076131
OSCAR	1.551591641	2.04E-06	5.689619694
METRN	1.552987922	4.16E-60	59.38045386
C1QL1	1.553028508	6.67E-21	20.17615704
RNU6-2	1.557152673	0.00734328	2.134109884
CDKL1	1.557301461	6.04E-07	6.218987244
OPRD1	1.56096462	8.58E-27	26.06637985
SNHG1	1.565931577	6.37E-132	131.195936
PBX3	1.566245334	1.64E-68	67.78536719
ADAMTS1	1.57079243	4.39E-172	171.3574721
SNORA73B	1.572141932	1.95E-09	8.709904118
FAM102B	1.574643486	2.33E-99	98.63252088
LMO2	1.575221561	4.63E-06	5.334645916
MN1	1.575931691	2.08E-19	18.68209763
XKRX	1.578260945	6.70E-15	14.17413111
AK5	1.578889817	5.79E-21	20.23726855
NCF2	1.579297114	6.98E-09	8.15625361
FSTL3	1.581132106	7.27E-213	212.1384403
TIGD3	1.581888987	0.000748016	3.12608901
AC005261.1	1.581934356	0.006302882	2.200460848
SMOX	1.58494015	9.84E-186	185.006853
DUSP8	1.585080588	9.50E-40	39.02245522
PRKCZ-AS1	1.586692672	7.59E-05	4.119620255
OSBPL6	1.588528484	0.004357909	2.360721859
DAGLA	1.589168605	4.25E-06	5.371162891
TMEM190	1.59030233	4.73E-07	6.325243422
BACH1-IT2	1.590583371	0.007581157	2.120264529
AC092117.1	1.592626757	2.91E-12	11.53621084
HIST1H2BJ	1.593504188	5.43E-16	15.26492136
KHDRBS3	1.597527674	3.50E-23	22.45637814
AC084018.2	1.602635437	2.89E-06	5.53911477
INHBC	1.607837899	5.23E-09	8.281327349
AC005076.1	1.610427161	2.44E-07	6.613339497
AL359504.2	1.610459516	1.31E-09	8.881956508
LINC02257	1.612737493	2.52E-07	6.598793548
AL137003.1	1.6160704	2.25E-06	5.648548509
HIST1H1C	1.616777905	2.61E-105	104.5832752
TMEM151A	1.617939041	0.008826641	2.054204558
HIST1H2BD	1.621832027	4.80E-40	39.31859473

Gene	log2(FoldChange)	p_{adj}	$-log_{10}(p_{adj})$
AC020765.2	1.622483203	0.007028039	2.153165812
ADAMTSL4-AS1	1.622541248	2.27E-11	10.64369879
AC093673.1	1.623269129	5.59E-22	21.25226906
NEU4	1.626633311	0.002340508	2.630689871
LINC00475	1.62971649	4.06E-09	8.391000671
AL023806.1	1.632753584	0.002164119	2.664718802
AC112198.2	1.632999751	0.002949945	2.530186136
AL365181.3	1.633091902	2.50E-09	8.601237707
SRGAP3	1.63329444	0.001395898	2.855146398
AC069544.1	1.634491773	4.31E-05	4.365644514
SLFNL1-AS1	1.635255919	4.71E-08	7.327051908
COL7A1	1.636565859	2.53E-42	41.5972526
GPR156	1.643159923	0.006217118	2.206410903
AC002985.2	1.645879388	3.48E-05	4.457811783
HRH1	1.647255456	8.28E-45	44.08179827
NKAIN1	1.649193209	0.006113035	2.213743084
KLC3	1.649708191	0.000107446	3.968809945
CYP1A1	1.651875712	0.001109749	2.954775398
ADAM19	1.655268818	1.17E-281	280.9309852
AL133342.1	1.657399447	0.000374118	3.426990959
LINC01144	1.657836641	0.001175706	2.929701437
AC017104.1	1.659685679	8.22E-05	4.08537408
AC002470.1	1.659899317	0.005620157	2.250251585
AL034417.2	1.661625218	0.003795247	2.420759947
AL008729.1	1.665086517	0.000927612	3.032633499
MMP2	1.665447945	1.52E-236	235.8181369
CACNA1H	1.666059141	0.000186691	3.728876255
AC027117.2	1.670542213	0.006436185	2.191371507
SRGN	1.671077974	7.98E-06	5.097752364
KCND1	1.672998973	4.36E-13	12.36070392
CTGF	1.676135078	3.21E-178	177.4932817
CD3EAP	1.676603413	1.44E-120	119.8401855
TRPM3	1.679135173	0.004362473	2.360267263
IL31RA	1.679161867	0.000168876	3.772433017
IFIT1	1.680055542	6.20E-07	6.207719881
TOR4A	1.680789902	9.85E-12	11.00661114
KBTBD8	1.68294773	2.34E-16	15.6305306
CNTNAP3	1.684757191	1.21E-51	50.91898365
RN7SL832P	1.68646702	0.000463093	3.334331857
SRPX	1.689501774	4.11E-10	9.386591668
HIST1H2BC	1.694415663	1.07E-14	13.97133681
AC010894.2	1.69493414	5.45E-05	4.263580177
AC104109.2	1.695918482	0.001902854	2.720594531
HIST1H2AK	1.699490342	6.59E-05	4.181220279
P2RY6	1.699606905	0.005063192	2.295575615

Gene	log2(FoldChange)	p_{adj}	$-log_{10}(p_{adj})$
MSH4	1.703272072	0.002039757	2.690421491
PGF	1.706423745	2.31E-16	15.63623744
ASPHD1	1.707197802	5.15E-28	27.28851107
TNFRSF12A	1.707533788	1.63E-128	127.7891434
ELMOD1	1.707943336	1.84E-06	5.734331059
HNRNPA1P27	1.713281325	8.27E-08	7.082495008
SCN8A	1.719228627	0.00210472	2.67680563
DUSP1	1.719587188	3.53E-63	62.45265322
PRKG1	1.719648765	0.001060715	2.974401172
CSGALNACT1	1.728730663	3.95E-31	30.40385191
NAV3	1.729538071	1.04E-71	70.98313287
ABAT	1.730004169	0.000118722	3.925469166
MICAL2	1.730445932	0	#ZAHL!
AL158151.3	1.730933868	0.001002613	2.998866666
MIR17HG	1.734702975	1.76E-05	4.753873716
AC026803.2	1.734824141	0.007112149	2.147999145
S100A14	1.736708594	1.38E-06	5.860957822
AC007952.4	1.738158438	4.31E-06	5.365292427
MYB	1.738231768	9.05E-05	4.043430367
COL8A2	1.743289186	4.27E-12	11.36944042
OVGP1	1.744121501	7.18E-09	8.143842123
BX276092.9	1.745875059	0.007416804	2.129783193
AL139393.2	1.750098769	1.02E-63	62.99232518
DCAF4L1	1.750129129	3.35E-05	4.474451043
PLAT	1.750368001	3.75E-265	264.4253956
AC026304.1	1.752956886	0.000695022	3.15800158
LIMS2	1.752960212	7.22E-18	17.14132427
AC073611.1	1.75363567	3.38E-08	7.471535176
PGM5P2	1.75510704	7.11E-15	14.14820144
COL27A1	1.758218944	3.70E-13	12.43125531
AC020916.1	1.759488068	1.31E-23	22.88271805
MX1	1.760384235	3.78E-11	10.42194932
TINAGL1	1.7650483	1.88E-09	8.726668936
PDZD2	1.765131657	2.11E-82	81.67477824
ADAM12	1.765698484	4.91E-60	59.30895434
NR4A3	1.768952327	1.98E-30	29.70242342
HIST1H2BO	1.770985203	7.33E-05	4.135084602
PTPRF	1.772252756	3.36E-286	285.4733536
LINC01125	1.773177844	5.16E-08	7.287135875
AC116407.1	1.773442137	0.005620157	2.250251585
BST2	1.774852474	7.22E-27	26.14136821
UNC79	1.775755913	0.000123209	3.909355835
AC068647.2	1.778303443	6.47E-26	25.18884999
CDH6	1.779371256	1.98E-295	294.70256
STARD13	1.782536914	7.01E-171	170.154129
OLFM2	1.784683169	4.93E-07	6.307481195

Gene	log2(FoldChange)	p_{adj}	$-\log_{10}(p_{adj})$
FN1	1.786435617	2.69E-295	294.5709366
KCNJ2-AS1	1.787437201	3.29E-05	4.483394541
KCNMA1	1.789603254	3.05E-161	160.5154056
RAB11FIP1	1.794630333	7.79E-10	9.108491039
KREMEN2	1.795862048	0.005481537	2.261097668
ZIC2	1.799951994	2.84E-19	18.54598311
NAP1L4P1	1.800209237	0.004017574	2.396036137
AL356356.1	1.801879145	0.000145747	3.836399255
LINC01191	1.802454182	0.001013967	2.993976298
RAD21-AS1	1.806068724	0.005662349	2.247003371
SRPX2	1.80664365	2.15E-40	39.66848195
ATF3	1.807966757	3.49E-129	128.4576009
KCNN4	1.809465959	7.54E-106	105.1227913
CEP83-AS1	1.813777572	0.000303154	3.518336979
FAM180A	1.814281489	0.007231053	2.140798436
NRARP	1.815974155	4.41E-10	9.355261042
DLX2	1.817717587	2.69E-42	41.57099753
ROS1	1.818466022	1.60E-58	57.79709169
AL021154.1	1.822283148	0.007529019	2.123261602
HAS3	1.823568317	3.19E-18	17.49649512
NRCAM	1.825037824	2.18E-56	55.66142845
SLCO4A1	1.831904485	1.59E-08	7.798427198
AL158819.1	1.832706601	0.003257469	2.487119667
LNX1	1.834233605	0.004266939	2.369883608
C1QTNF12	1.834581002	0.000212088	3.673483333
SLC22A4	1.834889614	7.85E-25	24.104886
PRRX1	1.835431389	3.62E-134	133.4413116
GPRIN3	1.837455706	3.34E-09	8.476348009
NR2F1	1.838595203	2.48E-145	144.6048453
B3GNT7	1.840540681	0.00722777	2.140995689
FZD4	1.841765355	4.08E-116	115.3898679
RNU6-8	1.847853393	0.000638236	3.195018579
AL365203.1	1.848140803	4.10E-07	6.38750123
FNDC5	1.848251634	7.55E-55	54.12198808
CDHR3	1.854290436	8.47E-08	7.072263395
GPR35	1.856454693	0.005771077	2.238743129
AL355312.3	1.858897147	0.001758089	2.754959085
BDKRB2	1.861184591	2.42E-32	31.61649456
UNC13A	1.863800117	1.76E-08	7.753770829
IFI44L	1.864073587	0.00348368	2.457961725
KCNJ2	1.865955773	1.32E-57	56.87950235
PAK6	1.866986913	2.46E-11	10.60872477
MAP3K7CL	1.866987852	1.08E-19	18.96842415
F2R	1.86766302	0	#ZAHL!
KCP	1.867683456	2.31E-12	11.63673915
SEMA4A	1.870914272	0.001512663	2.820257769

Gene	log2(FoldChange)	p_{adj}	$-log_{10}(p_{adj})$
TGFB3	1.873041172	1.29E-08	7.890872187
DIRC3-AS1	1.876100383	9.99E-06	5.000624784
LINC00513	1.876190072	0.001881295	2.725543046
HBEGF	1.876936737	2.30E-203	202.6383538
HAPLN3	1.877740929	1.52E-60	59.81858352
CARD9	1.880578931	3.45E-05	4.461928938
MRPS24	1.881277437	3.52E-25	24.4535501
TPPP	1.884557635	2.79E-05	4.55380644
RIN1	1.887040042	3.57E-61	60.44678244
TFPI2	1.887377073	9.11E-54	53.0406818
DNM1	1.887437465	9.00E-90	89.04596434
ZDHHC22	1.887489886	0.002155321	2.666488122
AL355512.1	1.89250048	4.07E-05	4.390381352
AP001437.1	1.895394398	0.000251075	3.600196324
SHANK3	1.899867583	2.65E-06	5.57709249
TNFAIP3	1.900579099	1.80E-61	60.74520148
GEM	1.902573684	1.05E-158	157.979313
METTL27	1.902752868	1.32E-11	10.87967196
AC010864.1	1.905331713	3.82E-06	5.418039224
CATSPERG	1.907472322	2.19E-08	7.659239196
SNORD104	1.910158987	1.20E-08	7.922489438
WNT5B	1.91203745	1.65E-146	145.7824491
AC012447.1	1.912115992	0.00193376	2.713597394
PAX6	1.912342674	5.72E-05	4.242738478
AL157756.1	1.913452762	0.000189599	3.722163964
AL365436.2	1.915299617	0.003369713	2.4724071
KRTAP5-AS1	1.918957359	0.000961204	3.017184651
BX088645.1	1.928813373	3.03E-05	4.51814336
NALT1	1.932735542	0.001584207	2.800188132
FCGBP	1.935775296	2.75E-06	5.560292474
S1PR5	1.938330239	0.009569635	2.019104612
C2orf66	1.938625409	0.005103359	2.292143868
AL807752.5	1.944012797	0.000683071	3.165533849
EOMES	1.945151018	5.81E-12	11.23582415
ZMIZ1-AS1	1.949192214	5.39E-05	4.268474318
AC104506.1	1.951052327	0.000267155	3.57323738
LINC01023	1.953891525	0.004538951	2.343044503
NFE2L3	1.954050747	2.31E-94	93.63599194
AL139289.2	1.954973347	0.001955786	2.7086786
ALMS1-IT1	1.958412592	0.004189724	2.377814543
AC079684.1	1.958992135	0.005378537	2.269335876
CLDN6	1.959582934	0.000804708	3.094361838
RPSAP52	1.964050439	1.50E-13	12.82487434
SCARNA15	1.966951882	1.22E-08	7.912513778
AC116366.1	1.969028274	0.003982215	2.399875315
LOXL1	1.969701265	6.24E-29	28.20502507

Gene	log2(FoldChange)	p_{adj}	$-log_{10}(p_{adj})$
LIF-AS1	1.971955593	0.000684473	3.164643516
AL365181.2	1.975830812	0.002924746	2.533911801
KCNK6	1.976731411	6.11E-06	5.213787858
RGS17	1.979482342	5.51E-22	21.2588003
HIST1H2BH	1.989924073	1.91E-15	14.72002059
HTR7P1	1.992674102	6.62E-14	13.17899669
LINC02535	1.998061378	0.004184396	2.378367199
AL139274.2	1.999686957	0.000921298	3.03559989
CSF1R	2.000946151	2.46E-10	9.608290485
CLDN1	2.002145302	5.76E-10	9.239876387
AC010491.1	2.002484816	0.000184677	3.733587932
SNHG25	2.003319445	0.00015058	3.822233101
FAM84B	2.004100979	0.002758377	2.559346453
SPINT1	2.006270122	3.86E-17	16.41344184
YTHDF3-AS1	2.006648361	8.47E-06	5.072284806
AHNAK2	2.008330953	5.90E-99	98.22908947
KCNMB4	2.011298678	1.05E-05	4.978734894
LINC01655	2.016485921	0.000271968	3.565481828
CHRM2	2.023757491	4.05E-09	8.392388545
CDO1	2.027191756	0.006280011	2.202039569
ANO9	2.027909639	0.006370654	2.195816014
PACERR	2.029318216	7.93E-05	4.100956811
NFKBIZ	2.030402298	5.21E-52	51.28329135
HCG20	2.032669173	0.003918304	2.406901914
CITED1	2.035240884	0.000517496	3.286093034
BCAS4	2.035802983	8.09E-51	50.09215333
IL12RB1	2.036819523	0.000311	3.507240066
DNER	2.036855643	0.000126201	3.898937518
PTPN22	2.039008417	9.87E-05	4.005479559
FIBCD1	2.039394467	3.73E-05	4.428442578
MIR222HG	2.03960466	7.95E-19	18.09989244
C7	2.039966542	0.000304703	3.51612357
UCN2	2.041064538	7.00E-77	76.15480607
MAP3K8	2.041763185	1.28E-06	5.891318488
HIF3A	2.041986207	0.004959476	2.30456417
TAF4B	2.042670529	7.54E-42	41.12258133
GUCA1B	2.042980957	0.008457314	2.072767551
AC011611.3	2.048529322	4.65E-06	5.332925964
ARHGAP30	2.051803608	2.09E-12	11.68063343
AC026124.2	2.052410847	0.005214391	2.282796394
AADACP1	2.054264913	2.54E-53	52.59548227
EXTL1	2.056489463	3.22E-30	29.49247818
ACTA1	2.056980428	2.15E-07	6.66784117
STMN3	2.058796812	3.02E-28	27.51989674
LMOD1	2.058874539	8.36E-05	4.077620582
LINC01588	2.060214539	0.000173041	3.761850054

Gene	log2(FoldChange)	p_{adj}	$-\log_{10}(p_{adj})$
CELF3	2.064674878	0.009905481	2.004124428
AC009237.14	2.068332735	2.02E-06	5.695237399
LINC00565	2.071634862	3.84E-13	12.41590679
OAS1	2.072186702	2.21E-05	4.65526248
ANK1	2.078504421	1.19E-14	13.92376352
AC009549.1	2.081560293	4.59E-15	14.33854744
ACTBP7	2.083422816	5.37E-05	4.270428121
FAP	2.085112516	3.99E-28	27.39924134
CD44	2.087495808	0	#ZAHL!
PCDH10	2.08953754	2.73E-11	10.56342955
DLL3	2.095573168	0.006395818	2.194103911
TRPM2	2.095713527	2.28E-10	9.641769654
AC083902.2	2.099436576	0.000702606	3.15328838
RGS2	2.101433919	5.66E-18	17.24728085
TFAP2E	2.1042976	0.002499017	2.602230853
AL356512.1	2.105295494	1.31E-08	7.881398686
SERINC4	2.108910661	0.003806304	2.41949657
AADAC	2.110085176	5.23E-56	55.28144025
AC017074.1	2.112805297	8.69E-06	5.060977663
GPD1	2.114469474	0.00144612	2.83979559
SDK2	2.115297366	0.007088062	2.149472517
SEMA3F	2.11542281	6.54E-05	4.184640977
AC010336.1	2.11940084	0.000339419	3.469263798
CABP1	2.120232452	3.22E-10	9.491596461
PTGER3	2.121961507	0.004129466	2.384106096
PTGER4	2.123969416	9.17E-79	78.03740674
AL031710.2	2.126680544	0.000800962	3.096387893
FBXO32	2.127403305	0	#ZAHL!
METTL12	2.127564378	4.53E-21	20.34357682
SNHG11	2.127716067	1.36E-18	17.86506929
AP001527.2	2.127765664	7.91E-05	4.101778441
AC006511.3	2.128964698	0.000168815	3.772589174
LYPD1	2.12940466	7.45E-217	216.1275624
GCNT4	2.130404061	3.96E-05	4.402795768
SMC2-AS1	2.130465877	0.009069807	2.042401972
AC106047.1	2.133633441	0.001331824	2.875553203
SLC45A3	2.134499457	1.73E-46	45.76219548
SEMA7A	2.135739049	7.79E-142	141.1083478
PROX1	2.136092943	1.44E-15	14.84053481
KCNH1	2.136430989	6.46E-85	84.18969023
AC087239.1	2.137049252	0.003857326	2.413713646
LDB3	2.137212731	0.007054867	2.151511169
AP000845.1	2.138997852	0.001185395	2.92613701
AL731571.1	2.141225948	2.66E-07	6.575590382
ST6GALNAC5	2.141330721	0.007168753	2.144556362
GFPT2	2.143031695	1.52E-47	46.81683853

Gene	log2(FoldChange)	p_{adj}	$-\log_{10}(p_{adj})$
CYP27C1	2.143233655	2.60E-16	15.58536684
MCAM	2.14393503	0	#ZAHL!
C9orf24	2.144642407	0.003919607	2.406757487
WISP1	2.146762006	1.03E-05	4.985373466
AC006262.1	2.146837955	9.83E-35	34.0074869
SPRED3	2.151987363	2.35E-21	20.62959449
MDGA1	2.157117591	2.98E-35	34.52594783
AL138966.2	2.158029015	0.000256748	3.590492298
FRMD6	2.164249701	0	#ZAHL!
CD274	2.165768551	7.31E-69	68.13586297
FZD8	2.167660656	1.75E-181	180.7578575
PIM1	2.168165813	0	#ZAHL!
LINC01119	2.171899018	1.85E-06	5.732417426
RHPN1-AS1	2.173160009	0.0034945	2.456614953
KIAA1683	2.179967301	7.72E-18	17.11249694
CABLES1	2.184410903	1.25E-126	125.902977
MED12L	2.18469077	2.93E-26	25.53347824
EPHB2	2.186118777	0	#ZAHL!
RTN4RL2	2.193939074	0.000172033	3.764388935
RTL3	2.197514445	9.34E-05	4.029440922
AL121983.1	2.205516758	0.001237863	2.907327271
NR4A2	2.205619549	2.23E-90	89.65232096
AC102945.2	2.209296527	1.94E-11	10.71291539
CTRC	2.211637381	0.000666362	3.176289534
LHX6	2.213047364	4.18E-43	42.37850689
AL390719.1	2.220335327	4.32E-22	21.36440189
ABCC2	2.220826868	3.46E-06	5.460653209
IL2RB	2.224912155	0.005183642	2.285364998
LINC00452	2.22990301	0.008274947	2.082234796
SNORA66	2.23406946	0.003973202	2.400859377
COL1A2	2.239987546	4.30E-05	4.366806755
INHBA	2.241255434	0	#ZAHL!
LINC01444	2.25044453	1.34E-05	4.873324904
CCDC168	2.251188098	0.009370023	2.02825935
ST6GAL2	2.251206833	0.003264646	2.48616395
HSPB8	2.252046714	2.02E-06	5.695106879
SYT7	2.253399091	1.56E-05	4.806841535
AHRR	2.253972423	2.93E-05	4.532618218
ITGA3	2.259961448	0	#ZAHL!
CXCL3	2.260433931	1.49E-11	10.82561676
TENM3	2.261848142	7.53E-11	10.12297918
NMNAT2	2.265313071	0.004699654	2.327934122
ADAMTS16	2.266252722	9.90E-75	74.00451285
MYO1D	2.267367806	0.003733351	2.427901182
HSPA12A	2.267404911	0.00371532	2.430003755
MEIOC	2.272199141	0.006792792	2.167951699

Gene	log2(FoldChange)	p_{adj}	$-log_{10}(p_{adj})$
TRPV2	2.27346737	0.000238059	3.6233163
FLJ31104	2.274652425	0.001295768	2.887472686
LINC00944	2.277204043	2.19E-11	10.65870187
LYPLAL1-AS1	2.277207028	0.00069684	3.156866803
ZG16B	2.280348671	2.70E-11	10.56857748
KRT16	2.281376983	2.14E-09	8.670276616
IL23A	2.282322553	0.000125168	3.902506438
RALGPS2	2.285856546	5.02E-67	66.29939833
FAM167A	2.290183275	0.000565522	3.247550196
SGK1	2.291935313	0	#ZAHL!
CRISPLD2	2.292000552	1.69E-82	81.77213073
CARMIL2	2.30029306	6.94E-06	5.158727667
FP565324.1	2.302511828	1.22E-09	8.912042928
PADI1	2.302744608	0.001435638	2.842955068
COX6B2	2.304622557	3.18E-09	8.497950507
CMPK2	2.307335266	1.09E-07	6.964055653
PITPNM3	2.309573092	4.06E-06	5.391551003
BICDL1	2.312647483	0.009744256	2.011251332
SNORD83A	2.315370841	0.001599124	2.796117729
ISLR	2.315797555	7.95E-09	8.099816867
CCL20	2.318118049	4.10E-07	6.387579855
AC092127.2	2.318869928	5.14E-05	4.289131605
ICAM4	2.323346583	0.000273473	3.563085688
LPAR6	2.323695216	1.17E-06	5.933314528
STARD8	2.32627509	0.003015367	2.52065982
CMYA5	2.326963523	2.67E-10	9.573505684
AL353759.1	2.328570062	1.18E-05	4.927030333
IGFL3	2.330947421	3.23E-08	7.490525194
RASL10B	2.33124377	0.000179436	3.746091449
AL121761.2	2.333644187	0.005084885	2.293718822
KIF17	2.337411857	0.000774819	3.110799891
AC007032.1	2.33948044	6.79E-07	6.168188752
CMTM2	2.339781884	0.000698153	3.156049495
LINC00702	2.340236374	1.53E-13	12.81453753
NFATC2	2.341798241	3.80E-243	242.4205247
FAM131B	2.34824466	2.37E-06	5.624447974
SENCR	2.348819559	0.000147234	3.83199173
JAM3	2.353225401	1.25E-18	17.90187069
LAPTM5	2.35430292	2.61E-42	41.58394446
OSR2	2.354340878	2.99E-22	21.52377522
TAGLN	2.357766397	1.63E-259	258.7883749
ASGR1	2.36436175	0.000251783	3.598973488
SLIT2	2.365984599	3.83E-45	44.41630172
JAG1	2.370886251	0	#ZAHL!
ENOX1	2.372616898	4.58E-77	76.33923006
WTIP	2.386507397	5.48E-22	21.26103403

Gene	log2(FoldChange)	p_{adj}	$-\log_{10}(p_{adj})$
AC080023.1	2.389825276	0.002086123	2.680660163
IL1A	2.389905156	0.002409186	2.618129756
LPXN	2.394564025	1.55E-128	127.8101923
GRID1	2.395181256	0.007227253	2.141026752
CACNA1G	2.400363604	0.000175629	3.755404389
AP000695.1	2.405053537	0.000219881	3.657811789
AC017083.2	2.405836904	0.000165809	3.780391938
DUSP5	2.406779275	5.80E-235	234.2366711
CEMIP	2.410599119	3.80E-124	123.4206742
MT1X	2.411290596	1.38E-52	51.86067561
GADD45G	2.413816124	0.001898762	2.721529363
CSPG4	2.417305174	8.54E-34	33.06861833
KIAA1549L	2.418317853	0.000528808	3.276702135
FAM182B	2.420256985	2.07E-05	4.685060399
NOTCH3	2.426841825	3.38E-13	12.47099722
GPRC5A	2.429506071	2.41E-66	65.61791903
HIST1H3J	2.430385321	0.001915511	2.717715316
ZFP69	2.434571964	0.001991868	2.70073952
SSC5D	2.436002901	1.77E-88	87.75283975
MYO5B	2.437007566	0.000240883	3.618194518
CYP2S1	2.43922201	7.01E-36	35.1540065
GNG12-AS1	2.440119646	0.000362957	3.440144981
CILP2	2.449494104	0.000139018	3.856929388
BGN	2.449775577	0	#ZAHL!
AL132780.1	2.450146503	0.000958588	3.01836788
FAM83G	2.452029318	2.06E-107	106.6866231
NBPF13P	2.454187589	0.008523499	2.069382077
CDKN1C	2.454259758	8.44E-22	21.07376278
SPEG	2.455208872	1.07E-08	7.969523498
NEB	2.455761816	0.000184409	3.734216714
ADGRG1	2.45852078	2.75E-88	87.56070189
MX2	2.458861248	2.91E-05	4.536172678
VTN	2.464672698	0.002246216	2.648548563
C10orf55	2.472508852	3.37E-07	6.472610034
AC112715.1	2.473438796	0.003280368	2.484077405
FCMR	2.473904089	3.04E-06	5.51708869
FGF18	2.474368269	0.008340392	2.078813537
ZEB2-AS1	2.475991553	0.009988692	2.0004914
AC112907.3	2.477596374	0.000855729	3.067663876
HSPA6	2.479776605	9.08E-14	13.04174293
H19	2.488458456	2.27E-22	21.64471538
AC026250.1	2.496386439	7.16E-07	6.144937791
WNT9A	2.497505738	6.37E-60	59.19620067
COL20A1	2.501808054	0.000342715	3.465067294
RGL3	2.502548222	0.000351418	3.454176239
MLXIPL	2.508902812	0.000127538	3.89436065

Gene	log2(FoldChange)	p_{adj}	$-\log_{10}(p_{adj})$
HSP90B2P	2.508990091	6.13E-08	7.212625561
XIRP1	2.513328486	2.26E-30	29.64662503
STX1A	2.515629274	2.42E-233	232.6155303
NKD1	2.518805319	3.63E-52	51.44037641
ALOX5AP	2.519052517	0.004632641	2.334171342
VDR	2.519328938	6.31E-49	48.19984022
RN7SL600P	2.531616088	0.001002833	2.998771213
LINC01415	2.533349873	1.38E-08	7.86103154
FGFR4	2.535208002	5.30E-06	5.275404386
TMEM204	2.536477549	0.000165263	3.781824798
AL078621.1	2.541927847	0.008428233	2.074263449
FLNC	2.542968466	1.21E-83	82.91811922
AC098864.1	2.54496512	9.02E-17	16.04500388
CCL2	2.54827378	1.98E-89	88.70249551
AC079305.3	2.548632513	1.18E-10	9.928589271
TMOD1	2.558919222	5.11E-10	9.291924635
UBE2E2	2.561449611	1.56E-05	4.805614114
AL590096.1	2.561639785	0.001571107	2.803794119
KLK14	2.564824636	0.001170491	2.931631745
FLVCR2	2.566362405	0.000335394	3.474444099
SPHK1	2.566922796	4.49E-188	187.3473908
RNU1-2	2.569675178	0.007127882	2.147039468
AP001033.2	2.577909532	0.000253228	3.596488819
SNORD99	2.579423697	0.000524178	3.280521586
PEG13	2.581376791	1.36E-05	4.866664331
POM121L9P	2.582603886	5.60E-10	9.25176433
AC012377.1	2.583061773	0.001865654	2.72916888
TFEC	2.583971102	0.001330095	2.876117379
TRPV3	2.585086094	0.009821917	2.007803755
EN2	2.588742532	0.002598016	2.585358109
NLRP1	2.590340059	2.98E-06	5.526305793
STOX2	2.590760353	0.009859355	2.006151496
KCNIP3	2.591089416	3.57E-06	5.446915742
AC008013.1	2.59323861	0.002980127	2.525765166
PKP3	2.594382447	2.02E-05	4.693838126
HIST1H3D	2.594761114	1.44E-16	15.84175875
MT2A	2.59748012	2.08E-114	113.682784
CTSW	2.598546836	0.000845257	3.073011376
AP001160.1	2.602058748	6.60E-06	5.180597196
AC132192.2	2.604311375	5.13E-27	26.29011308
CCM2L	2.60483557	0.000719645	3.142881655
ADPRHL1	2.605486633	9.24E-149	148.0344785
AC137932.2	2.6085599	0.000335126	3.474791673
AL590004.4	2.611828903	1.61E-10	9.793099685
OASL	2.617240274	2.59E-09	8.5867768
MMP24	2.620476121	3.78E-08	7.422991689

Gene	log2(FoldChange)	p_{adj}	$-log_{10}(p_{adj})$
IRF4	2.623278479	2.03E-09	8.691750376
FLT1	2.623722494	3.07E-05	4.513145101
Z95331.1	2.623813177	1.49E-12	11.82688385
OAF	2.623929979	3.03E-05	4.51804035
C3	2.62585661	4.81E-05	4.31790778
TNFAIP8L3	2.626635992	1.20E-08	7.921303488
OAS2	2.636798964	1.54E-05	4.811993535
ALPK2	2.647964362	1.36E-12	11.86800737
RAMP3	2.651629678	0.000417238	3.379616356
AC013400.1	2.654111399	0.002527636	2.597285422
MNX1	2.654221125	0.001473943	2.831519189
UMODL1	2.660248049	8.80E-08	7.055738137
PSG5	2.661868405	4.77E-06	5.32192232
SHC3	2.662302384	0.008687529	2.06110374
RTL5	2.663089761	3.47E-12	11.45932244
SZT2-AS1	2.664659077	1.42E-06	5.84746444
GAREM2	2.6702489	0.008438365	2.07374167
SLC14A1	2.675913848	2.56E-184	183.592609
PTGS2	2.677055857	0	#ZAHL!
AC062017.1	2.678046069	1.52E-05	4.817937804
AC021188.1	2.68141214	0.003191838	2.495959154
SP140	2.681487696	2.84E-05	4.54608311
AL136038.3	2.695322712	0.00071813	3.143797173
P4HA3	2.696013202	0.0029322	2.532806483
ACHE	2.696504844	4.85E-15	14.31404403
EFNB3	2.703666674	0.001628668	2.788167408
CTSH	2.706056875	8.12E-05	4.090670705
SCG5	2.712424506	2.03E-35	34.69163674
ABCA1	2.716677705	9.66E-111	110.0149558
FST	2.718182574	0	#ZAHL!
KLK4	2.721342863	1.39E-09	8.858189808
DIRAS1	2.721934739	1.36E-05	4.865967577
INPP5J	2.730147925	2.69E-07	6.569610717
NGFR	2.734550043	2.81E-94	93.55118686
ESM1	2.734917604	6.46E-209	208.1895893
EGR2	2.74310642	1.37E-102	101.8625278
TLR5	2.74797334	5.03E-05	4.298527221
COL5A3	2.748141066	1.84E-14	13.73607859
LINC00704	2.749931796	0.009070087	2.042388535
C2orf91	2.753063288	0.0051645	2.286971693
AC114811.2	2.754440897	2.84E-12	11.54720062
SPRR2D	2.754471153	0.003919659	2.406751715
IPCEF1	2.771148196	0.006495219	2.18740618
THBS1	2.772589076	0	#ZAHL!
GLIS1	2.775673077	8.39E-08	7.07611393
AL137077.2	2.778809683	4.30E-15	14.36693571

Gene	log2(FoldChange)	p_{adj}	$-\log_{10}(p_{adj})$
AL353807.2	2.781543725	0.00608142	2.215995036
FGF5	2.788895999	4.56E-15	14.34072194
LINC01619	2.789398671	0.000918559	3.036892991
RNF112	2.789576825	2.06E-05	4.687083247
MGAM	2.796334502	0.00260068	2.584913098
ITGAM	2.796407689	0.008115434	2.090688245
HIST1H4E	2.796661104	2.55E-22	21.59431006
SH2D2A	2.797006302	0.009569635	2.019104612
PICART1	2.804313449	1.62E-05	4.78914777
C8orf4	2.804652597	0.007054574	2.151529222
AC095055.1	2.80558659	5.38E-06	5.26913786
FOSL1	2.81516486	0	#ZAHL!
RND3	2.815890688	0	#ZAHL!
RNVU1-15	2.818441103	0.000736908	3.132586929
AC022028.2	2.826054322	0.005287208	2.276773606
SUGT1P3	2.826191283	0.000184976	3.732884103
EFNB2	2.826244475	5.99E-117	116.2227648
AMPD3	2.831307912	4.34E-13	12.36216262
PAPPA	2.831415547	1.70E-19	18.76925919
SEZ6L2	2.837731055	6.75E-25	24.17070446
NKAIN4	2.840648587	0.00162999	2.787815129
AC110769.2	2.845659222	4.66E-06	5.332042517
NLRC3	2.853704238	0.000670527	3.173584021
CREB3L1	2.854252609	1.75E-11	10.75669128
AC092117.2	2.866213214	0.004446837	2.351948813
AC002401.4	2.870476352	2.27E-10	9.643331478
HIST2H3D	2.877175261	1.80E-09	8.74375332
HIST2H2BE	2.880241973	2.40E-218	217.6192559
PHLDA2	2.883721681	6.50E-290	289.1868136
RPL13AP20	2.883864256	5.79E-05	4.237572472
VWA7	2.885323267	1.78E-05	4.749890267
ZFPM2	2.887213911	0.000383332	3.416424745
SNX18P3	2.888405959	0.004405263	2.356028134
MISP	2.888814639	4.93E-15	14.30687714
CD82	2.890914371	1.97E-58	57.70592019
KCNH1-IT1	2.892672618	1.40E-07	6.852514675
C17orf105	2.903003708	0.008496403	2.070764897
PRG4	2.903719256	1.15E-09	8.940693267
AC010999.2	2.91403949	0.009439706	2.025041552
AC007666.1	2.915945982	0.002660358	2.575059844
C7orf61	2.922728211	0.000331907	3.478983812
LINC01816	2.923593039	1.52E-07	6.818513841
Z97832.2	2.924318429	0.004891787	2.310532431
AL031777.1	2.927557336	0.00014123	3.850073764
AC026691.1	2.930331181	0.003324908	2.478220326
PLAU	2.930650426	0	#ZAHL!

Gene	log2(FoldChange)	p_{adj}	$-\log_{10}(p_{adj})$
NAT8L	2.931871257	7.03E-15	14.15302951
SLC7A8	2.934339197	1.28E-05	4.893936799
POU2F2	2.946651579	9.58E-12	11.01855944
LINC02392	2.947658482	0.000264728	3.577199866
EPPK1	2.952678306	4.10E-09	8.387664103
SPOCD1	2.955006711	2.75E-154	153.5611019
ACP5	2.955523613	1.09E-47	46.96388856
LY6K	2.959498396	0.000663059	3.178448055
ZMAT1	2.961721532	0.008933536	2.048976627
BEND7	2.96896034	4.49E-05	4.347977812
KIF21A	2.971111675	8.88E-10	9.051706983
MIR181A1HG	2.975837217	2.36E-05	4.626514903
BMP2	2.976467151	0	#ZAHL!
TARSL2	2.980095992	2.49E-07	6.604378412
HIST2H2AB	2.983970431	0.008277884	2.082080642
LINC02551	2.988503772	0.008111219	2.090913893
PSG4	2.998641176	9.22E-25	24.03543207
PHYHIP	3.001026112	1.40E-08	7.852894925
AC007881.3	3.001764933	0.001083587	2.965136329
IL16	3.004355278	0.001870557	2.728029111
PDE2A	3.004913143	0.000328706	3.483192046
CD44-AS1	3.005321144	0.001263115	2.898557109
TM4SF19	3.014130994	0.000311935	3.5059364
AL354732.1	3.017910982	5.67E-06	5.246549459
PTHLH	3.020751209	7.27E-101	100.1384162
PADI3	3.025784403	8.78E-10	9.056394134
PLPP4	3.028659633	1.57E-07	6.804543698
ITGA11	3.035301032	3.06E-23	22.51391517
AL133551.1	3.040556563	0.006098742	2.214759705
CHMP4BP1	3.044081225	0.000125935	3.899853099
AOC3	3.051524712	9.84E-20	19.00679183
TMEM154	3.052172814	7.25E-15	14.13967317
LBP	3.059273099	8.82E-05	4.054713879
AC005332.1	3.076100701	0.004380683	2.358458201
TINCR	3.076350487	4.09E-10	9.388346337
SPACA6P-AS	3.083828604	1.36E-06	5.866652875
CILP	3.088805003	0.005026065	2.298771926
KRT8P36	3.091383593	0.000336947	3.472438123
PTPRN	3.093250249	3.76E-07	6.425098519
AC015912.3	3.094972893	3.91E-18	17.40738174
AL359834.1	3.100587563	0.000285771	3.543982561
RNU5D-1	3.104202001	0.002760981	2.558936614
PLAUR	3.107558313	0	#ZAHL!
AL365356.5	3.11023132	6.78E-05	4.168685189
HRK	3.111828168	0.005450517	2.263562282
BIRC3	3.119904986	2.76E-38	37.55956842

Gene	log2(FoldChange)	p_{adj}	$-\log_{10}(p_{adj})$
RRAD	3.120878081	2.21E-82	81.65592302
NIPAL4	3.130100015	2.62E-05	4.58191817
AP005432.2	3.144047628	4.43E-05	4.353512306
TRIB1	3.145384503	0	#ZAHL!
AC020922.3	3.148207092	0.000387301	3.411951136
GOLGA7B	3.148355782	3.67E-06	5.435257856
S100A16	3.14843599	0	#ZAHL!
PTPRS	3.15058553	5.45E-25	24.26323484
PYY2	3.154992085	0.007399271	2.130811044
IMPDH1P10	3.162548385	0.000212586	3.67246442
LINC00598	3.169619724	0.000240917	3.618132007
NKX3-1	3.176475429	1.48E-129	128.8293587
KCNQ5	3.177235701	0.008117085	2.090599932
IRAK2	3.182020505	7.23E-63	62.14087455
AL627171.1	3.18503725	0.0008022	3.095717163
AL050403.2	3.191327998	0.000146109	3.835324349
NXPH3	3.199295381	4.40E-05	4.356410356
STAC2	3.202345625	2.81E-06	5.550558264
SUCNR1	3.208188019	1.36E-10	9.868018991
AC093510.1	3.208795669	0.000116947	3.932009559
NUDT11	3.216918715	9.82E-05	4.007960126
AC026471.2	3.221274083	0.002788585	2.554616167
AC012462.3	3.224923392	0.004978471	2.302904009
WNK4	3.235659399	1.48E-13	12.83019582
IL4I1	3.238790694	1.92E-07	6.717023916
RSAD2	3.245789457	2.61E-10	9.583177265
PTGER2	3.249540757	1.04E-20	19.98464695
DHRS9	3.253807416	0.000341242	3.466937253
POU3F1	3.254076661	5.77E-07	6.238790654
LINC00184	3.260656797	0.003607075	2.44284478
C1GALT1C1L	3.262810084	0.007615533	2.11829971
CPNE7	3.264063879	1.24E-70	69.90702745
LRRC32	3.270712337	5.88E-14	13.23035775
ABCA13	3.272355532	3.94E-14	13.40469322
ANKRD1	3.272431859	4.58E-272	271.3389269
AP000569.1	3.277085233	0.002113126	2.675074611
AZU1	3.278568337	0.00325166	2.4878949
AL450992.1	3.280008956	0.000254797	3.593805764
AC073352.1	3.282143878	0.002037879	2.690821703
SLC37A2	3.288119538	1.11E-07	6.955010889
SLC2A5	3.292564244	0.001231891	2.909427548
DMKN	3.310061548	7.95E-07	6.099679625
KRTAP20-2	3.316013098	0.004754396	2.322904614
HIST1H4D	3.318166075	0.007361075	2.133058763
BAAT	3.319849101	0.001886973	2.724234204
CACNA1I	3.32024232	2.44E-06	5.612227083

Gene	log2(FoldChange)	p_{adj}	-$\log_{10}(p_{adj})$
AC243772.2	3.322707823	5.65E-07	6.24794691
CRABP2	3.336236183	1.07E-35	34.97000672
AC013652.1	3.341347656	2.73E-07	6.563302811
KPNA7	3.347398262	0.00017185	3.76484962
SPOCK1	3.357333504	1.79E-10	9.74750132
PSG1	3.361085635	4.44E-05	4.353006177
NPTX1	3.362449515	3.10E-42	41.50923261
LINC00327	3.370946802	0.000405133	3.392401998
PSG9	3.37284102	0.002277839	2.642477031
SLC22A17	3.374746567	0.000348319	3.458023311
AMTN	3.375056507	2.47E-77	76.60754388
PCDH1	3.377148753	9.64E-13	12.01571232
MERTK	3.38367403	4.84E-06	5.314946039
HIST2H2BF	3.393481974	2.09E-52	51.67901963
EBI3	3.400288211	0.001999167	2.699150821
AP002478.1	3.401942968	0.005506079	2.259157537
FAM184B	3.403121283	0.004298719	2.366660988
TMEM59L	3.405742598	6.60E-24	23.18037303
GSX2	3.40683203	0.000761513	3.118322697
IL34	3.410327076	0.007246148	2.139892794
AL390037.1	3.418501581	0.008352195	2.078199357
IRX3	3.4204961	0.000297445	3.526593213
AOX1	3.421692723	2.49E-16	15.60346148
CNN1	3.426222645	1.74E-79	78.76051422
AC091212.1	3.436314629	0.007539776	2.122641564
AL591846.2	3.437752047	5.81E-08	7.235684724
HIST1H2AE	3.438032113	9.70E-05	4.013404229
AL359182.1	3.438974156	0.002116067	2.67447061
AC007728.2	3.445696364	0.000405984	3.391490613
MC5R	3.445967106	1.18E-12	11.92786966
COL13A1	3.447706835	2.68E-07	6.571652658
CD79A	3.450179973	0.000195	3.709964718
AC113410.3	3.452487651	0.000328984	3.482824761
AL139819.1	3.456320089	0.002229935	2.65170785
AC097634.1	3.457608696	7.42E-05	4.129843241
HKDC1	3.467129454	6.16E-14	13.2105692
LTA	3.472584196	0.009125781	2.039729977
LINC01705	3.476127568	1.43E-28	27.84515306
NPTXR	3.480805895	4.71E-87	86.32709735
Z93241.1	3.483033082	2.63E-05	4.580755887
KIAA1755	3.483381235	2.22E-22	21.65411559
G0S2	3.490189242	0.009965625	2.001495479
HIST1H2BG	3.492282503	1.06E-16	15.97559832
ELAVL3	3.498611333	0.000631939	3.199325124
KRT18P31	3.527633923	0.000188631	3.724387328
FAM71F1	3.550419334	0.00948451	2.022985107

Gene	log2(FoldChange)	p_{adj}	$-\log_{10}(p_{adj})$
TNFRSF9	3.558103926	4.04E-31	30.39389016
IL12A	3.558424908	6.57E-10	9.182238815
SH2D5	3.559532255	1.65E-25	24.78156504
NUP210L	3.57160532	4.09E-06	5.388005809
GPER1	3.578484882	2.21E-14	13.65575247
CNTN1	3.588751525	0.002045393	2.689223202
AC012557.3	3.591938972	8.66E-05	4.062407027
AC139256.1	3.592168609	0.005793362	2.237069348
CNTNAP3B	3.599359198	0.00921051	2.035716328
DLL4	3.60163195	1.24E-05	4.906061614
AL451050.2	3.607657902	0.003495555	2.456483904
PAX8-AS1	3.609546917	2.07E-08	7.683474529
RND1	3.636895468	2.04E-41	40.68948483
FMNL1	3.642600554	1.34E-09	8.874201629
ESPNL	3.643586491	0.002557445	2.592193741
AC004817.3	3.64974701	1.42E-05	4.846300497
MEGF6	3.655944244	7.18E-156	155.1435903
MYCT1	3.660983947	0.001582747	2.800588563
HIST1H4K	3.663267824	0.000239006	3.621590818
PAX8	3.666297619	1.49E-08	7.828015697
AC007663.3	3.667521251	0.003357014	2.474046865
AQP1	3.670203062	8.56E-05	4.067559594
NEURL3	3.670852969	5.46E-09	8.263008664
CLDN4	3.671016186	4.56E-08	7.341223718
CST7	3.676933966	0.005026065	2.298771926
LINC01647	3.678049677	0.004352819	2.361229383
AC005077.4	3.679111025	3.28E-10	9.483581876
DNAH17	3.686836055	7.36E-12	11.13311883
PDCD1LG2	3.687229085	3.56E-57	56.44844739
ACTBL2	3.692156181	1.20E-24	23.91935305
BIRC7	3.692983706	7.82E-08	7.106900545
SLC16A6	3.700745899	1.36E-47	46.86544325
RET	3.701633666	0.000421774	3.374920108
LINC01060	3.702601608	0.009871539	2.005615124
ATP6V0A4	3.70768484	0.007798227	2.108004133
SLC44A5	3.70818119	0.007006718	2.154485369
HSD11B1	3.708507895	0.00016582	3.780363877
VGF	3.712146031	6.87E-27	26.16281859
COL2A1	3.715941938	4.10E-15	14.38701942
LAMC2	3.750777851	3.61E-09	8.442548234
RASGRF1	3.756048568	0.000106462	3.972807336
XDH	3.758196773	5.83E-19	18.23429311
MYOSLID	3.758503867	0.002311378	2.636128991
PDE6G	3.767835198	0.000381211	3.418834687
TNS1	3.774731133	3.02E-11	10.52003438
ANKRD55	3.783594278	0.000489133	3.310573186

Gene	log2(FoldChange)	p_{adj}	$-log_{10}(p_{adj})$
JCAD	3.789564655	1.70E-61	60.77068012
TGM2	3.795389408	0	#ZAHL!
HIST1H2BF	3.798980421	1.71E-15	14.76698327
AP003419.4	3.801547375	0.000151265	3.820261193
PITX1	3.804832867	0.007178587	2.143961025
AC120024.1	3.80485043	0.007120724	2.147475856
HAGLR	3.806074224	0.005242484	2.280462926
CEACAMP10	3.80654399	0.000228033	3.642002266
SP6	3.809507765	0.008596684	2.065669027
LGALS9	3.812825789	0.006679322	2.175267609
PRKCG	3.825130404	0.000286413	3.54300799
MAP7D2	3.85210576	0.00044603	3.350635566
LINC01182	3.853191538	0.009726578	2.012039924
FAM225A	3.854905178	0.007503747	2.124721792
COL9A1	3.860798997	0.006668322	2.175983435
PMP2	3.86302549	0.006783185	2.168566351
RTL9	3.863102813	0.007279069	2.137924187
PEAR1	3.86623747	0.004954758	2.304977571
U1	3.866760348	1.66E-12	11.78009111
TRIM63	3.871187835	0.009811721	2.008254811
LRRC15	3.878067539	4.43E-79	78.35361711
AP003733.4	3.878285702	0.000245614	3.609747038
PRKG1-AS1	3.882499919	0.008044617	2.094494613
SPINK1	3.882791031	8.69E-11	10.06119223
AC109326.1	3.884488648	1.81E-18	17.74173079
RNU4ATAC	3.885507799	0.000162253	3.789808273
AC087482.1	3.899782745	0.006635353	2.17813595
SEMA3D	3.911731756	0.000622436	3.205905076
PPP1R14A	3.940536112	0.001577116	2.802136307
PRDM1	3.941303381	1.90E-48	47.72140269
F2RL3	3.943413757	5.96E-05	4.224788782
MEST	3.949692653	2.59E-08	7.587505656
TMEM158	3.955461122	1.47E-172	171.8320253
AC037198.2	3.957234729	2.77E-09	8.557698089
AL353803.4	3.966308021	1.32E-05	4.878068424
HTRA3	3.968588479	5.42E-11	10.2663838
AC055811.3	3.974182872	0.003039633	2.517178827
LCK	3.983010824	0.004200138	2.376736476
AC005593.1	3.983254808	0.001445303	2.840041139
PINLYP	3.997096606	7.69E-14	13.1143018
YPEL4	4.002117893	0.00062063	3.207167542
CXCL10	4.005748835	3.06E-06	5.514273271
HMGA1	4.008488524	0	#ZAHL!
SIGLEC15	4.013155283	4.44E-24	23.35231443
AMZ1	4.014417114	1.59E-30	29.79944304
HAP1	4.019237292	5.19E-05	4.284579814

Gene	log2(FoldChange)	p_{adj}	$-log_{10}(p_{adj})$
TRIML2	4.025570776	0.008598579	2.065573306
AC007780.1	4.026939888	0.008455627	2.072854166
IGSF9B	4.027938213	0.00413452	2.383574898
DES	4.028488205	0.005664785	2.246816542
SLFN11	4.029544123	0.004218111	2.374881995
AC090825.1	4.029730701	0.004200138	2.376736476
PAK3	4.031592734	0.00407209	2.390182653
SNORD3A	4.032716686	0.004922411	2.307822155
ANO5	4.036661927	0.008878786	2.051646393
BPI	4.038820672	0.005679721	2.245672978
AC004988.1	4.050052307	1.26E-09	8.900900989
NCAN	4.052811203	0.003837098	2.415997096
WNT7B	4.060158242	1.52E-205	204.8179138
AC004840.1	4.065402039	0.006111104	2.213880301
CABP7	4.069288717	1.97E-71	70.70640112
APBA2	4.069443244	0.002590909	2.586547843
AL512652.2	4.078392468	0.004874603	2.312060761
COLEC10	4.086417719	1.73E-13	12.76287719
ACE	4.088404587	0.004803615	2.318431847
ADRA2A	4.096712642	8.12E-06	5.090201021
ZNF341-AS1	4.099772041	0.000259979	3.585062509
CADM1	4.132356579	0.000258089	3.58822985
MMP25	4.134136134	2.17E-06	5.662758004
MPP4	4.137973418	0.00038298	3.416824064
NRROS	4.152382666	0.002085968	2.680692287
CGB8	4.157640822	0.000142579	3.845944471
GZMB	4.177073915	4.06E-10	9.39139258
USP2-AS1	4.17918436	0.005083463	2.293840319
AL031651.2	4.179279339	0.002661854	2.574815776
MMP13	4.182199304	1.15E-09	8.939450015
NAP1L2	4.191103405	0.00920841	2.035815356
FOSB	4.192731215	2.98E-79	78.52521979
AP001269.4	4.206777276	0.000441123	3.355440097
AC062015.1	4.208844869	0.005092555	2.29306427
SH3TC2	4.214801475	0.000185811	3.730928778
IL1RL1	4.221158838	0.000743906	3.128481952
AL353719.1	4.229093971	0.000431812	3.364705482
CLSTN2	4.236280444	0.00788797	2.103034765
EPB41L3	4.240023788	0.00512305	2.290471399
NECTIN4	4.245331481	4.82E-14	13.31719795
AC083973.1	4.27914538	0.009275044	2.032684031
AC135048.4	4.28368811	0.005630726	2.249435633
LINC01468	4.287158872	0.005032025	2.298257226
PIFO	4.301548835	0.002726601	2.564378438
GALNT18	4.320656222	0.001624343	2.789322361
NAV2-AS5	4.322923142	0.001398601	2.854306282

Gene	log2(FoldChange)	p_{adj}	$-log_{10}(p_{adj})$
OSM	4.323083955	0.001014145	2.993899851
LHX2	4.358638712	0.001020055	2.991376293
FRG2C	4.363209392	0.005067929	2.295169464
CADM2	4.364527255	0.007468068	2.126791713
AC016737.1	4.37333868	0.002049206	2.688414423
LHX1	4.373537332	0.000187133	3.727849607
LINC02154	4.378051979	0.004237651	2.372874817
KISS1	4.386430929	0.000850689	3.070229383
INSM1	4.386661071	0.000189599	3.722163964
LRIT3	4.386812344	0.00768082	2.114592429
NPC1L1	4.399238183	1.02E-05	4.991124457
ROBO4	4.411313804	0.000405894	3.391587058
KSR2	4.412890943	1.73E-11	10.76143685
SYTL5	4.42368136	0.000835875	3.077858691
TNFAIP6	4.427663755	2.48E-23	22.60551036
Z69720.2	4.43106946	0.00387629	2.411583718
IL4R	4.435610437	0.001739898	2.759476119
PPP1R1B	4.438109026	0.00160112	2.795576119
TTC9B	4.440360962	0.002731917	2.563532509
ACOX2	4.442749655	0.001201064	2.920433707
AFF3	4.4437315	0.001182512	2.927194278
EPHB1	4.444024716	0.001319307	2.879653989
LGI4	4.444045563	0.001102134	2.957765538
TMEM178B	4.446731069	0.001114975	2.952734694
NBL1	4.447100908	2.26E-16	15.64606068
STK26	4.448108445	0.001168577	2.93234283
DENND5B-AS1	4.452142269	0.002893613	2.538559553
KANK3	4.465389254	0.00167366	2.776332877
SUN3	4.465978331	0.002906766	2.536589866
ARHGAP22	4.480970725	0.000709662	3.148948239
SERPIND1	4.481342617	0.005152856	2.287952009
IL11	4.497292132	0	#ZAHL!
RAMP1	4.506482005	5.36E-07	6.270437458
DRAXIN	4.507174899	3.94E-191	190.404748
CDCP1	4.514117573	0.001406266	2.851932408
CPNE9	4.517434496	0.002736788	2.562758889
PRSS22	4.518583337	4.03E-14	13.39463917
AC022424.1	4.524768454	1.81E-05	4.741219171
LINC00973	4.538460366	3.09E-13	12.51009814
FAM189A2	4.538892879	0.000573716	3.241302718
OSBP2	4.541878145	0.000546441	3.262456979
CARMIL3	4.553540026	0.000976936	3.010133837
PRSS3	4.557259535	0.002717198	2.565878662
NOD2	4.567065738	0.000912295	3.03986452
NUDT10	4.573727113	0.002367942	2.625628963
COL17A1	4.578554706	0.007151267	2.145617025

Gene	log2(FoldChange)	p_{adj}	$-log_{10}(p_{adj})$
NTNG1	4.598534643	0.000469523	3.328343298
BEAN1	4.605228775	6.56E-09	8.183398931
KLK6	4.607696	0.000522723	3.281728493
LINC01711	4.609552992	0.000861504	3.064742565
COLEC11	4.613539688	0.00053223	3.273900581
FLJ16779	4.620945739	2.14E-06	5.670101813
DKK1	4.624707656	0	#ZAHL!
AC007365.1	4.633718535	0.002787999	2.554707452
CGB5	4.656332909	0.000106884	3.971086587
AC090527.3	4.657578367	0.001641188	2.784841718
IFT74-AS1	4.661480435	0.001411734	2.850247274
RNU5A-8P	4.664240141	0.004539723	2.342970645
AL096829.2	4.66945541	0.001300093	2.88602573
AC010186.1	4.670467204	0.00282604	2.548821657
ADGRF4	4.671593581	0.004399244	2.356621959
RELN	4.67285837	0.009268058	2.03301124
KIF21B	4.684083184	0.000599432	3.222260164
LINC01050	4.684830733	0.000395377	3.402988303
MAL	4.686541288	0.001043184	2.981639076
AC016831.1	4.688131382	2.34E-19	18.63039404
AC006483.2	4.696148552	0.002375376	2.624267702
SERPINE1	4.735960537	0	#ZAHL!
CPA4	4.750959605	3.71E-43	42.43013305
SNORD15B	4.757216421	0.001652653	2.781818198
AC026310.2	4.763636174	0.00017185	3.76484962
AC015936.1	4.764270683	0.002019362	2.694785819
Z83847.1	4.76688049	6.26E-05	4.203182824
NPR1	4.773362073	0.004639438	2.333534594
TNFRSF10A	4.783056873	0.000965746	3.015137258
TNF	4.784245381	0.001306545	2.883875662
AL031985.4	4.796884705	0.001826616	2.73835283
INSR	4.806536406	0.000221617	3.654397689
SYN1	4.837153748	0.000307428	3.51225666
GAPDHP14	4.846176628	1.73E-05	4.762044223
ZNF280A	4.846746401	0.001735276	2.760631397
NBEAP1	4.846894263	0.000735432	3.133457469
SERPING1	4.854601894	0.00044783	3.348887126
CHST1	4.860294926	0.000257861	3.588614778
SNAP25	4.860309421	0.000259653	3.585606475
AC104137.1	4.866524702	0.002199366	2.657702521
AC097372.1	4.881444593	0.001694522	2.770952752
LAMB3	4.881687884	7.62E-24	23.11787258
TRAF1	4.885700143	4.50E-80	79.34689151
TUBG1P	4.914119526	0.004751212	2.323195562
KRTAP2-3	4.933180475	0.002297745	2.638698113
HTRA1	4.937441596	1.51E-15	14.82210781

Gene	log2(FoldChange)	p_{adj}	$-\log_{10}(p_{adj})$
RAMP2-AS1	4.942387415	0.000226592	3.644755625
XIRP2	4.956728299	0.001329952	2.876164105
MIR320A	4.970629636	0.000672888	3.17205703
SBK3	4.990145202	0.00317423	2.498361619
NTRK1	5.003986169	0.002008404	2.697148817
DLX3	5.013397404	0.000575649	3.239841991
CXCL8	5.015365842	0	#ZAHL!
MMP7	5.01537346	0.006635351	2.178136088
BX255923.2	5.02577725	0.002984516	2.525126161
AMPH	5.030337707	0.000136881	3.863657028
OLIG2	5.031267197	0.00013692	3.863531953
AC187653.1	5.036027011	0.000192356	3.715894426
GJA3	5.072024483	0.000264081	3.578262579
CST4	5.078029431	0.007696344	2.113715528
FCRLA	5.108877436	0.000100298	3.998707811
RFPL4A	5.109735552	0.000364189	3.438672658
DOCK2	5.112253198	0.000713721	3.146471574
AL713998.1	5.12858579	0.001590767	2.798393416
SBSN	5.137655983	2.51E-05	4.600814116
SUSD4	5.149419537	9.89E-05	4.004926207
MOBP	5.155425635	0.00175688	2.755257824
RCSD1	5.178160094	0.00056674	3.246616514
KLHL31	5.179422085	0.00016103	3.793092683
MUSK	5.204536663	0.001058685	2.975233356
AQP3	5.259214706	4.26E-05	4.370298624
NPPC	5.261614367	0.000926632	3.03309266
RPLP0P2	5.270997901	5.95E-10	9.22524372
LINC01828	5.304664296	0.000391851	3.406878624
AC017002.3	5.314390435	0.007162401	2.14494135
NDNF	5.323303253	3.37E-05	4.471970148
IL24	5.324057349	5.90E-05	4.229014783
SSX1	5.325194851	5.13E-05	4.290277767
PTPN6	5.325530331	6.41E-05	4.192908885
AC108134.1	5.331100069	0.00014106	3.850597608
AC002384.1	5.3565536	0.000618858	3.208409188
STX1B	5.373030379	5.31E-05	4.274518881
LINC02547	5.388795357	0.002751746	2.560391732
EVI2A	5.392799501	3.34E-05	4.476498097
ACP7	5.402560053	0.007795746	2.10814231
TRIM72	5.408679676	0.000241977	3.616225539
AC098818.2	5.438537304	6.31E-09	8.199750313
AL359182.2	5.451149893	0.000436148	3.360366559
DTX1	5.451593022	3.00E-05	4.523426904
MYO7B	5.451793332	0.000285812	3.543920011
RPL3L	5.468132665	0.000269494	3.569451666
STK24-AS1	5.472343806	6.20E-05	4.207669619

Gene	log2(FoldChange)	p_{adj}	$-\log_{10}(p_{adj})$
DUSP2	5.474500438	7.52E-18	17.12372183
LINC01449	5.474538062	0.000698716	3.155699052
LINC01920	5.522104283	0.005396361	2.267899022
AC009908.1	5.530885295	7.85E-05	4.105385012
CSF2	5.531237263	0.000466668	3.330991622
CD22	5.561035726	1.65E-05	4.782911319
AL391056.1	5.566494714	1.45E-08	7.839667007
DCDC2C	5.572030476	0.002114334	2.674826347
GPR83	5.591980093	0.00044497	3.3516688
MFNG	5.597768362	2.62E-05	4.58099327
LRRC8E	5.618837199	1.40E-13	12.85372758
TRIM43B	5.624014669	0.000666436	3.176241814
GPR84	5.624174614	0.00095406	3.020424407
MARCH4	5.638319316	0.001730508	2.761826405
PRLH	5.665794762	0.000680164	3.167386371
APCDD1L	5.668361984	1.04E-05	4.981765751
AL138828.1	5.673519279	5.61E-05	4.25073481
LINC01635	5.697522415	7.51E-05	4.124189511
KRT34	5.718919913	0.000449676	3.347100179
EVI2B	5.724933839	8.69E-07	6.061200148
IQGAP2	5.731482771	7.04E-06	5.152561446
PLVAP	5.750475241	0.000181747	3.740532256
FAM71E2	5.760456476	1.81E-06	5.742829826
CHRNA9	5.765451077	2.17E-06	5.66389995
MIR3190	5.771180324	0.000102806	3.987980206
IER3	5.77662868	2.96E-24	23.52875004
FNDC7	5.782624468	6.68E-05	4.175379779
AC133552.1	5.815576121	6.13E-05	4.212394662
KRTAP21-2	5.815681159	0.001099796	2.95868805
MYH16	5.901930454	2.20E-05	4.658316072
IL36RN	5.95724028	0.002341411	2.630522351
AC026461.3	5.979961844	0.001335197	2.874454735
SIRPA	5.99785553	1.36E-15	14.86628449
NRG1	6.008217724	1.90E-06	5.720908607
RAC2	6.032899551	3.29E-06	5.482170299
PSG7	6.037352739	0.002746224	2.561264005
IL1B	6.068883902	2.79E-07	6.553681432
F2RL1	6.082083811	1.37E-44	43.86179601
TBX1	6.105824543	0.000124722	3.904056071
SLCO3A1	6.108302061	1.50E-06	5.82388866
ZFX-AS1	6.137876407	7.94E-06	5.100299394
CYP24A1	6.16119056	1.13E-05	4.947234724
PTGES	6.185984558	3.93E-227	226.4050843
BX284668.6	6.203557883	9.47E-06	5.023707607
ENDOU	6.217261507	8.62E-06	5.064273357
AC003092.1	6.346373617	4.50E-06	5.347091028

Gene	log2(FoldChange)	p_{adj}	$-log_{10}(p_{adj})$
TRIM43	6.361045986	3.99E-05	4.399117873
ITGAX	6.499663498	2.74E-06	5.561621052
CGB3	6.524363578	6.34E-05	4.197934638
MMP1	6.559167551	4.64E-50	49.33315085
MMP3	6.588237592	1.77E-20	19.75298373
GAL	6.59854812	3.59E-06	5.444574479
AC117382.2	6.647995917	6.51E-07	6.186557784
MMP10	6.720147731	4.96E-13	12.30413711
CACNG7	6.757661591	2.88E-06	5.540935042
CALB2	6.763875954	2.82E-54	53.54993434
KRTAP1-5	6.767494499	6.59E-07	6.180940963
EGR3	6.987831589	2.43E-08	7.615179275
KCNJ12	7.736401495	1.55E-08	7.809086199

Appendix Table 5: Full list of antibodies used in DigiWest protein profiling analyses

Antigen	Mod-Site	Supplier	Product No.	Species	MW (kDa)
14-3-3 sigma		R&D	AF4424	gt	28
53BP1		Cell Signaling	4937	rb	450
53BP1 - phospho	Thr543	Cell Signaling	3428	rb	450
Akt		Cell Signaling	4685	rb	60
Akt - phospho	Ser473	Cell Signaling	4060	rb	60
Akt - phospho	Thr308	Cell Signaling	13038	rb	60
Apaf-1		Cell Signaling	8723	rb	135
ATM		Cell Signaling	2873	rb	350
ATM - phospho	Ser1981	Cell Signaling	5883	rb	350
ATR		Cell Signaling	2790	rb	250
ATR - phospho	Ser428	Cell Signaling	2853	rb	300
Aurora B (AIM1)		Cell Signaling	3094	rb	40
Aven		Cell Signaling	2300	rb	50
Bad		Cell Signaling	9239	rb	23
Bad - phospho	Ser136	Cell Signaling	4366	rb	23
Bax		Cell Signaling	2772	rb	20
Bcl2		Cell Signaling	4223	rb	26
Bcl2 - phospho	Ser70	Cell Signaling	2827	rb	28
Bcl-xL		Cell Signaling	2764	rb	30
BID		Cell Signaling	2006	ms	22
BRCA1		Cell Signaling	14823	rb	220
Caspase 3		Cell Signaling	9662	rb	35, 19, 17
Caspase 3 - cleaved	Asp175	Cell Signaling	9661	rb	19, 17
Caspase 7		Cell Signaling	9492	rb	35, 20
Caspase 8		Cell Signaling	9746	ms	43, 18
Caspase 9		Cell Signaling	9502	rb	35, 17
Caspase 9 - phospho	Ser196	ThermoFisher	PA5-40222	rb	46
CBP		Cell Signaling	7389	rb	300
cdc2 (CDK1)		Cell Signaling	9112	rb	34
cdc2 (CDK1) - phospho	Tyr15	Cell Signaling	4539	rb	34
cdc25A		abm	Y021163	rb	59
cdc25A - phospho	Ser75	abm	Y011138	rb	59
cdc25C		Epitomics	1302-1	rb	60
CDK2		Cell Signaling	2546	rb	33
CDK2 - phospho	Thr160	Cell Signaling	2561	rb	33
CDK4		Cell Signaling	12790	rb	30
CDK5		Cell Signaling	2506	rb	30
CDK6		Santa Cruz	sc-7961	ms	40
CDK6 - phospho	Tyr13	biorbyt	orb15013	rb	36
CDK6 - phospho	Tyr24	biorbyt	orb15014	rb	36
CDKN2A		ProteinTech Group	10883-1-AP	rb	17
CDKN2B		Bio-Techne	MAB6798	ms	15

Antigen	Mod-Site	Supplier	Product No.	Species	MW (kDa)
Chk1 - phospho	Ser345	Cell Signaling	2341	rb	56
Chk1 - phospho	Ser296	Cell Signaling	2349	rb	56
Chk1 - phospho	Ser296	Cell Signaling	2349	rb	56
Chk2		Cell Signaling	3440	ms	62
Chk2 - phospho	Thr68	Cell Signaling	2661	rb	62
CHOP		Cell Signaling	2895	ms	27
c-Jun		Cell Signaling	9165	rb	48, 43
c-Jun - phospho	Ser73	Cell Signaling	3270	rb	48
c-myc		Cell Signaling	9402	rb	70-57
c-myc - phospho	Thr58/Ser62	abcam (Epitomics)	ab32029 (1203-1)	rb	57
c-myc - phospho	Thr58	ThermoFisher	PA5-37654	rb	62
Cyclin A		abcam	ab53054	rb	49
Cyclin B1		abcam	ab32053	rb	58
Cyclin D1		Cell Signaling	2926	ms	36
Cyclin D2		Cell Signaling	3741	rb	31
Cyclin E1		Cell Signaling	4129	ms	48
Cytochrome c		Cell Signaling	4280	rb	14
DNA polymerase beta		abcam (Epitomics)	ab175197 (8220-1)	rb	38
DNA-PK		Cell Signaling	4602	rb	450
EGFR (ErB-1, HER1)		Cell Signaling	4267	rb	175
EGFR (ErB-1, HER1) - phospho	Tyr1068	Cell Signaling	2234	rb	175
EMSY		abcam (Epitomics)	ab32329 (1602-1)	rb	141
Erk1/2 (MAPK p44/42)		Cell Signaling	4695	rb	44, 42
Erk1/2 (MAPK p44/42) - phospho	Thr202/Tyr204	Cell Signaling	9101	rb	44, 42
Ezh2		Cell Signaling	5246S	rb	98
FAK1		Cell Signaling	3285	rb	125
FAK1 - phospho	Tyr397	Cell Signaling	8556	rb	125
FAS		Cell Signaling	4233	rb	50-40
FasL		Cell Signaling	4273	rb	40, 26
FGF receptor 1		Cell Signaling	9740	rb	145, 120, 92
GADD45 alpha		Cell Signaling	4632	rb	22
GADD45B		abcam (Epitomics)	ab128920 (5833-1)	rb	18
GSK3 beta		Cell Signaling	9315	rb	46
GSK3 beta - phospho	Ser9	Cell Signaling	9336	rb	46
Histone deacetylase 1 (HDAC1)		Cell Signaling	2062	rb	62
Histone deacetylase 2 (HDAC2)		Epitomics	1603-1	rb	55

Antigen	Mod-Site	Supplier	Product No.	Species	MW (kDa)
Histone H2A.X - phospho	Ser139	Cell Signaling	9718	rb	15
Histone H3 - acetyl	Lys9/Lys14	Calbiochem	382158	rb	17
Histone H3 - monomethyl	Lys4	Cell Signaling	5326	rb	17
Histone H3 - phospho	Ser10	Cell Signaling	9701	rb	17
Histone H3 - trimethyl	Lys27	Cell Signaling	9756	rb	17
HSF1		Epitomics	2043-1	rb	82
HSF1 - phospho	Ser326	Epitomics	2092-1	rb	82
IGFBP-3		abcam	ab137370	rb	32
IkappaB alpha		Cell Signaling	9242	rb	41
IkappaB alpha		Cell Signaling	9242	rb	41
IkappaB alpha - phospho	Ser32	Cell Signaling	9241	rb	41
IKK alpha		Cell Signaling	2682	rb	85
IKK alpha/beta - phospho	Ser176/177	Cell Signaling	2078	rb	87, 85
IKK beta		Cell Signaling	2370	rb	87
IKK epsilon		Cell Signaling	2905	rb	80
IL-6		Cell Signaling	12153	rb	21-28
IL-8		Cell Signaling	94407	rb	11
Jak 2		Cell Signaling	3229	rb	125
Jak 2 - phospho	Tyr1007/Tyr1008	Cell Signaling	3771	rb	125
JNK/SAPK		Cell Signaling	9252	rb	54, 46
JNK/SAPK 1/2/3 - phospho	Thr183/Tyr185	Santa Cruz	sc-6254	ms	54, 46
Ku80		Cell Signaling	2180	rb	86
Mcl-1		Cell Signaling	5453	rb	40, 35
MDM2		Santa Cruz	sc-965	ms	90, 60
MDM2 - phospho	Ser166	Life Technologies	44-1400G	rb	125
MEK1/2		Cell Signaling	9126	rb	45
MKK4 (SEK1) - phospho	Ser257/Thr261	Cell Signaling	9156	rb	44
MMP13		R&D	MAB511	ms	54
MMP7		R&D	MAB9071	ms	30
MMP-9		Cell Signaling	13667	rb	92, 84
Mre11		Cell Signaling	4847	rb	81
Mre11 - phospho	Ser676	Cell Signaling	4859	rb	81
mTOR (FRAP)		Cell Signaling	2983	rb	289
mTOR (FRAP)- phospho	Ser2448	Cell Signaling	5536	rb	289
NF-κB p100/p52		Cell Signaling	4882	rb	120, 52
NF-κB p105/p50		Cell Signaling	3035	rb	120, 50
NF-κB p65		Epitomics	2229-1	rb	70
NF-κB p65 - phospho	Ser468	Cell Signaling	3039	rb	65
P21 - phospho	Thr145	Invitrogen	PA512646	rb	18

Antigen	Mod-Site	Supplier	Product No.	Species	MW (kDa)
p21 (Waf1, Cip1, CDKN1A)		Cell Signaling	2947	rb	21
p27 (Kip1, CDKN1B)		Cell Signaling	3698	ms	27
p27 (Kip1, CDKN1B) - phospho	Ser10	abcam (Epitomics)	ab62364	rb	22
p53		R&D	af1355	gt	53
p53 - acetyl	Lys305	abcam (Epitomics)	ab109396 (3308-1)	rb	44
p53 - phospho	Ser15	Cell Signaling	9284	rb	53
p53 - phospho	Ser20	Cell Signaling	9287	rb	53
p53 - phospho	Ser37	Cell Signaling	9289	rb	53
p95 (NBS1) - phospho	Ser343	Cell Signaling	3001	rb	95
PAI-1		Cell Signaling	11907	rb	48
PARP		Cell Signaling	9532	rb	116, 89
PARP - cleaved	Asp214	Cell Signaling	9541	rb	89
PI3-kinase p110 alpha		Cell Signaling	4255	rb	110
PI3-kinase p110 beta		Millipore	04-400	rb	110
PI3-kinase p85 alpha		abcam (Epitomics)	ab40755 (1675-1)	rb	85
PI3-kinase p85/p55 - phospho	Tyr458/Tyr199	Cell Signaling	4228	rb	85, 60
PKR		Cell Signaling	2766	rb	67
PKR - phospho	Thr446	abcam	ab47377-100	rb	62
PTEN		Cell Signaling	9552	rb	54
PTEN - phospho	Ser380	Cell Signaling	9551	rb	54
Rad51		Epitomics	3161-1	rb	37
Rb		Cell Signaling	9313	rb	110
Rb - phospho	Ser780	Cell Signaling	3590	rb	110
Rb - phospho	Ser807/Ser811	Cell Signaling	8516	rb	110
Rb2 (p130)		abcam (Epitomics)	ab76234 (2130-1)	rb	128
Rb2 (p130) - phospho	Ser952	abcam (Epitomics)	ab68136 (2272-1)	rb	128
RecQL1		Santa Cruz	sc-25547	rb	75
Rictor		Cell Signaling	2114	rb	200
SMC1 - phospho	Ser957	Cell Signaling	4805	ms	145
STAT 3		Cell Signaling	4904	rb	86, 79
STAT 3 - phospho	Tyr705	Cell Signaling	9145	rb	86, 79
STAT 3 - phospho	Ser727	Cell Signaling	9134	rb	86
Survivin		Cell Signaling	2802	ms	16
Survivin - phospho	Thr34	Cell Signaling	8888	rb	18-16
TAK1		Cell Signaling	4505	rb	82-78
VEGF-A		Dako	M7273	ms	45
XIAP		Santa Cruz	sc-55550	ms	55
XLF		Cell Signaling	2854	rb	39

Appendix Table 6: List of all germline mutations detected in the MTB Neurooncology Cohort Tübingen

MTB@ZPM	Gene	Functional class	Diagnosis
TUE-0032	BRCA1	frameshift	Glioblastoma
TUE-0035	DPYD	missense	Glioblastoma
TUE-0044	FANCM	stop-gained	Glioblastoma
TUE-0052	NF1	missense	CNS metastasis
TUE-0054	MAGI2	frameshift	Glioblastoma
TUE-0065	FANCA	splice_region	Glioblastoma
TUE-0071	BRCA2	missense	Glioblastoma
TUE-0075	XPC	missense	Oligodendroglioma
TUE-0088	PIK3R3	frameshift	Medulloblastoma
TUE-0091	SDHD	missense	Glioblastoma
TUE-0093	VHL	initiator codon	Meningioma
TUE-0095	IFNGR1	frameshift	Astrocytoma
TUE-0099	PMS1	stop-gained	Astrocytoma
TUE-0106	TP53	missense	Glioblastoma
TUE-0107	NF2	deletion of exons 2-4	Multiple Meningioma
TUE-0114	PALB2	frameshift	Glioblastoma
TUE-0125	SRGAP1	missense	Astrocytoma
TUE-0131	1) MUTYH 2) NF1	1) splice_region 2) spice_region	Pilocystic Astrocytoma
TUE-0140	TP53	missense	Medulloblastoma
TUE-0143	NF1	stop-gained	Pilocystic Astrocytoma
TUE-0145	BRIP1	frameshift	CNS metastasis
TUE-0152	FANCC	frameshift	Glioblastoma
TUE-0170	CHEK2	missense	Solitary fibrous tumor
TUE-0172	1) NF1 2) FANCA	1) stop-gained 2) inframe	CNS metastasis
TUE-0180	MSH2	frameshift	Glioblastoma
TUE-0181	ERCC2	missense	Clivus Chordoma

MTB@ZPM	Gene	Functional class	Diagnosis
TUE-0197	1) LZTR1 2) PALB2	1) stop-gained 2) frameshift	Astrocytoma
TUE-0205	RAD54L	stop-gained	Oligodendroglioma
TUE-0233	BRCA2	frameshift	Vestibular Schwannoma
TUE-0257	NF1	frameshift	Pilocystic Astrocytoma
TUE-0318	MSH6	frameshift	Chondrosarkoma
TUE-0338	APC	stop_gained	CNS metastasis
TUE-0352	SDHD	stop_lost	Solitary fibrous tumor
TUE-0407	BRCA1	splice_donor	Vestibular Schwannoma
TUE-0410	POLQ	frameshift	Clivus Chordoma
TUE-0411	BRCA2	missense	Pilocystic Astrocytoma
TUE-0419	FANCA	splice_region	Glioblastoma
TUE-0428	ERCC3	frameshift	Glioblastoma
TUE-0440	NF1	essencial_splice_site	Glioblastoma
TUE-0441	MSH6	frameshift	Esthesioneuroblastoma
TUE-0453	XRCC2	stop_gained	Glioblastoma
TUE-0474	1) CDKN2A 2) CDKN2B 3) NF2	1) gene deletion 2) gene deletion, non-focal 3) frameshift	Meningioma
TUE-0475	DPYD	missense	Glioblastoma
TUE-0484	MSH6	stop_gained	Glioblastoma
TUE-0488	1) FANCA 2) MUTYH	1) heterocygous loss 2) splice_region	Hemangioblastoma
TUE-0491	1) NBN 2) DPYD	1) frameshift 2) essential_splice_site	Glioblastoma
TUE-0492	BAP1	frameshift	Meningioma
TUE-0494	 NF1	 splice_region	High-grade malignant peripheral nerve sheath tumor
TUE-0497	DYPD	missense intronic	Glioblastoma
TUE-0503	UGT1A1	intronic	Glioblastoma

MTB@ZPM	Gene	Functional class	Diagnosis
TUE-0504			Esthesioneuroblastoma (recurrence)
	DPYD	synonymous	
TUE-0505	1) NF1	1) frameshift	
	2) BRIP1	2) stop_gained	Astrocytoma
TUE-0536	NF2	stop_gained	Meningioma
TUE-0545	NF2	stop_gained	Neurofibroma grade 1
TUE-0556	FANCD2	stop_gained	Glioblastoma
TUE-0562			Pleomorphic Xanthoastrocytoma
	MUTYH	missense and splice_region	
TUE-0567	NRAS	missense	Glioblastoma
TUE-0573	SBDS	splice_donor	Glioblastoma
TUE-0577	PALB2	stop-gained	Metastasis